The Role of Immunological Receptors CD74 and CD44 in Association with the Macrophage Migration Inhibitory Factor (MIF) on Human Breast Cancer Derived Cells

Hussain M M Al Ssadh

A thesis submitted for the degree of Doctorate of Philosophy in Biological Sciences

School of Biological Sciences

University of Essex

February 2016

Abstract

Synergistic interaction between pairs of membrane-bound receptors has been linked to signalling, cell communication and tumour progression. This study has shown that cluster of differentiation (CD) 74 and CD44 act in synergy and are susceptible to the effect of the macrophage migration inhibitory factor (MIF). MIF is a 12.5 kDa chemokine-like inflammatory mediator, whose ligand is the transmembrane receptor CD74. Recent data suggests that CD74 is involved in proinflammatory responses and tumorigenesis but detailed mechanisms are not fully understood. In normal cells CD74 functions as a chaperone of human leukocyte antigen (HLA)-DR biosynthesis and is expressed in antigen presenting cells in the absence of tumours. Notably, CD44 is also a transmembrane receptor and member of a family of cell adhesion molecules responsible for adhesion between adjacent cells (e.g. antigen presenting cells) and cells in the extracellular matrix. Western blotting and flow cytometry were employed to determine the quantitative expression of CD74, MIF and CD44 in three distinct breast tumour cell lines: CAMA-1, MDA-MB-231 and MDA-MB-435. All three cell lines showed a high expression of CD74, MIF and CD44. Modulation studies showed that IFN-γ and LPS can play a significant role in regulating the expression of CD74, proliferation and cell migration in CAMA-1 and MDA-MB-231 cells; suggesting that CD74 might be involved in controlling immunogenicity and immunoediting of breast cancer cells. To investigate the interaction of CD74 with CD44 and MIF, confocal microscopy and co-immunoprecipitation techniques were used. The three molecules form a multimeric complex in cytoplasmic compartments as measured by confocal microscopy, suggesting a mechanistic mode of action; in addition CD74, MIF and CD44 showed significant quantitative variations on all breast cancer derived cells. Knockdown of CD74 by CD74 siRNA significantly reduced CAMA-1 and MDA-MB-231 cell proliferation but increased the level of apoptotic cells. These data suggests that CD74, MIF and CD44, might facilitate signalling and hence could affect tumour progression. Measuring the co-expression levels of CD74, MIF and CD44 could potentially be used as a 'biomarker signature' for monitoring breast cancer tumours at different stages of the disease.

Acknowledgment

First and above all, I praise Allah, the almighty for providing me this opportunity and granting me the capability to proceed successfully. My deepest gratitude goes to the Ministry of Higher Education, Saudi Arabia for awarding me a full scholarship to complete this research.

This thesis appears in its current form due to the assistance and guidance of several people. I would therefore like to offer my sincere thanks to all of them.

I would like to express my appreciation and thank my supervisor, Prof. Nelson Fernández for all that he has done for me over the past few years. I was extremely fortunate for the opportunity and am very grateful for the experience. Thank you for giving me the freedom to explore my research in my own way and encouraging me at every step. I am also indebted to my committee member, Prof. Christopher A. Reynolds for his guidance during the board meetings. His support and inspiring suggestions have been precious for the development of this thesis content.

I am very grateful to my colleagues in lab 4.13 and lab 5.20 at the School of Biological Sciences for their enthusiastic help and support. Also, I would like to express my best wishes to all the staff at the department for their co-operation and warm welcome.

I would like to acknowledge family and friends who supported me during my PhD. My deepest thanks to my mother, brothers and sisters for their continuous love, support and encouragement with their best wishes.

Finally, I would like to dedicate this work to the soul of my father who was always supporting and encouraging me to continue my studies, may Allah rest his soul in peace.

Contents

List of Figures

Table of Figures

List of Figures (Appendix 1)

List of Tables

Abbreviations

°C	Celsius
2 DE	Two-dimensional gel electrophoresis
3D	Three dimensional
aa	Amino acids
Ab	Antibody
Ag	Antigen
APC	Antigen presenting cells
APS	Ammonium persulfate
BMP4	Bone morphogenetic protein-4
BSA	Bovine serum albumin
C-terminal	The carboxyl terminal
CAMs	Cell adhesion molecules
CD	Cluster of differentiation
CD44	Cluster of differentiation 44
CD74	Cluster of differentiation 74
cDNA	Complementary deoxyribonucleic acid
CIC	Cancer initiating cells
CIITA	Class II transcriptional transactivator
CLIP	Class-II-accociated invariant chain peptides
CLL	Chronic lymphocytic leukemia
cm	Centimetre
Co-IP	Co-immunoprecipitation
CO_2	Carbon dioxide
CS	Chondroitin sulfate
CTL	Cytotoxic cells
CXCR	Chemokine receptor
DAPI	4', 6'-diamino-2-phenylindole, dihydrochloride
DCIS	Ductal carcinoma in situ
DMEM	Dulbecco's Minimal Essential Medium
DMSO	Dimethyl sulphoxids
DNA	Deoxyribonucleic acid

DNase	Deoxyribonuclease
dNTPs	2'-deoxynucleoside-5'-triphosphates
DTT	Dithiothreitol
ECM	Extra-cellular matrix
EDTA	Ethylene diamine tetraacetic acid
EMT	Epithelial-mesenchymal transition
EPG	Epidermal growth factor
ER	Endoplasmic reticulum
ERK	Extracellular-signal-regulated kinases
FACS	Fluorescence-actived cell sorter
FCS	Foetal calf serum
FITC	Fluorescein isothiocyanate
FL	Fluorescence
FRET	Fluorescence resonance energy transfer
FSC	Forward scatter
GAS	Interferon-gamma activated sequence
H. pylori	Helicobacter pylori
HLA	Human leukocyte antigen
hr	Hours
IDCs	Invasive ductal carcinoma
IFN-γ	Interferon Gamma
Ig	Immunoglobulin
IgG	Immunoglobulin G
Ii	Invariant chain
JAK	Janus tyrosine kinases
Kb	Kilo base pair
kDa	kilodaltons
LC-MS/MS	Liquid chromatography tandem mass spectrometry
LPS	Lipopolysaccharide
LSCM	Laser scanning confocal microscopy
mAb	Mouse antibody
mAb/MAB	Monoclonal antibody
MAPK	Mitogen-activated protein kinases
MFI	Mean fluorescence intensity

mg	Milligram
MIF	Macrophage migration inhibitory factor
ml	Milliliter
mm	Millimeter
MMPs	Matrix metalloproteinase
mRNA	Messenger ribonucleic acid
MS	Mass spectrometry
N-terminal	The amino terminal
NF-κB	Nuclear factor kappa-light-chain-enhancer of activated B cells
ng	Nanogram
NK	Natural killer
PAGE	Polyacrylamide gel electrophoresis
PBS	Phosphate buffered saline
PCR	Polymerase chain reaction
PFA	Paraformaldehyde
pmol	Picomole
PMSF	Phenylmethylsulfonyl fluoride
PS	Phosphatidylserine
PTHrP	Parathyroid hormone-related protein
RNA	Ribonucleic acid
rpm	Revolutions per minute
RPMI	Roswell Park Memorial Institute Medium
RT	Room temperature
SD	Standard division
SDS	Sodium dodecyl sulphate
siRNA	Small interfering RNA
SIRP-α	Signal regulatory protein-alpha
SSC	Side Scatter
STAT	Signal transducer and activator of transcription
TAAs	Tumour-associated antigen
TDLUs	Terminal ductal–lobular units
TEBs	Terminal end buds
TEMED	Tetrametylethylenediamine
Tetrazole	3-(4, 5-Dimethylthiazol-2-yl)-2, 5-diphenyltetrazolium bromide

Tm	Annealing temperature
TNBC	Triple-negative breast cancer
TNF-α	Tumour necrosis factor-alpha
TRITC	Tetramethyl rhodamine isothiocyanate
TSAs	Tumour-specific antigens
USF-1	Upstream stimulatory factor-1
α-Tubulin	Alpha- tubulin
β-Actin	Beta-actin
µg	Microgram
µl	Microliter
µm	Micrometer

Chapter 1 Introduction

1.1 Tumour immunology

The association between tumours and the immune system was first identified in the 19th century when Rudolf Virchow observed the presence of leukocytes within tumours (Igney and Krammer, 2002; Grivennikov et al., 2010). However, because the lack of knowledge and technology the molecular and cellular basis of immunity and the mechanistic action of cancer, the validity of this idea proved is difficult to establish. It is only during the last 10 years that true evidence has been obtained showing that inflammation plays a significant role in tumorgenesis and some of the molecular mechanisms were elucidated (Hakim et al., 2004; Bucala and Donnelly, 2007; Grivennikov et al., 2010).

The concept of tumour immunology is based on the assumption that the immune system plays a fundamental role in immune responses against a wide range of diseases including cancer (Melvold and Sticca, 2007). Due to the ability of the immune system to distinguish between normal and cancerous cells, it can eliminate abnormal cells and hence, protect the host in absence of external therapeutic agents. It is also believed that the immune system has a dual curial role in tumour progression. Therefore, the immune system is not only capable of suppressing growth by destroying cancer cells or inhibiting their outgrowth but it also has the features to promote tumour progression either by selecting for tumour cells that are more fit to survive in an immunocompetent host or by establishing conditions within the tumour microenvironment to facilitate tumour outgrowth. The process of protecting the host from the development of cancer and altering tumour progression by driving the outgrowth of tumour cells - with decreased sensitivity to immune attack - is known as cancer immunoediting (Dunn et al., 2004; Grivennikov et al., 2010; Schreiber et al., 2011).

Immuno-oncology research over the last 30 years has provided increasing evidence that tumours might be recognised and controlled by the immune system. Therefore, scientists have become more concerned with the study of interactions between the immune system and tumours as well as tumour progression (Finn, 2012). Recently, Butrym et al. (2013) have showed a correlation between high expression of CD74 and zeta-chain-associated protein kinase 70 (ZAB70) expression in B-cell chronic lymphocytic leukemia patients. In breast cancer, Jiang et al. (2013) have shown that wingless-type integration site family, member 5A (WNT5A) inhibits metastasis and alters splicing of CD44 in breast cancer cells. Moreover, Richard et al. (2014) confirmed the role of macrophage migration inhibitory factor (MIF) and CD74 in human breast cancer. In this context, breast cancer is one of the most common cancers with more than 1.3 million cases and 450,000 deaths every year worldwide (Ferlay et al., 2013). In order to understand the biology of breast cancer and its subtypes, the anatomy of breast will be reviewed.

1.2 Anatomy of the human breast

The breast (or mammary gland) is the organ that functions to produce the milk protein and fat to feed the offspring (Capuco and Ellis, 2013; Hassiotou and Geddes, 2013). The normal mature breast consisted of three main components known as the lobules (or gland), milk ducts and stroma (connective tissue) (Figure 1-1) (Ali and Coombes, 2002). The lobules are joined together by alveoli, which consist of the gland and cells that are responsible for milk production. However, the function of ducts is to carry the milk from the lobule to the nipple within the breast. The lobules and ducts are made up of epithelial cells and are embedded in a fat pad composed of adipocyte (Watson and Khaled, 2008; Lemaine and Simmons, 2013). The stroma is comprised of fibroblast (connective tissue), fat various immune cells, lymphatic vessels and blood (Macéa and Fregnani, 2006). A lymphatic vessel and blood vessel network is made up with endothelial cells. The

epithelial cells of the mammary gland are composed of two main types of epithelium; luminal and basal (Watson and Khaled, 2008). In response to various stages of breast development, the breast undergoes different stages in function, shape and size during growth (Turashvili et al., 2005; Geddes, 2007). Theses stages are known as embryonic, pubertal and adult (Russo and Russo, 2004). The embryonic stage of breast development is similar in males and females and it begins when the buds are formed in the ectoderm (Hynes and Watson, 2010). The formation of buds depends on the activation of parathyroid hormone-related protein (PTHrP) (Watson and Khaled, 2008). Association of parathyroid hormone-related protein (PTHrP) and bone morphogenetic protein-4 (BMP4) enhances the outgrowth and elongation of the buds. The interaction of (PTHrP) and (BMP4) is also responsible for signaling pathways in mammary mesenchyme to induce the proliferation and differentiation of the epithelium (Hens et al., 2007). This process is regulated by a number of hormones and growth factors (Hens and Wysolmerski, 2005; Hens et al., 2007). Before puberty, the growth of the mammary tree is algometric. Terminal end buds (TEBs) are formed by the tips of ducts that are responsible for invading mammary stroma and causing elongation of the milk ducts (Hinck and Silberstein, 2005). TEBs consist of two different cells type; an outer layer of cap cells and a bulk of cells at the duct tips. When estrogen levels increase in the serum during puberty, proliferation within TEBs causes ductal elongation. However, the surrounding fat and extra-cellular matrix (ECM) is involved in aiding tabular formation either physically or by secreting growth factors (Couldrey et al., 2002). In addition to elongation, cleft TEBs enhance splitting the ducts and forming the branches. It is suggested at this stage that apoptosis could be detected in TEB cells forming ductal lumens (Humphreys et al., 1996). Several factors regulate and control branching morphogenesis including hormones, growth factors, extra-cellular matrix (ECM), matrix metalloproteinase (MMPs) and immune cells (Kouros-Mehr et al., 2006; Sternlicht et al., 2006).

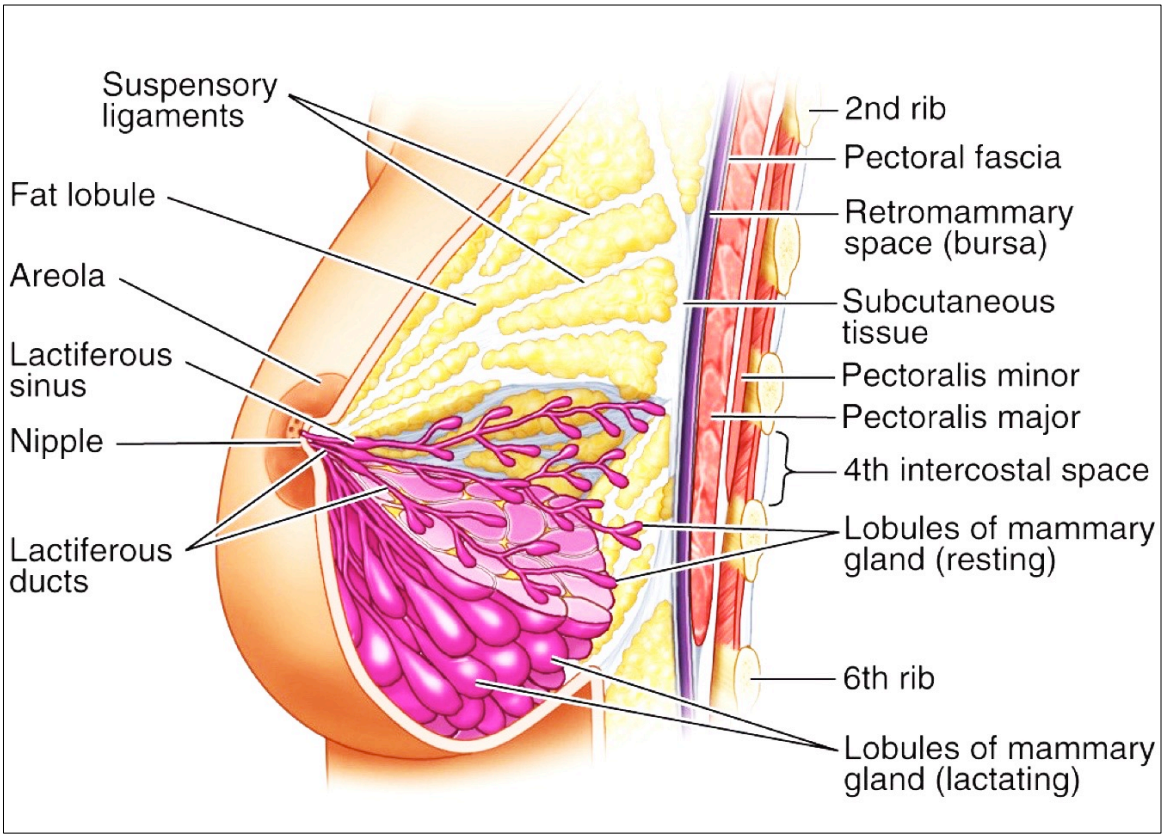

Figure 1-1:Anatomy of normal breast.

From the nipple long ducts terminate in alveoli networks called lobes. The ducts and alveoli penetrate the stroma and adipose tissue. The rib, as well as the muscle underlying the breast followed by loose connective tissue is also shown. Suspensory ligaments and the skin are indicated. Breast cancers most often arise in luminal epithelial cells lining the normal breast ducts and are called ductal carcinomas. (Ali and Coombes, 2002).

The mammary gland undergoes for further development unlike most other organs of the body during pregnancy and preparation for lactation (Figure 1-2) (Hassiotou and Geddes, 2013). At this stage, specialized cells are created for milk production and secretion (Hennighausen and Robinson, 2005; Topper, 2013). Progesterone stimulates the formation of alveolar and extensive branching, and in combination with prolactin promotes the differentiation of alveoli for future milk secretion (Watson and Khaled, 2008; Topper, 2013; Hassiotou and Geddes, 2013). Once the mother stops feeding the infant, the mammary gland returns to its original non-milk secreting state through the process of involution. The process of breast-feeding cessation induces apoptosis and the shedding of detached cells from the lumens (Sloane, 2012). As a result, matrix metalloproteinases (MMP) are activated, which break down the ECM around each alveolus resulting in alveolar collapse. Re-differentiation of adipocytes via plasmid and MMP3 activation complete the remodeling (Fata et al., 2003; Watson, 2006). During lifetime, normal mammary gland development undergoes many phases and processes including cell proliferation, migration and break down of the ECM (Lanigan et al., 2007). These processes are regulated by several soluble factors such as hormones and growth factors as well as ECM and stromal interactions (Wiseman and Werb, 2002). As a result, it is expected that dysregulation of any of these processes could lead to a pathophysiological outcome (Lanigan et al., 2007; Schedin and Keely, 2011). Specifically, the similarities between developmental processes and the characteristics of breast cancer have been studied, and it is currently the most commonly diagnosed female disease throughout the world (DeSantis et al., 2011; Eccles et al., 2013). Statistical surveys have estimated that around 550,000-570,000 females are diagnosed with breast cancer in the United Kingdom (Maddams et al., 2009). Thus, it is believed that understanding the molecular processes and molecular biology of breast cancer initiation and progression would be greatly beneficial and add to current research.

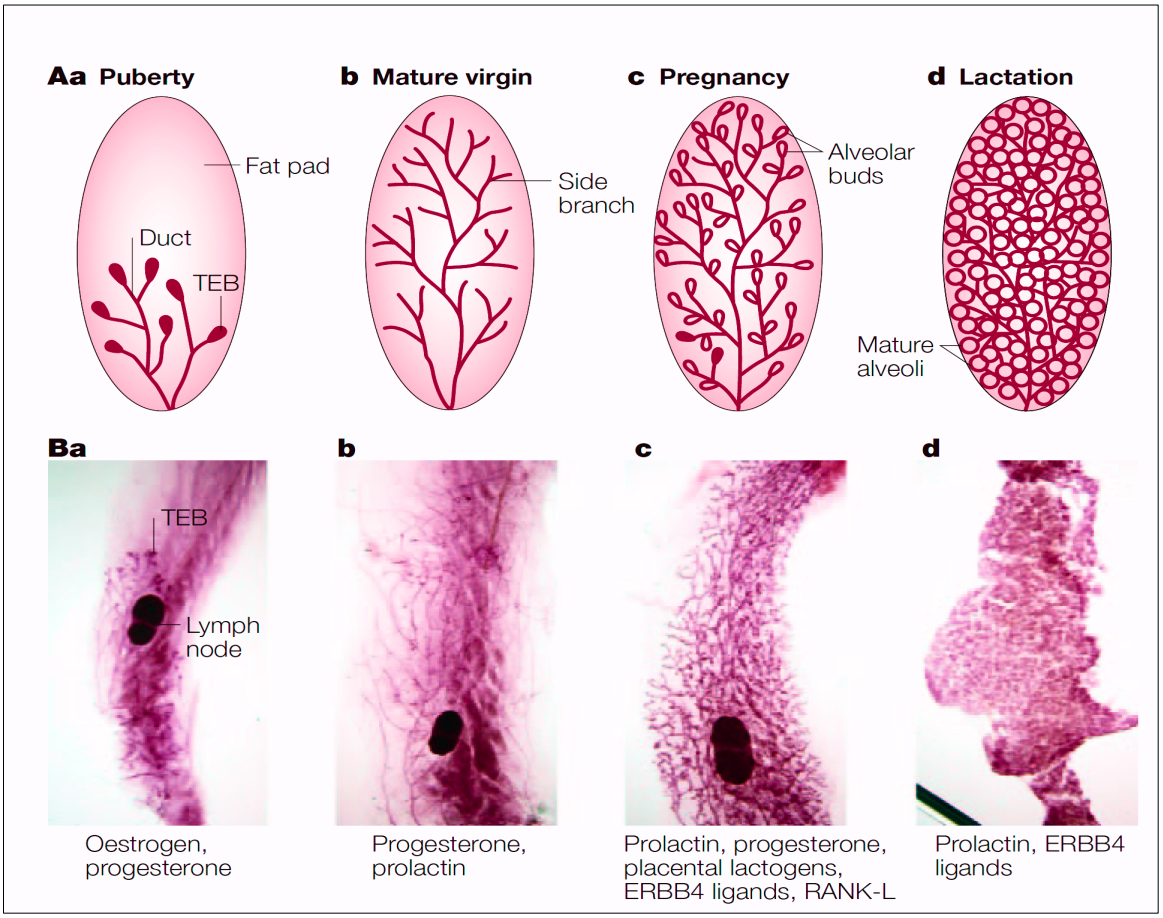

Figure 1-2: Mouse mammary gland development during puberty, mature virgin pregnancy and lactation.

Schematic (Aa–d) and wholemount (Ba–d) presentations of the different stages and the principal hormones that control development. A basic ductal design within the mammary fat pad is visible at birth, which grows at the same rate as the animal until the onset of puberty. (Aa, Ba). The cyclical production of ovarian oestrogen and progesterone during puberty promotes and accelerates ductal outgrowth. The highest level of cell division occurs in the stage of puberty where the structure of end buds (TEBs) are formed. (Ab, Bb) in the mature virgin stage, the entire fat pad is filled with primary and secondary ducts so the branches begin to form and disappear in each oestrous cycle. (Ac, Bc) During pregnancy, the secretion of prolactin, placental lactogens and progesterone increase cell proliferation and the formation of alveolar buds. (Ad, Bd) Alveoli are fully matured and the luminal cells synthesize and secrete milk components into the lumina in preparation for lactation. (Hennighausen and Robinson, 2005).

1.3 Biology of breast cancer

Breast cancer is the most frequently diagnosed cancer in women over the world and the fifth most common cause of malignancy associated death (Götte and Yip, 2006; Hutchinson, 2010; Richard et al., 2014). Breast cancer is found in breast sites and it is more common in females than males (Richard et al., 2014). 50,000 cases in females are recorded yearly in the UK alone. Every year, 458,000 people die from breast cancer over the world making it the most common cause of female cancer death in both the developed and developing world (Eccles et al., 2013). In the UK, the age-standardised incidence of breast cancer in women has increased by 6% over the last decade, between 1999 to 2001 and 2008 to 2010 (Ferlay et al., 2010). Based on current projection it is expected that the number of women who are diagnosed with breast cancer will increase three-fold by 2040 (Maddams et al., 2012). Recently, breast cancer research indicated that the annual cost of breast cancer healthcare has increased by over a third compared to the last 10 years (Eccles et al., 2013).

Breast cancer is a condition in which normal cellular regulation ceases to function and cells in the breast are allowed to proliferate unchecked, abnormally and then escape the DNA repair mechanisms (Helzlsouer et al., 1996; Hanahan and Weinberg, 2000; Culver et al., 2003; Hanahan and Weinberg, 2011). Breast cancer is considered as a heterogeneous group of diseases caused by both non-genetic and genetic factors that vary in morphology, biology and behaviour rather than a single disease (Vargo-Gogola and Rosen, 2007; Rakha and Ellis, 2009; Polyak, 2011). Most breast cancers are considered adenocarcinomas and arise from epithelial cells and other types constitute less than 5% of the total (Elenbaas et al., 2001; Dimri et al., 2005; Kumar et al., 2005). Moreover, most breast cancers arise form terminal ductal–lobular units (TDLUs) (Dimri et al., 2005). Figure 1-3 describes briefly the biology of breast cancer.

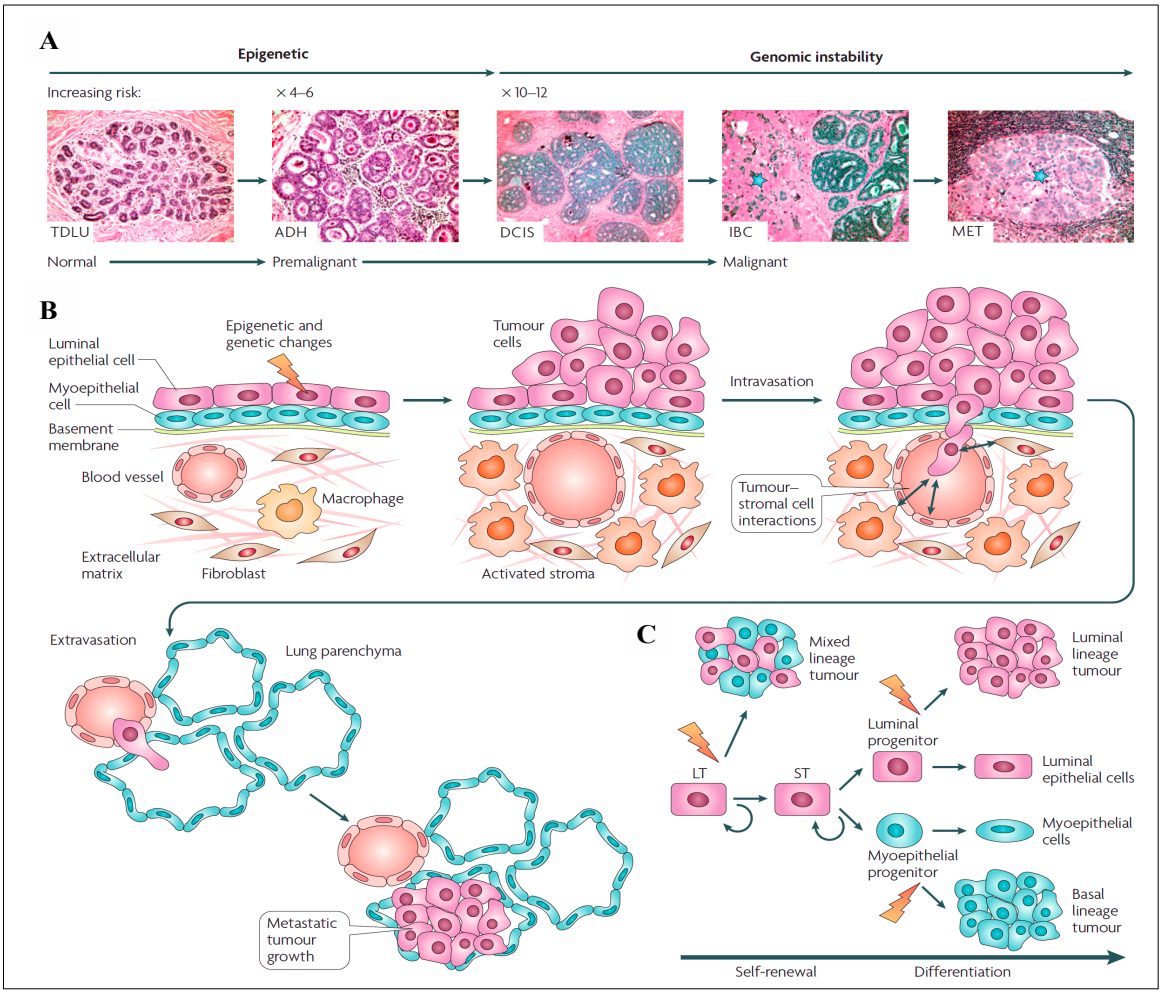

Figure 1-3: The biology of breast cancer.

(A) Breast cancer is a heterogeneous disease. The terminal ductal lobular unit (TDLU) of normal breast contains lobules and ducts, which consist of a bi-layered epithelium of luminal and myoepithelial cells. Atypical ductal hyperplasia (ADH) is a premalignant growth characterized by abnormal cell layers within the duct or lobule. ADH is classified as precursor of ductal carcinoma *in situ* (DCIS), which is a non-invasive lesion that contains abnormal cells. The risk of developing malignant or invasive breast cancer (IBC) increases with each stage. Ductal carcinoma in situ (DCIS) may develop into IBC (indicated by a blue star adjacent to a DCIS lesion), but it is unclear how to predict which lesions will progress. The primary site for breast cancer metastasis (MET; indicated by a blue star) is the lymph nodes. (B) A schematic of breast cancer progression is shown. The transformation of breast epithelial cells to breast cancer is controlled by an amalgamation of epigenetic and genetic changes and aberrant interactions within the microenvironment. The process of transformation itself is controlled by proliferation, survival, differentiation and migration advancing into deregulated, and aberrant tumour–stromal cell interactions. When the cells invade the basement membrane, they enter the vasculature (intravasate), survive in the absence of adhesion, exit the vasculature (extravasate) and establish a new tumour in a foreign microenvironment. Thus they become metastatic. (C) There are several links between normal breast stem or progenitor cells and cancer cells, such as dormancy, self-renewal and differentiation capabilities, that have lead researchers to propose that cancer cells with stem cell-like characteristics (called 'cancer stem cells' or 'tumour-initiating cells', which is a more appropriate designation), drive breast cancer initiation, progression and recurrence. This hypothesis is depicted as epigenetic and genetic alterations that occur in different stem or progenitor cells, including the long term (LT), short term (ST) and luminal or basal (myoepithelial) progenitors, and give rise to different subtypes of tumours that consist of different cell types (mixed, luminal or basal lineage), which display characteristic gene-expression profiles and exhibit distinct prognoses. (Vargo-Gogola and Rosen, 2007).

Several genetic mutations have been identified in human breast cancer, yet the exact mechanisms and events that are responsible for the transformation of normal cells and tumour formation remain unclear (Elenbaas et al., 2001; Dimri et al., 2005). However, it is well known that breast tumour formation is linked to intrinsic factors such as genetics, mutations and genomic instability in a number of genes that promote breast cancer progression (Elenbaas et al., 2001; Vollebergh et al., 2012). The most significant genes that are involved in breast cancer are the breast cancer susceptibility genes (BRCA1 and BRCA2) in high-risk families. It has been noticed that only 10 % of all breast cancer cases are caused by the lack of a tumour suppressor gene, as opposed to the gain of an oncogene (Laakso et al., 2005; Ligresti et al., 2008). BRCA1 and BRCA2 are responsible for 80-90% of breast cancer cases. These genes are rarely mutated in irregular forms, suggesting they play a pathogenetic role in the promotion of carcinogenesis (Welcsh and King, 2001; Ligresti et al., 2008).

Moreover, loss of function of p53 and phosphatase and tensin homolog (PTEN) genes are associated with aggressive breast cancer phenotypes (Elenbaas et al., 2001; Cheah and Looi, 2001; Lane, 2004). PTEN and p53 are both tumour suppresser genes (Ligresti et al., 2008). p53 is a transcriptional factor involved in cell cycle regulation and DNA repair. Dysregulation of p53 production in the cell cycle will allow cells to proliferate unchecked and as a result, inhibit apoptosis (Monti et al., 2007). PTEN is a tumour suppressor gene that is located at human chromosome 10q23. PTEN has a crucial role in cell proliferation, the cell cycle and the apoptosis of cancer cells (Li et al., 2007).

Additional genes that are commonly thought to play a role in tumour information include HER-2/neu and PI3K (Ligresti et al., 2008). Human epidermal growth factor receptor 2 (HER-2/neu) is a member of the oncogene family and it is related to the epidermal growth factor receptor (EGFR) although it has a unique form (Zhang and Liu, 2008). It has been

confirmed that this oncogene has a role in human breast cancer cell line progression, and many studies indicate a close correlation between its expression and prognosis in breast cancer (Zhang and Liu, 2008; Revillion et al., 2008). The phosphoinositide-3-kinase (PI3K) gene consists of an 85-kDa regulatory subunit that contains two domains; SH2 and SH3 and a 110-kDa catalytic subunit. PI3K has a critical role in oncogenic transformation and control of cellular proliferation (Chang et al., 2003a; Chang et al., 2003b; Lai et al., 2008).

There are two main hypotheses that have been proposed to explain the cellular nature of breast cancer formation (Molyneux et al., 2007). The first hypothesis suggests that all cells within a tumour have equal potential to be tumourigenic. So, it is believed that in response to outside signals or treatment, spontaneous mutations occur within normal breast cell populations leading to the formation of tumour cells. However, it has been suggested recently that the formation of a tumour has been linked to tumour initiating cells or cancer stem cells. It is proposed that breast cells are heterogeneous to begin with and therefore have a high potential for tumourigenesis (Reya et al., 2001; Molyneux et al., 2007). Since during pregnancy the normal mammary gland undergoes different stages of proliferation, differentiation and involution, it is believed that their growth is sustained with the aid of mammary epithelial stem cells. Interestingly, it is has been reported that females who are pregnant at a young age are less likely to develop breast cancer cells (Gabriel and Domchek, 2010). Under the given conditions, cancer stem cells enhance the differentiation and tumour growth of non-tumourgenic cells, in turn affecting normal tissue development (Molyneux et al., 2007). Consequently, it has been proposed that the eradication of cancer stem cells fails using conventional breast cancer therapies.

Based on the mentioned above theory regarding the origin of breast cancer, it has been suggested that breast cancer stem cells are formed by epithelial-mesenchymal transition

(EMT). This is because cells that underwent EMT have been shown to have similar features, characteristics and behaviours to normal and neoplastic cells (Thiery and Sleeman, 2006; Mani et al., 2008). It has been also reported that the induction of EMT in normal epithelial cells of the mammary gland can produce cell populations with similar characteristics to stem cells (Morel et al., 2008). The alternative theory suggested that cancer stem cells are formed by deregulation, self-renewal and differentiation of normal stem cells. The evidence of this theory is based on the similarity between normal and cancer stem cells in the level of features and biochemical characteristics (Dontu et al., 2003). In addition, since normal stem cells have long lifespans, this might increase their potential to gain mutations and oncogenic transformation (Ponti et al., 2005; Velasco-Velázquez et al., 2012). A study by Al-Hajj et al. (2003) suggested that breast cancer stem cells originate from basal mammary stem/progenitor cells based on the surface protein expression profiles of the two cell types (Al-Hajj et al., 2003). The theories about the origin of cancer stem cells are not considered exclusive. Recently, it has been suggested that normal and malignant breast cancer stem cells exist in inter-convertible states of EMT and mesenchymal-epithelial transition MET under the regulation of micro-RNAs (Liu et al., 2012). In this context, different states of breast cancer stem cells and their various differentiation states give rise to breast cancer heterogeneity and different tumour subtypes.

1.4 Breast cancer classification

Since breast cancer is considered both a genetically and clinically heterogeneous disorder, a classification system for breast cancer types has been established (Wen et al., 2015). It is believed that these classification schemes would assist the biologist in diagnosis, treatment and prognosis (Stingl and Caldas 2007; Malhotra et al., 2010; Viale, 2012). Breast cancer is classified based on histological level, molecular level, staging of cancer

and the function of cancer (Bauer et al., 2007; Eroles et al., 2012). However, histological and molecular classifications are the most common classification and they have been used widely in clinical settings (Malhotra et al., 2010).

1.4.1 Histological classifications of breast cancer subtypes

Breast cancer can be classified histologically into two main types; non-invasive or ductal carcinoma in situ (DCIS) and invasive ductal carcinoma (IDCs) (Viale, 2012; Wen et al., 2015). Ductal carcinoma in situ (DCIS) is an early form of breast cancer and it is developed within the milk ducts (Malhotra et al., 2010; Viale, 2012). This type of cancer does not invade the basement membrane and is thus confined within the terminal in-situ cancers. Ductal carcinoma in situ (DCIS) is classified into lobular carcinoma in-situ and ductal carcinoma in-situ (Fabbri et al., 2008). In contrast, invasive breast cancer often has the potential to invade the basement membrane (Andersson, 2005). In addition to this, there are two main types of invasive breast cancer; invasive lobular and ductal carcinoma (Pestalozzi et al., 2008). The main difference between in-situ and invasive cancers is the ability of the invasive forms to spread through the lymphatic and vascular vessels located under the basement membrane leading to regional lymphatic and distant organ metastases (Bauer et al., 2007; Eroles et al., 2012; Viale, 2012). DCIS has traditionally been further subclassified based on the architectural features of the tumour, which has given rise to five well recognized subtypes; Comedo, Cribiform, Micropapillary, Papillary and Solid (Figure 1-4) (Malhotra et al., 2010).

1.4.2 Molecular classifications of breast cancer subtypes

Breast cancer can be also classified into five subtypes distinguished by different gene and protein expressions at the molecular level (Polyak, 2011) (Figure 1-5). Two hormone-receptor positive subtypes are luminal A and luminal B, and three hormone-receptor

negative subtypes include human epidermal growth factor receptor-2 (HER-2$^-$), basal-like and normal breast-like (Weigelt et al., 2010; Elias, 2010; Reddy, 2011; Shastry and Yardley, 2013). However, each of these subtypes has its own risk factors for breast cancer incidence, preferential organ sites of metastases, risk of disease progression and response to treatment. For example, luminal tumours are positive for oestrogen receptors (ER$^+$) and progesterone receptors (PR$^+$) therefore the majority respond to hormonal interventions. However, HER-2$^+$ tumours have amplification and overexpression of the ErbB2; the member of oncogene family and it is related to the epidermal growth factor receptor (EGFR) and has been effectively controlled by anti-HER-2 therapies (Wen et al., 2015). General basal-like tumours lack hormone receptors and HER-2 so the majority of these tumours are also called triple-negative breast cancer (TNBC) (Greenwood et al., 2011; Wen et al., 2015). The molecular subtypes of breast cancer have been associated with tumour progression and thus have been widely used in clinical settings to predict cancer prognoses and guide treatment options (Weigelt et al., 2010; Elias, 2010).

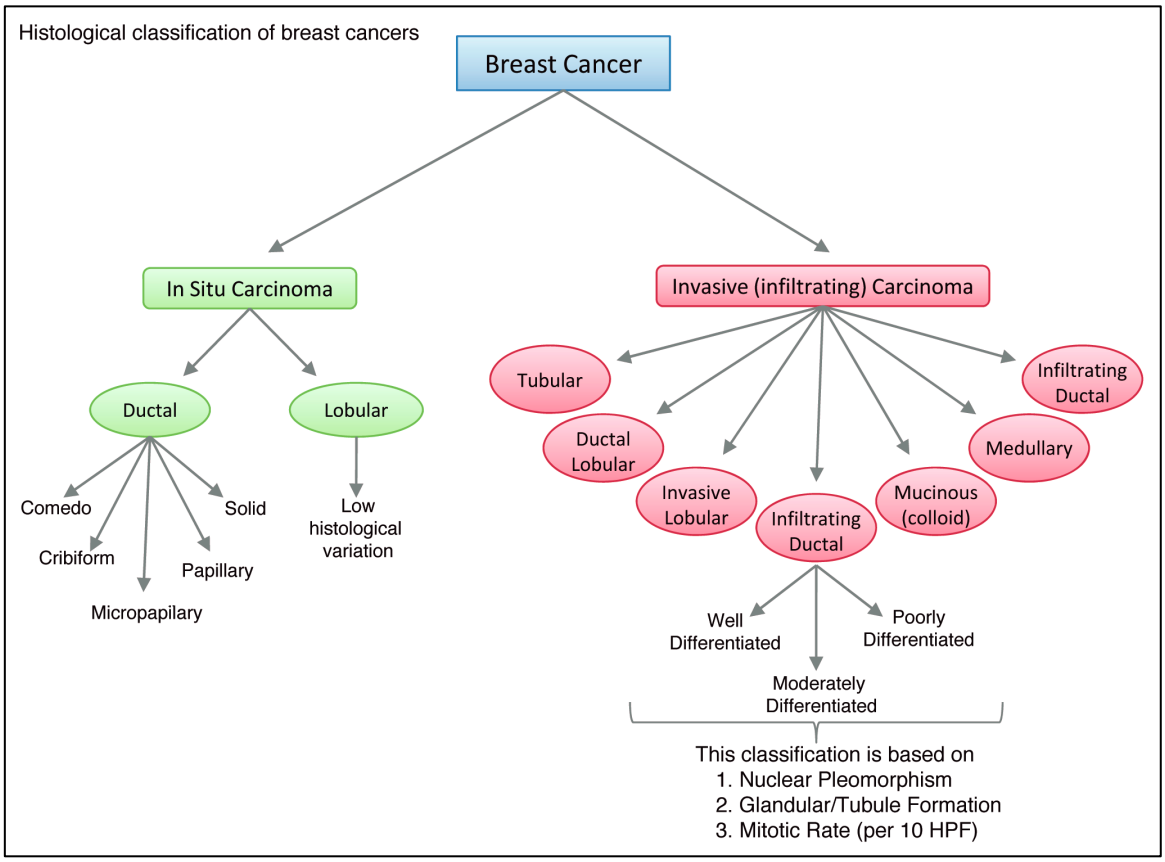

Figure 1-4: Histological classification of breast cancer subtypes.

This scheme, currently used by clinicians, categorizes the heterogeneity found in breast cancer based on architectural features and growth patterns. HPF: high power field. (Malhotra et al., 2010).

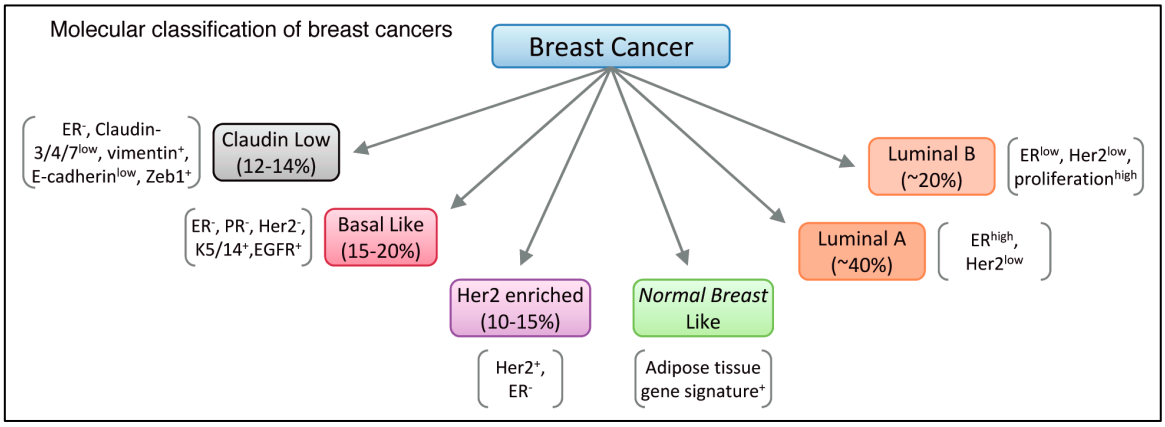

Figure 1-5:Molecular classification of breast cancer.

This classification is based on the intrinsic molecular subtypes of breast cancer identified by microarray analysis of patient tumour specimens. (Malhotra et al., 2010).

1.5 Models of human breast cancer

Breast cancer cell lines have been used widely in research as a model to investigate their morphology, structure, features and characteristics including proliferation, apoptosis and migration during the breast cancer progression (Carlsson et al., 2007; Vargo-Gogola and Rosen, 2007; Holliday and Speirs, 2011). The use of these cell lines has allowed much information to be obtained regarding the genetic and molecular mechanisms of various signalling pathways (Vargo-Gogola and Rosen, 2007). Breast cancer cell lines share many of the genetic and genomic features of human breast cancers, including representing several breast cancer subtypes. There is also evidence that gene-expression profiles of primary tumours and their metastatic counterparts are not markedly different (Lacroix and Leclercq, 2004). However, most breast cancer cell lines are obtained from advanced tumours so may represent the most malignant variants that could be adapted to culture (Charafe-Jauffret et al., 2006).

1.5.1 CAMA-1

The CAMA-1 cell line is classified as luminal-type human breast cancer cells that have a rounded morphology in adherent tissue culture. CAMA-1 cells were isolated from mammary gland/breast, and derived from metastatic pleural effusion. They are weakly invasive. These cells are considered negative for human epidermal growth factor receptor ($HER\text{-}2^{-}$) but positive for estrogen receptors (ER^{+}) and progesterone receptors (PR^{+}) ($ER^{+}/PR^{+}/$ $HER\text{-}2^{-}$). They are responsive to estrogen and sensitive to growth inhibition by tamoxifen. CAMA-1 cells have an in-frame mutation in the E-cadherin gene, resulting in a truncated, non-functional protein. In addition, they have oncogenic mutations in PTEN and p53 as well as amplification of the cyclin D1; the protein coding gene (Wang et al., 2007; Kenny et al., 2007).

1.5.2 MDA-MB-231

The MDA-MB-231 cell line is classified as a triple negative breast cancer cell line since it is negative for estrogen receptors (ER^-), progesterone receptors (PR^-), and human epidermal growth factor receptor ($HER\text{-}2^-$) (ER^-, PR^-, $HER\text{-}2^-$)(Liu et al., 2003). These cells are derived from a metastatic adenocarcinoma of the mammary gland of a 51-year-old Caucasian woman, according to the data sheet of the American Type Culture Collection (ATCC). This adherent epithelial cell line likely contains more than one cell population and is a highly aggressive, invasive and poorly differentiated human breast cancer cell line. Similar to other invasive cancer cell lines, the MDA-MB-231 cells display invasiveness by mediating the proteolytic degradation of the extracellular matrix (ECM), including the basement membrane and several mechanical barriers to the ECM, through the increased expression of matrix metalloproteinases (MMPs), including gelatinases, en route to their destinations (Yin, 2011).

1.5.3 MDA-MB-435

In the past, as shown by a paper authored by Rae JM has been argued that MDA-MB-435 cells are derived from M14 melanoma cells, results showed that MDA-MB-435 and M14 melanoma cell lines were identical in respect of gene expression patterns, cytogenic characteristics and other minor differences which they explained to be caused by phenotypic and clonal drifts (Creighton et al., 2007). However, another study released two years later revealed a contradictory view, in which despite the subsequent expression arrays studies and gene expression profile studies, MDA-MB-435 cells are indeed from metastatic breast cancer origin, the alternate conclusion was drawn from the explanation that many cell lines can display “lineage infidelity” and that it would be unreliable to conclude that MDA-MB-435 cells are derived from M14 cell lines, based on expression patterns (Chambers, 2009). Therefore it can be safely assume that MDA-MB-435 cells

used in this experiment are derived from metastatic breast cancer origin and several researches still used as model for human breast cancer (Prasad and Gopalan, 2015).

The MDA-MB-435 cell line was derived in the late 1970s from the pleural effusion of a female patient with breast cancer, and has been shown to be highly metastatic in nude mice (Cailleau et al., 1978; Chambers, 2009). This cell line has been used for a large number of studies on the biology and molecular biology of breast cancer. These cells are considered positive for human epidermal growth factor receptor (HER-2^{+}) but negative for estrogen receptors (ER^{-}) and progesterone receptors (PR^{-}) (ER^{-}/PR^{-}/ HER-2^{+}) (Holliday and Speirs, 2011).

Breast cancer and breast cancer cell lines are considered highly tumourigenic since the investigation has shown that patients who suffer from the breast cancer have pre-existent immune responses, both humoral and cellular, against a variety of proteins expressed in their tumours (Disis, 2002). In addition, it has been shown that tumour cells are uniquely able to utilize the immune cells and the tumour microenvironment leading to initial propagation of carcinogenesis (Zamarron and Chen, 2011). In this respect, understanding the immune system and its role against tumour initiation would provide a better understanding of tumour cell survival.

1.6 Immune system

The immune system is divided into two main parts known as innate and adaptive (acquired) response systems. They are determined by speed, memory and specificity of the reaction, even though in practice there is much association between them (Crotzer and Blum, 2010). The physical, chemical and microbiological barriers are usually referred to as innate immunity. However, specifically innate immunity consists of the basic elements of the immune system (neutrophils, monocytes, macrophages, complements, cytokines

and acute phase proteins), which present instant host defence and protection against pathogens. Innate response is termed as the nature of the response since it can be seen even in the simplest animals thus it corroborates its crucial role in survival. In contrast, adaptive immunity is considered as the hallmark of the immune system of higher animals including human beings. The adaptive response consists of T-lymphocytes and B-lymphocytes, which are produced via antigen specific reactions. The innate immunity is quick to respond however; it can cause damage to normal cells and tissues due to the lack of specificity. On the other hand, adaptive immunity takes several days or even weeks to show a response but it is highly specific and precise. Moreover, the adaptive immunity is highly distinct because it has memory cells and as a result, subsequent exposure leads to more various and rapid responses even though it is not immediate (Parkin and Cohen, 2001; Abbas and Lichthman, 2005; Whiteside, 2006).

1.6.1 Immune system and breast cancer

The interaction between tumour cells and the immune system is complex and its mechanism for the protection of the human body is not yet clear (Goldsby et al., 2003; Thibodeau et al., 2012). The complexity of the tumour increases immunodeficiency and therefore increases the level of tumourigenicity in tumour cells (Poschke et al., 2011). In addition, it has been reported that many tumours downregulate the expression of major histocompatibility complex (MHC) molecules suggesting a significant role of the immune system in controlling and evaluating the progression of tumours cells (Poschke et al., 2011; Thibodeau et al., 2012). Consequently, solid tumours, stromal cells and neighboring tissues are often infiltrated by a vast array of immune cells (Bindea et al., 2011).

T cells are the key cells of adaptive immune responses for tumour immunosurveillance. The recognition of antigens on tumour cells by T cell receptors (TCR) activates $CD8^+$ T cells to cytotoxic cells (CTL) that can kill the tumour cell target (Igney and Krammer, 2002; Grivennikov et al., 2010; Thibodeau et al., 2012). The activation of $CD8^+$ T cells is achieved by one subset of $CD4^+$ T cells, which is known as T helper cells type 1 (Th1) (Swann and Smyth, 2007; Gajewski et al., 2013). Th2 cells (the second subset of $CD4^+$ T cells) are involved in the stimulation of hormonal responses and suppression of the development of Th1 responses. Interestingly, in the same manner to $CD8^+$, $CD4^+$ cells can also show cytotoxic activity once it is required (Standish et al., 2008). The recognition of antigens as peptides by $CD8^+$ and $CD4^+$ tumour cells is presented via major MCH class I class II molecules respectively (Igney and Krammer, 2002).

T cells can recognize a number of tumour antigens that have been identified in several solid tumours (Igney and Krammer, 2002; Grivennikov et al., 2010; Coulie et al., 2014). The antigens that are expressed exclusively by tumours are known as tumour specific antigens (Thibodeau et al., 2012). These antigens arise from mutations or translocation of normal cellular genes such as cyclin-dependent kinase-4 (CDK-4), and these mutations may involve directly in carcinogenesis. In contrast, the antigens that are expressed by tumour cells are known as tumour-associated antigens. Additionally, overexpression of mutated proteins such p53 and HER-2/neu may serve as tumour antigens for T cells (Igney and Krammer, 2002). Tumour-infiltrating lymphocytes that are reactive against differentiation antigens present on normal melanocytes as well as melanomas have also been identified (e.g., MART-1/Melan-A, tyrosinase, gp100) (Lee and Margolin, 2012; Lee et al., 2012). Moreover, antigens from tumourigenic viruses can be expressed on tumour cells. The expression of tumour antigens may be heterogeneous within the tumour

so the patient can develop an immune response to multiple antigens (Wortzel et al., 1983; Lee et al., 1999; Igney and Krammer, 2002).

Natural Killer (NK) cells are the main component of the innate immune system, and also play a significant role in the immunosurveillance of tumours (Igney and Krammer, 2002; Gajewski et al., 2013). The main role of NK cells is to kill MHC class I-deficient cells, a phenomen leading to the "missing self" hypothesis. The activity of NK cells is controlled by a number of events and different signalling pathways (Igney and Krammer, 2002; Vesely et al., 2011). MHC class molecules block signalling activity through engagement with specific inhibitory receptors. There are two families of inhibitory receptors that have been identified in humans known as the immunoglobulin-like killer cell inhibitory receptors and the lectin-like CD94-NKG2 receptors. Stimulatory receptors including CD16, CD94-NKG2 and natural cytotoxicity receptors bind to fundamentally expressed ligands and NKG2d receptors, which bind to induced molecules by cellular stress (Boyton and Altmann, 2007; Moretta et al., 2009). In humans, the MHC class I chain related (MIC) glycoproteins MICA and MICB are the ligands for NKG2d receptors. Macrophages and neutrophils are additional cells of the innate immune system that are involved in immune responses against tumours (Nowarski et al., 2013). These cells are responsible for killing tumour cells directly through the destruction of tumour cells and vessels and by inhibition of angiogenesis (Igney and Krammer, 2002; Nowarski et al., 2013). They also present tumour antigens and enhance other immune cells such as CTL, NK cells and APCs (Maruyama et al., 2011). In contrast, the role of inflammatory cells is to increase progression by production of tumour growth factors and stimulation of angiogenesis. Macrophages and neutrophils are recruited to the tumour site by expression of adhesion molecules on endothelial cells and by chemotactic proteins (Igney and Krammer, 2002; Vesely et al., 2011).

Two different mechanisms have been proposed to protect the human body against tumours by the immune system. These mechanisms are known as the concept of immunosurveillance (cancer immunoediting) and the danger model (Möller and Möller, 1976; Igney and Krammer, 2002). In 1994, Polly Matzinger presented a new theory called the danger model suggesting that specific immune response develops as a result of danger detection rather than discrimination between self and non-self antigens (Matzinger, 1994; Kowalczyk, 2002). Although this model refers mainly to immune tolerance its assumptions are valid for such distant subjects as tumors or apparently unrelated with immunology gene therapy. The danger model mechanism proposes that tumour cells do not seem to be dangerous to the immune system so the presence and response of T cells to tumours is not initiated. Because danger model suggests that the immune system may be concerned with the detection of damaged cells rather than recognition of non-self (Matzinger, 2001, 2002), cancer immunoediting theory will be discussed in more detail.

1.6.2 Cancer immunoediting

In 1957, Burnet and Thomas hypothesised that the immune system is capable of recognising and destroying or eliminating nascent transformed cells in cancer immunosurveillance (Burnet, 1957; Dunn et al., 2002, 2004; Urosevic and Dummer, 2008). The concept of immunosurveillance was based on evidence that the adaptive response was responsible for protecting the immunocompetent host through preventing cancer development. However, the hypothesis of immunosurveillance was poorly supported by Stutman's studies (Dunn et al., 2004; Schreiber et al., 2011). By the 1990s, some studies rekindled the concept of immunosurveillance by discovering the importance of interferon-gamma (IFN-γ) in promoting immunologically induced rejection of transplanted tumour cells and also by demonstrating that mice lack either IFN-γ or adaptive immunity, T cells, B cells and NK cells. These studies were carried out in order

to reassess the role of immunity in cancer control (Schreiber et al., 2011). However, a major revision was made in the immunosurveillance hypothesis in 2001 when it was discovered that the immune system is not only responsible for controlling the tumour quantity but also tumour quality (immunogenicity). This study demonstrated that tumours formed in mice that lacked an intact immune system were highly immunogenic and classified as "unedited" compared to tumours that were derived from immunocompetent mice and were termed "edited". Therefore, the hypothesis of immunosurveillance was replaced with cancer immunoediting, which stresses the protective, and tumour promoting actions of immunity for the host, in developing tumours (Dunn et al., 2004; Schreiber et al., 2011). The process of cancer immunoediting consists of three main phases: elimination (also known as immunosurveillance), equilibrium and escape. Specifically, the elimination phase is divided into four phases (phases 1-4) with each phase having a critical role. Therefore, it is believed that a full understanding of cancer immunoediting and immunosurveillance will hopefully stimulate the development of effective immunotherapeutic approaches to eliminate or at least control human cancer (Dunn et al., 2002, 2004; Schreiber et al., 2011). The three phases of cancer immunoediting process are illustrated in (Figure 1-6).

The cells and molecules of innate and adaptive immune responses to tumour cells have the potential to eradicate the developing tumour and protect the host from tumour formation, through the process of elimination. However, the tumour cells may also go through the equilibrium phase if the elimination phase is not completely successful. In the equilibrium phase, tumour cells may be either maintained chronically or immunologically, sculpted by the immune editor to produce a new population of tumour variants. These variants may eventually evade the immune system through a variety of mechanisms and become clinically detectable in the escape phase. Several cells are

involved in cancer immunoediting, such as NK cells, NK T cells, macrophages, together with molecules like IFN-γ and TNF-α. Therefore, it is believed that studying the mechanism of action of one of the aforementioned molecules might enable scientists to design an appropriate drug for treating cancer at least in the level of *in vitro* (Dunn et al., 2002, 2004; Schreiber et al., 2011; DuPage et al., 2012; Matsushita et al., 2012).

A number of molecules are involved in cancer immunoediting; CD74, a cell-surface molecule, is believed to enable tumours to escape immune system (Chao et al., 2012). It has also been suggested that high levels of CD74 expression is associated with class II MHC expression and might prevent tumour antigen presentation by blocking the peptide-binding cleft, thus leading to a lack of recognition of tumour cells by immune cells (Beswick and Reyes, 2009; Borghese and Clanchy, 2011; Zheng et al., 2012). Several studies have shown that upregulation of CD74 expression in human cancers also appears to influence tumour growth and dissemination suggesting that CD74 may have a role in escaping the equilibrium phase of cancer immunoediting (Chao et al., 2012).

Current biomarkers cannot accurately target all breast cancer subtypes, so further research is required to discover new tumour antigens. This study will be emphasising the importance of CD74, MIF and CD44 potential as biomarkers. CD74 and CD44 along with MIF have been previously shown to be co-expressed in metastatic prostate cancer cell lines LNcap and DU-145. CD74 serves as a cell-surface receptor for MIF in association with CD44, which when bound to the encoded protein initiates cell survival signalling pathways through extracellular signal-regulated kinase (ERK1 and ERK2) activation. Furthermore, both LNcap and DU-145 had increased gene MIF overexpression in comparison to normal and benign prostate human cells (Meyer-Siegler et al., 2006).

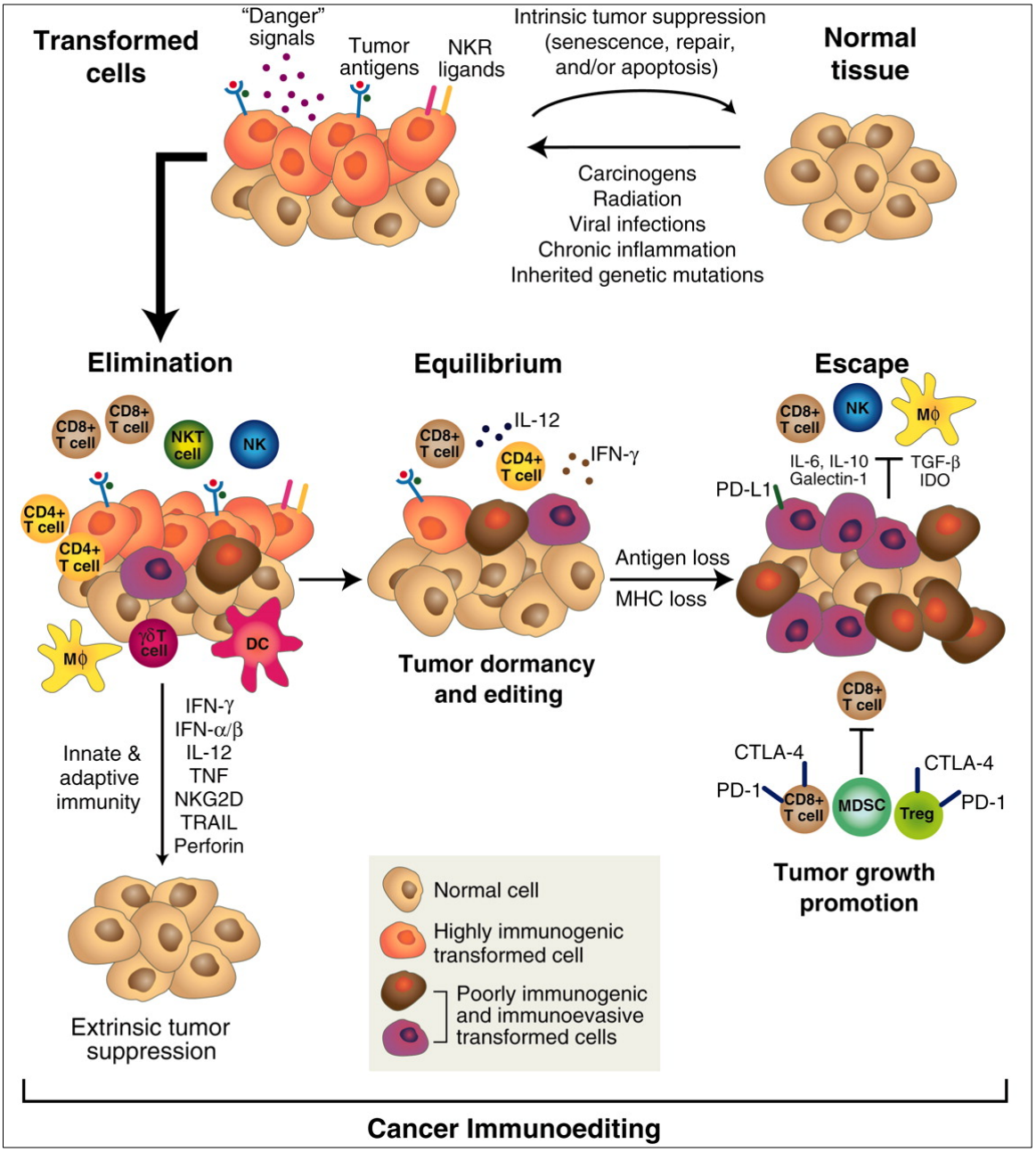

Figure 1-6:The phases of cancer immunoediting process.

Cancer immunoediting is an extrinsic tumour suppressor mechanism that engages only after cellular transformation has occurred and an intrinsic tumour suppressor has failed. Cancer immunoediting consists of three phases: elimination, equilibrium and escape. Innate and adaptive immunity are included in the elimination phase in order to destroy developing tumours before they appear clinically. However, the tumour cells may also go through the equilibrium phase if the elimination phase is not completely successful. In the equilibrium phase, tumour cells may be either maintained chronically or immunologically, sculpted by the immune editor to produce a new population of tumour variants. These variants may eventually evade the immune system by a variety of mechanisms and become clinically detectable in the escape phase (Dunn et al., 2004).

1.7 Cluster of differentiation 74 (CD74)

In humans, the gene that encodes the CD74 or invariant chain (Ii) molecule is found on chromosome 5 whereas in mice, the gene is located on chromosome 18 (Yamamoto, 1985). Jones and his colleagues were the first to recognize the Ii protein in 1979, specifically when the MHC class α chain and Ii was separated in 2D-gels. In spite of this, in 1989 it was found that Ii has a crucial role in antigen presentation through influencing the expression and peptide loading of MHC class II molecules (Badve et al., 2002). In 1995, the name CD74 was given to Ii by 'Leukocyte Typing Workshop' (Landsverk et al., 2009). Cluster of differentiation (CD) 74, also known as invariant chain, Ii or MIF receptor, is classified as a type II transmembrane glycoprotein that is expressed on antigen presenting cells and has diverse immunological functions (Burton et al., 2004; Stein et al., 2007; Beswick and Reyes, 2009). CD74 is post-translationally glycosylated and exists in various isoforms. There are four isoforms of CD74 in human beings, P33, P35, P41 and P43. Through alternative splicing of the Ii transcript where the P41 isoform has an extra exon, (exon 6b) these isoforms can be distinguished. However, the most common isoform (P33) has a molecular weight of 33 kDa (Landsverk et al., 2009; Beswick and Reyes, 2009). The structure of CD74 (shown in Figure 1-7) consists of 30 NH_2- terminal, intracytoplasmic residues, a 26 amino acid hydrophobic transmembrane region and 244 amino acid extracytoplasmic domains containing two N-linked carbohydrate chains (Stein et al., 2007; Landsverk et al., 2009; Shachar and Haran 2011; Gil-Yarom et al., 2014). CD74 is synthesized on the rough endoplasmic reticulum in same manner as MHC class II molecules despite the genes of these molecules being located on different chromosomes (Badve et al., 2002).

The most well known function of CD74 is its ability to associate with MHC class II α and β chains, directing the transport of the αβIi complex to the endosome and lysosome (Pyrz

et al., 2010). Specifically, the role of CD74 in antigen presentation has been divided into three main functions. Firstly, CD74 acts as a chaperone that is responsible for stabilizing nascent human leukocyte antigen (HLA)-DR αβ-heterodimers by formation of a trimetric structure. Secondly, by means of various sorting and internalization signals in its N-terminal cytoplasmic tail, CD74 directs HLA-DR molecules to subcellular compartments. Thirdly, CD74 prevents loading of antigenic peptides into the groove of HLA-DR molecules outside endosomes/lysosomes through a stretch called CLIP (class II-associated invariant chain) (Moldenhauer et al., 1999). CD74 has begun to emerge as a more versatile molecule beyond its well-known function of regulating class II MHC trafficking. Several studies have revealed that cell-surface expression of CD74 is not always dependent on class II MHC (Wilson et al., 1993; Beswick and Reyes, 2009). In this context, CD74 has been suggested to function as a cytokine and bacterial receptor. CD74 has also been shown to be involved in signalling along with MIF and CD44 pathways as a survival receptor (Stein et al., 2007; Beswick and Reyes, 2009). CD74 was also demonstrated to be involved the maturation of B cells through a pathway involving NF-κB (Stein et al., 2007).

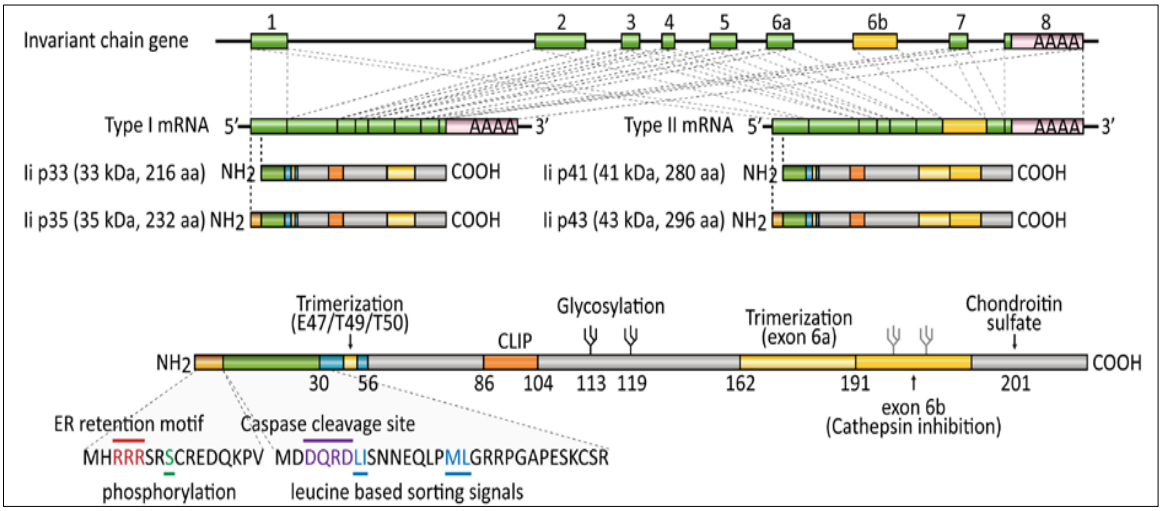

Figure 1-7: Schematic diagram of gene and protein structure of CD74.

The corresponding gene of CD74 consists of nine exons. The 33 kDa and 35 kDa forms of Ii, are both encoded by eight exons but they differ in 16 N-terminal residues as a result of alternative translation initiation. The 41 kDa isoform is encoded by nine exons generated by the alternative splicing of a common pre-mRNA. Theoretically, an additional 43-kDa form could be expected but is not yet unequivocally detected in immunoprecipitates from human cells. The additional exon 6b in Ii41 and Ii43 encodes a cysteine-rich stretch of 64 amino acids near the C-terminus that displays a striking homology to a repetitive sequence of thyroglobulin. (Strubin et al., 1986 and Gregers et al., 2003).

1.7.1 CD74 and the antigen presentation process

The MHC class II molecule is restrictedly expressed by a limited set of cells called professional antigen presenting cells (APCs), which include cells of the monocyte-macrophage lineage, dendritic cells (DCs) and B-lymphocytes, unlike MHC class I molecules which are ubiquitously expressed on all nucleated cells. The function of MHC class II is to present antigenic peptides from exogenous origin to a specialized T cell, $CD4^+$ in the presence of invariant chain (CD74). Hence, when CD74 is synthesized, it begins to associate with MHC class II (HLA-DR-α) and MHC class II (HLA-DR-β) within the endoplasmic reticulum (Burton et al., 2004; Stein et al., 2007; Landsverk et al., 2009; Neefjes et al., 2011). The association between these molecules is believed to take place in the rough endoplasmic reticulum through the sequential addition of DR α and β heterodimers to a trimeric core of CD74 molecules in order to from a nine-subunit complex with an equimolar amount of CD74–MHC class II. The resulting complex of CD74 and MHC class II is then gradually transported through Golgi apertures to the late endosomal compartment that is termed the MHC class II compartment (MIIC) either directly or within the plasma membrane. Here, CD74 is digested and cleaved into peptide fragments by endosomal/lysosomal proteases, leaving residual class II-associated Ii peptides (CLIP; amino acids 91-99) in the peptide-binding groove of the MHC class II heterodimer. In order to facilitate the exchange of CLIP fragments for specific peptides derived from a protein degraded in the endosomal pathway, MHC class II molecules require HLA-DM. By reaching this stage, MHC class II molecules are ready for transporting via the plasma membrane to present their peptides to $CD4^+$ cells (Burton et al., 2004; Stein et al., 2007; Landsverk et al., 2009; Beswick and Reyes, 2009; Neefjes et al., 2011).

1.7.2 The role of CD74 in breast cancer

The expression of CD74 has been found in several normal tissues, such as HLA class II-positive cells, including B cells, monocytes, macrophages, langerhans cells, dendritic cells, a subset of T activated cells and thymic epithelium. However, several studies have confirmed that CD74 is highly expressed in inflammatory disorders and several types of tumours (Stein et al., 2007; Beswick and Reyes, 2009). For example, 90% of B-cell cancers and the majority of cell lines derived from these cancers express CD74 in high levels compared to normal tissues (Stein et al., 2007). In particular, CD74 is expressed on different cancer cells, such as myeloma; prostate cancer cells, cancers of the gastrointestinal tract as well as breast cancer (Beswick and Reyes, 2009; Verjans et al., 2009). CD74 expression has also been shown to be correlated positively with gastric cancer stages (Zheng et al., 2012). Recently, CD74 has been classified as a new prognostic factor for patients with malignant pleural mesothelioma (Otterstrom et al., 2014). Moreover, Cheng et al. (2015) have also revealed that CD74 has a high potential in treating thyroid carcinoma.

Verjans et al (2009) have shown that breast cancer tissues and breast cancer cell lines overexpressed CD74. Interestingly, Leth-Larsen et al. (2009) observed that CD74 was present in tumour cells of 61% of ER^-/PR^- breast cancer biopsies but in only 33% of the ER^+/PR^+ biopsies. Greenwood et al. (2011) also revealed that triple negative breast cancer highly expressed signal transducer and activator of transcription (STAT-1) and CD74. Similarly, Tian et al. (2012) have shown that CD74 was negatively expressed in non-triple negative breast cancer while it is highly expressed on triple negative breast cancer and metastatic lymph nodes. Richard et al. (2014) showed that stromal CD74 expression significantly correlated with triple-negative receptor status and the absence of estrogen receptors. Recently, according to Yaprak et al. (2015) patients who suffer from breast

cancer with no CD74 expression had significantly better surgical outcomes than CD74-positive.To emphasize the role of CD74 in tumourigenicity and immunogenicity, the expression of CD74 has been assessed under proinflammatory and inflammatory conditions using interferon-gamma and lipopolysaccharide (Greenwood et al., 2011; Zheng et al., 2012). Since then CD74 has been identified as a potential novel target for breast cancer therapies as well as other types of cancer such as prostate, gastric cancer and thyroid carcinoma (Meyer-Siegler et al., 2006; Leth-Larsen et al., 2009; Verjans et al., 2009; Tian et al., 2012; Zheng et al., 2012; Richard et al., 2014; Cheng et al., 2015).

1.7.3 CD74 and interferon-gamma (IFN-γ)

In terms of proinflammatory cytokines, Möller and Moldenhauer (1999) have shown that the expression of CD74 can be induced using several types of cytokines such as IFN-γ, TNF-α and IL-4. Maubach et al. (2007) revealed that CD74 expression was upregulated when hepatic stellate cells (HSCs) were treated with IFN-γ for 30 hr. Martín-Ventura et al. (2009) demonstrated that the expression of CD74 increased after IFN-γ treatment in human aortic VSMCs and THP-1 cells. Moldenhauer et al. (1999) also showed that the expression of CD74, HLA-DR and HLA-A, B, C increased when colon carcinoma cell lines (HT-29 cells) were incubated with recombinant-IFN-γ (rIFN-γ). Similarly, Burton et al. (2010) revealed that cell-surface and cytoplasmic expression of CD74 was upregulated in acute myeloid leukaemia (AML) lines after IFN-γ exposure in AML patient specimens and cell lines. In the same manner, Greenwood et al. (2011) recently demonstrated that the expression of CD74 is upregulated in breast cancer cell lines. Their findings suggested that overexpression of CD74 using IFN-γ treatment increased adhesion of tumour cells (Greenwood et al., 2011). Interferon-gamma (IFN-γ) is a potent proinflammatory cytokine that has many critical roles including; promoting immune responses, immunopathological processes, cell maturation, differentiation, activation, and apoptosis

(Pestka et al., 1987; Platt and Hunt, 1998; Dranoff, 2004). INF- γ is a member of a family of proteins originally identified by their capacity to non-specifically protect cells from viral infections. IFN-γ is divided into two main classes on the basis of structural and functional criteria as well as the stimuli that induce their expression (Farrar and Schreiber, 1993; Ikeda et al., 2002; Schroder et al., 2004). It is know that IFN-γ plays a critical role in cancer and cancer progression by controlling apoptosis, cell proliferation, angiogenesis and the expression of MHC class I and II (Sikora and Smedley, 1983; Gooch et al., 2000; Brandacher et al., 2006; Zaidi and Merlino, 2011;). However, IFN-γ has another face that functions against the immune system, and increases the tumourigenicity of tumour cells (Zaidi and Merlino, 2011). There is now emerging evidence that IFN-γ may also be involved at the equilibrium and/or evasion stages, roles that may be more pro-tumourigenic. IFN-γ has been shown to upregulate the suppression of CTL- and NK cell-mediated immune responses, and is central to tumour immune escape (Brody et al., 2009). IFN-γ has also been suggested to enable tumours to escape innate immune system surveillance and influence tumour growth and dissemination by induction of CD74 (Greenwood et al., 2011; Chao et al., 2012).

IFN-γ is a pleiotropic cytokine involved in aspects of immune regulation including transcription. Upon engagement of IFN-γ with its receptors; interferon gamma receptor (IFNGR1 and IFNGR2), janus tyrosine kinases (JAK) are activated and subsequently phosphorylate the signal transducer and activator of transcription-1 (STAT-1) protein, which dimerises and translocates to the nucleus to induce target gene transcription by binding to gamma activated sequences (GAS) in the promoter of IFN-γ- responsive genes (Ma et al., 2005).

1.7.4 CD74 and lipopolysaccharide (LPS)

During bacterial infection, it has been reported that the expression of CD74 is increased under inflammatory conditions.In, *Helicobacter pylori* (*H.pylori*) infection the bacterium can also use CD74 as a point of attachment to gastric cancer cell lines (Beswick et al., 2006; Beswick and Reyes, 2009; Zheng et al., 2012). *H.pylor*i is classified as a gram-negative spiral bacterium that colonizes the human gastroduodenal mucosa. In this context, Zheng et al. (2012) reported that CD74 expression is upregulated after exposure to lipopolysaccharide (LPS) in gastric cancer cell line MKN-45.

Lipopolysaccharide (LPS) is unique for gram-negative bacteria, present in the outer membrane, and is made of both hydrophobic and hydrophilic domains. It is important for bacteria to survive and protects them from hydrolytic degradation by other organisms. LPS consists of three components: (i) Lipid A, (ii) core Oligosaccharide (iii) O-specific side chain or O-antigen (Qiao et al., 2014). A lipid, which connects with epitopes of CD14, contains two acylated GIcNAc-P residues (GIcN). The core part consists of KDO (3-deoxy-D-manno-octulosonic acid), heptoses (Hep), and neutral sugars such as galactose. The outer O-antigen is made of repeating units of two to eight sugars (Hardaway, 2000; Hashimoto, 2003; Qiao et al., 2014).

1.7.5 The role of CD74 in cancer immunoediting

Research has shown that CD74 plays a significant role in tumour immunosurveillance and cancer immunoediting. Chao et al. (2012) hypothesised that over expressed CD74 might enable tumours to escape the immunosurveillance recognition via evasion of phagocytosis. It is believed that CD74 inhibits phagocytosis via the ligation of expressed signal regulatory protein-α (SIRP-α) by phagocytes leading to tyrosine activation and inhibition of myosin accumulation at the submembrane assembly site of the phagocytic

synapse (Tsai and Discher, 2008). So, CD74 functions as a 'don't eat me signal' and a marker of self, as loss of CD74 may lead to homeostasis of phagocytosis of damaged and aged cells (Oldenborg et al., 2000; Blazar et al., 2001; Chao et al., 2012). This process occurs when CD74 on tumour cells binds to SIRP-α on phagocytes leading to promotion of phagocyte inhibition and tumour survival (Chao et al., 2012). In support of this hypothesis, it has been shown that forced expression of CD74 enhances dissemination and fulminantes death in xenografted mice in a CD74-deficient myeloid leukaemia cell lines (Jaiswal et al., 2009).

CD74 expression by tumour cells has been linked to the process of tumour recognition by T cells and antigen presentation (Beswick and Reyes, 2009). CD74 is thought to be a link molecule between the endogenous and the exogenous antigen presentation pathway as shown recently by Basha and his group (Basha et al., 2012). It has been also shown that CD74 exhibits physical association with HLA-DR promoting re-cycling of HLA-DR into the endosomes. It was proposed that the high level expression of CD74 might prevent the antigen presentation process by blocking the peptide binding cleft rendering tumours less immunogenic. Moreover, it has been demonstrated that upregulation of CD74 in human cancer cells directly influences tumours growth and dissemination suggesting that CD74 may have a role in escaping the equilibrium phase of cancer immuneediting (Chao et al., 2012).

In addition, it has been confirmed recently that blocking CD74 expression on tumour cells by anti-CD74 antibodies may facilitate the elimination of tumour cells by the immune system (Zheng et al., 2012; Otterstrom et al., 2014). It has been suggested that the anti-CD74 antibody eradicates tumour cells through the Fc-dependent mechanism including complement dependent cytotoxicity (CDC) and antibody-dependent cellular cytotoxicity (ADCC) (Chao et al., 2012). Interestingly, it was found that the anti-CD74 antibody

induces cytotoxicity of NK cells against head and neck cancer (Kim et al., 2008). Another suggestion proposed is that blocking CD74 may induce the level of tumour cells apoptosis *in vivo* and *in vitro* (Kikuchi et al., 2005; Uno et al., 2007). Anti-CD47 antibody-mediated apoptosis occurred independent of the caspase cell death pathway and may also involve ligation and activation of thrombospondin, an additional ligand of CD47 (Mateo et al., 2002; Manna and Frazier, 2004). In support of this finding, CD74 has been suggested to be involved in signalling pathways via MIF and CD44 increasing tumour cell survival and inhibition of apoptosis (Tillmann et al., 2013; Yaddanapudi et al., 2013; Richard et al., 2014). Further, Verjans et al. (2009) found that MIF/CD74 interactions play a crucial role in breast tumourigenesis.

1.7.6 The interaction of CD74 along with MIF and CD44

Several studies have shown that MIF can bind to the extracellular domain of CD74 to promote signalling pathways including inflammatory processes, activation of ERK1 and ERK2 members of the family of mitogen-activated protein kinases (MAPKs), cell proliferation, prostaglandin E2 (PGE_2) production, chemokine-mediated signalling and apoptosis (Leng et al., 2003; Shi et al., 2006; Starlets et al., 2006; Bach et al., 2009; Fan et al., 2011; Tillmann et al., 2013). However, the short cytoplasmic tail of CD74 lacks a signal-transducing intracellular domain, although phosphorylation of the serine residues takes place on the P35 variant of CD74 and requires CD44 (Zernecke et al., 2008; Borghese and Clanchy, 2011). CD44 binding is necessary for MIF mediated signalling cascades to start along with Src-tyrosine kinase (Shi et al., 2006). So, CD74 that has been modified by the addition of chondroitin sulfate interacts with CD44, a polymorphic transmembrane protein with kinase activating properties, forming a receptor complex (Naujokas et al., 1993; Borghese and Clanchy, 2011). This leads to phosphorylation of ERK1 and ERK2, which further triggers various effector proteins involved in

inflammatory processes and cell proliferation. ERK1 and ERK2 remain phosphorylated for many hours and hence this cascade continues for a longer time (Mitchell et al., 1999; Lue et al., 2006). Along with this, the Akt pathway is also activated by MIF (Lue et al., 2007). This leads to phosphorylation of pro-apoptotic proteins, namely BAD and BAX and the cells acquire signals to withstand apoptosis (Lue et al., 2007). In B-lymphocytes, MIF induces a signalling cascade that leads to nuclear factor-κB (NF-κB) activation, proliferation and survival (Matza et al., 2001; Starlets et al., 2006). These findings suggest that CD74 stimulation initiates a pro-survival signal.

1.8 Macrophage migration inhibitory factor (MIF)

Rich and Lewis originally reported MIF as immunological mediators in 1932 when they noticed an apparent active inhibition of inflammatory cell migration *in vitro* (Rich and Lewis, 1932; Flaster et al., 2007). In the 1950s, the name macrophage migration inhibitory factor was given to substances that were believed to be responsible for arresting the movement of monocytes *in vitro* by cellular inflammatory reactions. MIF is considered one of the first cytokines that have been described and its role in both innate and adaptive immunity was shown approximately 50 years ago in 1966 (Bach et al., 2008). MIF was classified as a T-cell-derived factor, which is believed to be responsible in macrophage migration inhibition in research carried out to characterize delayed-type hypersensitivity (Calandra and Roger, 2003; Bucala and Donnelly 2007; Conroy et al., 2010). In addition, MIF and interferon have been identified as the first two cytokines that have a central role in immune responses. However, the precise role of MIF in biological activities remained unclear until the cloning of human MIF complementary DNA in 1989 (Weiser et al., 1989). In 1991, research showed that MIF showed activity similar to hormones after the exposure of the anterior pituitary gland to the endotoxin LPS. Therefore, these observations suggest that MIF might be a mediator that links the immune

system to endocrine via its activity (Calandra and Roger, 2003; Bucala and Donnelly, 2007).

The expression of MIF has previously been linked to be the main cellular source of T cells in the immune system (Leng and Bucala, 2006). However, it was later confirmed that the expression of MIF could be found in several types of immune cells, such as monocytes, macrophages, blood dendritic cells, B cells, neutrophils, mast cells and basophils (de Dios Rosado and Rodriguez-Sosa, 2011). Since MIF is constitutively expressed and stored in intracellular pools, its secretion does not require *de novo* protein synthesis. In addition to its expression by immune cells, MIF was found to be expressed by cells and tissue in direct contact with the host's natural environment, such as gastrointestinal and genitourinary tracts, the lung and the epithelial lining of the skin. Another feature that makes MIF unique is that it can be highly expressed by some tissues of the endocrine system specifically by the hypothalamus, pituitary and adrenal glands (Flaster et al., 2007; Calandra and Roger, 2003).

The human MIF gene was first reported in 1994 by Paralkar and Wistow (Paralkar and Wistow, 1994; Donn and Ray, 2004). The MIF gene of the human genome is located on chromosome 22 (22q11.1). The human gene of MIF is composed of three different short exons of 107, 172 and 66 base pairs; and two introns of 188 and 94 base pairs as shown in Figure 1-8. The 5' end region has several consensus DNA-binding sequences for transcription factors, such as activator protein 1 (AP1), NF-κB, EST, erythroid transcription factor (GATA), SP1 and cAMP response element binding protein (CREB). However, knowledge concerning these putative DNA-binding sites in the regulation of expression of the human MIF gene is still limited (Brunner and Bernhagen, 2000; Calandra and Roger, 2003).

Three laboratories first determined the three-dimensional structure of the MIF protein in 1996. These observations have shown that human and rat MIF is a homotrimer. It has been also demonstrated that determination of MIF showed that there is a marked three-dimensional structural homology between MIF and three microbial enzymes; oxalocrotonate tautomerase, 5-carboxymethyl-2-hydroxymuconate isomerase and chorismate mutase (Calandra and Roger, 2003; Leng and Bucala, 2006; Conroy et al., 2010). Furthermore, unlike any other cytokine or pituitary hormones, the primary structure of MIF consists of 115 amino acids with a molecular weight of 12.5 kD. It has also been shown that the secondary structure of MIF consists of 6 β-plated sheets and 2 antiparallel α-helices with a high similarity to major histocompatibility complex (MHC) molecules (Bach et al., 2009; Cornry et al., 2010). Three-dimensional structural homology of top and side view of MIF is shown in Figure 1-9.

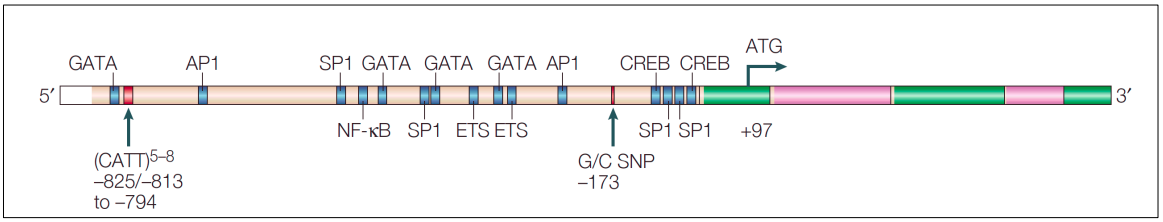

Figure 1-8: The structure of human MIF gene.

The green regions show short exons, pink regions illustrate the introns. It is known that exons are codes of proteins, while introns are not involved with the coding for proteins (Calandra and Roger, 2003).

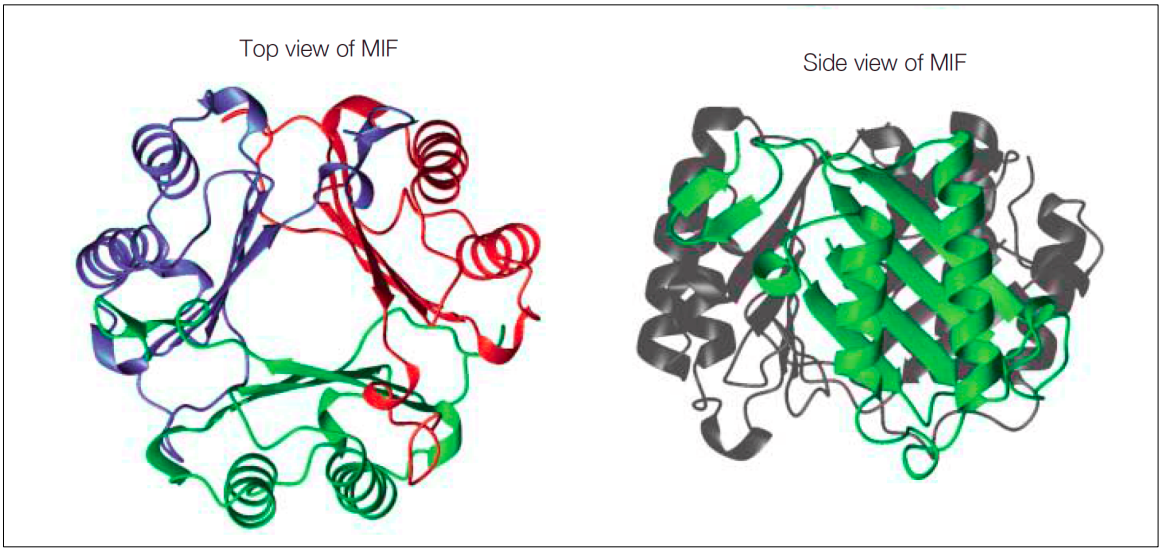

Figure 1-9: Three-dimensional structural homology of top and side view of MIF.

Three identical monomers are shown; each monomer consists of 2 anti-parallel α-helices that pack against 6 β-plated sheets (Calandra and Roger, 2003).

MIF is also known as a pleiotropic cytokine and plays a pivotal role in both innate and adaptive immunity. MIF is one of the most important cytokines since it is considered a multi-functional molecule that has several roles in immune responses (Verjans et al., 2009). It has been found that MIF is capable of stimulating other cytokines to the site of infections. With regards to MIF structure, Rosengren et al. (1996) suggested that MIF might play an enzymatic role; however knowledge regarding its activity as enzyme is still limited (Bach et al., 2009). MIF has been found to be a modulator in the immune system. Since MIF is highly expressed by most cells of immune system, such as monocytes, macrophages, dendritic cells and B cells, it is believed that MIF has a central role in both innate and adaptive immunity (Rice et al., 2003). Monocytes/macrophages are the first defensive line of immune cells that are activated against foreign invaders. MIF is released from macrophages for cytokine production, such as IFN-γ, IL-2, TNF-α and IL1-β. However, mRNA production and protein synthesis are required in order to secrete TNF-α and IL1-β. In general, the main function of MIF in the presence of these cytokines is to attract the other immune cells to the sites of infections and to elevate inflammatory interactions against intracellular pathogens (Calandra et al., 1994, 2000; Benigni, 2000).

MIF has a critical role in tumourigenesis due to its overexpression by cancer cells. It has been found that MIF is overexpressed in various tumours, such as breast cancer, prostate cancer and colon carcinoma. For instance, the expression of MIF was higher in tumour tissue compared to normal tissue in a mouse model for intestinal cancer (Bach et al., 2008; Conroy et al., 2010). It has been confirmed that MIF may play a significant role in inducing angiogenesis, promoting cell cycle progression, inhibiting apoptosis, inhibiting the lysing of tumour cells by NK cells, inhibiting p53-dependent gene expression, activating ERK1 and ERK2 signalling and upregulating TLR4 expression. The expression of MIF is chiefly controlled by cell stress and growth factors. Chesney and Takahashi

have demonstrated that using anti-MIF treatment can alter the proliferative state of tumour cells (Takahashi et al., 1998; Chesney et al., 1999; Calandra and Roger, 2003). MIF is capable of inhibiting acute inflammation and killing cells; a function that is thought to be the first step in tumourigenesis. It is believed that MIF inhibits the action of glucocorticoids by preventing the activation of NF-κB, a primary target of steroids. Steroids play a central role in the induction of mitogen-activated protein kinase phosphatases. This mechanism is regulated by MIF, which is essential in down-regulation of MKA kinase activation (Bach et al., 2008; Tillmann et al., 2013).

Within the breast, Bando et al. (2002) documented the overexpression of MIF in 93 primary breast cancer tissues with MIF localization to tumour, as well as stromal cells. Xu et al. (2008) found that MIF was overexpressed in breast cancer tissues compared with normal tissues. In the same manner, Verjans et al. (2009) have also shown that MIF is overexpressed in non-invasive breast cancer cells lines such as MDA-MB-468 and ZR-75-1 as well as breast cancer tissue. High expression of MIF in breast tumour tissue has also been correlated with tumour size and hormone receptor status and is associated with favourable survival (Verjans et al., 2009). Surprisingly, MIF overexpression in breast cancer cells was most abundantly observed in non-invasive breast cancer cells, but not in invasive cells, which in turn expressed higher levels of the MIF receptor CD74 (El Bounkari and Bernhagen, 2012). Richard et al. (2014) also observed an inverse correlation between stromal MIF expression and tumour size, as well as an elevated MIF presence in fibroblasts surrounding the tumour tissue. Their findings suggested that there is a positive correlation between the expressions of MIF and CD74 in breast cancer (Richard et al., 2014). In support of this hypothesis, McClelland et al. (2009) demonstrated that co-expression of MIF and CD74 was associated with greater vascularity and higher levels of pro-angiogenic chemokine receptors (CXC).

Despite knowledge about the role of MIF in tumourigenesis, identification of potential receptor of MIF and obtaining information concerning the intracellular signalling cascade took some time. It was believed that MIF might interact with a constituent of albumin known as sarcolectin although no studies have been carried out to support these observations. Kleemann et al. (2000) showed that MIF is taken up by cells and binds to c-Jun activation domain-binding protein-1, inhibiting the activation of the transcription factor AP-1. Leng et al. (2003) were the first to demonstrate that there is a relationship between MIF and CD74 as a potential MIF receptor in signalling pathways. It has also been shown that fluorescence-coupled MIF binds with high affinity to the CD74 receptor. CD74 has been known to play a role in the transport of export enzymes from the Golgi apparatus to the endoplasmic reticulum. However, CD74 is expressed on the cell-surface, so it appears very likely that it also serves as receptor for MIF in the presence of CD44. CD44 is classified as a transmembrane co-receptor that is required for MIF-induced ERK1 and ERK2 kinase phosphorylation. The binding of MIF is also associated with serine phosphorylation of both CD74 and CD44 receptors. However, protection from apoptosis is required in order to activate both CD74 and CD44 receptors. MIF has been known as a non-cognate ligand for chemokine receptors (CXCR4 and CXCR2) in addition to its capability to interact with CD74 and CD44. CXCR4 and CXCR2 have been described previously as functional receptors (Bernhagen et al., 2007; Tillmann et al., 2013).

1.9 Cluster of differentiation 44 (CD44)

Cluster of differentiation 44 (CD44) is a transmembrane glycoprotein that acts as the major receptor for hyaluronan and it is considered a member of a large family of cell adhesion molecules (CAMs). The human gene of CD44 is located on the short arm (p13) of chromosome 11. The CD44 gene consists of 20 exons spanning approximately 60 Kb of human DNA and they are classified to two main groups (Sneath and Mangham, 1998; Cichy and Puré, 2003). The first five exons 1-5 as well as exons 16-20 are spliced together to form a transcript and encode the ubiquitously expressed isoforms that are abbreviated to CD44s or CD44H. The 10 variable exons 6-15 (also known as v1-10) can be alternatively spliced and included within the standard exons at the insertion site between exons 5 and 16. CD44 expressed from the variable exons is abbreviated, to CD44v. Theoretically, more than 1000 isoforms of CD44 would be allowed for expression based on alternative splicing. Since CD44 is a transmembrane glycoprotein, the extracellular domain of protein is encoded by exons 1-17, the short transmembrane domain is encoded by exon 18 and the cytoplasmic domain is encoded by part of exon 18 and by exons 19 and 20 (Sneath and Mangham, 1998; Lesley and Hyman, 1998; Goodison et al., 1999; Cichy and Puré, 2003).

The molecular weights of CD44 proteins range from 80-230 kDa for three reasons. Firstly, the variety of mRNAs generated by alternative splicing of ten variant exons during its pre-mRNA. Secondly, the posttranslational modifications including N- and O-linked glycosylation and the attachment of glycosaminoglycans generate additional structure of diversity of CD44. Thirdly, the proteins often get shortened *in vivo* owing to partial cleavage by matrix metalloproteases; this affects most CD44 in human cancer types (Naor et al., 1997; Iczkowski, 2011). Gene and protein structures of CD44 are shown in Figure 1-10.

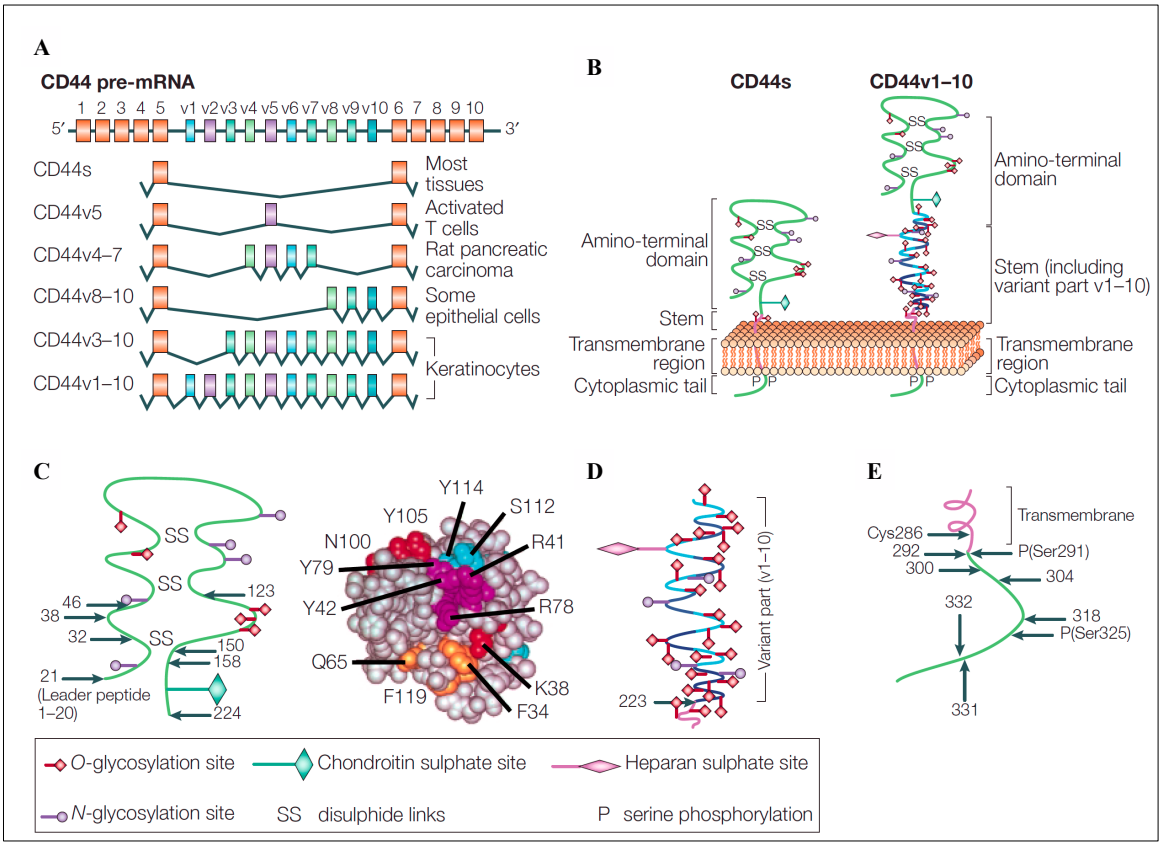

Figure 1-10: Schematic diagram of gene and protein structure of CD44.

(A) CD44 pre mRNA consists of 20 exons, some of which are constant region exons that are used in every CD44 mRNA and protein (orange bars) and others are variant exons (coloured bars) that are used in the CD44 variant proteins and are selected by alternative splicing. (B) The protein structure of CD44s is compared with the largest variant isoform CD44v1–10. The CD44 protein is composed of an extracellular link domain, a stalk-like region in the extracellular domain close to the transmembrane region, where the variant exon products (green) are inserted, the transmembrane region (TM) and the cytoplasmic tail (CP). (C) The amino-terminal domain of CD44 proteins contains the hyaluronan-binding motifs, which are in the link domain and a basic motif that is outside the link domain. The stability of the link module is contributed to by four highly conserved cysteine residues that form interchain disulphide links 141. (D) The stem structure of CD44s consists of 46 amino acids, but can be enlarged by up to 381 variant-exon-encoded amino acids in human or 423 in mouse, as shown for CD44v1–10. The unique heparan sulphate addition site that is encoded by exon v3 is important for the binding of heparan-sulphate-dependent growth factors. (E) The carboxy-terminal cytoplasmic domain supports the binding of proteins with crucial functions in cytoskeletal organization and signalling. Ezrin, radixin, moesin (ERM) proteins bind to amino acids 292–300 and ankyrin to amino acids 304–318. Amino acids 331 and 332 are necessary for basolateral distribution of CD44 in polarized epithelia145 (Zöller, 2011).

The smallest isoform of human CD44 proteins (CD44s), which lacks the variant exons contains 363 amino acids and its theoretical molecule mass is 37 kDa. The CD44 protein consists of three different regions; C-terminal cytoplasmic domain 72 (aa), transmembrane domain 21 (aa) and extracellular domain 270 (aa). The predominant form of CD44 has an approximate molecular weight of 80 to 95 kDa, and has been denoted as CD44 standard form (CD44s). In addition, a large number of higher molecular weight variant isoforms (CD44v) exist (Sneath and Mangham, 1998; Lesley and Hyman, 1998; Goodison et al., 1999; Cichy and Puré, 2003).

The function of CD44 is diverse due to its varied structure and distribution in tissues and cells. CD44 is involved in cellular adhesion (aggregation and migration), hyaluronate degradation, lymphocyte activation, lymph node homing, angiogenesis and release of cytokines (Sneath and Mangham, 1998; Marhaba and Zöller, 2004). Interestingly, CD44 also has several roles in neoplasia such as tumourigenesis and metastasis formation (Klingbeil et al., 2010; Orian-Rousseau, 2015). It has been found that CD44 expression is associated with a high rate of cell division. The proliferation status of tumour cells increases when CD44 is overexpressed (Sneath and Mangham, 1998). Several studies have also shown that CD44 isoforms are associated with metastatic behaviour (Goodison et al., 1999; Cichy and Puré, 2003). Additionally, CD44 plays a significant role in PI3K signalling which increases cell proliferation and survival (Torre et al., 2010). The ERK1 and ERK2 pathway can be stimulated by CD44/CD74/MIF complex activation, which in turn leads to Scr association with the cytoplasmic tail of CD44 and subsequent ERK1 and ERK2 phosphorylation (Shi et al., 2006).

Generally, the expression of CD44 has been found in wide range of cells and tissues including hematopoietic, central nervous system, lung, liver, pancreatic, endothelial and fetal tissues (Naor et al., 1997). In particular, CD44v expression has lower distribution

than CD44s because the process of alternative splicing is normally tightly regulated (Lesley and Hyman, 1998). As a result, it is expressed on a variety of endothelial cells and epithelial linage in a tissue specific pattern. The expression of CD44 on endothelial cells can vary between layers and also between cells. For example, it has been reported that the expression of CD44v6 was restricted to the serum basal and the stratum spinosum of normal uterine cervical squamous epithelium. It was later shown that normal melanocytes and naevi do not express CD44 although the keratinocytes express CD44vs-10 (Lesley and Hyman, 1998; Goodison et al., 1999; Cichy and Puré, 2003).

The expression of CD44 has been linked to several tumour types such as prostate tumour, head and neck squamous tumour, nervous system tumours, respiratory tract tumours, melanomas and breast cancer (Jaggupilli and Elkord, 2005; Fillmore and Kuperwasser, 2007). It has been reported that most CD44v forms were present in pancreatic cancer cases. Interestingly, CD44v, v2/v6 expression was associated with not only a poorer prognosis but also favourable prognosis. On the other hand, several reports indicated that loss of CD44 expression could be considered a predictor of a poor prognosis in some types of tumours, including tongue cancer laryngeal cancer and colorectal cancer. However, another study reported conflicting findings, where it was demonstrated that positive CD44 expression can be the most important indicator of poor prognosis in patients with colorectal cancer (Sneath and Mangham, 1998; Assimakopoulos et al., 2002; Eberth et al., 2010; Iczkowski, 2011; Olsson et al., 2011).

CD44 has been the subject of extensive research for more than three decades due to its role in breast cancer. Importantly, it has been shown that the role of CD44 can be involved in both tumour suppression and progression (Götte and Yip, 2006). CD44 expression has also been reported to promote pro-tumourigenic signalling and advance the metastatic cascade (Louderbough and Schroeder, 2011a). Conversely, CD44 has been

shown to suppress growth and metastasis (Louderbough and Schroeder, 2011a). In the same manner, Louderbough et al. (2011b) reported conflicting results regarding the role of CD44 as a tumour suppressor or promoter, which highlights the importance of studying the cell type–specific function of proteins important to cancer progression. Histological researches of CD44 expression in human breast cancer have been correlated to both favourable and unfavourable clinical outcomes (Anand and Kumar, 2014). Recently, significant attention has been paid to CD44 expression in stem cells as a potential therapeutic target (Götte and Yip, 2006; DeLisser, 2009; Louderbough and Schroeder, 2011a). CD44 has been shown to mark cancer-initiating cells (CIC), thus indicating its significant role in maintaining cancer cells including progression, proliferation and metastasis (Sieuwerts et al., 2009; Trapé and Gonzalez-Angulo, 2012; Anand and Kumar, 2014). Huang et al. (2007) reported that over expressed serine/arginine gene (SRp40) in breast cancer correlates with the alternative splicing of CD44, forming variants such as CD44v2, v3, v5 and v6.

1.10 Project description

1.10.1 Overview

In recent years there has been a rapid growth of interest in breast cancer immunotherapy. Of particular current interest is the question of which of the many immunogenic proteins present in a breast tumour should be harnessed for therapeutic purposes, an outgrowth of research on whether breast cancer is immunogenic (Disis, 2002; Wolchok and Chan, 2014). The present study sought to determine the expression and function of CD74, MIF and CD44 in the breast tumour cell lines CAMA-1, MDA-MB-231 and MDA-MB-435. To date, co-expression of CD74, along with MIF and CD44, has not been studied in breast cancer. However, it has been described in prostate and non-small cell lung cancer. In prostate cancer, MIF staining was intense, but CD74 staining was weak and patchy (Meyer-Siegler et al., 2006). In lung cancer, CD74 was mainly detected in the stromal compartment or in stromal and epithelial cells (McClelland et al., 2009). Recently, Richard et al. (2014) studied the involvement of MIF and its receptor CD74 in human breast cancer. However, they did not consider the relationship between CD74 and MIF and the expression of CD44. It is proposed herein that co-expression of CD74/MIF and CD44 might play a significant role in breast tumour progression and survival, in addition to the role that each molecule individually has in breast tumour.

1.10.2 Aims

The overall aim of this project was to study the expression and the role of CD74, MIF and CD44 in human breast cancer derived cell lines. The aims of this study were:

- To analyse and profile the expression of CD74, MIF and CD44 in human breast cancer cell lines (CAMA-1, MDA-MB-231 and MDA-MB-435). To validate the study by investigating the expression of CD74, MIF and CD44 in immortalized normal breast luminal cells (226LDM), normal breast tissue lysate (Abcam, USA) and normal breast tissue slides.
- Modulation studies: study of the effect of interferon-gamma (IFN-γ) and lipopolysaccharide (LPS) on the migration, proliferation and expression of CD74 in CAMA-1 and MDA-MB-231cells.
- To study of CD74 and its potential interaction with MIF and CD44 in the breast cancer-derived cell lines (CAMA-1, MDA-MB-231 and MDA-MB-435); the interactive partners of CD74, along with MIF and CD44, were analyzed using target imaging and co-immunoprecipitation.
- To study the effects of apoptosis and cell proliferation in CD74 siRNA transfected cells (CAMA- 1 and MDA-MB-231).
- Proteomics study of IFN-γ in the CAMA-1 and MDA-MB-231 cell lines.

Chapter 2 Materials and Methods

2.1 Materials

2.1.1 General laboratory chemicals

The majority of chemicals used in this study were from Sigma (Poole, England, UK) specifically; Accutase, Dimethyl Sulphoxide (DMSO), Cellytic M Cell Lysis Reagent, Protease Inhibitor Cocktail, Ponceau S solution, Paraformaldehyde (PFA), Tween-20, Saponin and Triton-x 100. Other chemicals such as Sodium chloride, acetone, methanol and Virkon were from Fisons (Leicester, England, UK); Fetal Calf Serum (FCS) was from Imperial Laboratories, England. Recombinant Human Interferon Gamma (IFN-γ) was from Immuno Tools, Germany. Lipopolysaccaride (LPS) from *E. coli* serotype EH100 was purchased from Sigma Aldrich, UK. Dulbecco's Modified Eagle's Medium (DMEM), Dulbecco's Modified Eagle's Medium (DMEM)/F-12 and RPMI-1640 were from Fisher Scientific, UK.

2.1.2 Commercial kits

The commercial kits used in this study were:

- Protease Inhibitor Cocktail Set III (Calbiochem, UK)
- Breast (Human) Tissue Lysate - Normal tissue (Abcam, UK)
- Breast Tissue Slide (Normal) (ProSci, USA)
- DNAse treatment kit (Life technologies, UK)

These kits were used according to the manufacturer's recommendations.

2.1.3 Cell lines

For the purpose of the present study, we employed two kinds of cell lines. First, we used breast cancer cell line CAMA-1 and MDA-MB-231 as the main cell lines. Also, we included other cell lines as positive control, including; 226LDM, THP-1, Raji, Jurkat and HeLa. The CAMA-1 breast cancer cell line was isolated from mammary gland/breast; derived from metastatic site: pleural effusion (Ji et al., 1994). This cell line was maintained in RPMI-1640 supplemented with 10% (v/v) Foetal Calf Serum (FCS) from Imperial Laboratories. MDA-MB-231 breast cancer cell line was obtained from a patient in 1973. This cell line was maintained in D-MEM (high glucose) supplemented with 10 % FCS. 226LDM are immortalized normal breast luminal cells, kindly provided by Elena Klenova (School of Biological Sciences, University of Essex). This cell line was maintained in Dulbecco's Modified Eagle's Medium (DMEM)/F-12 and was supplemented with 10% (FCS), 50 mg/ml gentamicine, 5 µg/m Insulin, 1 ng/ml Hydrocortine, 20 ng/ml EGF and 20 ng/ml cholera toxin.

Secondary cell lines were used in the present study as a positive control since they express a considerable level of CD74, MIF and CD44. The secondary cell lines that were used in this study are as follows: THP-1, Raji, HeLa and Jurkat. All the types of secondary cell lines were kindly provided by Prof. Nelson Fernandez, (School of Biological Sciences, University of Essex, UK). The cell lines were cultured in RPMI-1640 medium and maintained at 37 °C and 5% CO_2. The cell lines used in this study were obtained from different sources as shown in Table 2-1 below:

Table 2-1: Details of cell lines used in this study.

Cell line	Origin	Cell culture
MDA-MB-435	Cell lines was originally derived from pleural effusion of a female breast cancer	RPMI-1640 supplemented with % FCS
CAMA-1	Epithelial cells was derived from a human breast carcinoma	RPMI-1640 supplemented with % FCS
MDA-MB-231	Epithelial cells was derived from pleural effusion of breast cancer	D-MEM (high glucose) supplemented with 10 % FCS
226LDM	Immortalized normal breast luminal cells	DMEM/F-12 supplemented with 10% (FCS), 50 mg/ml gentamicine, 5 µg/m Insulin, l ng/ml Hydrocortine, 20 ng/ml EGF and 20 ng/ml cholera toxin.
THP-1	Human monocyte was derived from patients with Acute Lymphocytic Leukaemia (ALL)	RPMI-1640 supplemented with % FCS
Raji	Human lymphoblastoid cells derived from a Burkitt lymphoma.	RPMI-1640 supplemented with % FCS
Jurkat	Established from the peripheral blood of a 14-year-old boy with Acute Lymphoblastic Leukemia (ALL)	RPMI-1640 supplemented with % FCS
HeLa	Epithelial cells was derived from human cervical carcinoma	D-MEM (high glucose) supplemented with 10 % FCS

The details and features of each cell lines are available in American Type Culture Collection (ATCC) website; (http://www.lgcstandards-atcc.org/).

2.1.4 Antibodies

The primary and secondary used in this study were obtained from different sources as shown in Table 2-2 below:

Table 2-2: List of the antibodies used for all the applications in the project.

Specificity	Type	Clone	Cat. no.	Company
Mouse anti-human HLA-A, B, C	Primary	W6/32	311415	Cambridge Biosciences
Mouse anti-human HLA-A, B, C	Primary	W6/32	Supernatant	Cambridge
Mouse anti-human HLA-DR	Primary	LN3	327001	Biolegand
Mouse anti-human CD74	Primary	By2	sc-20062	Santa Cruz
Mouse anti-human CD74	Primary	BU45	Supernatant	Cambridge
Mouse anti-human MIF	Primary	D-2	sc-271631	Santa Cruz
Mouse anti-human MIF	Primary	Polyclonal	ab55445	Abcam
Mouse anti-human CD44	Primary	156-3c11	3570	Cell signalling
Mouse anti-human α Tubulin	Primary	TU-02	sc-8035	Santa Cruz
Mouse IgG2b antibody	Isotype	MPC-11	400301	Biolegand
Rabbit anti-human β-actin	Primary	poly6221	622102	Biolegand
Goat anti-mouse Alexa 488	Secondary	Polyclonal	A-10667	Invitrogen
Goat anti-mouse Alexa 555	Secondary	Polyclonal	A-21422	Invitrogen
Donkey anti-mouse IRDye® 800CW	Secondary	Polyclonal	925-32212	Li-Cor Bioescieces
Goat anti-Rabbit IRDye® 680LT	Secondary	Polyclonal	925-68022	Li-Cor Bioescieces
Mouse IgG2b antibody	Isotype	MPC-11	400301	Biolegand
Goat anti-mouse antibody	Secondary	Poly4053	405305	Biolegand

2.2 Methods

2.2.1 Cell cultures

2.2.1.1 Thawing of cells

Cryogenic vials with 1×10^6 cells/ml in a 9:1(v/v) solution of FCS: dimethyl sulphoxide (DMSO) were removed from liquid nitrogen. Special precautions were taken which included using a protective mask and heavy padded gloves. Cells were thawed rapidly at 37^{o}C and then transferred using a sterile glass pipette to a 10 ml centrifuge tube containing 5 ml of fresh complete medium to dilute out the DMSO. After centrifugation for 5 minutes at 1000 rpm, the medium was removed, the cell pellet was re-suspended in 5ml of fresh medium, and the number of the cells was counted using a haemocytometer. A final concentration of 1×10^5 cells/ml was transferred to either a flask or petri dish. Cells were cultured at 37^{o}C in a humidified tissue culture incubator with 5% (v/v) CO_2.

2.2.1.2 Cell cultures of cell lines

MDA-MB-435 cell line was of immense importance for all the experiments in this study as it was the control or model with which the new cell lines (CAMA-1 and MDA-MB-231) were compared. MDA-MB-435 cells were passaged at 70-80% confluence at every 3 to 4 days. The cells were washed with 1X Phosphate buffer saline (PBS) and lifted from the flask with 1 ml of accutase (Sigma-Aldrich; Dorset, UK) by incubating at 37°C for about 5-10 minutes. The cells were then counted with a hemocytometer and plated out at a density of 1×10^3 in new culture flask. CAMA-1, MDA-MB-231, 226LDM and HeLa cell lines were expanded in a similar way. The steps followed were exactly as for the MDA-MB-435 cell line. THP-1, Jurkat, and Raji are suspension cell lines. The cells were centrifuged at 1000 rpm for 5 minutes, supernatant was aspirated and fresh medium was added to the cell pellet. Then, cells were seeded at density of 1×10^5 in new culture flasks.

2.2.1.3 Cryopreservation of cells

Cells were cryopreserved at 70% confluence. Cells were briefly detached using accutase, counted and checked for viability as mentioned above and then centrifuged. Cells were then re-suspended so that they were about 1.25×10^6 cells/ ml of freezing mixture (90% FCS and 10% Dimethyl sulphide [DMSO]). 1 ml of the cell suspension was then dispensed into each cryo tube (Fisher Scientific, UK) and placed in -80 ^{o}C freezer for 1-2 days before transferring them to liquid nitrogen at -196^{o}C for long-term storage.

2.2.1.4 Growth curve

As both CAMA-1 and MDA-MB-231 cell lines are grown in culture; there are three distinct phases that can be detected. The first is the Lag Phase, which is usually no further than 1-2 days in length, during which there is slight increase in cell number. It is assumed that during this period of time, the cells are adjusting to the new media. This is followed by the Log Phase. During this phase, the cell number increases exponentially. The final phase is the confluent phase. During this phase, the number of cells remains constant. Eventually, the cells will die unless they are sub cultured or fresh media is added. Approximately 3×10^4 cells/ml was plated onto 35 mm dishes and cell number was determined at approximately 24 hr intervals for 192 hr. Three dishes were read every day using a haemocytometer and the mean number of the cells in the squares was calculated. This value multiplied by the amount of media in the dish gave the total number of cells.

2.2.1.5 Cell viability test

The following cell viability test, based on the trypan blue exclusion, was used to check whether the cells used here produce a result of dead or living cells. First the cells were washed with PBS (phosphate buffered saline). Then accutase treatment was used to split them and the cell suspension was placed in a conical centrifuge tube. Then a cell

suspension of 1:2 dilution in trypan blue (Sigma, UK) was prepared. Approximately 10 µl of diluted cell suspension was loaded into both the haemocytometer chambers, and cells were viewed under the light microscope. The cells were observed as total cells and non-viable (blue) cells. Live cells would have the cell membranes intact and would exclude the trypan blue dye, where dead cells did not.

2.2.2 Cell stimulations

2.2.2.1 Recombinant human interferon-gamma (IFN-γ)

Synthetic IFN-γ is a single, non-glycosylated, polypeptide chain containing 144 amino acids and was purchased from ImmunoTools, Germany, in white lyophilized (freeze-dried) powder. IFN-γ was dissolved in 1 ml of sterile H_2O (stock 1), 50 µl from stock 1 was added to 450 µl of sterile H_2O (stock 2) and was stored at -18° C in accordance to the manufacturer's instructions. CAMA-1 and MDA-MB-231 cells were grown in RPMI-1640 and D-MEM respectively containing 10% FCS overnight before stimulation. Cells were then stimulated with IFN-γ at a concentration of 100, 500 and 1000 IU/ml for 72 hr. Cells were counted using a haemocytometer, checked for viability and harvested for sample preparation.

2.2.2.2 Lipopolysaccharide (LPS)

LPS is unique for gram-negative bacteria, present in the outer membrane, and is made of both hydrophobic and hydrophilic domains. It was purchased from (Sigma Aldrich, UK) in freeze-dried powder form. LPS was dissolved in 1ml of sterile 1X PBS to a vial (1 mg) and gently swirled until the powder dissolved. Solutions would be further diluted to the desired working concentration with additional sterile balanced cell culture media and were stored at - 20°C in accordance with the manufacturer's instructions. CAMA-1 and MDA-MB-231 cells were grown in RPMI-1640 and D-MEM respectively containing

10% FCS, overnight before stimulation. Cells were then stimulated with LPS at a concentration of 100, 500 and 1000 ng/ml for 24 hr. Cells were counted using a haemocytometer, checked for viability and harvested for sample preparation.

2.2.3 MTT Cell proliferation assay

2.2.3.1 Principle

This is a colorimetric method for determining cell viability. Cell proliferation was determined using MTT reagent (Sigma-Aldrich, UK). This solution contains (3-(4, 5-Dimethylthiazol-2-yl)-2, 5-diphenyltetrazolium bromide, a tetrazole). Assays were performed by adding a small amount of the solution directly to culture wells and then incubated for 4 hr. The absorbance was measured at 595 nm with a reference wavelength of 620 nm.

2.2.3.2 Experimental protocol

Breast cancer cells CAMA-1 and MDA-MB-231 (1×10^4 cells/well) cells were cultured in 96 well flat bottom plates at 37 °C. After 24 hr incubation to allow cells to adhere, cells were exposed to varying concentrations of (IFN-γ or LPS) or no treatment (10 % FCS medium only). Cells were incubated for 24 or 72 hr after treatments. The MTT assay was then used to assess cell proliferation. Briefly, 20 µl of MTT solution (5 mg/ml in PBS) and 100 µl was added per well and cells were incubated at 37^oC with 5% CO_2 in a humidified chamber for 4 hr for colour development. The resultant Formazan crystals were dissolved in dimethyl sulfoxide (100 µl) and the absorbance intensity measured at 595 nm using a micro plate reader (Versamax). The percentage of cell proliferation was calculated relative to the rate of proliferation in untreated cells.

2.2.4 Cell migration assay

2.2.4.1 Principle

The transwell migration assay is a commonly used test to study the migratory response of endothelial cells to angiogenic inducers or inhibitors. This assay is also known as the Boyden or modified Boyden chamber assay. During this assay, endothelial cells were placed on the upper layer of a cell permeable membrane and a solution containing the test agent was placed below the cell permeable membrane. Following an incubation period (3–18 hr), the cells that had migrated through the membrane were stained and counted. The membrane was coated with an extracellular matrix component (e.g. collagen), which facilitated both adherence and migration.

The main advantage of this assay is its detection sensitivity since very low levels of angiogenic inducers can cause migration through the permeable filter. Prolonged studies are difficult, due to the fact that the test-agent concentration will quickly equalize between the compartment below the membrane and the compartment above the membrane. Another disadvantage is the relative difficulty in setting up the transwells. Commercially available transwells have alleviated this burden, but they are expensive.

2.2.4.2 Experimental protocol

Both CAMA-1 and MDA-MB-231 cells were detached, counted and seeded in serum free medium in the upper chamber of a 6-well cell culture plate placed with 24 mm polyester membrane transwell insert (pore size: 4.0 μm) from Corning Incorporated Life Sciences, UK. The cells were then allowed to attach with medium alone that was added to the upper chamber of the plate. Either medium containing 10% FCS was added or serum free medium was added to the lower chamber and the cells were allowed to migrate and invade for 24 hr. Migrated cells were washed twice in PBS and fixed with 4% paraformaldehyde (PFA) for 20 minutes at room temperature. The cells were then

permeabilized using 100% methanol for 20 minutes at room temperature followed by washing in PBS. The cells were then stained using Giemsa stain for 15 minutes and then washed three times in PBS. Non-migrated cells were then carefully scraped off with cotton swabs. Migrated cells were mounted and the slides were visualized under low magnification on a BX41 microscope.

2.2.5 Polymerase chain reaction (PCR)

2.2.5.1 Principle

The polymerase chain reaction (PCR) one of the most widely used techniques in molecular biology to amplify a single piece of DNA across several orders of magnitude, by multiplying a particular DNA sequence. PCR involves three steps; denaturation, annealing and extension. This method is useful in the investigation of a large number of diseases using DNA as a target, rather than RNA, due to the higher stability of the DNA molecule as well as the ease with which DNA can be isolated. Qualitative PCR can be used for detecting human, viral and bacterial genes.

2.2.5.2 Primer design

The primers of CD74 and β-actin were designed using primer plus 3 tools. All considerations were taken into account such as annealing temperature (Tm), GC content, the length of primers and the size of the PCR product. The primers were ordered from Fisher Scientific (Invitrogen).

2.2.5.3 RNA extraction

Total RNA from 1×10^6 CAMA-1, MDA-MB231 and THP-1 cells grown in a 75 cm^2 flask was extracted using 1 ml of TRIsure reagent (Bioline) according to the manufacturer's recommendations (Chomczynski and Mackey, 1995). The reagent was mixed well with a pipette and divided into an equal number of Eppendorf tubes. 200 µl of

chloroform was added to each tube and mixed thoroughly. The tubes were incubated at room temperature for 5 minutes, then centrifuged at 13,000 rpm for 20 minutes at 4°C. The supernatant from these was collected and put into new tubes. 500 µl of isopropanol (VWR chemicals, UK) was added to each tube and then mixed by inverting. After being incubated at room temperature for 10 minutes, the tubes were again centrifuged at 13,000 rpm for 20 minutes at 4°C. The supernatant was discarded, and the white pellet retained. The pellet was washed with ice cold 75% ethanol. The following supernatant was discarded and the tubes were spun briefly to remove any traces of ethanol, and air dried for 15-20 minutes.

2.2.5.4 DNase treatment

DNase treatment was carried out for total RNA using a DNase treatment kit. 300 µl of the master mix (3 µl buffer, 1 µl DNase enzyme and 26 µl sterile double distilled H_2O) was added to each tube and the pellet was dissolved into it. The tubes were then placed into a water bath at 37°C for 30 minutes. 5 µl of the inactivation reagent (Fermentas, UK) was then added, and the samples mixed thoroughly. After being incubated at room temperature for few minutes the tubes were then centrifuged at 13,000 rpm for 5 minutes at 4°C. The supernatant collected consisted of the RNA extracted. 270 µl of sterile double distilled H_2O, 750 µl of ice cold 100% ethanol and 3M Sodium Acetate (Fermentas, UK) were added to the collected supernatant. After an overnight incubation at -20 degrees, the tubes were spun at 13,000 rpm for 20 minutes at 4°C. The supernatant was discarded and pellet washed with 1 ml of ice cold 75% ethanol. The centrifugation step was repeated again at 13,000 rpm for 5 minutes at 4°C. The supernatant was then discarded and the tubes were spun briefly to remove any traces of ethanol. The pellet retained in the tubes was dissolved in 26 µl of sterile double distilled H_2O. The concentration of the RNA was

then determined using a NanoDrop. The quality of the RNA was also checked by electrophoresis in a 1% agarose denaturing gel.

2.2.5.5 Complementary DNA conversion

Tubes containing the RNA were vortexed, then prepared from 2 µg of total RNA using 1 µl of random hexamers and 1 µl of sterile double distilled H_2O (Fermentas, UK). The tubes were then placed into a water bath at 65°C for 10 minutes, and then chilled on ice for about 5 minutes. 8 µl of the master mix (4 µl of 5x buffer (enzyme buffer), 1 µl of sterile double distilled H_2O, 2 µl of dNTPs, and 1µl of Reverse Transcriptase) (Fermentas, UK) was added and mixed thoroughly by pipetting. The samples were then ready for use in PCR experiments.

2.2.5.6 Reverse transcriptase (RT-PCR)

The CD74 primers was PCR amplified using CD74-specific primers, CD74-F (5' TGACCAGCG CGACCTTATCT 3') and CD74-R (3' GAGCAGGTGCATCACATGGT 5') (Burton et al. 2004). PCR conditions were 95°C for 5 minutes; 35 cycles of 95°C for 30 seconds, 55°C for 30 seconds, and 72°C for 25 seconds; 5 minutes at 72°C. Control PCR amplification of β-actin using specific primers β-actin-F (5' ATCTGGCACCACACCTTCTACAATGAGCTGCC 3') and β-actin-R (3' CGTCATACTCCTGCTTGCTGATCCACATCTCC 5') was carried out so as to evaluate the RNA in all the samples. PCR conditions were 95°C for 5 minutes; 35 cycles of 95°C for 30 seconds, 60°C for 30 seconds, and 72°C for 1 minute; 6 minutes at 72°C. PCR products were then analysed by electrophoresis in a 1% agarose gel stained with ethidium bromide or safe view (NBS Biologicals, UK). The results of the gel were then analysed using an ultraviolet camera. To estimate the size of DNA bands we used the DNA ladder from (Fermentas, UK #SM0383) size from 80- 1031 bp.

2.2.6 Flow cytometry

2.2.6.1 Principle

Flow cytometry is a technique used to analyse and measure various properties of cells. The cells are usually labelled with a fluorescent probe, normally a fluorphore conjugated to an antibody. The cells are suspended in fluid, and the cells carrying fluid pass through a beam of light. This technique uses the principles of light scattering, light excitation, and the emission of fluorochrome molecules to generate specific multi- parameter data from cells. There are three parameters that are measured by photomultiplier tubes. These parameters are forward scatter (FSC), side scatter (SSC) and fluorescence (FL). One advantage of the flow cytometer is its ability to evaluate a large population of cells accurately and quickly with semi quantitative results. This makes the flow cytometry technique an ideal tool for quantitative analysis of certain cellular properties, especially when the cells of interest are a small fraction of other cell types in a cell population. The results are displayed in many ways, including histogram, dot plot, and contour. As standard practice, an irrelevant or nonspecific isotype antibody was used as a negative control to evaluate the degree of positivity for other surface proteins in terms of the fluorescence intensity.

2.2.6.2 Cell-surface and intracellular staining

For cell-surface staining of specific cell antigens, cell cultures of cell lines were washed twice with 1X PBS and incubated with accutase for 5-10 minutes at 37 ºC. Cell suspensions (1×10^6 cells/ sample) per sample were centrifuged at 300 rpm for 10 minutes. The cells were fixed with a fixation buffer to ensure free access of the antibody to its antigen 4 % PFA (Sigma, UK) followed by a washing step in PBS. Supernatants were discarded and the cell pellets resuspended in blocking buffer (PBS supplemented with 0.1% (w/v) bovine serum albumin [BSA]). The cells were incubated at 4 ºC for 1 hr

with saturating concentrations of the following primary human specific monoclonal antibodies: with an appropriate concentration of By2 (anti-CD74), ab55445 (anti-MIF), 156-3C11 (anti-CD44), W6/32 (anti-HLA-A, B, C), and LN3 (anti-HLA-DR). The cells were washed twice with PBS and incubated with secondary antibody fluorescein isothiocyanate (FITC) conjugated goat anti-mouse IgG at 4 ºC for 1 hr. Cells were used with either only secondary antibody or neither primary nor secondary antibody as negative controls. For intracellular staining, cells were permeabilised with 200 µl permeabilisation buffer (PBS supplemented with 0.1% (v/v) [Triton X-100 (Sigma, UK)]) for 20 minutes to facilitate the entry of antibodies inside the cells. The staining procedure for intracellular staining was the same as for the surface staining. Samples (10,000 cells) were analysed using a BDFACS Aria flow cytometer and a 488 nm beam for detection of the fluorochrome attached to the secondary antibody (PE, FITC). The results were analysed using FlowJo version 8.8.6 (Tree Star Inc., Ashland, OR, USA).

2.2.7 Laser scanning confocal microscopy

2.2.7.1 Principle

Confocal laser scanning microscopy is a valuable technique that has the ability to produce high resolution images of very small objects and produce a three-dimensional image of a specimen. There are many advantages of confocal microscopy over the conventional microscope due to many factors; firstly its ability to control the depth of the field, secondly the reduction of background interference away from the focal plane and thirdly its ability to analyse serial sections from thick specimens.

2.2.7.2 Colocalisation analysis

Colocalisation describes the presence of two or more types of molecules at the same physical location. Colocalisation of fluorescent signals from two or more different

proteins is an indicator of their association and potential interaction. Within the context of a cell or sub-cellular protein, often the molecules are attached to the same receptor, while in the context of digital imaging, the colours emitted by the fluorescent molecules occupy the same pixel in the image (Bolte and Cordelieres, 2006; Adler and Parmryd, 2010).

Colocalisation does not refer to the likelihood that fluorochromes with similar emission spectra will appear as overlapped in the composite image. It is important to note that cross-talk or "bleed-through" may occur if the emission spectra of the two fluorochromes are similar. Accurate colocalisation determination can only occur if emission spectra are sufficiently separated between fluorochromes and the correct filter sets are used during the acquisition step. To achieve this aim, red and green wavelengths are usually selected, and usually those dyes representing these wavelengths are carefully matched to the power spectrum of the illumination source to obtain maximum excitation wavelengths while still maintaining a degree of separation between the emission wavelengths. Often, colocalisation is assessed qualitatively, for example by showing yellow regions as the overlap between dual colour fluorescence images from green and red channels. If quantitation is sought, global statistical methods to determine overlap on a pixel-per-pixel basis are commonly chosen. (Press et al., 1992; Manders et al., 1993). Measuring the colocalisation can be divided into two main methods: pixel-based and object- based. Pixel-based methods look at all pixels in an image and determine various correlations between the channels. Object-based methods first segment the images into objects, and then make some comparison between the objects in the channels (Bolte and Cordelieres, 2006; Adler and Parmryd, 2010).

The Pearson correlation coefficient and Mander's overlap coefficient are the most common colocalisation measurement for pixel-based approaches. However, Adler and

Parmryd (2010) have reported that the Pearson correlation coefficient is superior to the Mander's overlap coefficient. The PCC is a well-established measure of correlation, originating with Galton in the late 19th century but named after a colleague, and has range of −1 (perfect correlation) to +1 (perfect but negative correlation) with 0 denoting the absence of a relationship (Adler and Parmryd, 2010).

Bolte and Cordelieres (2006) also describe object-based approaches, which allow more spatial information to be inferred about colocalisation, helpful in determining in which subcellular compartment(s) of the cell the stains may colocalise. Proper segmentation is very important in object-based methods, since different segmentations will give different colocalisation results. Pre-processing of the image, including filtering or illumination correction, may be necessary for proper segmentation. Once images have been properly segmented (that is, the cells and subcellular compartments correctly identified in both channels), Bolte and Cordelieres (2006) described several methods by which to compare the colocalisation. The first was to compare the centroids of the identified objects and define colocalised objects as those whose centroids are within some specified distance (usually, less than the optical resolution of the microscope). Another method was to multiply the two channels by one another after pre-processing and then to segment the structures of interest; the result of the multiplication is composed of only pixels present in both channels. However, we applied segmentation using regional maximum detection tools followed by manual threshold (Manders, 1997; Lachmanovich et al., 2003; Bolte and Cordelieres 2006; Rizk et al., 2014)

2.2.7.3 Experimental protocol

Cell monolayer culture and double staining: CAMA-1 and MDA-MB-231 cell lines were separately cultured in LabTek 8 well chambers (Thermo Fisher Scientific) at a density of

10×10^3 cell per well, for two days following seeding. For the staining procedure, all the steps were carried out at room temperature. The cells were fixed with 4% PFA (Sigma, UK) for 20 minutes and blocked with 2% (w/v) BSA (Bovine serum albumin) prepared in 1X PBS for 1 hr at room temperature. For intracellular staining, the cells were permeabilized with 0.1% Triton X-100 and then blocked as described above. The incubation steps were also carried out at room temperature. For staining, the cells were incubated with specific monoclonal antibody for 1 hr and washed three times with PBS. For the secondary antibody, anti-mouse IgG conjugated with Alexa Fluor® 488 or Alexa Fluor® 555 (Invitrogen, Carlsbad, CA, USA) was used for 1h. For double staining, cells were blocked again for 1h and stained with specific monoclonal antibody for 1 hr. After 3 washes cells were incubated with anti-mouse IgG TRITC conjugated antibody for 1h. Isotype controls were stained with only secondary antibody. Cells were then thoroughly washed and chambers were removed from the slide. Slides were rinsed in a beaker containing 1XPBS and dried. The cells were mounted with anti-fade mounting medium and carefully covered with the cover slip avoiding any air bubbles. Edges of the cover slip were sealed with transparent nail polish and dried in air. Prepared slides were stored at 4^oC in the dark for further analysis. The slides were then examined under a Bio-Rad confocal microscope using an x 60 oil immersion objective (numerical aperture 1.4) and FITC filter for Alexa Fluor® 488 and PE filter for Alexa Fluor® 555. The images obtained were then analysed using the Fiji software and NIS elements.

2.2.7.4 Image acquisition

For image acquisition, a Nikon A1si confocal microscope was used with a plan-apochromatic VC1.4 N.A. 60x magnifying oil-immersion objective. The software used for image acquisition was NIS-Elements AR 4.13.01 (Build 916). Three dimensional (3D) images were acquired in three channels, using one-way sequential line scans. DAPI was

excited at 398.7 nm with laser power 1.6 arbitrary units, and its emission collected at 450 nm with a PMT gain of 86. Alexa Fluor® 488 was excited at 488 nm with laser power 5.8, its emission collected at 525 nm with a PMT gain of 117. Alexa Fluor® 555 was excited at 560.5 nm with laser power 3.7, and collected at 595 nm with a PMT gain of 98, the scan speed was ¼ frames/s (galvano scanner). The pinhole size was 35.76 μm, approximating 1.2 times the Airy disk size of the 1.4 N.A. objective at 525 nm. Scanner zoom was cantered on the optical axis and set to a lateral magnification of 60 nm/pixel. Axial step size was 105 nm, with 80-100 image planes per z-stack.

2.2.7.5 Image processing

NIS-Elements software (version 3.21.03, build 705) was used for image processing. MIF (green) and CD74 (red) or CD74 (green) and CD44 (red) channels were segmented using regional maximum detection tools followed by manual threshold. The generated binary areas were visually inspected; the overlap of the green and red channels was generated by the overlay tool, resulting in a new layer (yellow) that represents the intersection of CD74 and MIF or CD74 and CD74. Finally, automated volume measurement was carried out for CD74, MIF, CD44 and their intersection by volume measurements tool.

2.2.8 Preparation of total protein

For Lysate preparation, a pellet of 1×10^6 cells for control, untreated and treated cells were collected and washed twice in ice cold 1X PBS. Following this, 500 μl of cell lysis mixture (Cell Lytic™ MT Reagent and Protease Inhibitor, Sigma, UK) was added. The pellet was resuspended by gentle pipetting and incubated on ice for 20 minutes. Then, the lysate was clarified by centrifugation at 15,000 rpm for 20 minutes. Finally, the protein containing supernatant was moved to a chilled test tube and the lysate was stored at -80°C for long-term use.

2.2.8.1 Bradford assay

This method is used for calculating the protein concentration in the lysate so as to calculate the amount of protein that should be loaded into each well before running the gel. This assay was based on the principal that when the Coomassie Blue Dye is bound to the protein in an acidic medium, a shift in absorbance occurs from 465 nm to 595 nm resulting in a colour change from brown to blue. The amount of complex now present in the solution is a measure for the protein concentration by means of an absorbance reading. Standard concentrations of BSA (Bovine Serum Albumin) 0.015, 0.031, 0.06, 0.125, 0.50, 1, and 2 mg/ml were prepared. A series of dilutions for the sample were prepared in PBS. 5 µl of the standards and samples respectively were added to the 96 well-plate. 250 µl of Bradford reagent was added to each well and the plate was left for incubation at room temperature for 5 minutes. The Micro-titre plate reader was switched on and set up to an absorbance of 595 nm. The plate was read and results were read three times to minimise experimental error. A graph for concentration vs. absorbance was plotted on Microsoft Excel and the protein concentration was found out using the y = mx + c equation.

2.2.9 One dimensional gel electrophoresis

2.2.9.1 SDS- PAGE

Electrophoresis is currently the most commonly technique used for the isolation and identification of proteins. This technique is based on the unique idea of separating polypeptides based on their molecular weight. The ability of a molecule to move across an electric field is inversely proportional to molecular friction (which depends on the shape and size of the molecule) and directly proportional to the voltage and the charge of the molecule. Total protein complexes can then be separated electrophoretically according to molecular weight in gels containing sodium dodecyl sulphate (SDS), in a semi-solid matrix at a set voltage. In the presence of SDS (sodium dodecyl sulphate),

proteins bind the SDS anions, and all become negatively charged and thus separated within a matrix of polyacrylamide gel in an electric field according to their molecular weights. The polyacrylamide gel concentration used determines the effective separation range of SDS-PAGE. For example, low porosity gels 15 % (w/v) total acrylamide concentration are suitable for analysis of small proteins (less than 50 kD), whereas high porosity gels 5% (w/v) total acrylamide concentration should be used for large molecular weight proteins (above 100 kD).

In this study, the protein samples were separated in 12 % resolving gels and 4% stacking gels and prepared in sterile universals, using a BioRad Mini PROTEAN Electrophoresis system. Care was taken during the addition of TEMED (tetrametylethylenediamine) and APS (ammonium persulfate) were added as they enhance the process of polymerization. Thus, these two components were only added after the system was completely set up. Once the resolving and stacking gels were polymerised completely, they were loaded with electrophoresis buffer into to the system. The previously measured protein lysate was used in sample preparation. The samples were diluted in 5X SDS-sample buffer and heated for 4 minutes at 95^{o}C before loading on 12 % SDS-PAGE. The mixture of 5 µl of sample buffer was added to 20 µl of the lysate loaded into each well. The sample and protein markers thus prepared were loaded into the wells of the gel. The system was connected to a power supply unit and run at 60V until the samples crossed the stacking gel and then increased to 120V until the samples reached the bottom of the resolving gel for approximately 2 hr. Following separation by SDS-PAGE, the gels were stained with sliver or Coomassie Blue to check the success of the transfer or processed for immunoblotting. Recipes for buffers and solutions are in the (Appendix 2 Buffer Recipes).

2.2.9.2 Coomassie blue staining

The polyacrylamide gel was carefully removed from between the plates and then placed into coomassie blue stain, covering the gel completely, for 2 hr at RT on a rocking table. Following that, the gel was placed into 100 ml of destain solution and replaced with fresh one until the gel was clear and the stained protein bands were visible. Recipes for buffers and solutions are in the (Appendix 2 Buffer Recipes).

2.2.9.3 Western transfer

Following protein separation by electrophoresis, proteins were moved to polyvinylidene fluoride (PVDF) membrane (Immobilon-FL, Merck Millipore, Merck KGaA, Darmstadt, Germany) by opening the gel system and placing the gels in a transfer buffer. Two cassettes were lined with a sponge and the gels were positioned on a filter paper above the sponge. The methanol pre-soaked PVDF membrane was positioned above the gel while an additional filter paper and sponge were stacked above. A glass pipette was rolled over to eliminate air bubbles, and the two cassettes were positioned into the Bio Rad Mini PROTEAN Electrophoresis system. Then a cooling unit and transfer buffer were added, and the system was run overnight at 30V. At the end of the transfer period, the system was disconnected from a power supply unit and the gel also stained with coomassie blue stain to check the success of the transfer.

2.2.9.4 Immunoblotting

This technique is used to detect a target protein in a sample through the monoclonal or the polyclonal antibody specific to that protein. The blocking method was the first step to this procedure. A membrane was incubated in a 5% semi skimmed milk solution with PBS-Tween-20 (Sigma-Aldrich) for 1 hr to prevent non-specific protein binding between the membrane and the antibody. The primary antibody was then diluted in PBS-T. Since the

primary antibody was specific for the protein, it would not bind to any other protein on the membrane. After incubation, the membrane was washed about 3 times with PBS-T at 10 minutes intervals to eliminate any unbound primary antibody. The membrane was then incubated with a secondary antibody to bind with the primary antibody. The membrane was washed again to remove unbound secondary antibody. Finally, the membrane was scanned with ODYSSEY Infrared Imaging System from LI-COR Biosciences. To estimate the molecular weight of the proteins being studied we used the PageRuler™ Plus Prestained Protein Ladder (#26619) from Fermentas (Thermo Fisher Scientific).

2.2.10 Co-immunoprecipitation

Immunoprecipitaion techniques are very sensitive methods to reveal molecular weights of specific antigens. Immunoprecipitaion is often used to study the interaction of different proteins with each other as part of a complex. As with most other proteins, clock proteins physically interact with one another. Immunoprecipitation is a useful method for isolating proteins of interest from cellular extracts using specific antibodies. Co-immunoprecipitation (Co-IP) is the most straightforward technique to study protein-protein interactions *in vivo*, if antibodies against the proteins of interest are available. To perform coIP, first an antibody against a target protein was coupled to Sepharose beads through protein A or G, and then the complexes containing the target protein were immunoprecipitated with the antibody-coupled beads by centrifugation. Protein components in the complexes were visualized by western blotting using antibodies specific to the different components. In this study, we utilized co-immunoprecipitation to investigate the interaction of CD74 along with other partners such as MIF and CD44 (Kaboord and Perr, 2008; van der Geer, 2013).

2.2.10.1 Experimental protocol

During this procedure, cells were lysed with RIPA lysis buffer system (Santa Cruz Biotechnology, USA) and incubated for 20 minutes. This was achieved by mixing the following: 1 ml of RIPA lysis buffer with 10 µl of protease inhibitor cocktail in DMSO, (200mM) PMSF (phenylmethylsulfonyl fluoride) in DMSO (Dimethyl sulfoxide) and (100mM) sodium orthovanadate in water. After incubation, cells were centrifuged at 14,000 rpm for 15 minutes, and the total protein concentration was determined by Bradford assay. 1 mg/ml of each sample was incubated with 4 µg of specific primary antibody for the protein overnight at 4°C. Then, 40 µl of protein A/G PLUS- Agarose (Santa Cruz Biotechnology, USA) was added and kept overnight on a rotator at 4°C. After incubation, the samples were spun down for 30 seconds and the supernatant was discarded. Beads were then washed twice using PBS and the samples were boiled at 100°C after adding 50 µl of SDS-PAGE sample loading buffer containing Dithiothreitol (DTT). Then, 20 µl of each sample was loaded in each well of the gel and they were left for 1 hr and 30 minutes at 120V. After electrophoresis, protein was transferred to a polyvinylidene fluoride (PVDF) membrane (Immobilon-FL, Merck Millipore, Merck KGaA, Darmstadt, Germany). Membranes were blocked with 5% skimmed milk in PBS-Tween-20 (Sigma) for 1 hr at room temperature and incubated in primary antibody specific for protein co-immunoprecipitation (Co-IP) followed by washing in PBS-T for 30 minutes. The membranes were then incubated with secondary antibody, the IRDye 800CW Donkey anti-Mouse IgG (Li-Cor Bioscience, Licoln, NE, USA) for 1 hr and then by washed in PBS-T for 30 minutes. Signals were detected using the ODYSSEY Infrared Imaging System (Li-Cor Biosciences).

2.2.11 siRNA transfection

2.2.11.1 Principle

Mammalian cell transfection is a technique commonly used to express exogenous DNA or RNA in a host cell line (for example, for generating RNAi probes). Transfection is the introduction of foreign material into eukaryotic cells. It typically involves the opening of transient pores or 'holes' in the cell plasma membrane to allow the uptake of molecules, such as supercoiled plasmid DNA or siRNA constructs. There are many different ways to transfect mammalian cells, depending on the cell line characteristics, desired effect, and downstream applications such as transient transfection, stable transfection and siRNA transfection. In this study, siRNA transfection was used as described below.

2.2.11.2 siRNA transfection protocol

CAMA-1 and MDA-MB-231 cell lines were seeded in six well plate at density of 2×10^5 per well in 2 ml normal growth medium supplemented with 10% FCS. The cells were then allowed to grow until they reached 60-80% confluency. For each transfection, 4 µl of CD74 siRNA duplex at dose of 80 pmols (sc-35023) (Santa Cruz Biotechnology, USA) was diluted and 4 µl of siRNA transfection regent was added at dose of 80 pmols (sc-29528) (Santa Cruz Biotechnology, USA) into 100 µl of siRNA transfection medium (sc-36868) (Santa Cruz Biotechnology, USA) separately without serum or antibiotics. Both diluents were mixed together and incubated for 15-45 minutes at room temperature. Cells were then washed with 2 ml of siRNA transfection medium. The siRNA transfection regent mixture was then added to each well and the volume made up to 1 ml by adding 800 µl of siRNA transfection medium (Santa Cruz Biotechnology, USA). In the same manner, this was applied for negative control siRNA (sc-44230) (Santa Cruz Biotechnology, USA). The cells were then incubated overnight at 37ºC in a CO_2 incubator for 18-24 hr. Following incubation, the medium was aspirated and replaced

with fresh 1X normal growth medium. Cells were assayed using the appropriate manufacturer's protocol 24-72 hr after the addition of fresh medium in the step above. Transfection efficiency was confirmed by western blot and microscopy. Once the transfection was confirmed, the effect of CD74 siRNA on the proliferation and apoptosis of CAMA-1 and MDA-MB-231 could then be studied.

2.2.12 Apoptosis assay

2.2.12.1 Principle

Apoptosis, or programmed cell death, is a normal physiological process occurring to remove unwanted cells. An early apoptotic event is the translocation of membrane phosphatidylserine (PS) from the inner side of the plasma membrane to the surface. Annexin V, a Ca2+-dependent phospholipid-binding protein, has high affinity for PS, and fluorochrome-labelled Annexin V can be used for the detection of exposed PS using flow cytometry.

2.2.12.2 Experimental protocol

CAMA-1 and MDA-MB231 cell lines were cultured in 6 well plate at a density of (15×10^3 cell/well) at 37°C, and then transfected with CD74 siRNA duplex as explained previously. The cells were then washed twice with 1X PBS and incubated with 2 µl of Annexin V-FITC (BioLegend, UK) at room temperature for 20 minutes in the dark. Cells were then thoroughly washed and then fixed with 4 % PFA followed by washing steps in PBS. Finally the samples were read using BD FACSAria and analysed by FlowJo 8.8.6.

2.2.13 Two-Dimensional gel electrophoresis

2.2.13.1 Preparation of cell lysate

Untreated and IFN-γ treated CAMA-1 and MDA-MB-231 cells cultured in 100 mm cell culture dishes (Nunc, UK), and 1×10^7 cells were used per sample to make cell lysate.

Cells were detached from culture dishes using accutase, counted and washed with 1X PBS as described earlier. The cell pellet was resuspended in 1 ml of the protein extraction buffer containing 7M urea, 2M Thiourea, 4% CHAPS, 1X protease inhibitor cocktail, 20 mM DTT, 1% ampholyte, and Bensonase. All reagents were purchased from Sigma, UK. Cells were vortexed and sonicated for 5 minutes at 4°C. Cell lysates were spun at 20,000 rpm for 10 minutes, supernatant was collected into a clean micro-centrifuge tube and stored at -80°C for later use. The protein concentration of cell lysates was estimated using the Coo Assay (Uptima, Interchim, France) following manufacturer's instructions.

2.2.13.2 First dimensional gel isoelectric focusing (IEF)

The Immobiline dry strip gel pH 3-10NL, 18cm (GE Healthcare Bio-Sciences AB) used in this study was rehydrated in an immobiline dry strip reswelling tray. The dry strip was rehydrated for 24 hr at room temperature in 350 µl of rehydration buffer (7M urea, 2M thiourea, 4% CHAPS, 1X protease inhibitor cocktail, 20 mM DTT, 1% ampholyte, 0.1% bromophenol blue, 0.05% SDS) containing 80 µg of sample proteins. The IPG strip was overlaid using approximately 3 ml of immobiline PlusOne dry strip cover fluid (GE Healthcare Bio-Sciences AB). After rehydration, the IPG strip was briefly rinsed with ultrapure water to remove crystallized urea.

For isoelectric focusing, the IPG-Phor was cleaned with Strip holder cleaning solution (GE Healthcare Bio-Sciences AB). The Ettan IPG Phor3 was switched on and connection with the IPG Phor3 control software was established. IPG Phor mainfold was covered with 108 ml of Immobiline PlusOne dry strip cover fluid and the rehydrated strips were then placed in individual lanes of Ettan IPG strip holder (GE Healthcare Bio-Sciences AB) under the fluid using tweezers with the positive end towards the anode end of the mainfold. Hydrated filter wicks were placed between the IPG strips and the electrodes.

The cathodic (-ve) filter wick was rehydrated with 150 µL of 100 mM DTT. The anodic (+ve) filter wick was hydrated with 150 µL miliQ water. The lid was closed and IPG-Phor programme was run according to the programme below. A holding step at the end was added to so that it could be left overnight.

Step 1	200 V	500 V hr
Step 2	500 V	500 V hr
Grad 3	1000 V	800 V hr
Grad 4	10,000 V	16,500 V hr
Step 5	10,000 V	6,200 V hr
Step 6	200 V	24 hr

At the end of the programme, the computer was disconnected and IPG-Phor was stopped. The paper wicks were removed with tweezers and discarded. The IPG strips were placed in a petri dish, rinsed briefly with deionized water, labelled and stored at –80 °C for later use.

2.2.13.3 SDS-PAGE gel preparation

For second dimension gel electrophoresis, the PROTEAN® II System (BIO-RAD, UK) was used. Glass plates were cleaned with 70% ethanol, dried, assembled with 2 mm spacers and clipped into the casting frame. Purite water was poured between the plates to check for leakage. Assemblies that leaked were taken apart and re-clipped and the process was repeated. Upon establishing a non-leaking system, the water was removed and the system was dried in situ with pressurized airflow. The gel solution 12% SDS PAGE was made with water, 1.5 M Tris-HCl and 30% acrylamide solution. These were placed in a flask and degassed for 15 minutes at ambient temperature. The TEMED, APS and SDS were added and mixed by stirring. The gel solution was poured in between glass plates,

avoiding any air bubbles, to 1 cm below the lowest plate. The top of the gels was covered with overlay buffer (water saturated isopropanol 80%) and allowed to polymerise overnight.

2.2.13.4 Equilibration of the IPG strips

Prior to the second dimension gel run, the Immobilized pH Gradient (IPG) strips containing isoelectrically focussed proteins were equilibrated and reduced. For each strip, two vials of 10 ml aliquots of frozen equilibration buffer were thawed at room temperature. In one vial of equilibration buffer 100 mg of DTT was added while in the other 400 mg of iodo-acetamide was added and allowed to mix gently. The IPG strips were first equilibrated in equilibration buffer containing 1% DTT, then in a buffer containing 4% iodo-acetamide for 15min each at room temperature. The IPG strips were rinsed with 1X electrophoresis buffer before placing on second dimension gel.

2.2.13.5 Assembly and running of second dimensional gel

Agarose sealing solution was heated to liquefy. IPG strips were trimmed from each end up to 0.6 cm thus giving a final length of 16 cm. A small square of paper electrode wick (2 × 3 cm half thickness) was loaded with 10 µl of molecular weight marker and placed on the top of left hand corner of the gel. The IPG strip was placed into the well of the 12% SDS PAGE gel with the acidic side facing the glass plate hinge and sealed with agarose solution, avoiding any air bubbles. The electrophoresis tank was filled with 1.5 L of gel running buffer. The gels with strips were removed from the casting assembly and clipped onto the core unit of the protean tank. The core unit was lifted into the tank, running buffer was added to the top of the upper buffer chamber and air bubbles were removed with a glass rod. The lid was fitted to the tank and cables were connected to the power Pac (Bio-Rad, Power Pac 1000). Electrophoresis was carried out first at 50V for 30

minutes and then at 150V for about 4.5 hr or until the bromophenol blue dye front had reached to the lower end. The core unit was then removed from the tank disassembled and gels were removed from the clamps. The spacers were loosened and one edge of the glass plate was lifted up with a spatula. The gel was then placed in a glass container containing gel fixing solution.

2.2.13.6 Silver staining

For visualization of protein spots a modified silver staining protocol was used as previously described (Yan et al., 2000; Yan and Chen, 2005). Briefly, after electrophoresis gels were fixed for half an hour in fixing solution they were sensitized for 30 minutes and washed with ultrapure water. Staining was carried out using 2.5% silver nitrate solution for 20 minutes followed by a careful wash with ultrapure water for a maximum of 1 min. The gels were developed for 10-15 minutes until spots appeared, and the reaction was stopped by washing with stop solution for 10 minutes. The gels were washed 3 times with ultrapure water and stored in gel preserving solution at 4°C.

2.2.13.7 Gel image capture and spot analysis

Gels were scanned using the scanner (Epson image scanner III) with LabScan 6.0 software. First the scanner was calibrated and set to use the transparent settings at 300 dpi with the blue filter. The scanner surface was cleaned with 70% ethanol and a little purite water was poured on the surface. The gel was placed directly on the scanner, previewed and air bubbles were smoothed out if any were present. The scan area of the gel was then selected and scanned. Gel images were saved as mel and tiff files. Scanned gel images were characterised with Progenesis SameSpot software package (Nonlinear Dynamics Limited, UK).

2.2.13.8 Statistical analyses

All results in this research were carried out in at least triplicate experiments. The mean of each set of data was calculated and the standard error (±SD) was also included in order to present the reliability of the mean reading.

Chapter 3 Immunophenotyping of CD74, MIF and CD44 expression on human breast cancer derived cell lines

3.1 Introduction

In the light of numerous instances of the breakdown of immunologic self-tolerance, the former paradigm that the primary function of the immune system is to discriminate between self and non-self (e.g. foreign antigens or mutated self-antigens) has recently been queried. The identification of a handful of potentially immunogenic cancer antigens shows that they are not truly foreign. Although the boundary between self and non-self is not well defined, this first look at cancer antigens fits more with a self/altered self paradigm than with the non-self paradigm for antigens recognized in infectious diseases (Houghton, 1994). Resultantly, the likelihood that the immune system does not recognize between self and non-self has led to the proposal of the "Danger" model of the immune system (Matzinger, 1994, 2001; Fuchs and Matzinger, 1996; Aickelin and Cayzer, 2008). This model suggests that the immune system may be concerned with the detection of damaged cells rather than recognition of non-self (Matzinger, 2001, 2002). Tumour cells might exemplify the "Danger" model, threatening the host immune system. The contemporary self-non-self discrimination model assumes that immune system protects the organism against everything, which is foreign, thus immune responses are directed towards external entities, which are non-self antigens. According to the danger model the immune system detects and then responds to anything dangerous and not necessarily foreign (Matzinger, 1994; 1998; Fuchs & Matzinger, 1996). The whole model is based on the principle that the presence or absence of the so called second signal determines immune responsiveness or tolerance. Whereas the first signal comes from specific antigen recognition, the second signal is generated from either help delivered by T-helper lymphocytes or co-stimulation from professional antigen presenting cells (Kowalczyk, 2002).

As described previously, tumour antigens are identified and eliminated through the

process known as immunoediting (based on tumour immune surveillance). In fact, tumour immune surveillance is considered an important process that prevents the formation of cancers and maintains cellular homeostasis (Dunn et al., 2002, 2004). It has been suggested that the immune system recognizes tumour cells as "non-self" and then rejects them. Tumours that arise from non-virally transformed cells are considered, as "self", and therefore the immune system cannot recognize the tumours as "non-self" (Klein and Klein, 2005; Swann and Smyth, 2007).

Based on the above, efforts have been made to manipulate the immune system in order to identify tumour cells that are carrying 'foreign antigens'. One way to achieve this is to monitor the expression of selected molecules that are required for immunological responses. In this context, MHC class II molecules that are normally found only on APCs, are considered to be significant molecules due to their role in antigen presentation (Vyas et al., 2008; Neefjes et al., 2011). In contrast, MHC class I molecules are expressed by all nucleated cells and present fragment of cytosolic and nuclear origin at the cell surface allowing for cytotoxic cell based elimination upon infection or transformation (Neefjes et al., 2011). However, a previous study was carried out on the breast cancer cell lines TD7D and ZR75-1, which showed low expression of MHC class I molecules and no expression of MHC class II molecules. Surprisingly, the expression of MHC molecules can be found in non-professional antigen presenting cells such as epithelial cells (Tsunawaki et al., 2002). Since most breast cancers are considered adenocarcinomas and arise from epithelial cells, it is believed that these cells could express MHC molecules normally however these molecules may behave differently (Elenbaas et al., 2001; Dimri et al., 2005; Kumar et al., 2005). It is suggested that high levels of CD74 expression is associated with class II MHC expression and might prevent tumour antigen presentation by blocking the peptide-binding cleft, thus leading to a lack of recognition of tumour cells

by immune cells (Beswick and Reyes, 2009; Borghese and Clanchy, 2011; Zheng et al., 2012).

A number of molecules play a key role in to play a crucial role in tumour progression. These include CD74, MIF and CD44 (Meyer-Siegler et al., 2004). These molecules have been identified in several types of cancers and are believed to play a role in immunotolerance (Becker-Herman et al., 2005). CD74 expression has been observed in several types of cancer, including multiple myeloma, as well as in solid tumour cancers, such as gastric cancer, kidney and small-cell lung cancer (Ishigami et al., 2001; Young et al., 2001; Burton et al., 2004; Butrym et al., 20013). CD74, along with CD44, has been suggested to mediate MIF signalling pathway in bladder and prostate cancer cell lines (Meyer-Siegler et al., 2004; Meyer-Siegler et al., 2006). MIF has a critical role in tumourigenesis due to its overexpression by cancer cells; it is widely documented that MIF is overexpressed in breast cancer, prostate cancer and colon carcinoma tumours (Conroy et al., 2010). CD44 is able to promote tumour cell invasiveness, self-renewal and sustained survival, and for these reasons has the ability to prompt many types of cancer (Toole and Slomiany, 2008; Fedorchenko et al., 2013).

The key aim of this study was to investigate the expression profile of CD74, MIF and CD44 molecules on the breast cancer derived cell lines CAMA-1, MDA-MB-231 and MDA-MB-435. To validate this study the expression of CD74, MIF and CD44 on the normal breast cell line 266LDM, whole cell lysate obtained from adult normal breast tissue and normal breast tissue section were investigated. In order to test this flow cytometry, Western blotting and microscopy were employed.

3.2 Results

3.2.1 Granularity, viability and size of malignant and non-malignant cells

The viability and granularity of the breast cancer cell lines CAMA-1, MDA-MB-231 and MDA-MB-435 and normal breast cells (226LDM) were tested using flow cytometry. This was achieved using cells with no staining. The obtained results show that all breast cells, whether they were malignant or benign, were the same cell size and almost all the cells showed the same viability, which was around 88% to 92 %. Figure 3-1 shows results obtained from a flow cytometer.

3.2.2 Cell-surface expression of HLA-A, B, C and HLA-DR

The expression of HLA-A, B, C and HLA-DR molecules on the cell-surface of CAMA-1, MDA-MB-231 and MDA-MB-435 cells and normal breast cells was tested to examine the immunogenicity of these cell lines as models of malignant and non-malignant cells. Figure 3-2 shows results obtained from a flow cytometer. The results showed that MDA-MB-231 and MDA-MB-435 cells express the same level of HLA-A, B, C and HLD-DR respectively. In contrast, CAMA-1 and 266LDM cells did not express HLA-A, B, C and HLA-DR or the expression was very weak.

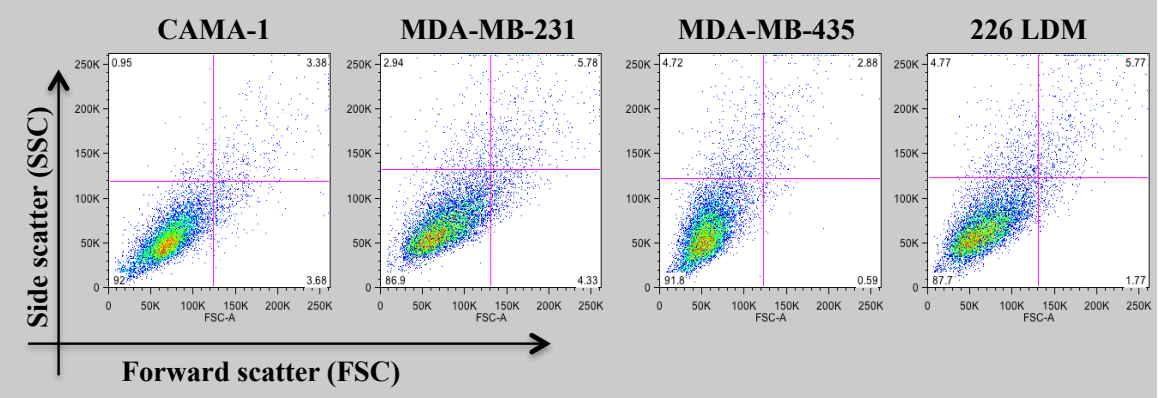

Figure 3-1: Scatter plots displaying forward scatter (FSC) *(X-axis)* and side scatter (SSC) *(Y-axis)* of breast cancer cell lines CAMA-1, MDA-MB-231 and MDA-MB-435 and normal breast cell lines (226LDM).

The FCS scatter data provide information on the relative size of the cells whereas SSC scatter data estimate the granularity. The units indicate the level of light scatter brightness with 0 being the dullest and 1000 being the brightest. Each dot is a cell ranked by its brightness. Data is representative of three independent experiments.

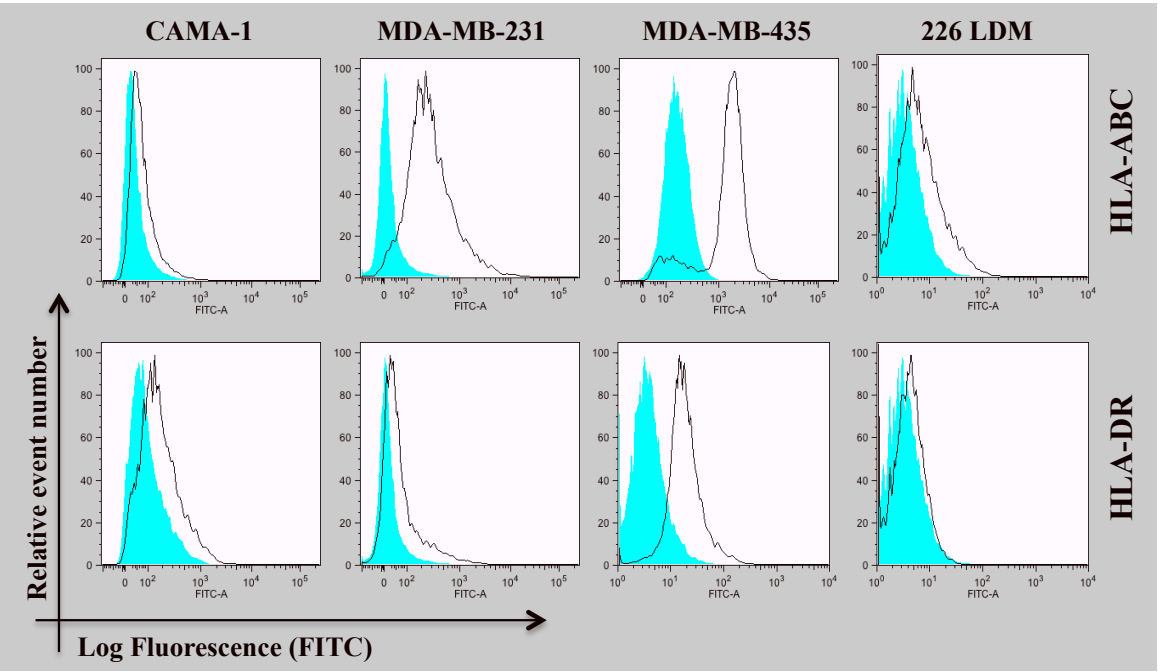

Figure 3-2: Analysis of the expression of cell-surface of HLA-A, B, C and HLA-DR in the breast cancer cell lines CAMA-1, MDA-MB-231 and MDA-MB-435 and in the normal breast cell line (226LDM).

Flow cytometry analysis showing HLA-A, B, C and HLA-DR expression (empty histograms), displayed as mean fluorescence intensity at the cell-surface for CAMA-1, MDA-MB-231, MDA-MB-435 and 226LDM cells. Negative controls were performed by using an isotype-matched control antibody (blue-filled histograms). Data is representative of three independent experiments.

3.2.3 Identification and quantification of CD74, MIF and CD44

The cell-surface and intracellular expression of CD74, MIF and CD74 was analysed in CAMA-1, MDA-MB-231 and MDA-MB-435 cells. Non-permeabilized and permeabilized cells with 0.1 % Triton x-100 were stained with an appropriate concentration of By2 (anti-CD74), ab55445 (anti-MIF) and 156-3C11 (anti-CD44) antibodies followed by 1 µl RAM-FITC secondary antibody. Cells without staining and isotype cells, stained with only secondary antibody, were used as a negative control. CD74, MIF and CD44 expression was detected on the cell-surface and cytoplasmic of CAMA-1, MDA-MB-231 and MDA-MB-435 cells (Figures 3-3, 3-4 and 3-5). Monocytes, Raji cells, cervical cancer HeLa cells and lymphocytes, (Jurkat) cells, were used as a positive control as they express high levels of CD74, CD44 and MIF respectively.

Results are shown as histograms where mean fluorescence intensity (MFI) is along the horizontal axis (x-axis) versus total cell count on vertical axis (y-axis). This is displayed in (Figures 3-3 A, 3-4 A and 3-5 A) where empty histograms show CD74, MIF or CD74 protein expression as indicated while blue histograms represent isotype-matched negative control. Mean fluorescence intensity (MFI) values were further used to plot the bar graphs and CAMA-1, MDA-MB-231 and MDA-MB-435 cell lines under study were compared for the level of CD74, MIF and CD44 expression separately (Figures 3-3 B, 3-4 B and 3-5 B).

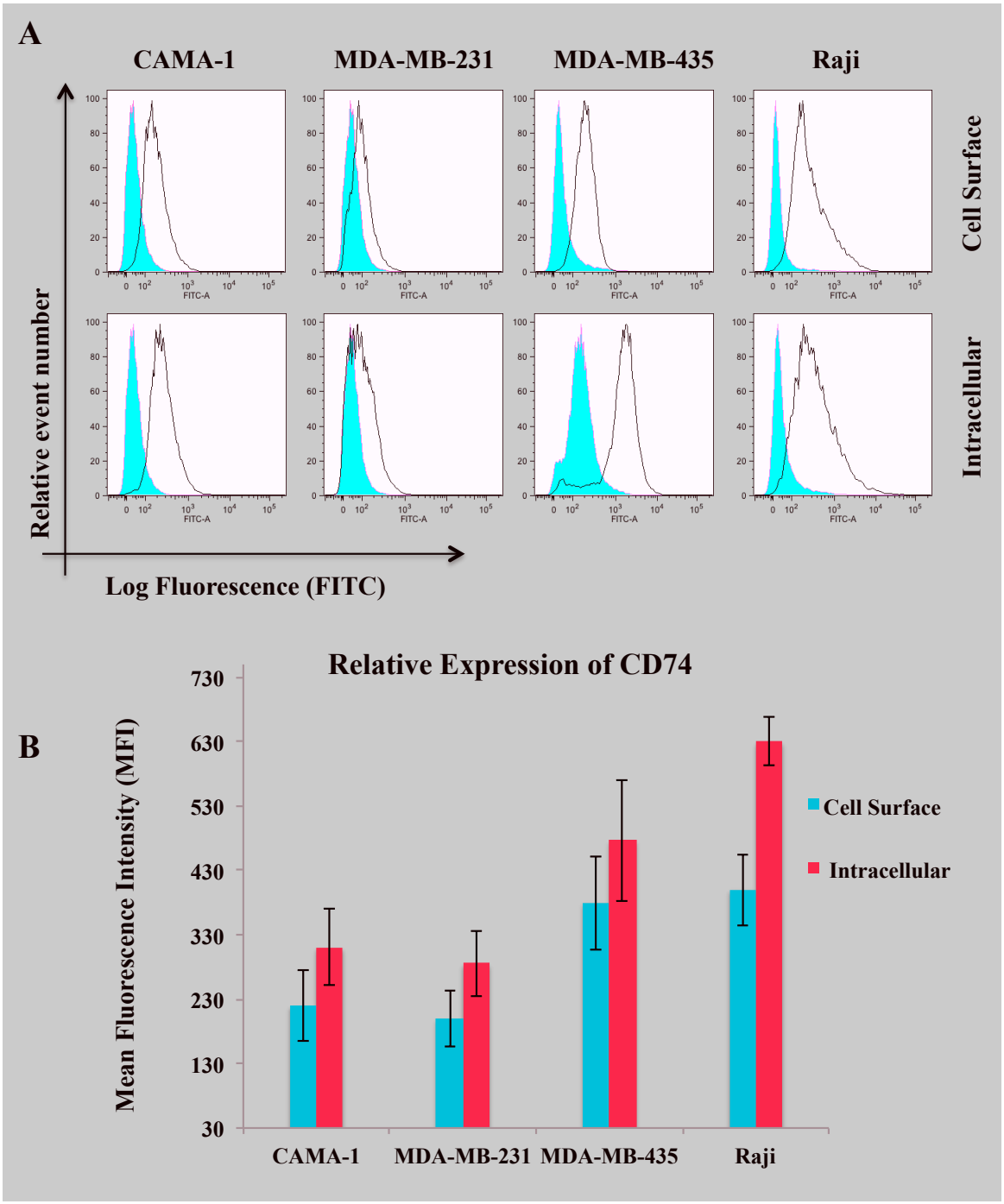

Figure 3-3: Analysis of the expression of cell-surface and intracellular CD74 in the breast cancer cell lines CAMA-1, MDA-MB-231 and MDA-MB-435.

(A) Flow cytometry analysis showing CD74 expression (empty histograms), displayed as mean fluorescence intensity, on the cell-surface and intracellularly for CAMA-1, MDA-MB-231 and MDA-MB-435 cells. Surface and intracellular expression of CD74 in Rji cells are shown as a positive control. Negative controls were performed by using an isotype-matched control antibody (blue-filled histograms). (B) Graphical representation of CD74 surface and intracellular protein expression on CAMA-1, MDA-MB-231 and MDA-MB-435 cells. Bar graphs represent level of each protein in mean values ± SD in each cell line. Data is representative of three independent experiments.

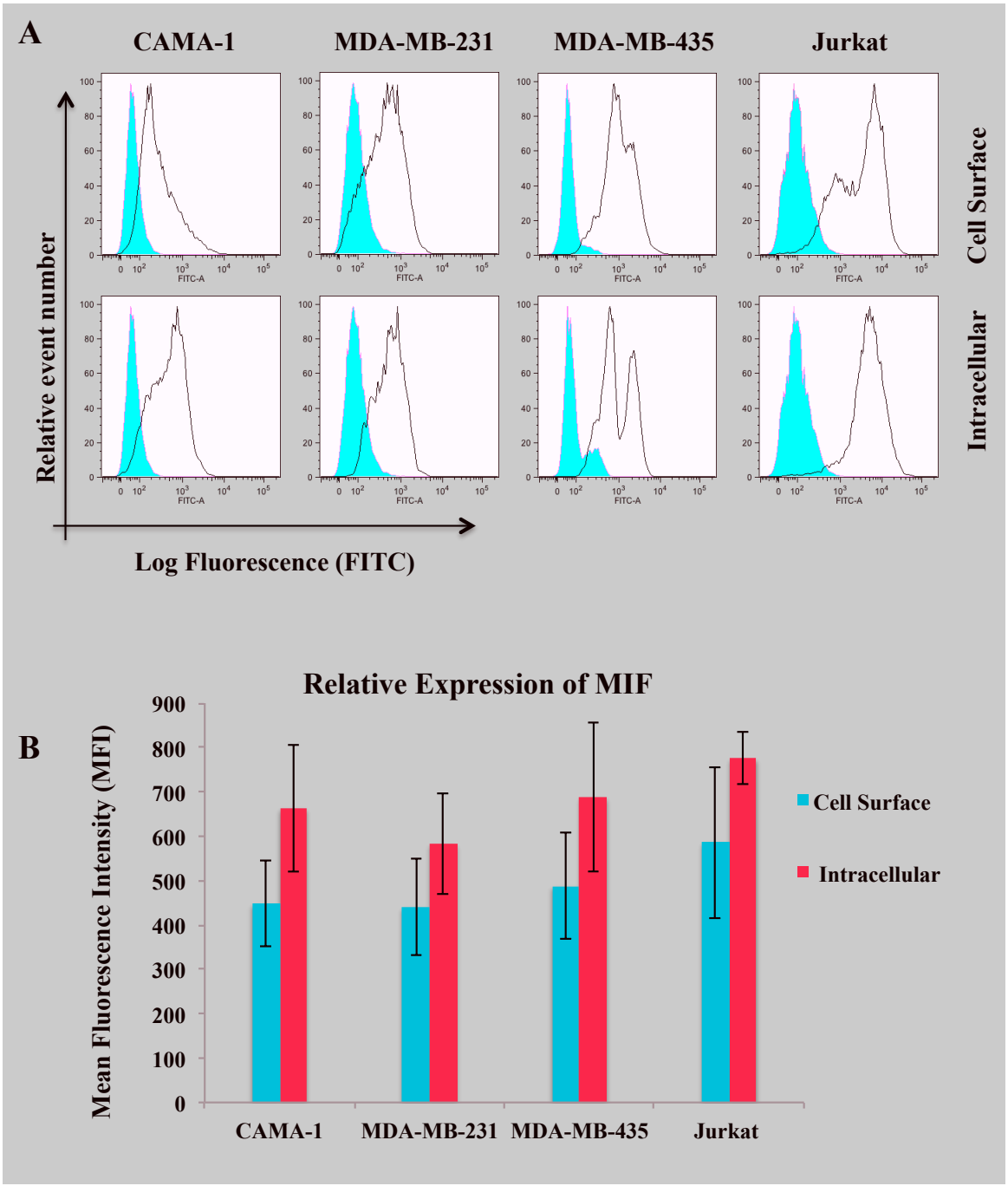

Figure 3-4: Analysis of the expression of cell-surface and intracellular MIF in the breast cancer cell lines CAMA-1, MDA-MB-231 and MDA-MB-435.

(A) Flow cytometry analysis showing MIF expression (empty histograms), displayed as mean fluorescence intensity, on the cell-surface and intracellularly for CAMA-1, MDA-MB-231 and MDA-MB-435 cells. Cell -surface and intracellular expression of MIF in Jurkat cells are shown as a positive control. Negative controls were performed by using an isotype-matched control antibody (blue-filled histograms). (B) Graphical representation of MIF surface and intracellular protein expression on CAMA-1, MDA-MB-231 and MDA-MB-435 cells. Bar graphs represent the levels of each protein in mean values ± SD in each cell line. Data is representative of three independent experiments.

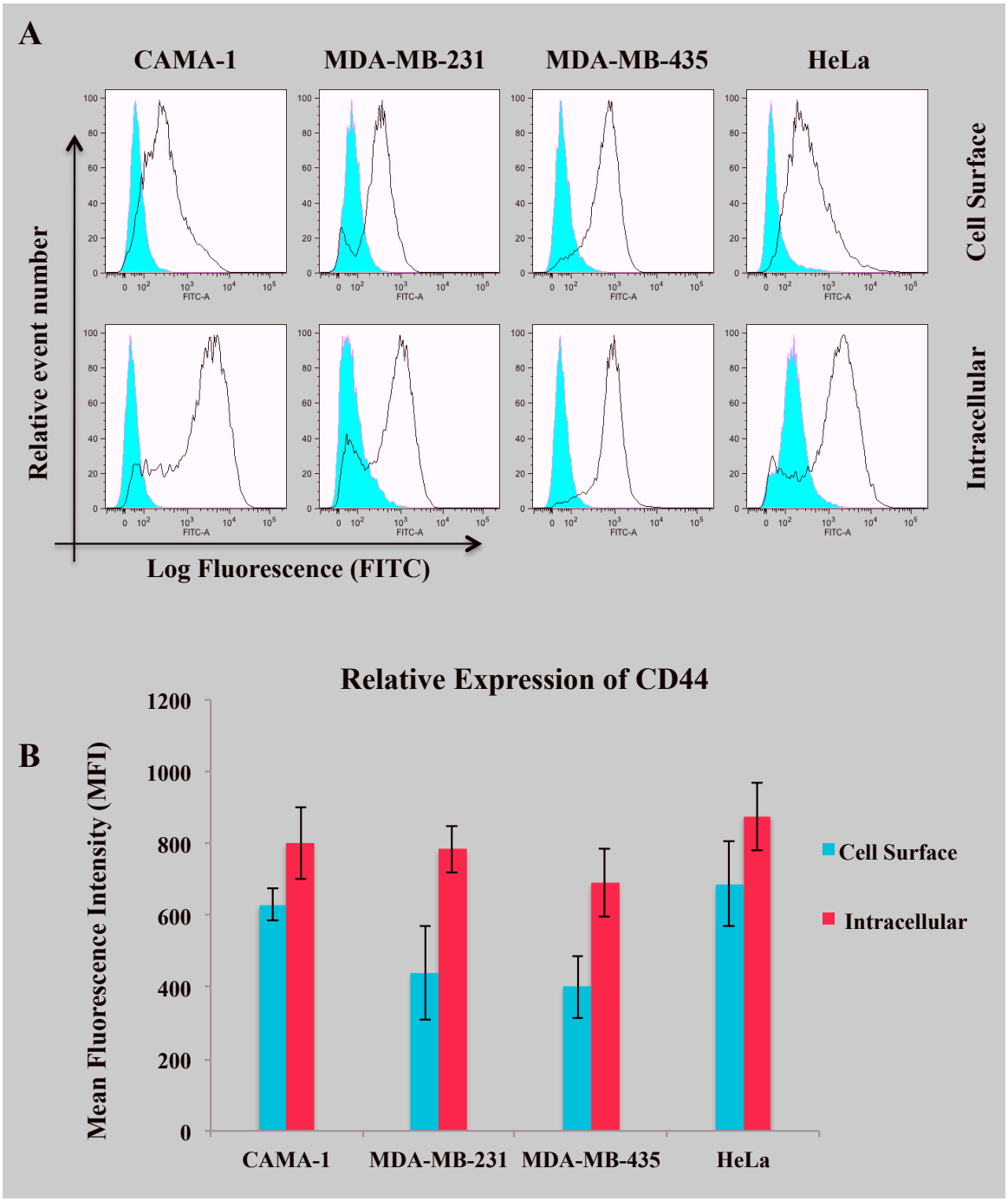

Figure 3-5: Analysis of the expression of cell-surface and intracellular CD44 in the breast cancer cell lines CAMA-1, MDA-MB-231 and MDA-MB-435.

(A) Flow cytometry analysis showing CD44 expression (empty histograms), displayed as mean fluorescence intensity, on the cell-surface and intracellularly for CAMA-1, MDA-MB-231 and MDA-MB-435 cells. Surface and intracellular expression of CD44 in HeLa cells are shown as a positive control. Negative controls were performed by using an isotype-matched control antibody (blue-filled histograms). (B) Graphical representation of CD44 surface and intracellular protein expression on CAMA-1, MDA-MB-231 and MDA-MB-435 cells. Bar graphs represent the levels of each protein in mean values ± SD in each cell line. Data is representative of three independent experiments.

3.2.4 Immunoblot analysis of CD74, MIF and CD44

CD74, MIF and CD44 protein expression in CAMA-1, MDA-MB-231 and MDA-MB-435 cells was analysed by Western blot analysis using By2 (anti-CD74), D-2 (anti-MIF), 156-3C11 (anti-CD44), and TU-02 (anti- α-Tubulin) and Poly6221 (anti β-Actin). By2 (anti-CD74) is specific for CD74 isoforms 31-45 kDa and 156-3C11 (anti-CD44) is a mouse mAb that detects endogenous levels of total CD44 protein and is specific for most isoforms (80-90 kDa). The MIF-specific antibody, D-2, is a mouse monoclonal antibody mapping an epitope between amino acids 7 to 39 at the N-terminus of the MIF protein. THP-1 monocytic cells, Jurkat cells and cervical cancer HeLa cells were used as a positive control, expressing high levels of CD74, MIF and CD44.

The results obtained show that the molecular weight of CD44, α-tubulin, β-actin, CD74 and MIF are 80-90 kDa, 50-55 kDa, 42 kDa, 33-41 kDa and 12 kDa respectively. β-actin and α-tubulin were used as a loading control, since their expression not affected by any treatments such as IFN-γ or LPS. CAMA-1, MDA-MB-231 and MDA-MB-435cell lines expressed CD74 isoforms, MIF and CD44 however CAMA-1 cells expressed two isoforms of CD44 (CD44s and CD44v) (Figure 3-6 A). To evaluate the differences in protein loading during the experiment, the percentage of regulation was calculated after the intensity of each band was adjusted according to its respective β-Actin band intensity (Figure 3-6 B) using the Image Studio Lite software (LI-COR Biosciences).

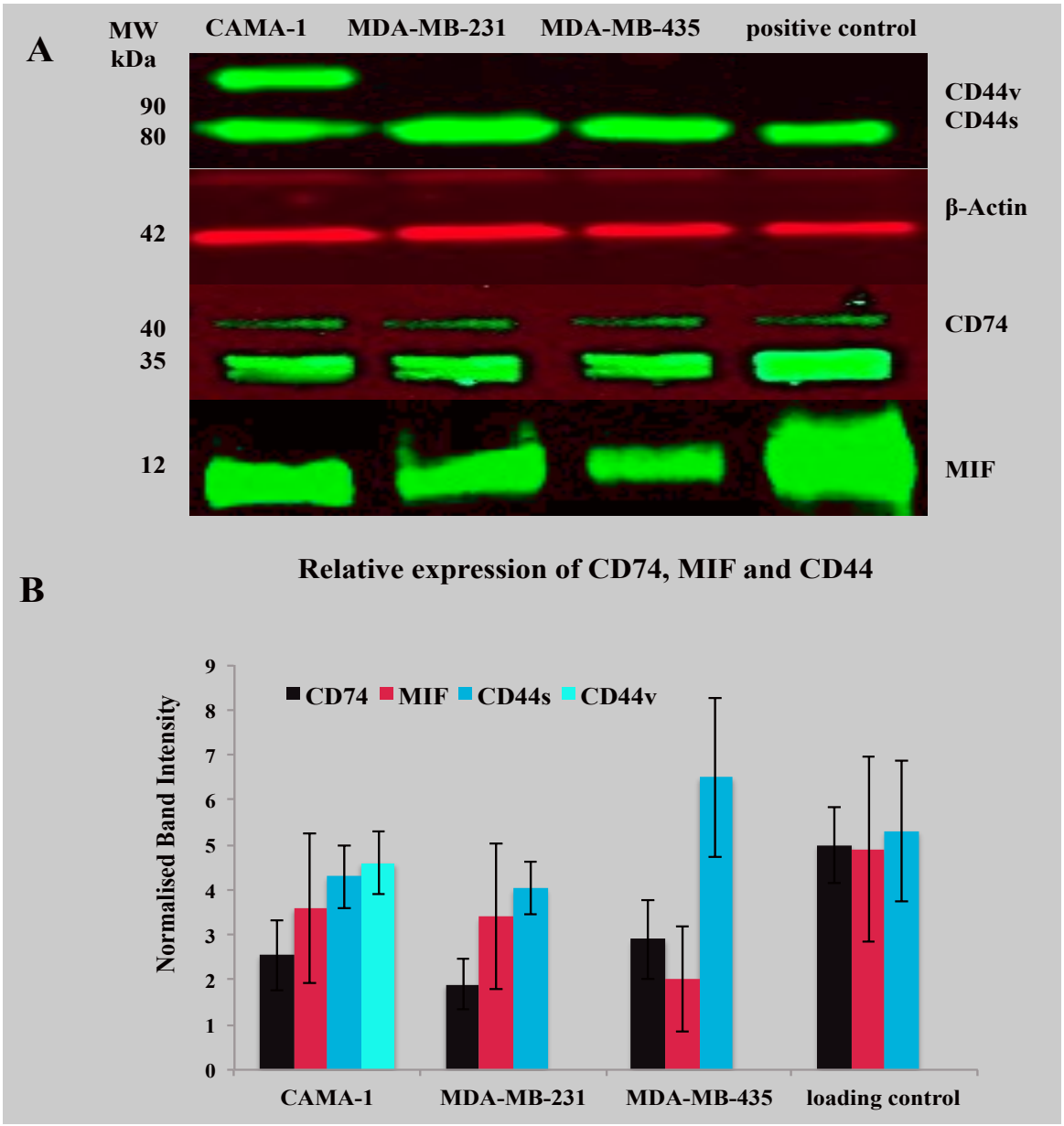

Figure 3-6: Semi-quantitative Western blot analysis of CD74, MIF, CD44 and β-Actin expression, detected according to their molecular weight in CAMA-1, MDA-MB-231 and MDA-MB-435.

(A) 12% SDS-PAGE was performed under reducing conditions, followed by Western blotting with primary monoclonal antibodies Poly 6221 (anti β-Actin as loading control), By2 (anti-CD74), 156-3C11 (anti-CD44), D-2 (anti-MIF). β-Actin is detected at a molecular weight of 42 kDa. Monocytes (THP-1 cells), cervical cancer HeLa cells and Jurkat cells were used as a positive control as they express high levels of CD74, CD44 and MIF respectively. CD44, CD74, β-Actin and MIF on untreated CAMA-1, MDA-MB-231 and MDA-MB-435 cells are also shown. CD44 isoforms were detected at expected molecular weights; 90 and 80 kDa, CD74 at 33, 35 and 41 kDa and MIF at 12 kDa. The expression of target proteins was normalised according to its respective β-actin band intensity using the Image Studio Lite software (LI-COR Biosciences). (B) Graphical representation of CD74, CD44 and MIF protein expression on CAMA-1, MDA-MB-231 and MDA-MB-435 cells. Bar graphs represent the level of each protein in mean values ± SD in each cell line. A representative immunoblot of three independent experiments.

3.2.5 Confocal microscopy

Cell-surface staining of CD74, MIF and CD44 in THP-1, Jurkat and HeLa cell lines as positive controls was performed as per the protocol for breast cancer cell lines since they express high level of above mentioned molecules (Figure 3-7). Negative control samples stained with IgG isotype and secondary antibodies were also imaged using the same acquisition protocol as for all data sets, where no signals above background fluorescence were observed (Figure 3-8), thus minimising false positive signals.

Cell-surface and intracellular expression of CD74, CD44 and MIF proteins was visualized by laser scanning confocal microscopy using different wavelengths. The CAMA-1, MDA-MB-231 and MDA-MB-435 cell lines all exhibited expression of CD74, CD44 and MIF on the surface and intracellular membranes of cells (Figure 3-9 A, B). CD74 or MIF was labelled with Alexa Fluor® 488 (green), CD44 Alexa Fluor® 555 (red) and cell nuclei were stained with 4 ', 6-diamidino-2-phenylindole (DAPI) (blue).

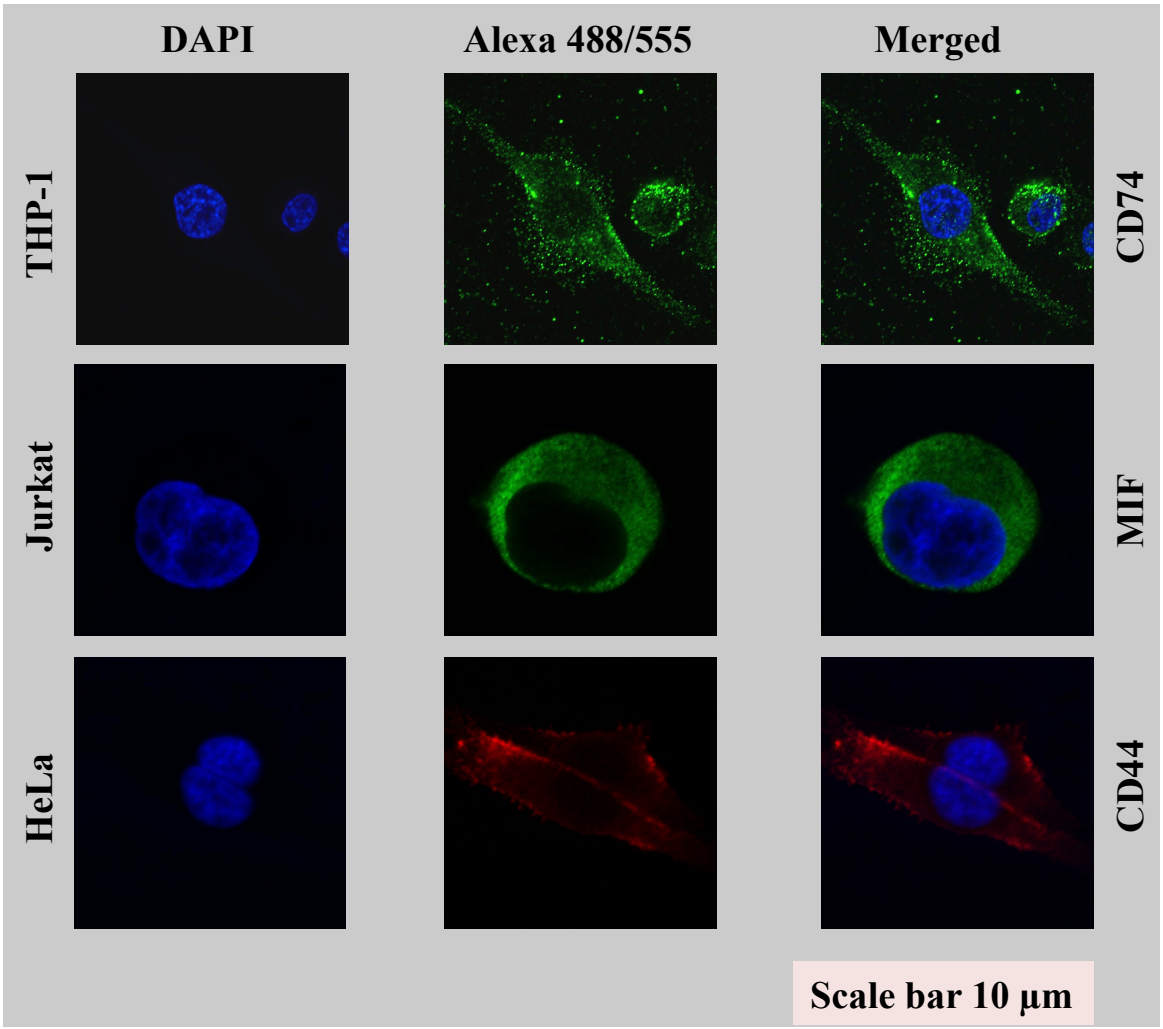

Figure 3-7: Cell-surface staining of CD74, MIF and CD44 of THP-1, Jurkat and HeLa cells as visualised by confocal laser scanning microscopy.

All cells were cultured in LabTek 8-well chambers at a density of 6×10^3 cells per well overnight. Cells were stained either with CD74 or MIF labelled with Alexa Fluor® 488 (green). CD44 was labelled with Alexa Fluor® 555 (red), cell nuclei were stained with 4', 6-diamidino-2-phenylindole (DAPI), which is shown in blue. Fluorochromes were acquired separately to evaluate the expression of CD74, CD44 and MIF using the Fiji software. Photomicrographs are representative of three independent experiments. Scale bar 10 µm.

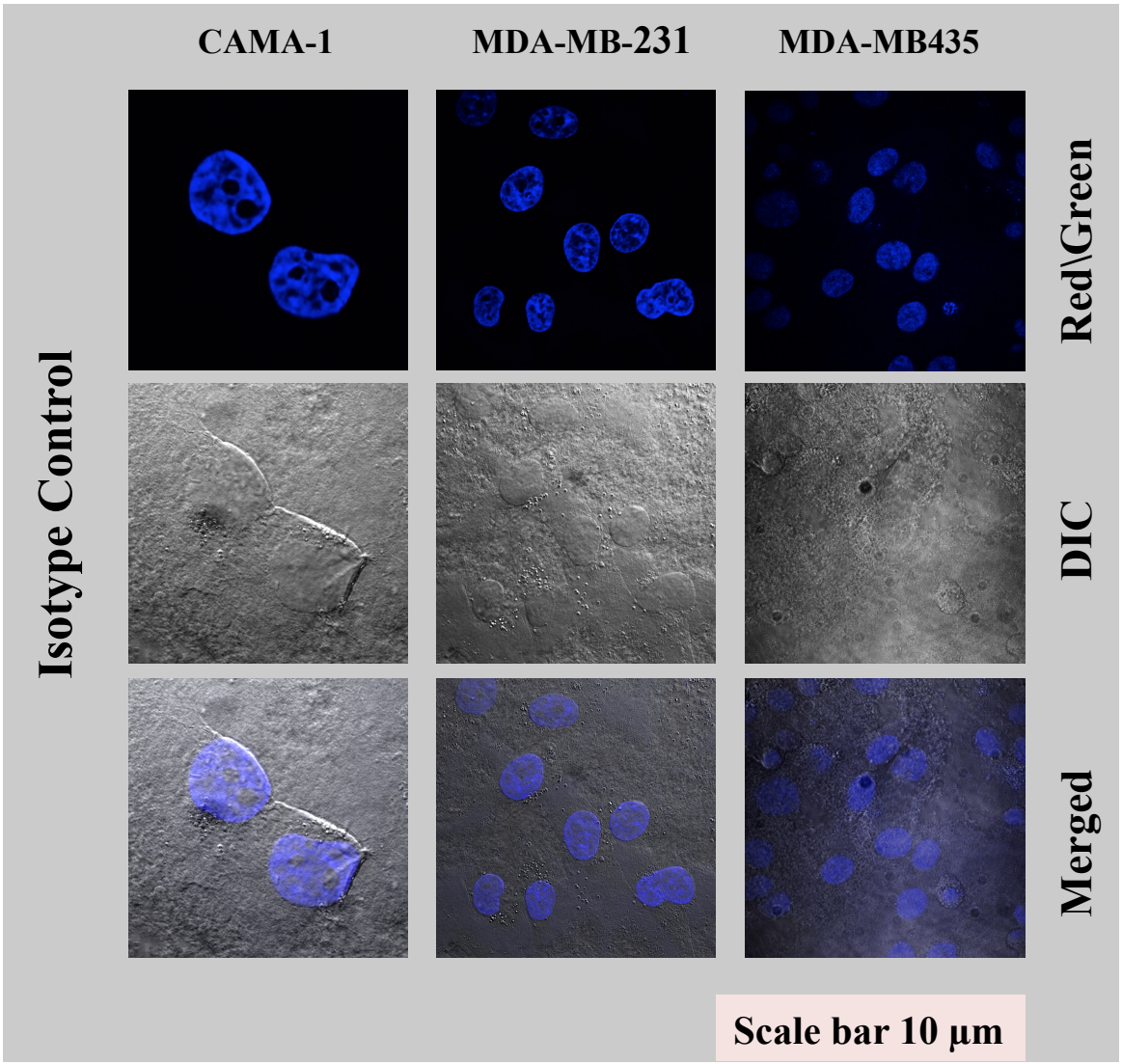

Figure 3-8:Confocal microscopy images of CAMA-1, MDA-MB-231 and MDA-MB-435 cells as isotype- negative controls.

The isotype control comprised cells stained with isotype control IgG primary and Alexa Fluor® 488 and Alexa Fluor® 555 secondary antibodies, visualised by using green 488 nm and red 555 nm wavelength lasers to measure non-specific antibody binding. Blue colour shows DAPI stained cell nuclei, red and green show the merged image, whereas DIC is the differential interference contrast image of corresponding cells. Scale bar 10 µm.

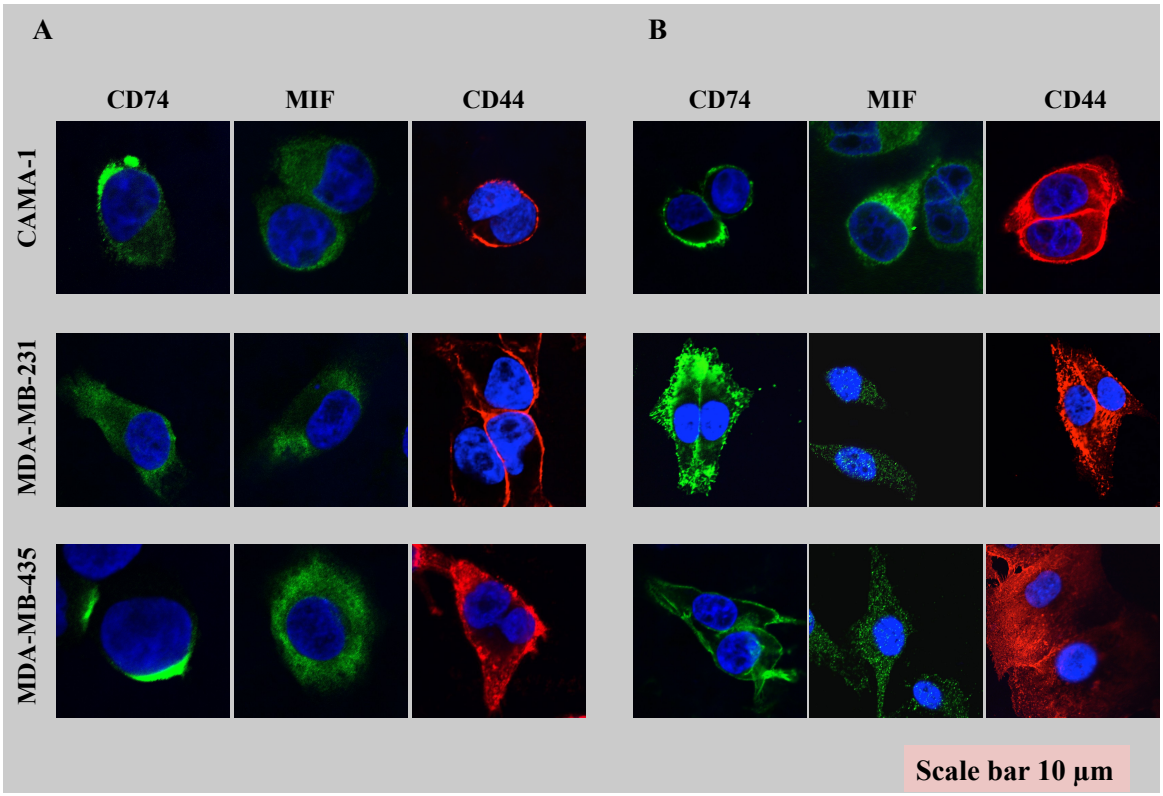

Figure 3-9: (A) Cell-surface and (B) intracellular staining of CD74, CD44 and MIF on CAMA-1, MDA-MB-231 and MDA-MB-435 cell, as visualised by confocal laser scanning microscopy.

All cells were cultured in LabTek 8-well chambers at a density of 10×10^3 cells per well overnight. Cells were stained either with CD74 or MIF labelled with Alexa Fluor® 488 (green). CD44 was labelled with Alexa Fluor® 555 (red). Cell nuclei were stained with 4', 6-diamidino-2-phenylindole (DAPI) that is shown in blue. Fluorochromes were acquired separately to evaluate the expression of CD74, CD44 and MIF using the Fiji software. Photomicrographs are representative of three independent experiments. Scale bar 10 µm.

3.2.6 Validation study of tumour antigens

In order to validate this study, the expression of CD74, MIF and CD74 in immortalized normal breast luminal cells (226LDM) was investigated. Cell-surface and intracellular expression of CD74, CD44 and MIF was assessed using flow cytometry (Figure 3-10 A). Total protein of CD74, MIF and CD44 was detected by Western blotting and α-Tubulin was used as a loading control (Figure 3-10 B). Confocal laser scanning microscopy was used to study the intracellular staining of CD74, MIF and CD44 in 226LDM cells (Figure 3-10 C). The results show that 226LDM cells do not seem to express CD74, but they do express MIF and CD44. Flow cytometry data show that MIF was not detectable and CD44 was very weak on the cell-surface but was higher intracellularly.

In the same manner, the expression of CD74, MIF and CD44 on normal breast lysate and tissues (available commercially) was examined. The results revealed that CD74 was not expressed on normal breast lysate and tissues in contrast to MIF and CD44 (Figure 3-11 A, B). Although normal breast lysate and tissues expressed MIF and CD44, the level was low compared to that in CAMA-1, MDA-MB-231 and MDA-MB-435 breast cancer cells.

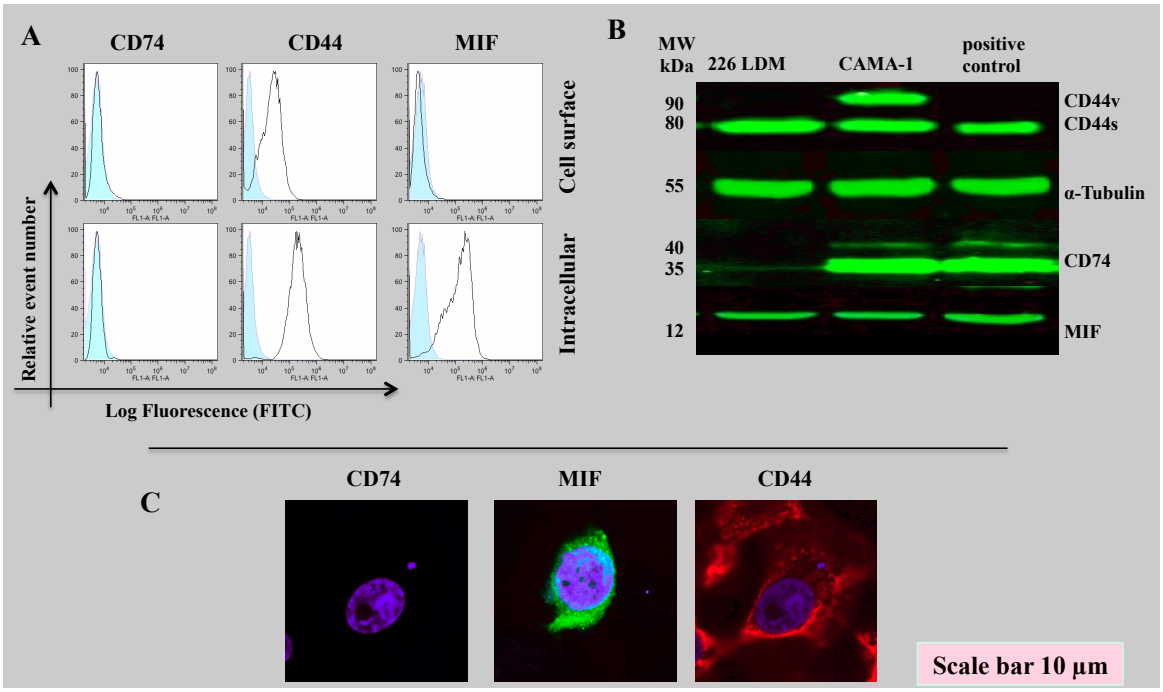

Figure 3-10: The expression of CD74, MIF and CD44 proteins in immortalized normal breast luminal cells (226LDM).

(A) Cell-surface and intracellular expression of CD74, MIF and CD44 was acquired by flow cytometry using By2 (anti-CD74), 156-3C11 (anti-CD44) and D-2 (anti-MIF). Empty histograms represent the 226LDM cells stained with indicated antibody as displayed. Negative controls were performed by using an isotype-matched control antibody (blue-filled histograms). (B) Total protein of CD74, MIF and CD44 was detected by Western blotting and α-Tubulin was used as a loading control. (C) Intracellular staining of CD74, MIF and CD44 in 226LDM cells, visualised by confocal laser scanning microscopy. Data is representative of three independent experiments. Scale bar 10 µm

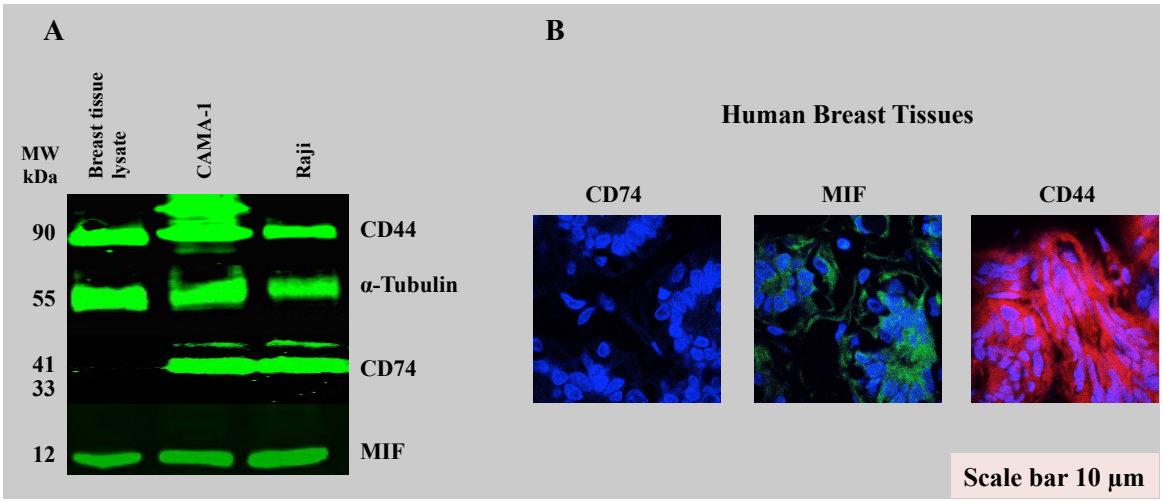

Figure 3-11: The detection of CD74, MIF and CD44 proteins in normal human breast lysate and tissues.

(A) Total protein of CD74, MIF and CD44 was detected by Western blot and α-Tubulin was used as a loading control. (B) Histological immunostaining of CD74, MIF and CD44 in normal breast tissue cells, as visualised by confocal laser scanning microscopy. Scale bar 10 µm.

3.3 Conclusions

The determination and identification of tumour antigens that are highly immunogenic in human tumours is important for the development of cell- and vaccine-based tumour therapies (Parmiani et al., 2007). The characterisation of tumour cells in terms of mapping the immunological molecules on those cells can provide further insight into whether these cells have the ability to be utilised by the immune system to work as non professional antigen-presenting cells.

This study has examined the immunophenotyping of HLA-A, B, C, HLA-DR, CD74, MIF and CD44 expression in the human breast cancer derived cell lines CAMA-1, MDA-MB-231 and MDA-MB-435. The expression of CD74, MIF and CD44 was studied in breast cancer cell lines, the immortalized normal breast luminal cell line 226LDM, normal breast tissues and lysate, and in THP-1 cells, Jurkat cells and HeLa cells which were used as a positive control. From the obtained results it is concluded that all breast cancer cells overexpress CD74 isoforms, MIF and CD44, in contrast to the normal cell lines and normal breast tissues, which express only CD44 and MIF in low levels. The data shown in this chapter also represents the first evidence of breast cancer cell lines expressing three different isoforms of CD74. Taken together, the results of the present study indicate a crucial role of CD74 in breast cancer cells along with MIF and CD44. The results also suggest that CAMA-1, MDA-MB-231 and MDA-MB-435 cells are poorly immunogenic, expressing low levels of HLA-A, B, C and HLA-DR.

Chapter 4 Modulation studies: effect of IFN- γ and LPS on the migration, proliferation and the expression of CD74 on CAMA-1 and MDA-MB-231 cells

4.1 Introduction

Tumour immunogenicity is the ability of a tumour to induce the immune response to prevent tumour growth and single-cell transplantation experiments have been widely used to study the immunogenicity of tumour cells. Cancer cells that are rejected in naive syngeneic mice (which are known as 'regressors') are considered highly immunogenic (Blankenstein et al., 2012). However, low immunogenicity of cancer cells has often been attributed to selective immune processes in the primary tumour-bearing host. The possible reasons for the poor immunogenicity of some tumour cells in allogeneic systems include the inability to produce, or to cause accessory cells to produce, the necessary 'costimulators' i.e. interleukin (IL)-1 and/or IL-2, a qualitative or quantitative deficiency of MHC encoded alloantigens, and the production of inhibitory molecules such as prostaglandins (Ashman, 1987). Although most tumour cells express antigens that can mediate recognition by host $CD8^+$ T cells, tumour cells can evade anti-tumour immune responses to grow progressively (Gajewski et al., 2013). The regulation of the tumour immunogenicity by tumour cells is believed to be through either tumour-specific (non-self) antigens (TSAs) or tumour-associated (self) antigens (TAAs) (B Janakiram, 2012; Blankenstein et al., 2012; Burgess, 2012; Gajewski et al., 2013).

Several mechanisms of immunomodulation within tumour cells have been described that render the cells less sensitive to immune attack (resistance) or inhibit anti-tumour immune responses (immunosuppression) (Uyttenhove et al., 2003; Gajewski et al., 2006; Mantovani et al., 2008). Tumour cells that directly suppress anti-tumour immune responses, or induce other cells to do so, are likely selected for by the spontaneous occurrence of anti-tumour immune responses. The most common cause of resistance is decreased antigenicity owing to HLA class I and II molecule downregulation or loss, which frequently occurs in human tumours (Garrido et al., 2010). It is also believed that

tumour formation in immunocompetent hosts is dependent on the ability of tumour cells to evade the immune system, as suggested by alterations in the expression of MHC molecules and other related molecules, such as CD74, in a number of cancers (Rangel et al., 2004). However, defects in HLA molecules can be reversed by cytokines, such as IFN-γ (Pandha et al., 2007). In consideration of these defects, it is believed that studying the expression of HLA molecules and related molecules would help to characterise the ability of tumour cells to be recognised by the immune system or to be utilized as APS (Dodson et al., 2011). Therefore, investigating the effect of proinflammatory and inflammatory conditions on the expression of HLA molecules by tumour cells might assist with targeting specific molecules for immunotherapy if inflammatory events in tumour microenvironments could be created. In this context, several researches have investigated the expression of HLA molecules and CD74 in tumour cells (Moldenhauer et al., 1999; Rangel et al., 2004; Burton et al., 2010; Greenwood et al., 2011). Rangel et al. (2004) demonstrated that ovarian cancer cells overexpress HLA-DR-α and HLA-DR-β, class II transcriptional transactivator (CIITA) and CD74. Matsushita et al. (2006) have also shown that overexpression of HLA-DR molecules in cancer cells relates to better prognosis of colorectal cancer patients. The immunogenicity of tumour cells is suggested to be regulated by HLA molecules; Malmberg et al. (2002) have shown that IFN-γ regulates the immunogenicity of target cells by increasing their expression of HLA class I molecules. Similarly, Propper et al. (2003) have also shown that low-dose IFN-γ induces tumour MHC expression in metastatic malignant melanoma, increasing the immunogenicity of tumour cells. Zheng et al. (2012) showed that LPS stimulation can greatly induce MIF and surface CD74 expression and enhance the MIF/CD74 pathway. Wu et al. (2014) also observed that the expression of CD74 in lung tissue was significantly increased after LPS induction in a mouse model.

The main aim of the present study was to investigate the role of CD74, the cell-surface form of the invariant chain, in respect to immunological molecules in breast cancer cell lines. This was achieved by studying the effect of IFN-γ or LPS on the expression of CD74 on CAMA-1 and MDA-MB-231 cells and by quantifying the cell-surface expressed CD74 receptors as well as proliferation and cell migration. To evaluate the response of the cells to stimulation, the cell- surface expression of HLA-A, B, C and HLA-DR was investigated after IFN-γ treatment. To achieve the aim of this study, RT-PCR, flow cytometry and Western blotting were employed.

4.2 Results

4.2.1 Effect of IFN-γ and LPS on the proliferation and invasion of CAMA-1 and MDA-MB-231 cells

The effect of varying concentrations of IFN-γ (100, 500 and 1000 IU/ml) for 72 hr or LPS (100, 500 and 1000 ng/ml) for 24 hr on proliferation of CAMA-1 and MDA-MB-231 cells was examined. Cells without IFN-γ or LPS treatment served as the control group. IFN-γ could inhibit the proliferation of CAMA-1 and MDA-MB-231 cells (Figure 4-1 A, B). Both cell lines showed a similar pattern of decreasing the proliferation. In contrast, LPS treatment positively affected the proliferation of CAMA-1 cell lines, since proliferation increased compared to untreated control cells. MDA-MB-231 cell lines showed a weak proliferative response to LPS treatment in comparison to CAMA-1 cells.

In the same manner, the ability of non-invasive CAMA-1 and highly invasive MDA-MB-231 cells to migrate was measured in the presence and absence of 10% FCS, as controls, using a transwell insert from Corning Life Science (Figure 4-1 C). The result showed that both cell lines had a tendency to migrate towards the serum. However, MDA-MB-231 cells migrated more than CAMA-1 cells. The migration of both CAMA-1 and MDA-MB-231 cells cultured with IFN-γ or ng/ml LPS for 24 hr was also evaluated. In the absence of 10% FCS, 1000 IU/ml of IFN-γ or 1000 ng/ml LPS were added in the upper chambers of the transwell insert. The results confirmed that both cell lines migrate against IFN-γ or LPS even in the absence of FCS, which functions as an effective chemoattractant for cells in the culture. This suggests that IFN-γ or LPS have a clear effect in the migration of both cell lines.

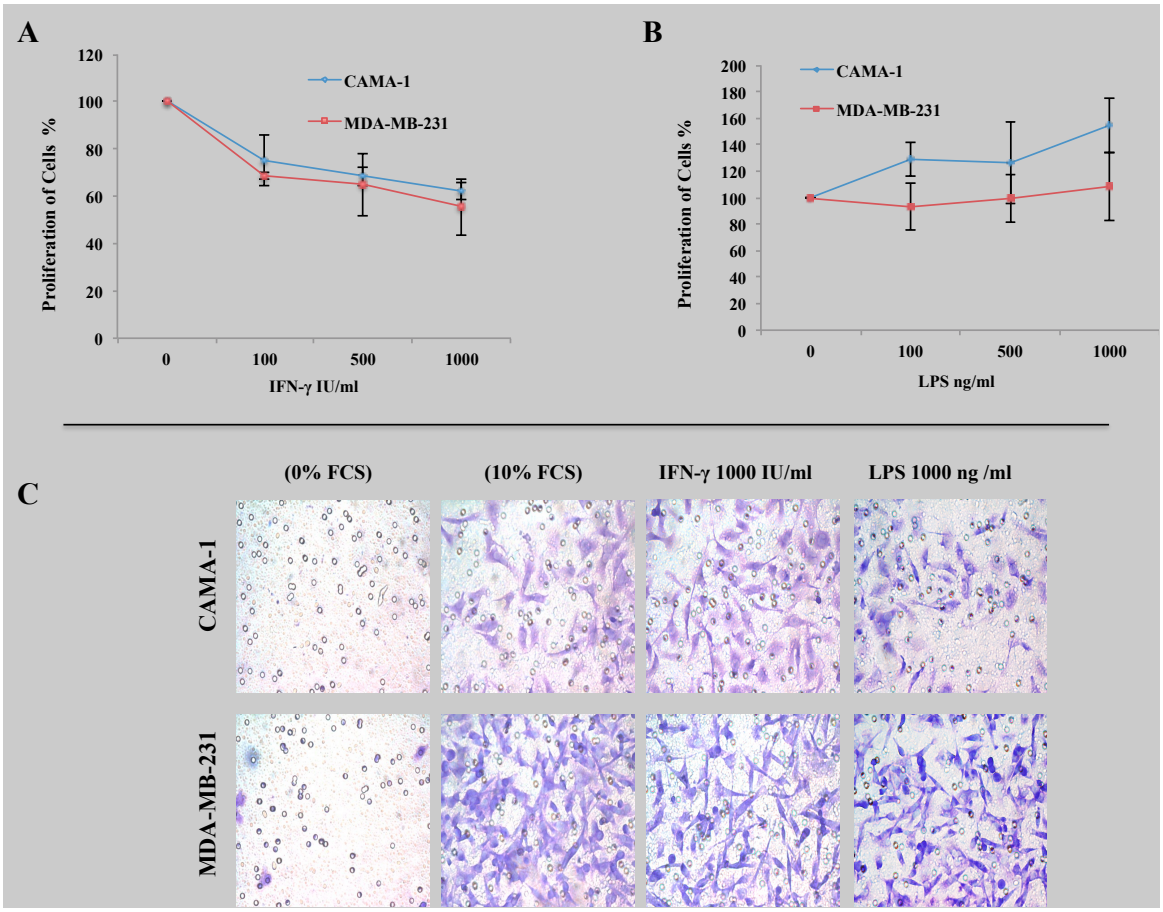

Figure 4-1: Effect of IFN-γ and LPS on proliferation and cell migration of human breast cancer cell lines.

(A and B) Validity of IFN-γ or LPS treated CAMA-1 and MDA-MB-231 cells. CAMA-1 and MDA-MB-231 cells were seeded in 96 well-plates and treated with indicated concentrations of IFN-γ (100-1000 IU/ml) for 72 hr or LPS (100-1000 ng/ml) for 24 hr. Untreated cells of both cell lines were used as positive controls. Each data point represents a mean of at least three independent experiments with triplicate wells and error bars represent SEM from three separate experiments. (C) CAMA-1 and MDA-MB-231 cells were cultured with an appropriate medium in the presence or absence of 10% FCS and were allowed to migrate overnight through the transwell membrane; 24 mm diameter inserts and a pore size of 0.4 µm. The negative control showed that there was no indication of cell migration in the absence of FCS in contrast to the positive control, which showed that CAMA-1, and MDA-MB-231 cells strongly migrated toward FCS. The migration of CAMA-1 and MDA-MB-231 cells was also evaluated in the presence of IFN-γ or LPS. 1000 IU/ml of IFN-γ or 1000 ng/ml LPS were added in the upper chambers of transwell insert in the absence of 10% FCS. Both cell lines migrated against IFN-γ or LPS.

4.2.2 Effect of IFN-γ on the expression of HLA-A, B, C, and HLA-DR

The cell-surface expression of HLA-A, B, C and HLA-DR was analysed in untreated and IFN-γ-treated CAMA-1 and MDA-MB-231 cells. Non-permeabilized cells were stained with an appropriate concentration of w6/32 (anti-HLA-A, B, C) and L243 (anti- HLA-DR) primary antibody followed by 1 µl RAM-FITC secondary antibody. Cells without staining and isotype cells, stained with only secondary antibody, were used as a negative control.

Weak expression of HLA-DR was detected on the cell-surface membrane of untreated CAMA-1 and MDA-MB-231 cells. In contrast to CAMA-1 cells, which showed a weak expression of HLA-A, B, C molecules, MDA-MB-231 cells showed high expression of the same molecules. It was observed that the expression of HLA-A, B, C and HLA-DR increased when CAMA-1 and MDA-MB-231 cells were incubated with (100, 500 and 1000 IU/ml) IFN-γ for 72 hr (Figures 4-2 and 4-3). However, maximum HLA-A, B, C and HLA-DR expression was detected in CAMA-1 cells treated with 1000 IU/ml of IFN-γ. In the same manner, MDA-MB-231cells treated with 1000 IU/ml of IFN-γ showed the maximum expression of HLA-A, B, C and HLA-DR molecules.

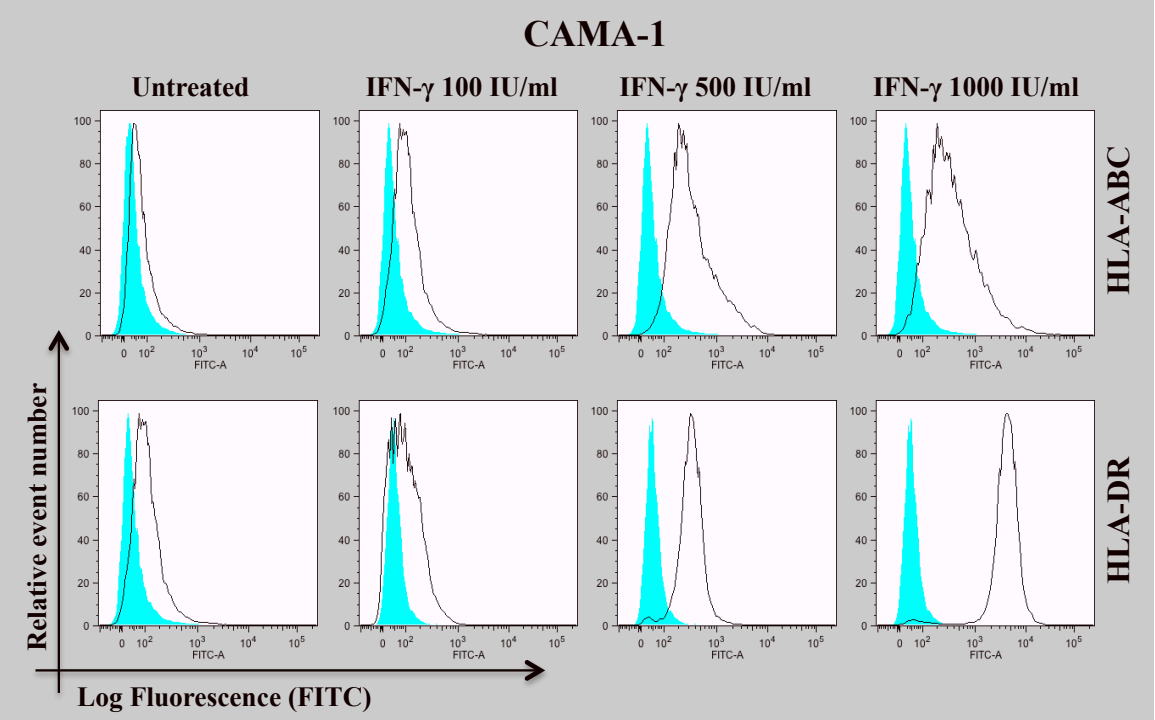

Figure 4-2: Cell-surface expression of HLA-A, B, C and HLA-DR on IFN-γ treated CAMA-1 cells.

CAMA-1 cells were cultured in the presence of the indicated concentrations of IFN-γ (100-1000 IU/ml) for 72 hr and were acquired by flow cytometry using w6/32 (anti-HLA-A, B, C) and L243 (anti- HLA-DR). Empty histograms represent the cells with indicated concentrations of IFN-γ and antibody. Blue-filled histograms show negative controls. Cells were labelled with an FITC-labelled secondary anti-mouse antibody. Cell-surface expression of HLA-A, B, C and HLA-DR on untreated and IFN-γ treated CAMA-1 cells is also displayed. The results show that HLA-A, B, C and HLA-DR expression increases upon IFN-γ treatment.

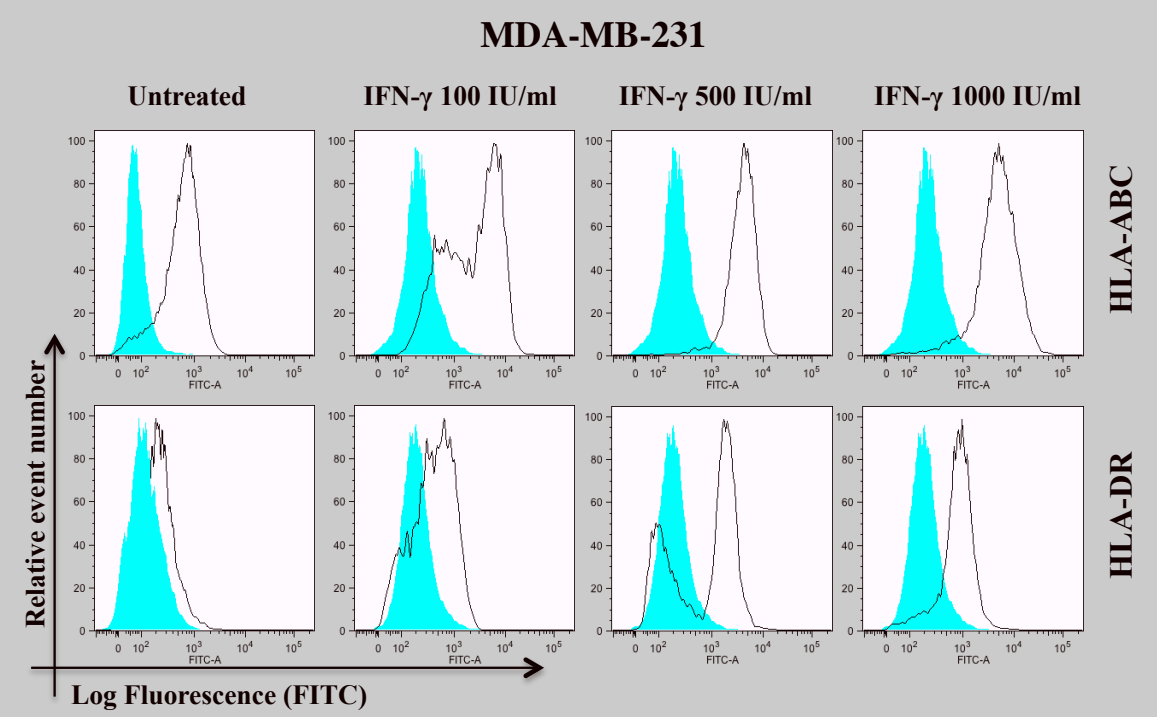

Figure 4-3: Cell-surface expression of HLA-A, B, C and HLA-DR on IFN-γ treated MDA-MB-231 cells.

MDA-MB-231 cells were cultured in the presence of the indicated concentrations of IFN-γ (100-1000 IU/ml) for 72 hr and were acquired by flow cytometry using w6/32 (anti-HLA-A, B, C) and L243 (anti-HLA-DR). Empty histograms represent the cells with indicated concentrations of IFN-γ and antibody. Blue-filled histograms show negative controls. Cells were labelled with an FITC-labelled secondary anti-mouse antibody. Cell-surface expression of HLA-A, B, C and HLA-DR on untreated and IFN-γ treated CAMA-1 cells is also displayed. The results show that HLA-A, B, C and HLA-DR expression increases upon IFN-γ treatment.

4.2.3 Gene expression

4.2.3.1 RNA extraction

To investigate the RNA expression of CD74 and β-actin in Raji, CAMA-1 and MDA-MB-231 cell lines, RT-PCR was performed. In order to achieve this, RNA was extracted and then measured using a NanoDrop spectrophotometer. The samples were then checked on a 0.1 % agarose gel, (Figure 4-4 A, B). Since the results showed that the extracted RNA was cross contaminated with DNA, DNAse treatment was carried out for RNA using a DNase treatment kit (Life technologies, UK). RNA was then converted to cDNA according the manufacturer's instructions. β-actin and CD74 primers were then evaluated with the cDNA to check the quality of the cDNA.

4.2.3.2 Effect of IFN-γ and LPS on CD74 mRNA expression in CAMA-1 and MDA-MB-231 cells

RNA extracted from IFN-γ or LPS treated CAMA-1 and MDA-MB-231 cells was reverse transcribed into cDNA using reverse transcriptase. This was achieved by converting an equal amount of each sample (2 μg of RNA). The resulting cDNA was used as a template for subsequent PCR amplifications using β-actin and CD74 primers. The results confirmed that the extracted RNA was converted successfully, using β-actin as a housekeeping gene. The CD74 amplicon migrated consistently as a single band at the appropriate molecular size (384 bp). These results served to confirm the expression of CD74 that was observed in untreated and treated CAMA-1 and MDA-MB-231 cells with IFN-γ or LPS. The results are illustrated in (Figure 4-5 A, B).

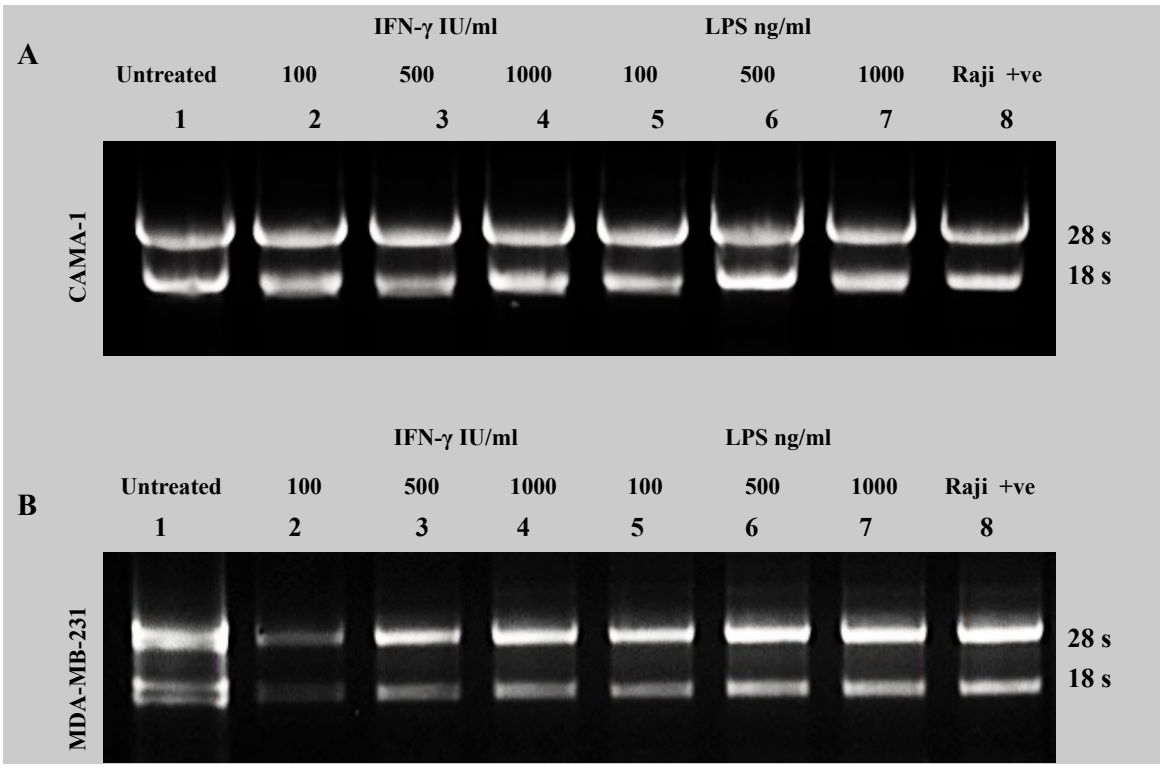

Figure 4-4: Total RNA extracted using TRIzol reagent.

RNA samples isolated from 1×10^6 Raji, CAMA-1 and MDA-MB-231 cells. Samples were subjected to electrophoresis in agarose gels to check the integrity of the RNA. According to this analysis, distinct ribosomal RNA bands 28s and 18s could be seen, indicating that all samples were in tact. Lane 1 represents the RNA for untreated (A) CAMA-1 and (B) MDA-MB-231 cells. RNA from (A; upper panel) CAMA-1 and (B; lower panel) MDA-MB-231 cells treated with indicated concentrations of IFN-γ for 72 hr is shown in lanes 2, 3 and 4 respectively. Lane 5, 6 and 7 shows the RNA samples isolated from CAMA-1 and MDA-MB-231 cells treated with indicated concentration of LPS for 24 hr. Lane 8; Raji cells used as a positive control. Data is representative of three independent experiments.

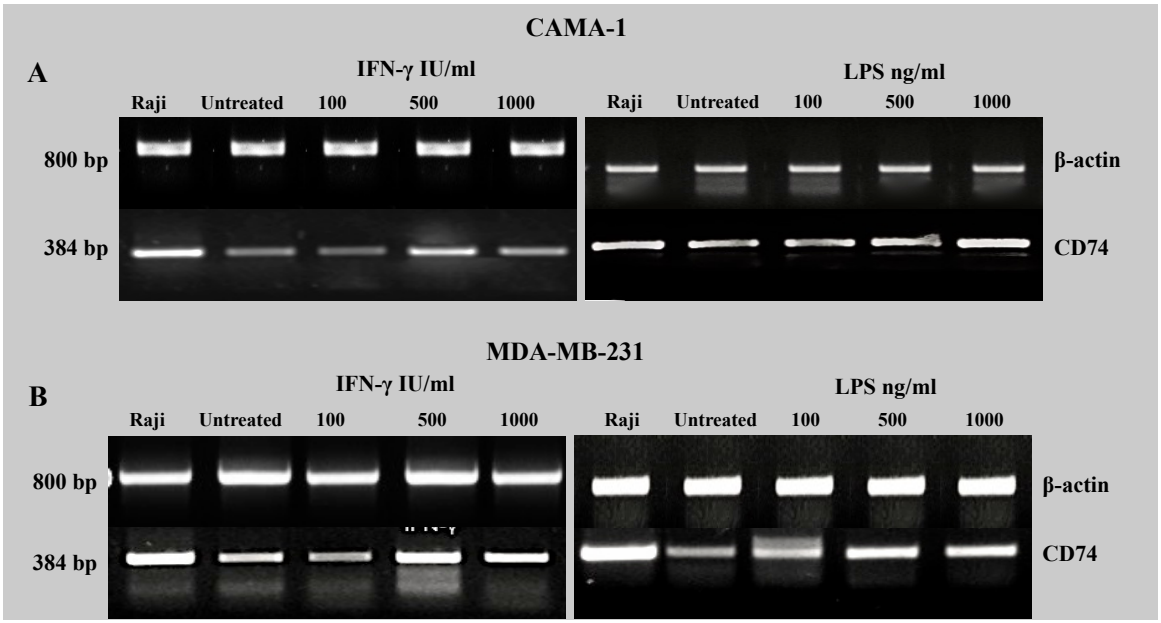

Figure 4-5: CD74 mRNA expression in CAMA-1 and MDA-MB-231 cells by RT-PCR.

Submaximal amplification (27 cycles) of cDNA from a representative subset of the positive control (Raji cells) and CAMA-1 and MDA-MB-231 cells treated with IFN-γ or LPS is shown for β-actin and CD74. β-actin was included as housekeeping gene. (A and B) The presence of bands corresponding to indicated molecular weights according to the DNA marker shows CD74 mRNA expression levels in untreated CAMA-1 and MDA-MB-231 cells as well as in cells treated with IFN-γ or LPS. (A) The band intensity of CD74 shows that mRNA expression increased when CAMA-1 cells were incubated with IFN-γ for 72 hr or LPS for 24 hr and maximum expression was detected in CAMA-1 treated with 500 IU/ml of IFN-γ or 1000 ng/ml of LPS. (B) CD74 mRNA expression in MDA-MB-231 cells increased upon the treatment of IFN-γ for 72 hr or LPS for 24 hr and the highest band intensity was obtained in cells treated with (500 IU/ml of IFN-γ or 1000 ng/ml of LPS). Data is representative of three independent experiments.

4.2.4 Flow cytometry

4.2.4.1 Effect of IFN-γ and LPS on the expression of CD74 on CAMA-1 and MDA-MB-231 cells

The cell-surface and intracellular expression of CD74 was analysed in untreated and IFN-γ or LPS treated CAMA-1 and MDA-MB-231 cells as explained in section 2.2.2. Cells permeabilized with 0.1 % of Triton X-100 and non-permeabilized cells were stained with an appropriate concentration of the By2 (anti-CD74) primary antibody followed by 1 µl RAM-FITC secondary antibody. Cells without staining and isotype cells stained with only secondary antibody were used as a negative control.

CD74 was found to be moderately expressed on the cell-surface membrane and intracellularly in untreated CAMA-1 and MDA-MB-231 cells. The expression of CD74 increased when CAMA-1 and MDA-MB-231 cells were incubated with (100, 500 and 1000 IU/ml) IFN-γ for 72 hr (Figures 4-6 A and 4-8 A). In the same manner, the expression of CD74 increased when CAMA-1 and MDA-MB-231 cells were incubated with (100, 500 and 1000 ng/ml) LPS for 24 hr (Figures 4-6 B and 4-8 B). However, maximum CD74 expression was detected in CAMA-1 and MDA-MB-231 cells treated with either 500 or 1000 IU/ml of IFN-γ or 1000 ng/ml of LPS. (Figures 4-7 A, B and 4-9 A, B) show cell-surface and intracellular expression of CD74 depicted by graphical representation of mean fluorescence intensity (MFI) in IFN-γ or LPS treated CAMA-1 and MDA-MB-231.

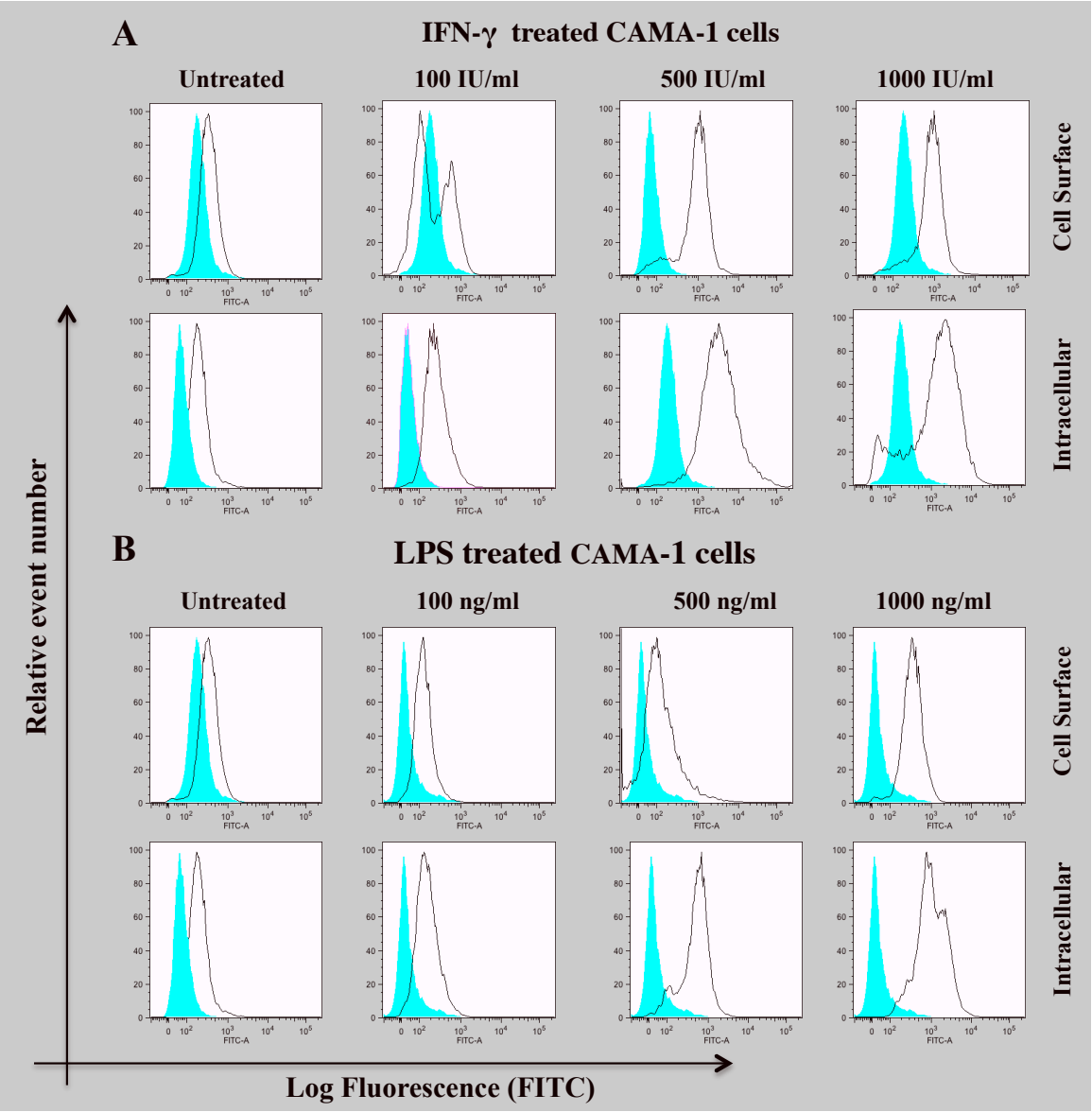

Figure 4-6: Cell-surface and intracellular expression of CD74 in IFN-γ or LPS treated CAMA-1 cells.

CAMA-1 cells were cultured in the presence of the indicated concentrations of IFN-γ (100, 500 and 1000 IU/ml) for 72 hr or LPS (100, 500 and 1000 ng/ml) for 24 hr and were acquired by flow cytometry using By2 (anti-CD74). Empty histograms represent the expression of CD74 on untreated CAMA-1 and IFN-γ or LPS treated CAMA-1 cells whereas blue-filled histograms show negative controls. Cells were labelled with an FITC-labelled secondary anti-mouse antibody. (A) Cells-surface and intracellular expression of CD74 in untreated CAMA-1cells and in IFN-γ treated cells. (B) The expression of CD74 after LPS treatment with indicated concentration. The results show that CD74 expression increases upon IFN-γ or LPS treatment. Maximum CD74 expression was detected in CAMA-1 cells treated with 1000 IU/ml of IFN-γ or 1000 ng/ml of LPS. Data is representative of three independent experiments.

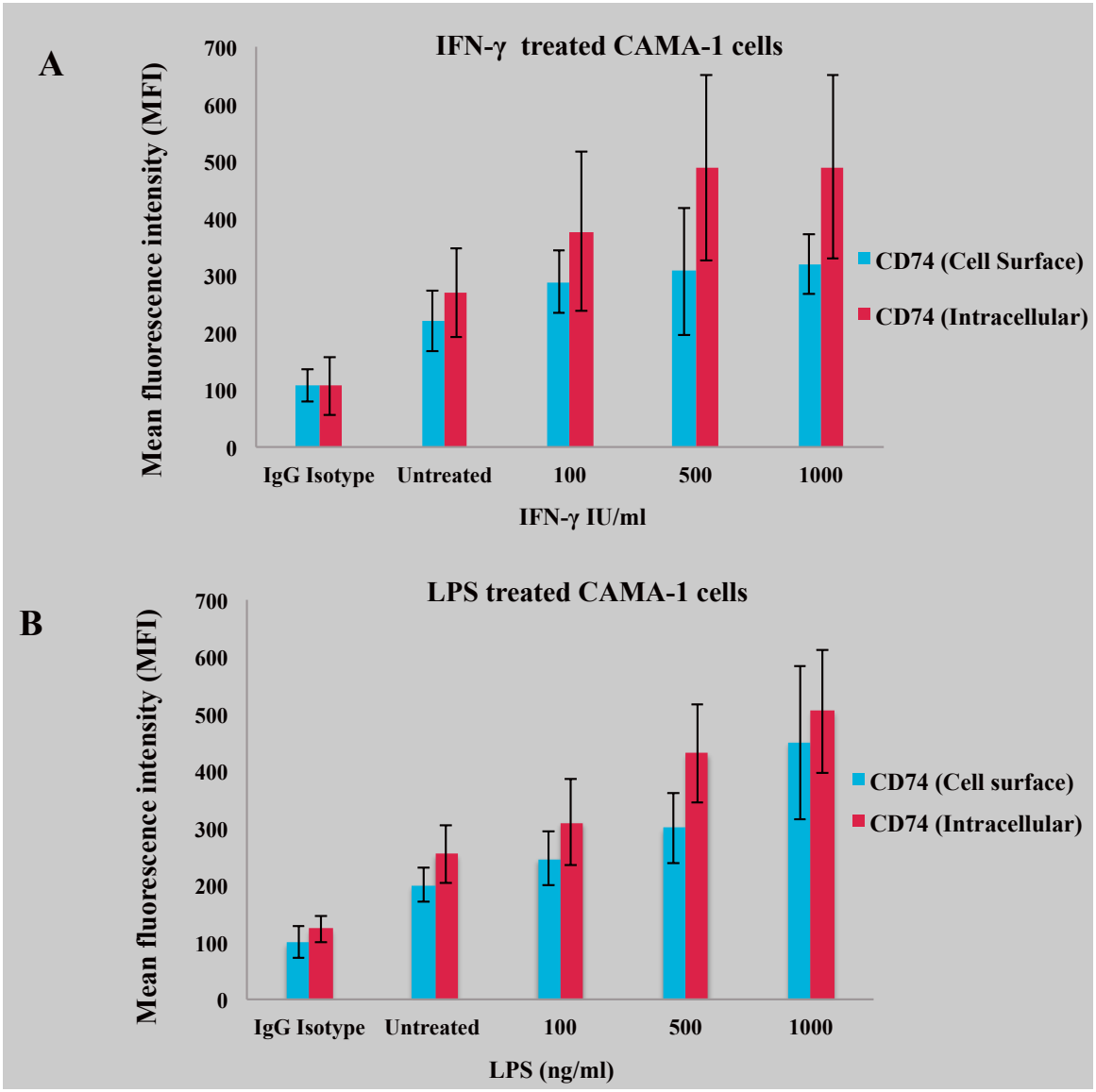

Figure 4-7: Graphical representation of CD74 surface and intracellular protein expression in untreated CAMA-1 and IFN-γ or LPS treated CAMA-1 cells.

(A and B) CAMA-1 cells cultured in RPMI-1640 supplemented with 10% FCS and treated with indicated concentrations of IFN-γ (100, 500 and 1000 IU/ml) for 72 hr or LPS (100, 500 and 1000 ng/ml) for 24 hr. Cells were stained with primary mouse anti-human (anti-CD74) mAb clone (By2) followed by staining with goat-anti-mouse secondary antibody labelled-FITC. The expression levels were analysed by flow cytometry (Aria cell sorter) and FlowJo 8.8.6 software was used to analyse the data. Mean fluorescence intensity (MFI) values were measured based on geometric means. Mouse IgG was used as a negative control. Blue bars represent cell-surface expression and red bars represent intracellular expression of CD74 in untreated and IFN-γ or LPS treated CAMA-1 cells. The results show the expression levels of cell-surface and intracellular levels of CD74 in untreated and LPS treated CAMA-1 cells. The increase in both blue and red bars confirms that the expression of CD74 was upregulated after exposing the cells to LPS. Maximum expression levels were detected when cells were incubated with 1000 ng/ml of LPS on the cell-surface and intracellularly. Bar graphs represent level of each protein in mean values ± SD in each cell line. It was noted that the level of CD74 expression increased after IFN-γ or LPS treatment. Data is representative of three independent experiments.

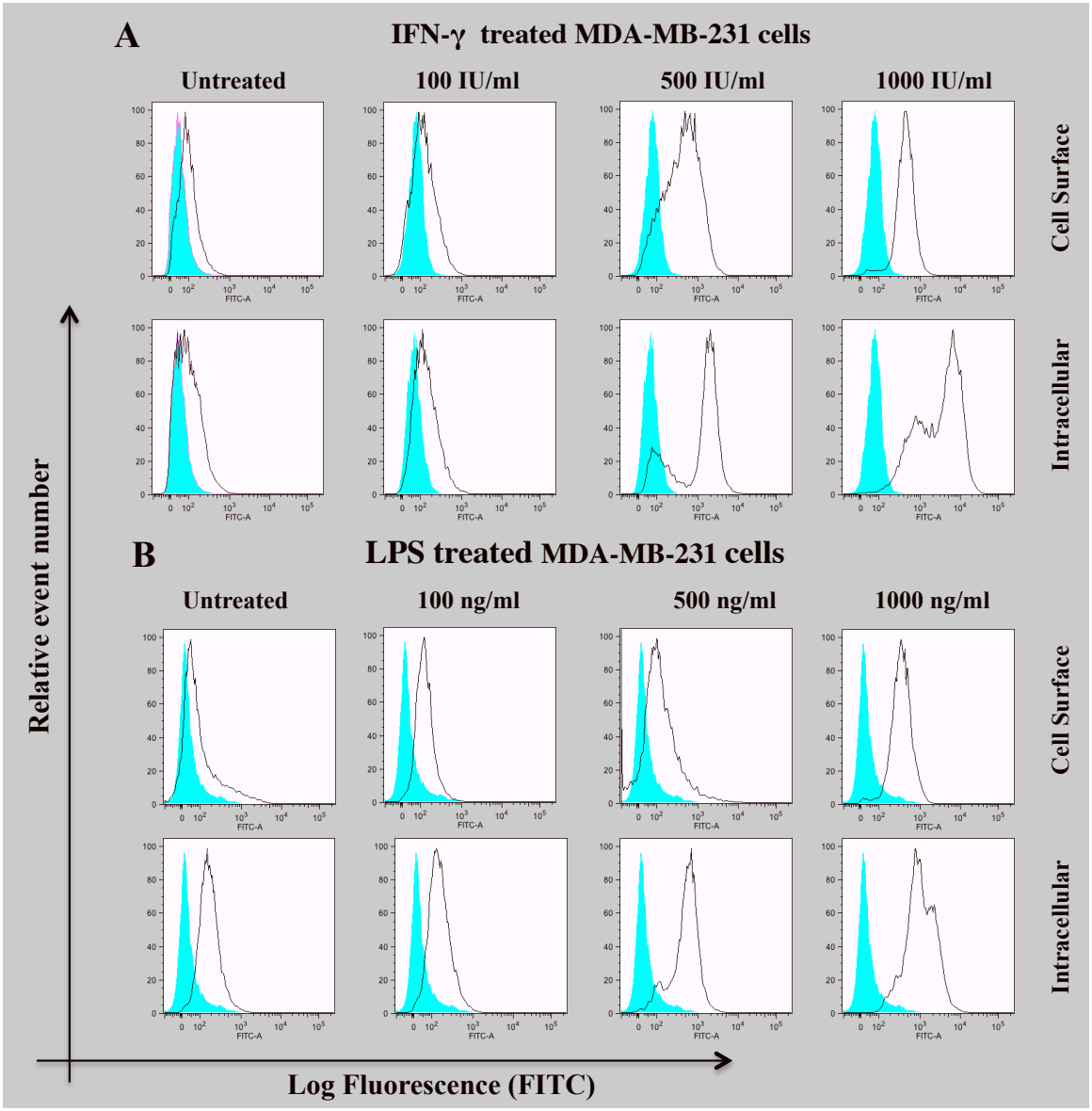

Figure 4-8: Cell-surface and intracellular expression of CD74 on IFN-γ or LPS treated MDA-MB-231 cells.

MDA-MB-231 cells were cultured in the presence of the indicated concentrations of IFN-γ (100, 500 and 1000 IU/ml) for 72 hr or LPS (100, 500 and 1000 ng/ml) for 24 hr and were acquired by flow cytometry using By2 (anti-CD74). Empty histograms represent the expression of CD74 in untreated CAMA-1 and IFN-γ or LPS treated CAMA-1 cells whereas blue-filled histograms show negative controls. Cells were labelled with an FITC-labelled secondary anti-mouse antibody. (A) Cell-surface and intracellular expression of CD74 in untreated MDA-MB-231 and in IFN-γ treated cells. (B) The expression of CD74 after LPS treatment with indicated concentration. The results show that CD74 expression increases upon IFN-γ or LPS treatment. Maximum CD74 expression was detected in CAMA-1 cells treated with 1000 IU/ml of IFN-γ or 1000 ng/ml of LPS. Data is representative of three independent experiments.

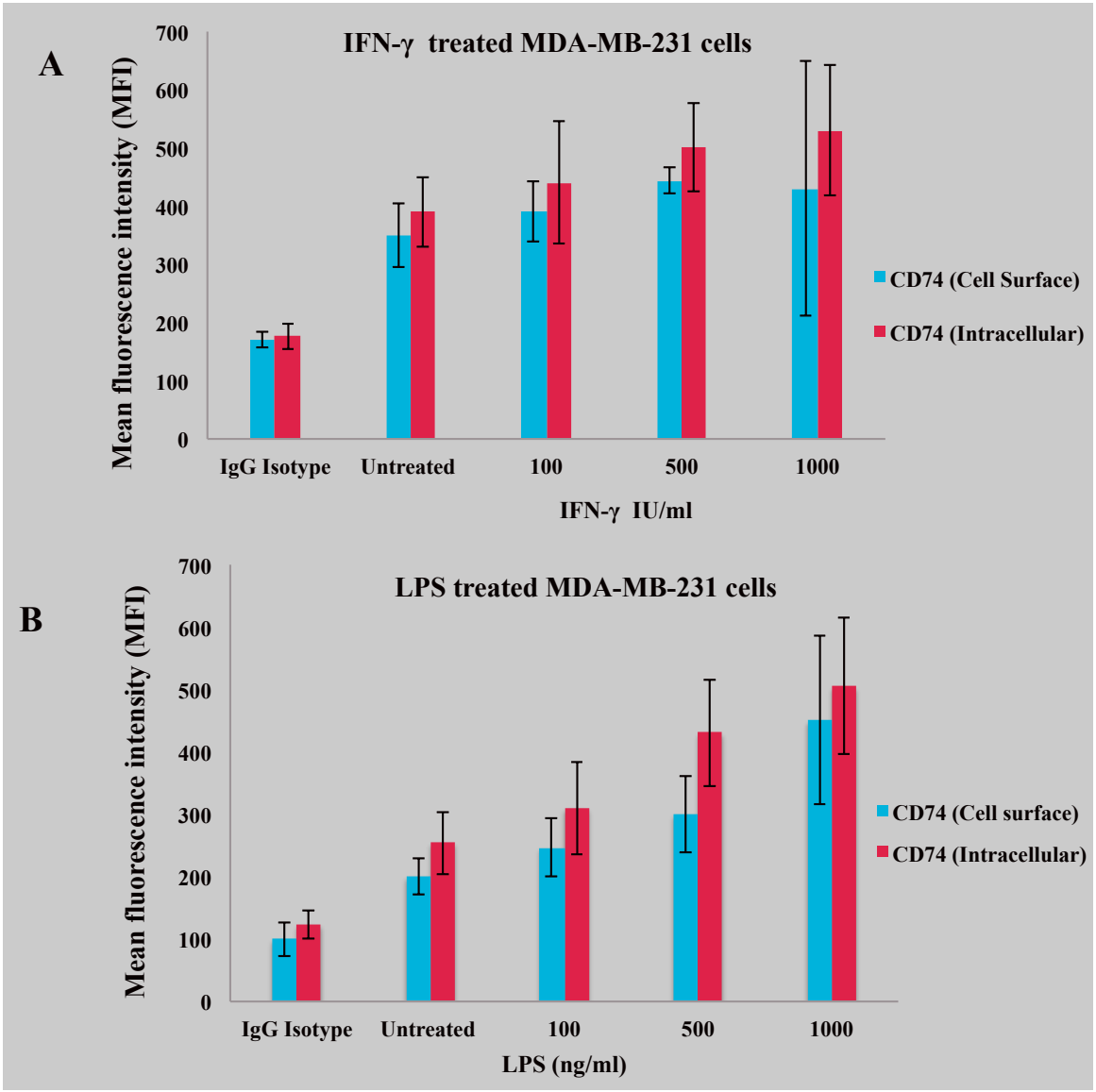

Figure 4-9: Graphical representation of CD74 surface and intracellular protein expression in untreated MDA-MB-231 and IFN-γ or LPS treated MDA-MB-231 cells.

(A and B) MDA-MB-231 cells were cultured in D-MEM supplemented with 10% FCS and treated with indicated concentrations of IFN-γ (100, 500 and 1000 IU/ml) for 72 hr or LPS (100, 500 and 1000 ng/ml) for 24 hr. Cells were stained with primary mouse anti-human (anti-CD74) mAb clone By2, followed by staining with goat-anti-mouse secondary antibody labelled-FITC. The expression levels were analysed by flow cytometry (Aria cell sorter) and FlowJo 8.8.6 software was used to analyse the data. Mean fluorescence intensity (MFI) values were measured based on geometric means. Mouse IgG was used as a negative control. Blue bars represent cell-surface expression and red bars represent intracellular expression of CD74 in untreated and IFN-γ or LPS treated CAMA-1 cells. The results show the expression levels of cell-surface and intracellular levels of CD74 in untreated and LPS treated CAMA-1 cells. The CD74 expression was upregulated after exposing the cells to LPS. Maximum expression levels were detected when cells were incubated with 1000 ng/ml of LPS on the cell-surface and intracellularly. Bar graphs represent level of each protein in mean values ± SD in each cell line. It was noted that level of CD74 expression increased after IFN-γ or LPS treatment. Data is representative of three independent experiments.

4.2.5 Western blotting

CD74 protein expression in Raji, CAMA-1 and MDA-MB-231 cells was studied by Western blot analysis using By2 (anti-CD74) and TU-02 (anti- α-Tubulin) mAbs. By2 (anti-CD74) is specific for 31-45 kDa CD74 isoforms. Results confirmed that the molecular weight of CD74 and α-tubulin are 33-41 kDa and 55 kDa respectively. α-tubulin was used as a loading control since it is expressed at the same level and it is not affected by the suggested treatments. Almost all cell lines expressed CD74 isoforms even though the expression varied before and after treatment with IFN-γ and LPS. To evaluate the differences in protein loading during the experiment, the percentage of regulation was calculated after the intensity of each band was adjusted according to its respective α-tubulin band intensity using the Image Studio Lite software (LI-COR Biosciences).

4.2.5.1 The effect of IFN-γ and LPS on total protein expression of CD74 on CAMA-1 and MDA-MB-231 cells

Total cell lysate was extracted and loaded on a gel from untreated and IFN-γ or LPS treated CAMA-1 and MDA-MB-231 cells, cultured in the presence of the indicated concentrations of IFN- γ (100, 500 and 1000 IU/ml) for 72 hr or LPS (100, 500 and 1000 ng/ml) for 24 hr (Figures 4-10 A, C and 4-11 A, C). The presence of bands corresponding to the expected molecular weight of CD74 confirmed its expression. The differences in band intensity between untreated and treated CAMA-1 or MDA-MB-231 cells confirmed that CD74 was upregulated in cells incubated with IFN-γ or LPS. CD74 isoforms were detected at expected molecular weights; 33 and 41 kDa. Maximum CD74 isoform expression was detected in CAMA-1 cells treated with 500 IU/ml of IFN-γ or with 1000 ng/ml of LPS. Density of the bands was normalized with internal α-tubulin loading control (Figures 4-10 B, D and 4-11 B, D).

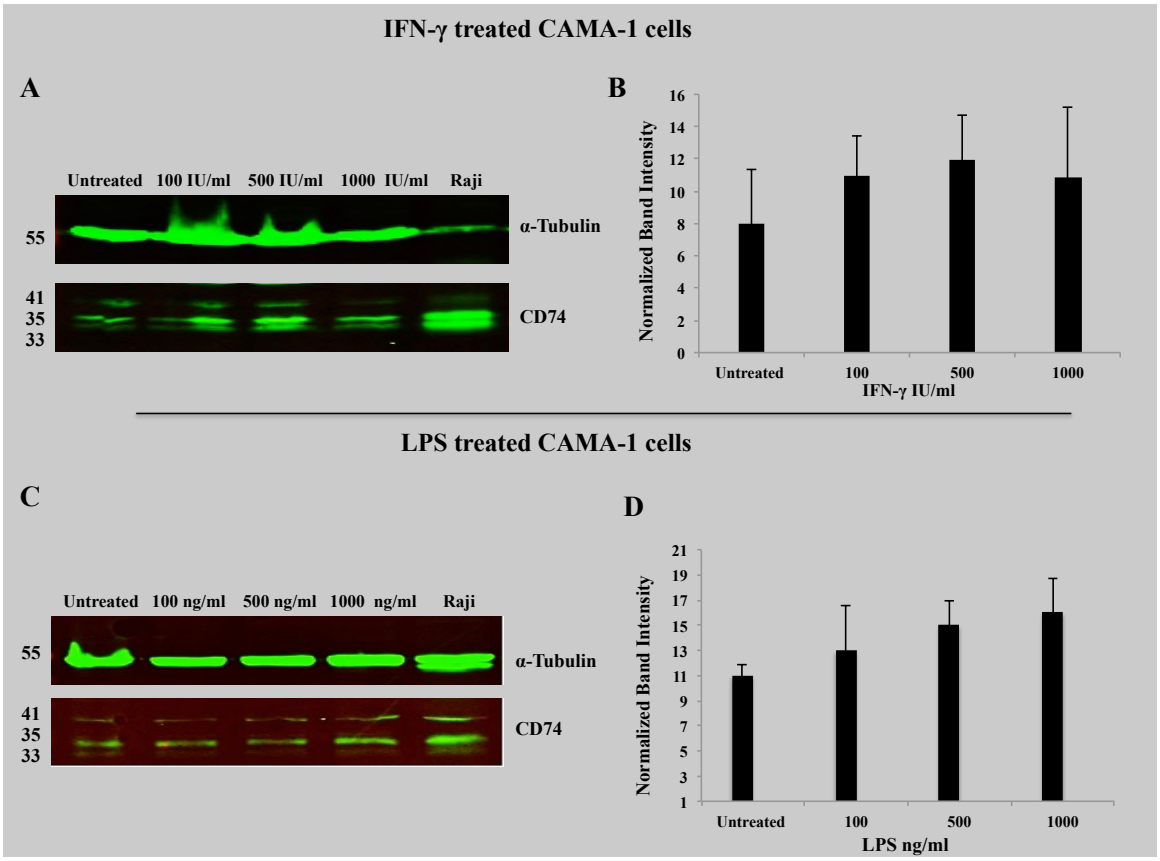

Figure 4-10: CD74 and α-Tubulin expression according to their molecular weight in IFN-γ or LPS treated CAMA-1 cell lines.

SDS-PAGE (12%) was performed under reducing conditions, followed by Western blotting with primary monoclonal antibodies TU-02 (anti α-Tubulin as loading control) and By2 (anti-CD74). α-Tubulin was detected at a molecular weight of 55 kDa. The monocyte cell line Raji was used as a positive control as it expressed high levels of CD74 without any stimulation of cytokines. CAMA-1 cells, cultured in the presence of the indicated concentrations of IFN- γ for 72 hr or LPS for 24 hr. (A and C) α-Tubulin, CD74 on untreated CAMA-1 and IFN-γ or LPS treated CAMA-1 cells with indicated concentrations. (B and D) Relative levels of CD74 in IFN-γ or LPS treated CAMA-1 cells. CD74 levels are normalized against α-tubulin to account for the difference in protein loading during the experiment. The percentage of regulation was calculated after the intensity of each band was adjusted according to its respective α-Tubulin band intensity using Image Studio Lite software (LI-COR Biosciences). Comparison of CD74 expression in untreated CAMA-1 and IFN-γ or LPS treated CAMA-1 cells were assessed using densitometry analysis. CD74 isoforms were detected at expected molecular weights; 33, 35 and 41 kDa. Maximum CD74 isoform expression was detected in CAMA-1 cells treated with 500 IU/ml of IFN-γ or 1000 ng/ml of LPS. A representative immunoblot of three independent experiments.

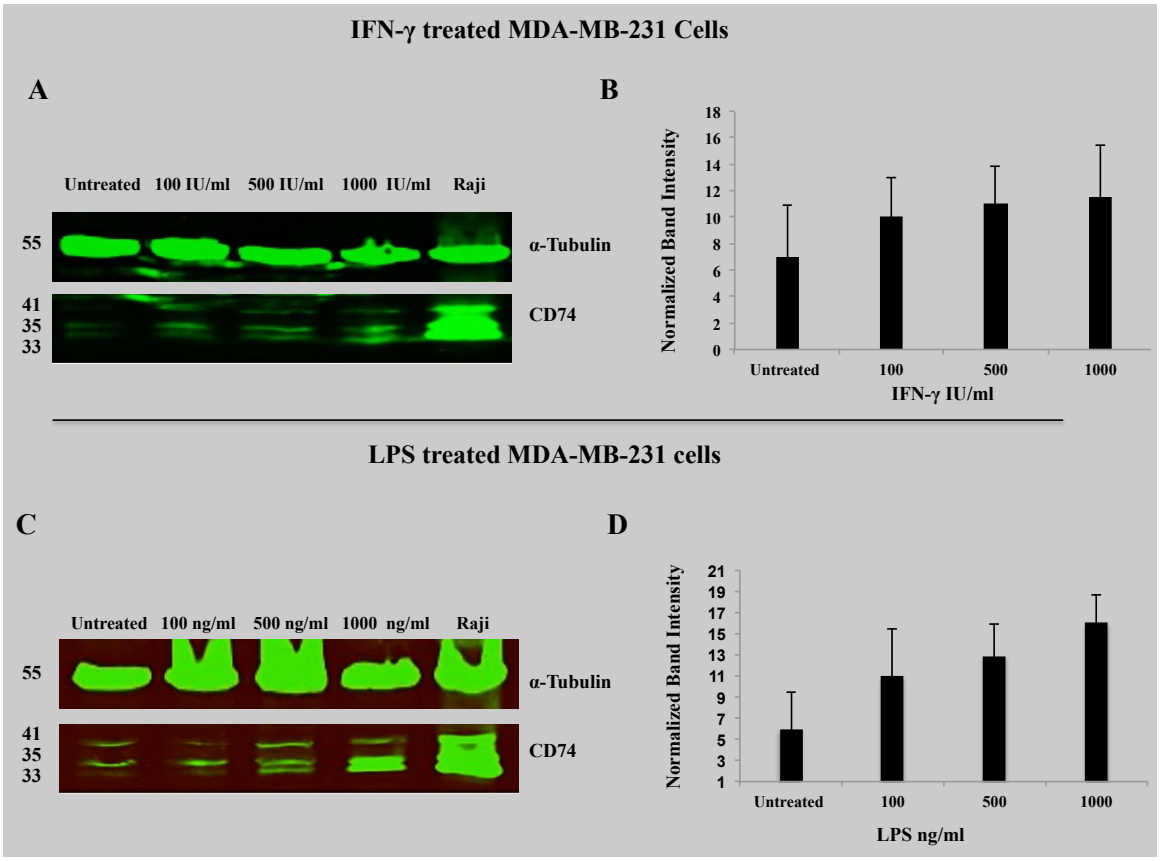

Figure 4-11: CD74 and α-Tubulin expression according to their molecular weight in IFN-γ or LPS treated MDA-MB-231 cell lines.

SDS-PAGE (12%) was performed under reducing conditions, followed by Western blotting with primary monoclonal antibodiesTU-02 (anti α-Tubulin as loading control) and By2 (anti-CD74). α-Tubulin is detected at a molecular weight of 55 kDa. The monocyte cell line Raji was used as a positive control as it expressed high levels of CD74 without any stimulation of cytokines. MDA-MB-231 cells, cultured in the presence of the indicated concentrations of IFN- γ for 72 hr or LPS for 24 hr. (A and C) α-Tubulin, CD74 on untreated MDA-MB-231 and IFN-γ or LPS treated MDA-MB-231 cells with indicated concentrations. (B and D) Relative levels of CD74 in IFN-γ or LPS treated MDA-MB-231 cells. CD74 levels are normalized against α-Tubulin to account for the difference in protein loading during the experiment; the percentage of regulation was calculated after the intensity of each band was adjusted according to its respective α-Tubulin band intensity using Image Studio Lite software (LI-COR Biosciences). Comparison of CD74 expression in untreated MDA-MB-231 and IFN-γ or LPS treated MDA-MB-231 cells were assessed using densitometry analysis. CD74 isoforms were detected at expected molecular weights; 33, 35 and 41 kDa. Maximum CD74 isoform expression was detected in MDA-MB-231 cells treated with 500 IU/ml of IFN-γ or 1000 ng/ml of LPS. A representative immunoblot of three independent experiments.

4.3 Conclusions

The characterization of the determinants of tumour immunogenicity may potentially help to inform the development of cell-based vaccines. The present study sought to map immunological molecules and related molecules in breast cancer cells to investigate the involvement of CD74 in proinflammatory and inflammatory pathways. As it was explained above, CD74 is a receptor for the proinflammatory cytokine, MIF. This ligand/receptor complex initiates survival pathways and cell proliferation, and it triggers the synthesis and secretion of major proinflammatory factors and cell adhesion molecules (Le Hiress et al., 2015). CD74 has been also suggested to be involved in tumour escape and dissemination (Chao et al., 2012). For this reason the influence of IFN-γ or LPS on the behaviour of the breast cancer derived cell lines CAMA-1 and MDA-MB-231 was studied. It is suggested that overexpression of CD74 by tumour cells might enhance their escape from immunoediting during the cancer immunoediting process (Kim et al., 2008; Chao et al., 2012). Recent studies by Fan et al. (2011) and Chao et al. (2012) have found evidence to link CD74 to tumour survival, suggesting that systemic inflammation and postoperative infections lead to cancer recurrence and survival. Therefore, investigation of the role of IFN-γ or LPS in the expression of CD74 in breast cancer cell lines has become critical.

The obtained results from this study showed the MIF-receptor CD74 could serve as a new putative prognostic factor, opening up possibility for further research. Growing interest focuses on the role of inflammatory signals in the initiation and development of breast cancer diagnosis and prognosis. Therefore, following profiling of CD74 expression, the effect of IFN-γ and LPS on CD74 expression in breast cancer cell lines was examined. It was found that CD74 positivity is significantly increased after incubation with IFN-γ or LPS. The results indicate that IFN-γ and LPS can play a key role in modulating the

expression of CD74 in the breast cancer cell lines CAMA-1 and MDA-MB-231as well as on the proliferation and the migration of both cell lines. This suggests that CD74 might play a role in tumour immunogenicity as well as in cancer immunoediting of breast cancer cells. Further research into CD74 and its effect on cellular processes, including the complex interactions between CD74 and its binding partners, such as MIF and CD44, will undoubtedly translate into clinical benefit for patients. However, on the whole, the present data support a role for CD74 in the inflammatory cascade during tumourigenesis. Its biological functions, and its association with surrogate markers, such as invasion and migration, could implicate CD74 as a potential therapeutic target in breast cancer therapy.

Chapter 5 CD74 and its interrelation with MIF and CD44 in the breast cancer derived cell lines

5.1 Introduction

Several studies have suggested that a small proportion of intracellular CD74 is modified by the addition of chondroitin sulfate (CD74-CS), a form of CD74. Chondroitin sulfate is a sulfated glycosaminoglycan usually found attached to proteins as part of a proteoglycan. CD74-CS is expressed on the surface of immune cells and can bind MIF, mediating MIF's signalling pathway (Naujokas et al., 1993; Matza et al., 2003; Binsky et al., 2010). Cell-surface expression of CD74 is not strictly dependent on the expression of class II MHC molecules in term of antigen presentation (Henne et al., 1995; Starlets et al., 2006), and numerous non-class II positive cells express CD74, in which it functions as a receptor for the initiation of different signalling cascades (Stumptner-Cuvelette and Benaroch, 2002; Maharshak et al., 2010). MIF has been found to be the natural ligand of CD74 and binds to the extracellular domain of CD74 with high affinity (KD = 1.40 Å~ 10-9 M) and initiates a signalling cascade (Leng et al., 2003).

When bound to the extracellular domain of CD74, MIF promotes signalling pathways, including cell proliferation and apoptosis (Leng et al., 2003; Shi et al., 2006; Starlets et al., 2006; Bach et al., 2009; Fan et al., 2011; Tillmann et al., 2013). The short cytoplasmic tail of CD74 lacks a signal-transducing intracellular domain, although serine phosphorylation, takes place in the P35 variant of CD74, requiring CD44, a polymorphic transmembrane protein with kinase activating properties (Zernecke et al., 2008; Borghese and Clanchy, 2011). CD74 forms a complex with CD44, which is essential for the MIF-induced signalling cascade (Gore et al., 2008; Shi et al., 2006). This cascade induces phosphorylation of ERK1 and ERK2, which then activates various effector proteins involved in inflammatory processes and cell proliferation. ERK1 and ERK2 remains phosphorylated for many hours and hence this cascade continues for up to 2 to 3 hours (Mitchell et al., 1999; Lue et al., 2006; Wortzel and Seger, 2011; Roskoski, 2012).

Concurrently, MIF binding to CD74 activates the P13K-Akt pathway, leading to phosphorylation of BAD and BAX proteins, involved in apoptosis (Lue et al., 2007). In addition, this cascade augments Bcl-2 expression, further supporting cell survival (Starlets et al., 2006; Lantner et al., 2007; Gore et al., 2008; Sapoznikov et al., 2008; Gordin et al., 2010; Cohen et al., 2012). Thus, the binding of MIF to the CD74/CD44 complex initiates a pathway resulting in proliferation of the mature B cell population and their rescue from death. In addition to activating the P13K-Akt pathway, MIF binding to CD74 induces a signalling pathway that involves the Syk tyrosine kinase (Gore et al., 2008; Starlets et al., 2006), induction of CD74 intramembrane cleavage, and the release of the CD74 intracellular domain (CD74-ICD) (Matza et al., 2002; Schneppenheim et al., 2013). CD74-ICD translocates to the nucleus where it induces activation of transcription mediated by the NF-κB p65/RelA homodimer and its co-activator, TAFII105, resulting in regulation of transcription of genes that control B cell proliferation and survival (Gore et al., 2008; Matza et al., 2001; Starlets et al., 2006). Therefore, the CD74-MIF-CD44 complex initiates a pro-survival signal leading to the increase of proliferation and inhibition of apoptosis.

The key question of this study was to investigate the interaction of CD74 as a related molecule to MIF and CD44 in CAMA-1, MDA-MB-231 and MDA-MB-435 cells. This was achieved by studying the colocalisation of CD74 and MIF as well as CD74 and CD44 by confocal microscopy and immunoprecipitation. Two different colocalisation analysis methods, pixel-based and object- based, were applied to study the interaction between CD74-MIF-CD44 complexes. Cell proliferation and apoptosis in CD74 siRNA transfected cells (CAMA-1 and MDA-MB-231) were also studied to address the hypothesis that blocking CD74 or MIF would affect apoptosis and cell proliferation.

5.2 Results

5.2.1 Colocalisation of CD74 and MIF

To investigate whether CD74 colocalised with MIF on CAMA-1, MDA-MB-231 and MDA-MB-435 cells, all cell lines were immunostained with an appropriate primary antibody followed by a secondary antibody. CD74 was labelled with Alexa Fluor® (red) and MIF Alexa Fluor® (green). MDA-MB-435 cells were used as a model in this study since they express high level of CD74, MIF and CD44. CAMA-1, MDA-MB-231 and MDA-MB-435 cells showed clear expression of CD74 and MIF. Merging green and red channels assessed the colocalisation and the Pearson's product-moment correlation coefficient (PCC) was used to analyse the degree of colocalisation. Figure 5-1 shows the colocalisation of CD74 and MIF on positive control THP-1 cells by merging green and red channels. 3D images are depicted in Figure 5-2, which were acquired in stack, with z-direction step size 0.14 μm using NIS element. Figure 5-3 shows the colocalisation analysis of CD74 and MIF which is performed on a pixel by pixel basis and based on the PCC using a scatter plot on the THP-1, CAMA-1, MDA-MB-231 and MDA-MB-435 as a comparison of colocalisation in all cell lines versus the (positive control; THP-1). It was found that CD74 and MIF were highly colocalised in the breast cancer cell lines CAMA-1, MDA-MB-231 and MDA-MB-435 compared to THP-1 cells, serving as positive control (Figures 5-1 and 5-3). The images used to calculate the Pearson's correlation coefficients of MIF and CD74 are presented in (Appendix 1; Figure A1.6). For more accuracy, the total colocalised volume of CD74 and MIF was acquired in stack, with z-direction and segmented by NIS-Elements program (Nikon).

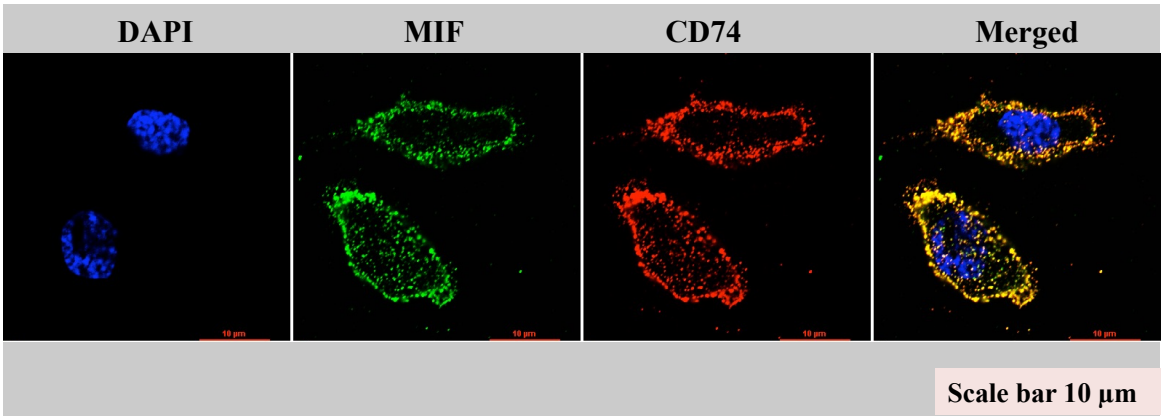

Figure 5-1: Colocalisation of CD74 and MIF on the cell-surface of THP-1 cells.

THP-1 cells were cultured in LabTek 8-well chambers at a density of 10×10^3 cells per well overnight. Colocalisation of CD74 and MIF on the cell-surface of THP-1 cells is shown. THP-1 cells were double stained with MIF primary antibody labelled with (FITC) Alexa Fluor® 488 (green) or with CD74 primary antibody labelled with (TRITC) Alexa Fluor® 555 (red). Colocalisation is shown as yellow fluorescence, the result of merging green and red channels; highly colocalised area of MIF and CD74 is shown. The Pearson's product-moment correlation coefficient was used to analyse the degree of colocalisation. The images represent three different experiments.

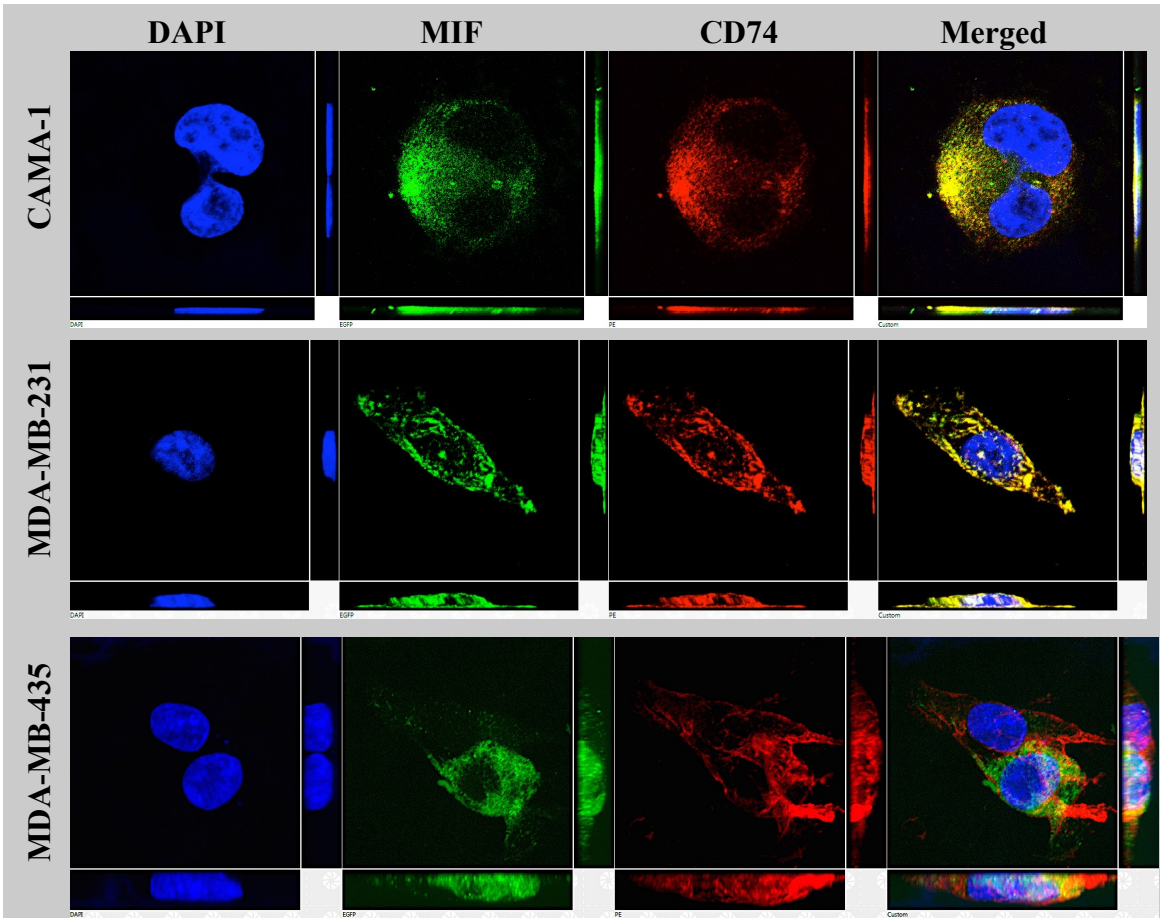

Figure 5-2: Colocalisation of CD74 and MIF on the cell-surface of CAMA-1, MDA-MB-231 and MDA-MB-435 cells, determined by confocal microscopy analysis.

CAMA-1, MDA-MB-231 and MDA-MB-435 cells were cultured in LabTek 8-well chambers at a density of 10×10^3 cells per well overnight. Cells were stained with MIF labelled with Alexa Fluor® 488 (green) or CD74 labelled with Alexa Fluor® 555 (red). Cell nuclei were stained with 4', 6-diamidino-2-phenylindole (DAPI) (blue). Fluorochromes were acquired separately to evaluate the expression of CD74 and MIF. Yellow/orange fluorescence reveals the potential colocalisation of the two antigens. 3D images were acquired in stack, with z-direction step size 0.14 µm using NIS element. Single-plane of z-stack is shown in three directions as xy, yz and zx. Data represents three different experiments.

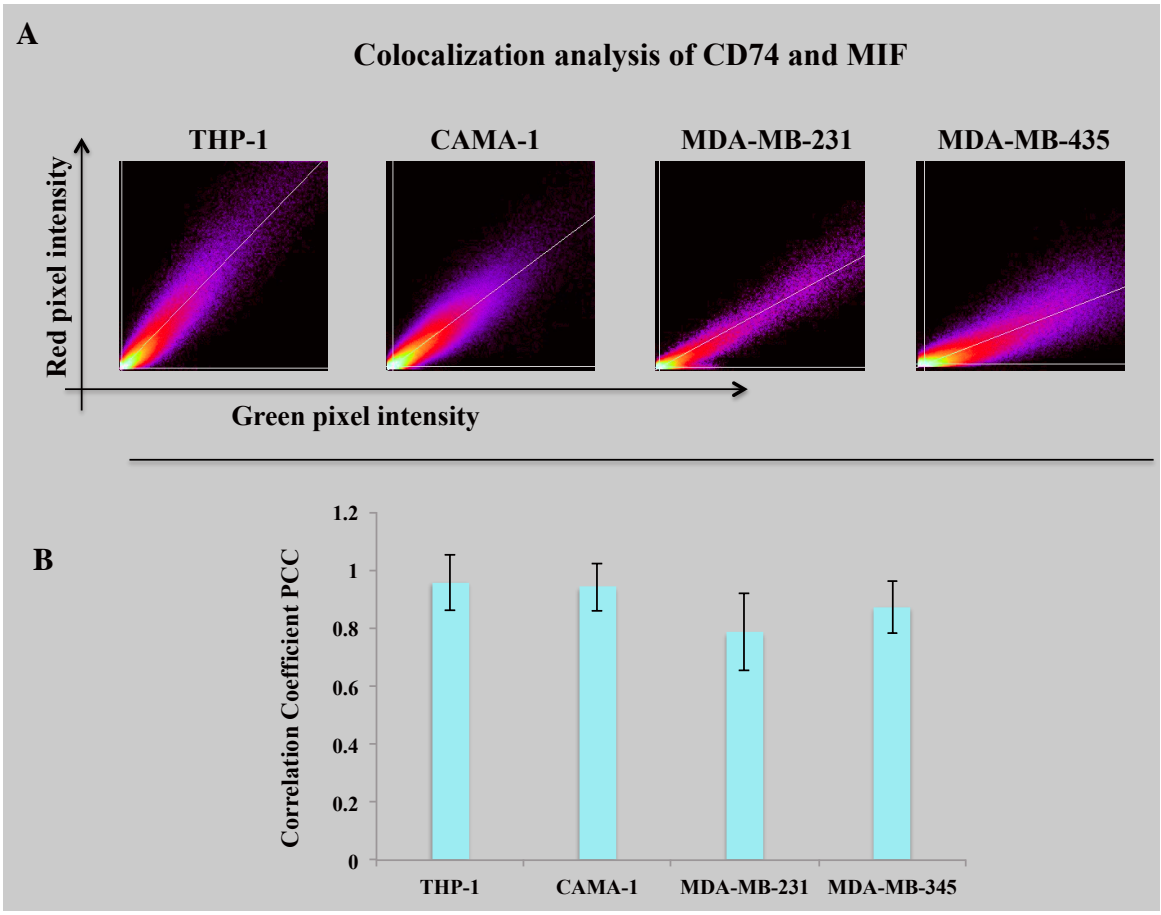

Figure 5-3: Colocalisation analysis of CD74 and MIF performed on a pixel by pixel basis and based on Pearson's product-moment coefficient correlation using a scatter plot on THP-1, CAMA-1, MDA-MB-231 and MDA-MB-435 cells.

(A) Each pixel in the image was plotted in the scatter diagram based on its intensity level in each channel. The colour in the scatterplot represents the number of pixels plotted in that region. In this example, green is shown on the x-axis and red is shown on the y-axis. The scatterplot shows high colocalisation and no bleed through either green or red channels. The scatter plot provides the rate of the area of association of two fluorochromes, calculated by linear regression. The scatter plot comprised of dots, appearing as cloud, indicates complete colocalisation. (B) Graphical representation of colocalisation analysis based on the Pearson product-moment correlation coefficient (PCC) on each cell. The value for PCC ranges from +1 and −1 inclusive. A value of +1 would mean the total positive correlation, every pixel that contains Alexa Fluor® 488 (FITC) also contains Alexa Fluor® 555 (TRITC), while a value of −1 would mean the total negative correlation, every pixel that contains Alexa Fluor® 488 does not contain Alexa Fluor® 555 and vice versa. The PCC was calculated based on different images and indicates strong colocalisation of CD74 and MIF on CAMA-1, MDA-MB-231 and MDA-MB-435 cells. THP-1 cells, serving as positive control. Data represents three different experiments.

5.2.2 Colocalisation of CD44 and MIF

The colocalisation of CD44 with MIF on the cell-surface of CAMA-1, MDA-MB-231 and MDA-MB-435 cells was also investigated. All cell lines were immunostained with an appropriate primary antibody followed by a secondary antibody. MIF was labelled with Alexa Fluor® (green) 488 and CD44 was labelled with Alexa Fluor® 555 (red). CAMA-1, MDA-MB-231 and MDA-MB-435 cells showed expression of MIF and CD44. Confocal microscopy confirmed that MIF and CD44 were not colocalised on the cell-surface so further analysis was not carried out. Figure 5-4 shows a weak colocalisation of CD44 and MIF on the cell-surface of CAMA-1, MDA-MB-231 and MDA-MB-435. 3D images of negative control samples stained with secondary antibodies were acquired in stack, with z-direction step size 0.14 μm using NIS element, the same acquisition protocol as for all data sets (Figure 5-5).

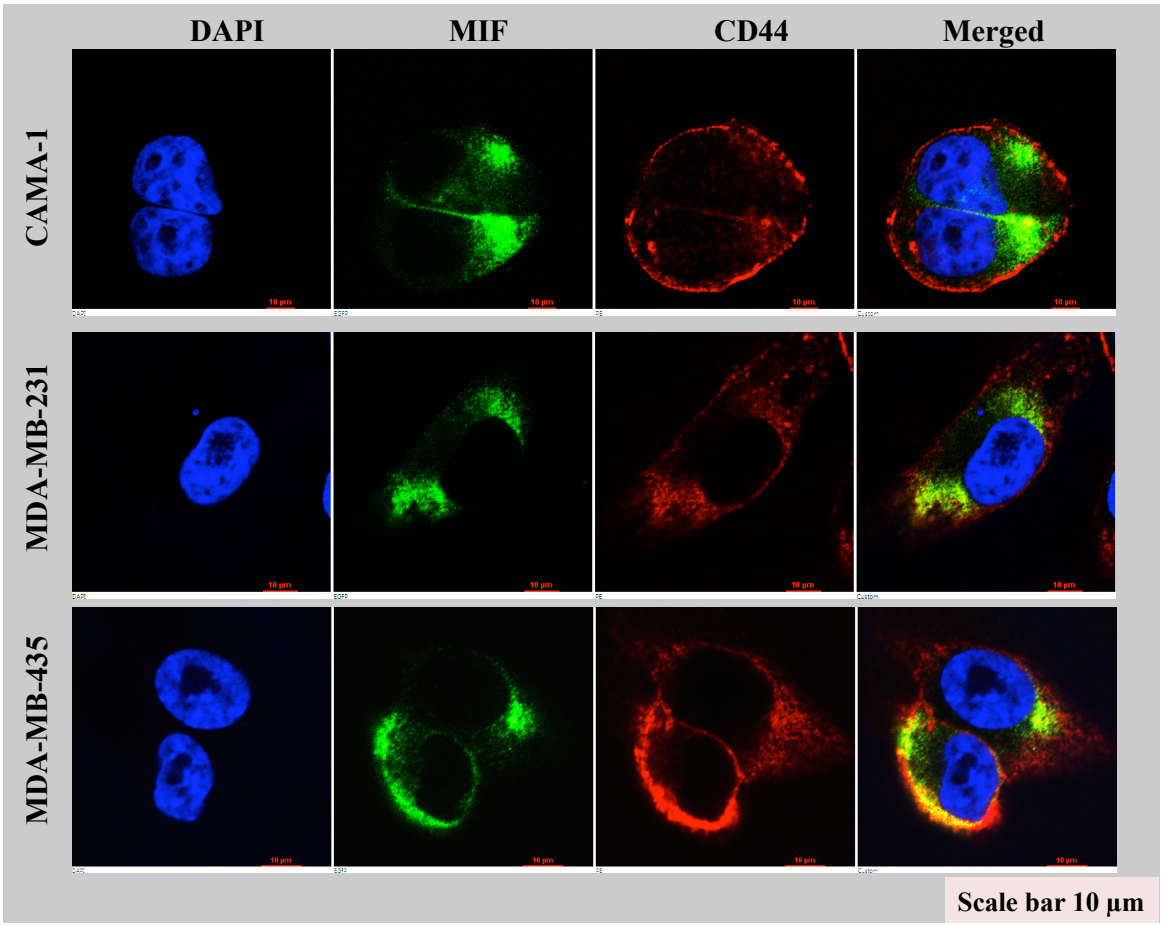

Figure 5-4:Colocalisation of MIF and CD44 on the cell-surface of CAMA-1, MDA-MB-231 and MDA-MB-435 cells, determined by confocal microscopy analysis.

CAMA-1, MDA-MB-231 and MDA-MB-435 cells were cultured in LabTek 8-well chambers at a density of 10×10^3 cells per well overnight. The cells were stained with MIF labelled with Alexa Fluor® 488 (green) or CD44 labelled with Alexa Fluor® 555 (red). Cell nuclei were stained with 4', 6-diamidino-2-phenylindole (blue). Fluorochromes were acquired separately to evaluate the expression of CD44 and MIF. Yellow/orange fluorescence reveals the potential colocalisation of two antigens. The images represent three different experiments.

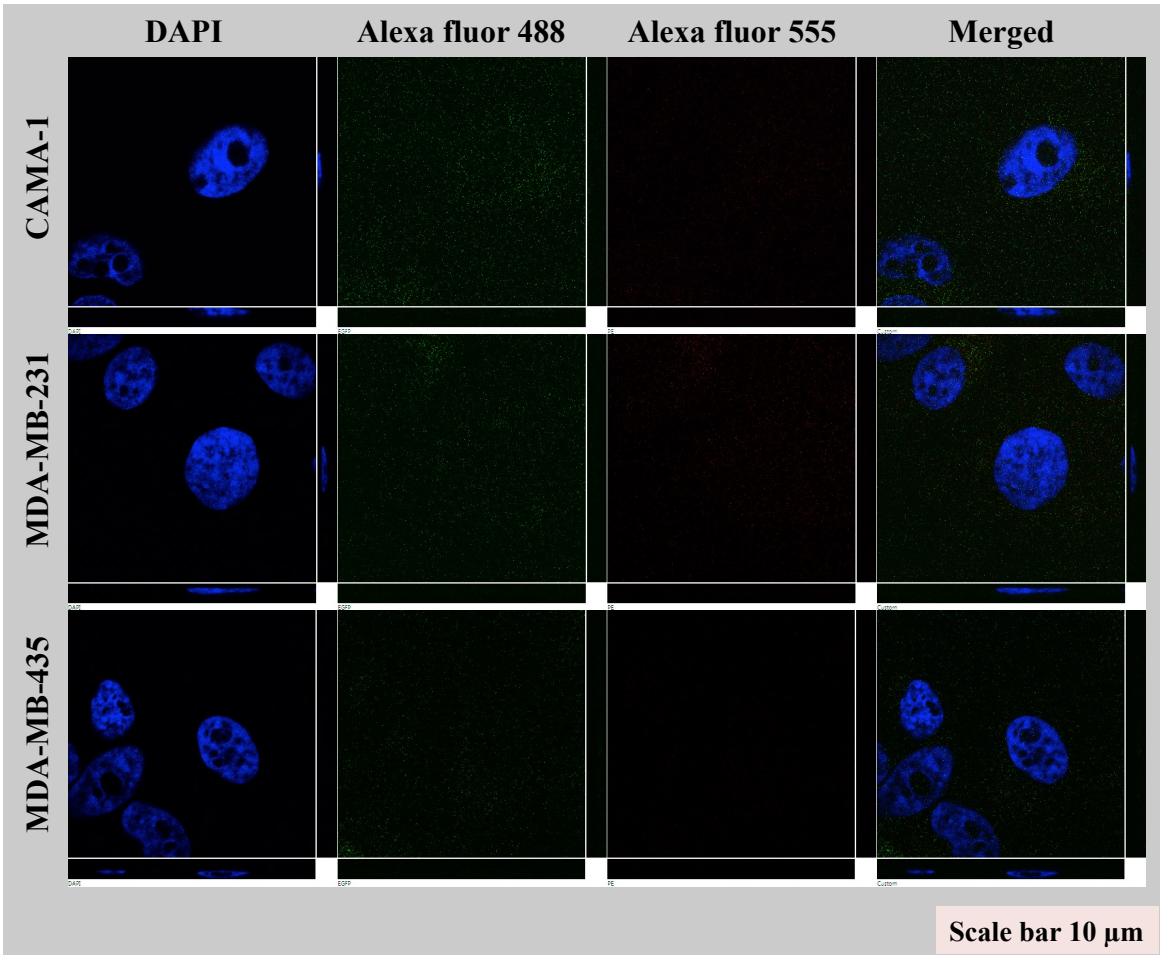

Figure 5-5: Confocal microscopy images of negative control samples of CAMA-1, MDA-MB-231 and MDA-MB-435 cells.

Isotype control representing cells stained with isotype control IgG primary and Alexa Fluor® 488 and Alexa Fluor® 555 secondary antibodies, visualised by using green 488 nm and red 555 nm wavelength lasers to measure non-specific antibody binding. Blue colour shows DAPI stained cell nuclei. Red Green shows merged image. 3D images were acquired in stack, with z-direction step size 0.14 µm using NIS element. Single-plane of z-stack is shown in three directions as xy, yz and zx. Scale bar 10 um.

5.2.3 Segmentation and colocalisation of CD74 and MIF

For more accuracy, 3D images were acquired in stack, with z-direction and segmented by NIS elements using regional maximum detection tools followed by manual threshold to calculate the exact percentage of colocalised molecules of CD74 with MIF against the total volume in each image. CD74 (red) and MIF (green) channels were segmented and the generated binary areas were visually inspected; the overlap of the green and red channels was generated by an overlay tool, resulting in a new layer (yellow) that represented the intersection of CD74 and MIF. Finally, automated volume measurement was carried out for CD74, MIF and their intersection with a volume measurements tool. The overlapped percentage of the green and red channels (yellow) in that CAMA-1, MDA-MB-231 and MD-MB-435 was calculated by NIS-Elements with values presented as a pie chart (20%, 15% and 22% respectively). The result of 3D images and pie charts are presented in (Figure 5-6 A, B and C). It was found that CAMA-1, MDA-MB-231 and MD-MB-435 cells labelled with CD74 and MIF displayed significantly high levels of colocalisation. This suggests that CD74 might serve important regulatory roles in signalling pathways along with MIF and CD44.

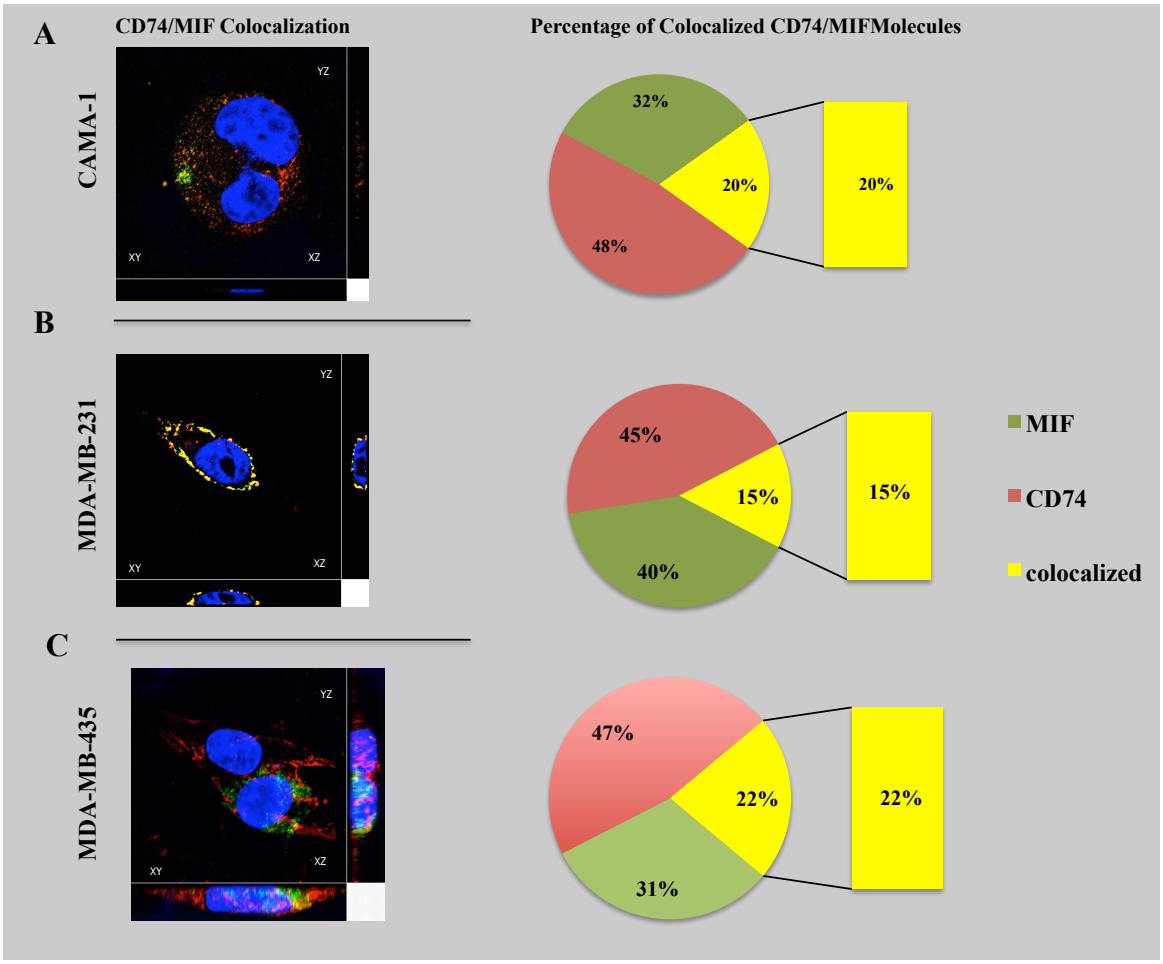

Figure 5-6: Colocalisation of CD74 with MIF, quantified on segmented 3D images by maximum intensity projections.

Maximum intensity projections of CAMA-1, MDA-MB-231 and MDA-MB-435 cells are represented in panels A, B and C. MDA-MB-435, MDA-MB-231 and CAMA-1 cells were stained with CD74 labelled with Alexa Fluor® 555 (red) and MIF labelled with Alexa Fluor® 488 (green). Cell nuclei were stained with 4', 6-diamidino-2-phenylindole (blue). Segmentation results from both channels were merged with the DAPI. The percentages of the total volumes of CD74, MIF and the colocalisation from each image are represented on pie charts. CAMA-1 cells have the highest correlation between CD74 and MIF followed by MDA-MB-435 and MDA-MB231. Data represents three different experiments.

5.2.4 Colocalisation of CD74 and CD44

To investigate whether the intra-cytoplasmic domain of CD74 colocalises with CD44 on the intracellular membranes of CAMA-1, MDA-MB-231 and MDA-MB-435 cells, cell lines were immunostained with an appropriate primary antibody followed by a secondary antibody. CD74 was labelled with Alexa Fluor® 488 (green) and CD44 was labelled with Alexa Fluor® (red). CAMA-1, MDA-MB-231 and MDA-MB-435 cells show expression of CD74 and CD44. Merging green and red channels revealed colocalisation of CD74 and CD44, and the PCC was used to analyse the percentage of colocalisation. Figure 5-7 shows colocalisation of CD74 and CD44 in positive control THP-1 cells. 3D images are shown in in Figure 5-8, which were acquired in stack, with z-direction step size 0.14 μm using NIS element. Figure 5-9 shows colocalisation analysis of CD74 and CD44, which was performed on a pixel by pixel basis and based on the PCC. This analysis used a scatter plot for the assessment of the THP-1, CAMA-1, MDA-MB-231 and MDA-MB-435 to compare colocalisation in all cell lines versus the (positive control; THP-1). It was found that CD74 and CD44 were highly colocalised in the breast cancer cell lines CAMA-1, MDA-MB-231 and MDA-MB-435 compared to THP-1 cells (Figure 5-7). For more accuracy, the total colocalised volume of CD74 and CD44 was acquired in stack, with z-direction and segmented by NIS elements. The images used to calculate the Pearson's correlation coefficients are presented in (Appendix 1; Figure A1.7).

Colocalisation of CD74 and CD44 was also investigated on the cell-surface membrane. Confocal microscopy confirmed that CD74 and CD44 were not colocalised on the cell-surface, so further analysis was not carried out. The merged images of CD74 and CD44 on the breast cancer cell lines are shown in Figure 5-10.

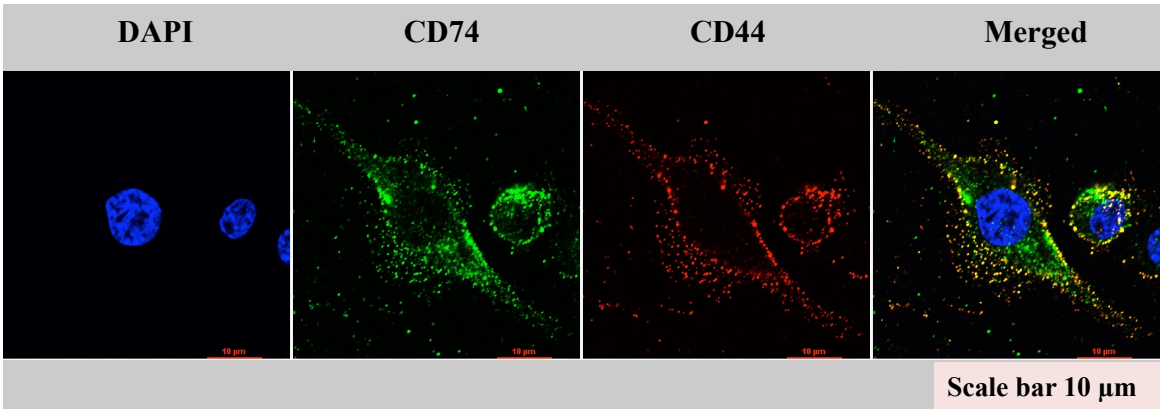

Figure 5-7: Colocalisation of CD74 and CD44 at intracellular level in THP-1 cells.

THP-1 cells were cultured in LabTek 8-well chambers at a density of 10×10^3 cells per well overnight. THP-1 double were stained with CD74 primary antibody and labelled with (FITC) Alexa Fluor® 488 (green), and with CD44 primary antibody and labelled with (TRITC) Alexa Fluor® (red). Colocalisation is shown as yellow fluorescence, the result of merging green and red channels; highly colocalised area of CD74 and CD44 is shown Pearson's correlation coefficient was used do analyse the degree of colocalisation. The images shown represent three different experiments.

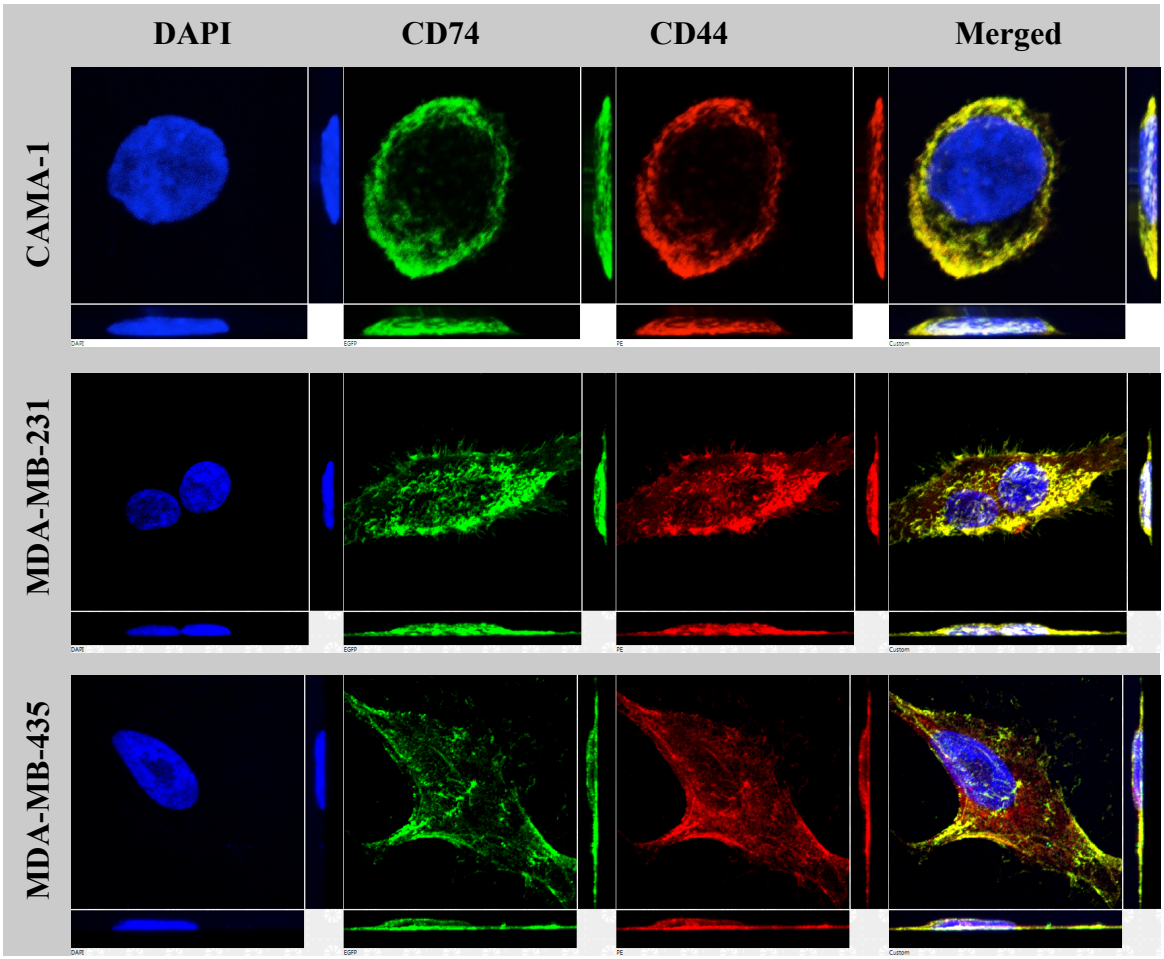

Figure 5-8: Intracellular colocalisation of CD74 and CD44 in CAMA-1, MDA-MB-231 and MDA-MB-435 cells, determined by confocal microscopy analysis.

CAMA-1, MDA-MB-231 and MDA-MB-435 cells were cultured in LabTek 8-well chambers at a density of 10×10^3 cells per well overnight. Cells were stained with CD74 labelled with Alexa Fluor® 488 (green) and CD44 labelled with Alexa Fluor® 555 (red). Cell nuclei were stained with 4', 6-diamidino-2-phenylindole (DAPI) (blue). Fluorochromes were acquired separately to evaluate the expression of CD74 and CD44. Yellow/orange fluorescence shows the potential colocalisation of two antigens. 3D images were acquired in stack, with z-direction step size 0.14 µm, using NIS element. Single-plane of z-stack is shown in three directions as xy, yz and zx. Data represents three different experiments.

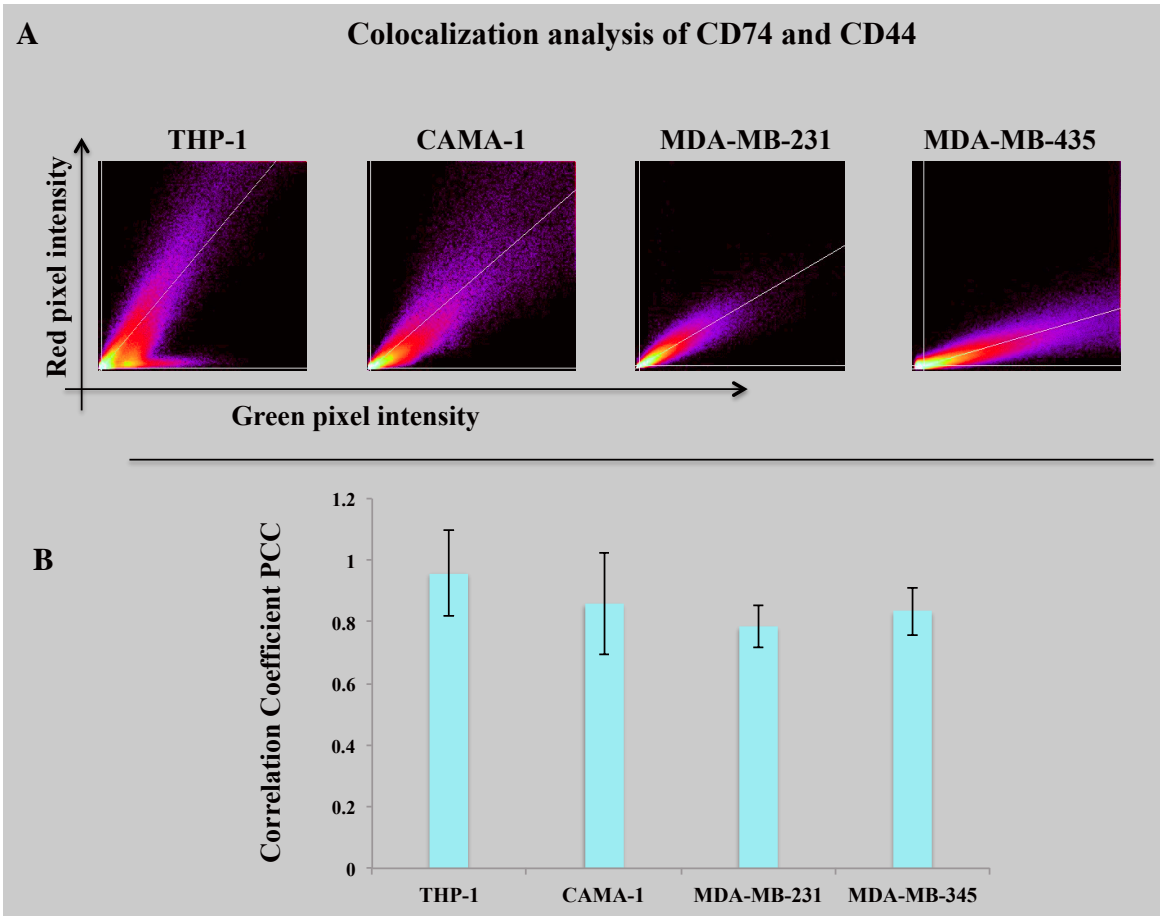

Figure 5-9: Colocalisation analysis of CD74 and CD44 is performed on a pixel by pixel basis and based on Pearson's product-moment coefficient correlation using a scatter plot on THP-1, CAMA-1, MDA-MB-231 and MDA-MB-435 cells.

(A) Each pixel in the image is plotted in the scatter diagram based on its intensity level in each channel. The colour in the scatterplot represents the number of pixels that are plotted in that region. Green intensity is shown on the x-axis and red intensity is shown on the y-axis. The scatterplot shows high colocalisation and no bleed through. It depicts the area of association of two fluorochromes, as calculated by linear regression. Dots, appearing as cloud, indicate complete colocalisation. (B) Graphical representation of colocalisation analysis based on the Pearson product-moment correlation coefficient (PCC) of each cell. The value for PCC can range from −1 to +1. A value of +1 would mean that the patterns are perfectly similar; i.e. pixels that contain Alexa Fluor® 488 (FITC) also contain Alexa Fluor® 555 (TRITC). A value of −1 would mean that the patterns are perfectly opposite; i.e. pixels that contain Alexa Fluor® 488 do not contain Alexa Fluor® 555 and vice versa. The PCC, derived from three different images, indicates a strong colocalisation of CD74 and CD44 on CAMA-1, MDA-MB-231 and MDA-MB-435 cells. THP-1 cells, serving as positive control. Data represent three different experiments.

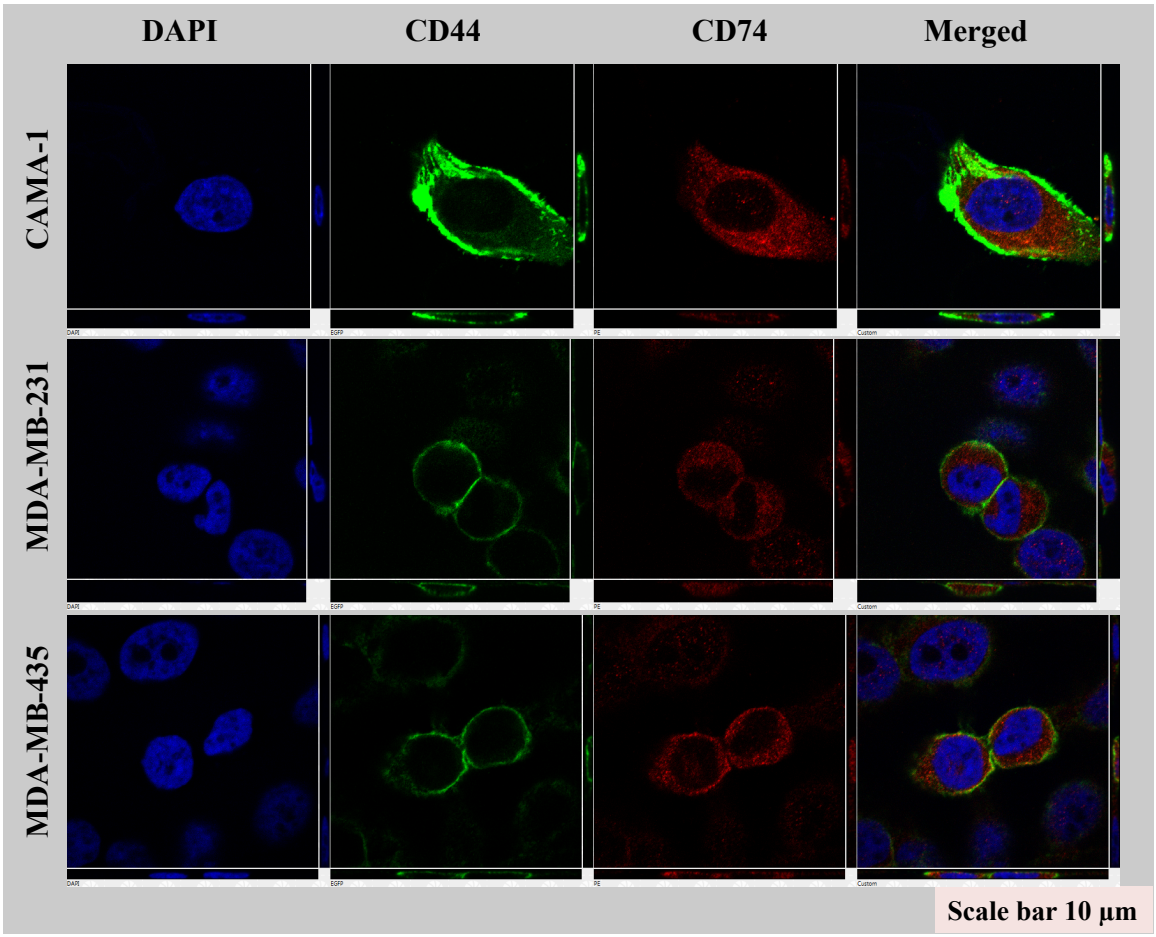

Figure 5-10: Colocalisation of CD74 and CD44 on the cell-surface of CAMA-1, MDA-MB-231 and MDA-MB-435 cells, determined by confocal microscopy analysis.

CAMA-1, MDA-MB-231 and MDA-MB-435 cells were cultured in LabTek 8-well chambers at a density of 10×10^3 cells per well overnight. Cells were stained with CD74 labelled with Alexa Fluor® 488 (green). Alexa Fluor® 555 (red) and CD44 labelled with Alexa Fluor® 555 (red). Cell nuclei were stained with 4', 6-diamidino-2-phenylindole (blue). Fluorochromes were acquired separately to evaluate the expression of CD74 and CD44. Yellow/orange fluorescence reveals the potential colocalisation of two antigens. 3D images were acquired in stack, with z-direction step size 0.14 µm using NIS element. Single-plane of z-stack is shown in three directions as xy, yz and zx. Data represents three different experiments.

5.2.5 Segmentation and colocalisation of CD74 and CD44

For more accuracy, 3D images were acquired in stack with z-direction and segmented by NIS elements using regional maximum detection tools followed by manual threshold to calculate the exact percentage of colocalised CD74 with CD44. CD74 (green) and CD44 (red) channels were segmented and the generated binary areas were visually inspected. The overlap of the green and red channels was generated by the overlay tool, resulting in a new layer (yellow) that represents the intersection of CD74 and CD44. Finally, automated volume measurement was carried out for CD74, CD44 and their intersection using the volume measurement tool. The overlapped percentage of the green and red channels (yellow) in that CAMA-1, MDA-MB-231 and MD-MB-43 was calculated by NIS-Elements with values presented as a pie chart (20%, 22% and 23% respectively). The resulting 3D images and pie charts are presented in (Figure 5-11 A, B and C). MDA-MB-435, MDA-MB-231 and CAMA-1 labelled with CD74 and CD44 displayed a significantly high level of colocalisation, suggesting that CD74 might play important regulatory roles in signalling pathways along with MIF and CD44.

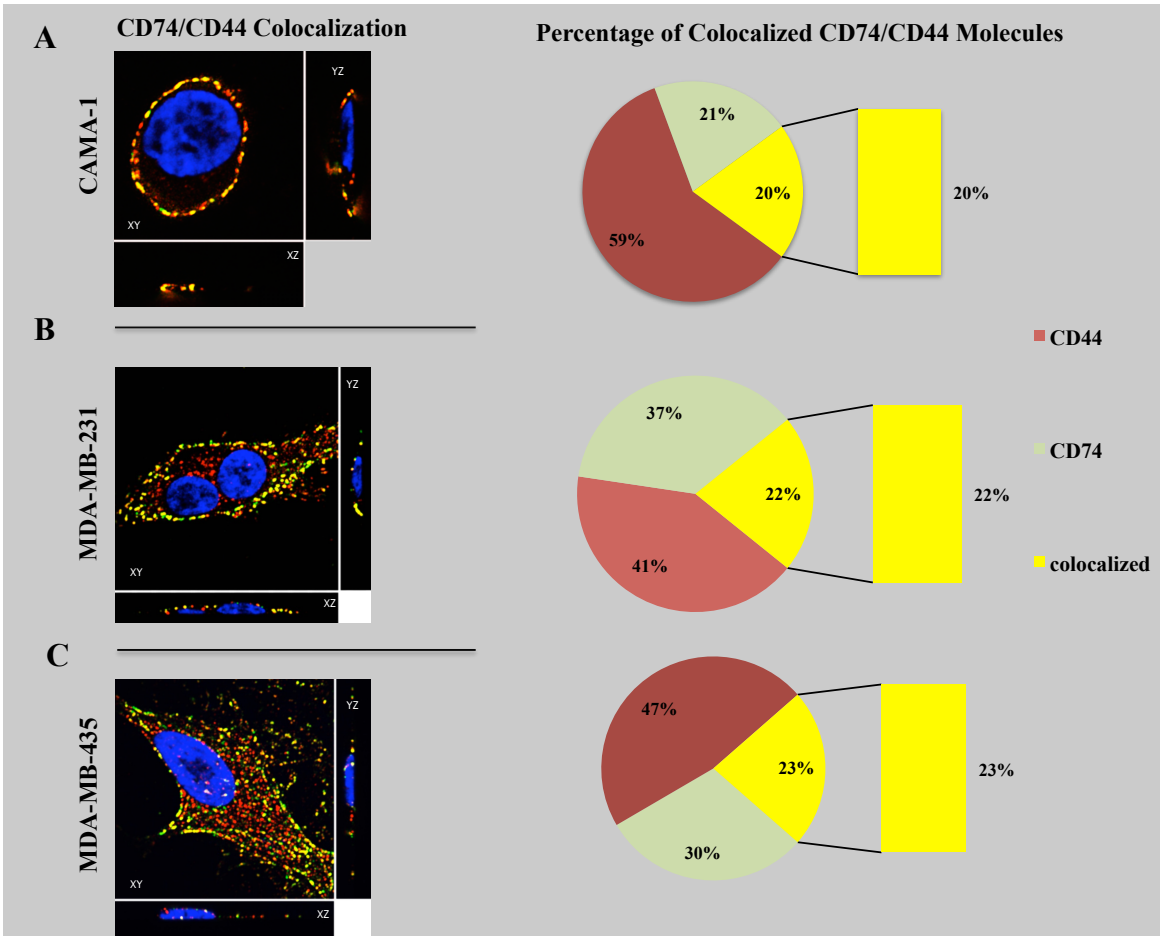

Figure 5-11: Colocalisation of CD74 with CD44, quantified on segmented 3D images by maximum intensity projections.

Maximum intensity projections of CAMA-1, MDA-MB-231 and MDA-MB-435 cells are represented in panels A, B and C. Cells were stained with CD74 labelled with Alexa Fluor® 488 (green) and CD44 labelled with Alexa Fluor® 555 (red). Cell nuclei were stained with 4', 6-diamidino-2-phenylindole (DAPI, blue). Segmentation results from both channels merged with the DAPI. The percentages of the total volumes of CD74, CD44 and the colocalisation from each image are represented in pie charts. The result shows that CAMA-1 cells have the highest correlation between CD74 and CD44, followed by MDA-MB435 and MDA-MB231. Data represents three different experiments.

5.2.6 Interaction of CD74 with MIF and CD44

To determine whether a physical association exists exclusively between the human-specific CD74 isoforms (P41, P35 and P33) and MIF as well as CD44 variant (CD44v) and CD44 standard (CD44s), a coimmunoprecipitation technique was used. Cell lysate was extracted from CAMA-1, MDA-MB-231 and MDA-MB-435 cells cultured in the presence of 10% of FCS with appropriate medium. The extracted lysate was incubated with anti-CD74 or anti-CD44 antibody and loaded on a gel. The probe was then incubated either with anti-CD74, anti-MIF or anti-CD44 antibodies as instructed.

CD74 or CD44 were first pulled down by immunoprecipitation in all breast cancer cell lines, as shown in (Figures 5-12 A and 5-13 A). CD74-MIF and CD74-CD44 interactions in cell lysates, as demonstrated by coimmunoprecipitation, showed that CD74 interacted with MIF and CD44 in breast cancer cells CAMA-1, MDA-MB-231 and MDA-MB-435 (Figure 5-12 B and C). The data also revealed that CD74 interacted with MIF, CD44s and CD44v in CAMA-1 cells. Figure 5-13 A, which demonstrates the pull of CD44, shows that MDA-MB-231 and MDA-435 cells expressed only CD44s, so were interacting with CD74 in the same manner, but in contrast to CAMA-1 cells, which expressed CD44v and CD44s. Co-IP of CD44-CD74 and CD44-MIF was performed to test whether CD44s and CD44v interacted exclusively with all isoforms of CD74 and MIF. The results showed that CD44s and CD44v bind only to P41 of CD74 (Figure 5-13 B and C). In contrast, no evidence was obtained for a cell-surface or intracellular interaction between CD44 and MIF (Figure 5-13). Bands at 55 and 25 kDa, corresponding to the heavy chain and light chain of the antibody coupled to the magnetic beads, were observed in all the samples and could be considered as a loading control. Additionally, no band was observed with protein G beads alone, which were loaded as the negative control.

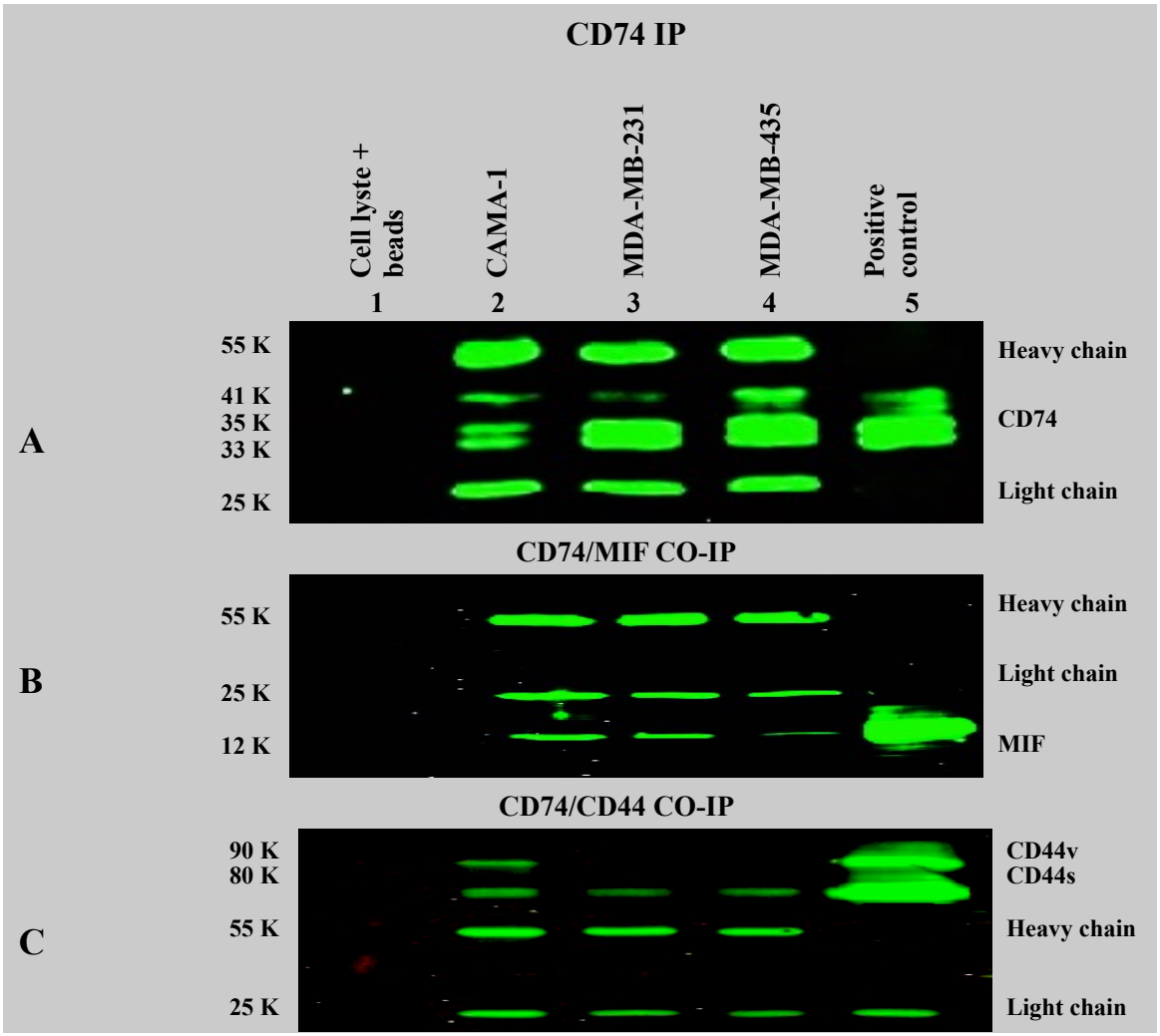

Figure 5-12: Co-immunoprecipitation (Co-IP) to study the interaction of CD74 with MIF and CD44 in CAMA-1, MDA-MB-231 and MDA-MB-435 cells.

Cell lysates from breast cancer cell lines were used for immunoprecipitation and immunoprecipitated proteins were separated by 12% SDS-PAGE. Blots were probed with mouse anti-CD74, anti-MIF or anti-CD44 antibodies. (A) Immunoprecipitation was subjected to pull down CD74 from breast cancer cells lysate. The blots were probed with mouse anti-CD74, anti-MIF or anti-CD44 antibodies. Molecular mass in kDa is shown on the left-hand side. The antibody (Ab) heavy and light chain bands are indicated so that Ab heavy and light chain fragments can be observed at approximately 55 and 25 kDa respectively. Lane 1 shows beads without added Ab, used in Co-IP as a negative control. (B and C) Co-IP applied to study the interaction of CD74/MIF and CD74/CD44. (B) The Co-IP of CD74/MIF confirmed that CD74 interacts with MIF. (C) The Co-IP of CD74/CD44 confirmed that all CD44 isoforms, including CD44s and CD44v, interact with CD74. No CD74 Co-IP was observed with Protein G beads alone, used as the negative control. The data represent three different experiments.

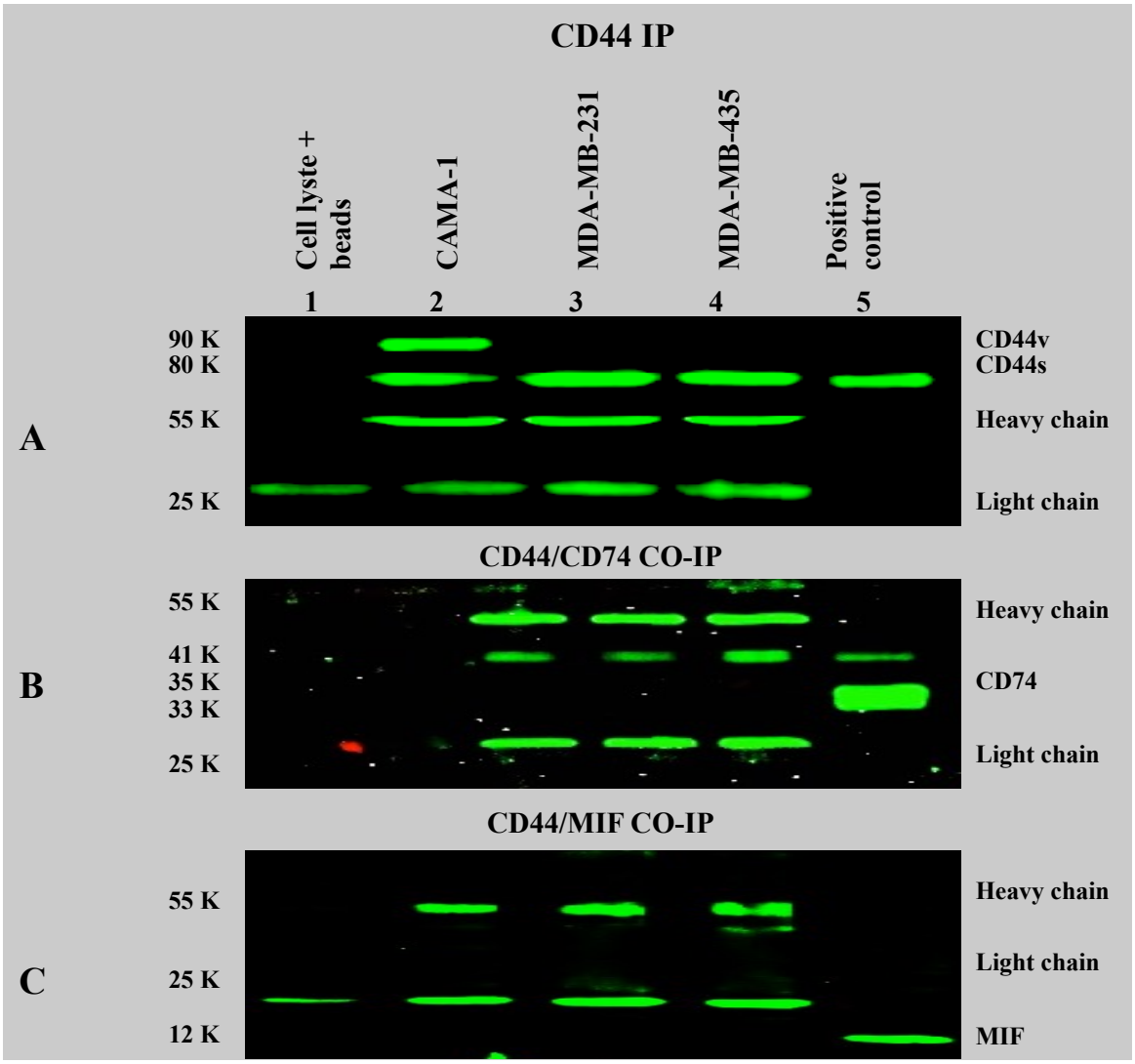

Figure 5-13: Co-immunoprecipitation (Co-IP) to study the interaction of CD44 with CD74 and MIF in CAMA-1, MDA-MB-231 and MDA-MB-435 cells.

Cell lysates from breast cancer cell lines were used for immunoprecipitation and immunoprecipitated proteins were separated by 12% SDS-PAGE. Blots were probed with mouse anti-CD74, anti-MIF or anti-CD44 antibodies. (A) Immunoprecipitation was subjected to pull down CD44 from breast cancer cells lysate. Molecular mass in kDa is shown on the left-hand side. The antibody (Ab) heavy and light chain bands are indicated so that Ab heavy and light chain fragments can be observed at approximately 55 and 25 kDa respectively. Lane 1 shows G beads without added antibody used in Co-IP, used as the negative control. (B and C) Co-IP was applied to study the interaction of CD44/CD74 and CD44/MIF. (B) The Co-IP of CD44 /CD74 confirmed that only P41 of CD74 interacts with CD44. (C) The Co-IP of CD44/MIF confirmed that there is no clear interaction between MIF and CD44 as no band consistent with MIF was observed. No CD74 Co-IP was observed with the negative control. Data represent three different experiments.

5.2.7 Knockdown of CD74 expression in CAMA-1 and MDA-MB-231 cells by siRNA CD74

Prior studies have reported that CD74 is over-expressed in human breast adenocarcinomas, and, along with MIF and CD44, has a role in tumour progression. The expression of CD74 in CAMA-1 and MDA-MB-231 cells was therefore evaluated. The expression of CD74 was found to be highest in CAMA-1 cells compared to MDA-MB-231 cells (Figure 5-14). In pilot experiments, it was found that a concentration of 80 pmol/ml for 24 hr of specific CD74 siRNA was optimal for disrupted expression of CD74. Therefore, a dose of 80 pmol/ml was selected for optimal transfection of CAMA-1 and MDA-MB-231 cells with siRNA for all subsequent experiments.

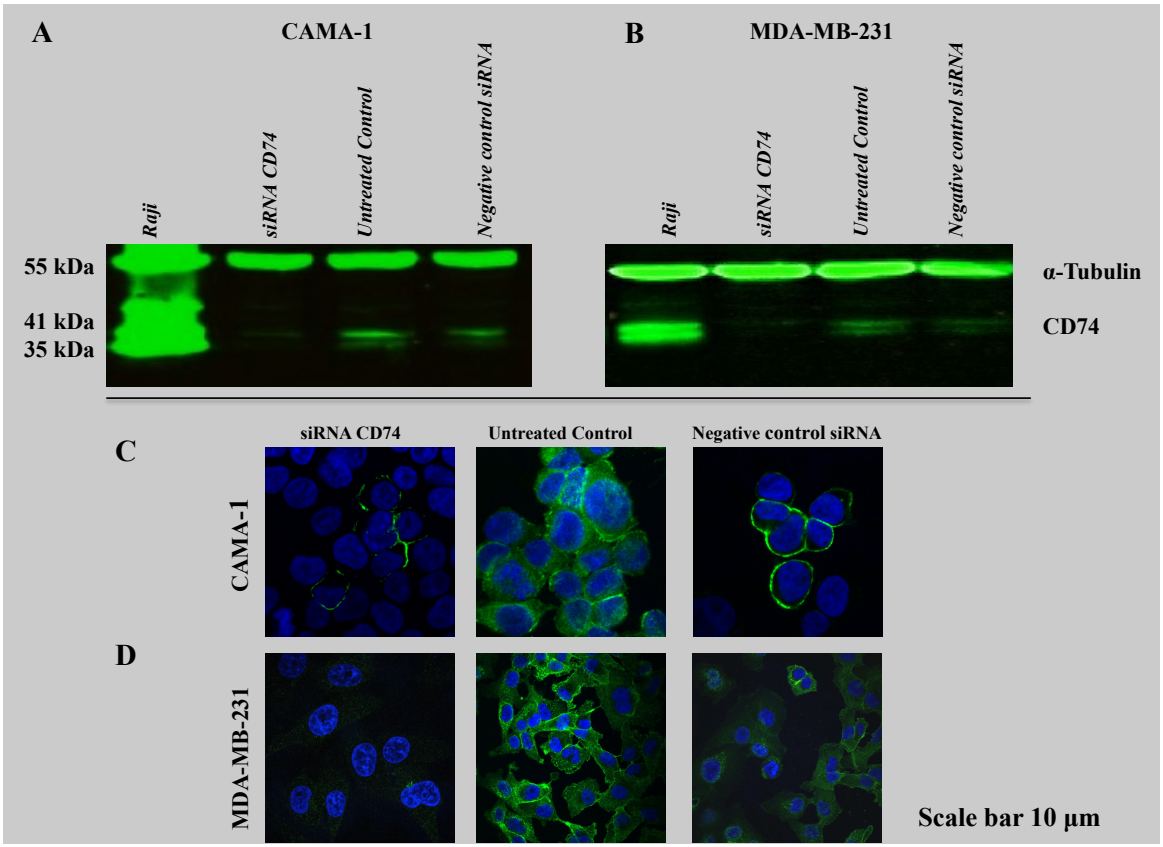

Figure 5-14: CD74 knockdown by CD74 siRNA transfection reagent in CAMA-1 and MDA-MB-231 cells.

(A and B) siRNA-mediated knockdown of CD74 expression in CAMA-1 and MDA-MB-231 cells detected by Western blot. An approximately two to five (siRNA) fold weaker signal of CD74 protein expression is apparent, as compared to the negative control siRNA group normalized to the expression of α-Tubulin. (C and D). Confocal images of CAMA-1 and MDA-MB-231 cells transfected with CD74 siRNA, untreated control and negative control siRNA. Data represent three different experiments.

5.2.8 Knockdown of functional CD74 expression promotes apoptosis

In the light of the observations indicating apoptotic modes of cell death in CAMA-1 and MDA-MB-231 cells treated with CD74 siRNA (Figure 5-14), next, multi-parameter flow cytometric analysis of siRNA-transfected CAMA-1 and MDA-MB-231 cells was pursued to obtain more sensitive and quantitative details of a possible apoptotic mode of cell death. Following 24 hr of culture of CD74 siRNA-transfected CAMA-1 and MDA-MB-231 cells, flow cytometry was used to detect the expression of annexin V in the absence of PI staining (Figure 5-15 A). Annexin V is a non- quantitative probe used to detect phosphatidylserine expressed on the cell-surface, an indication of apoptosis. CAMA-1 and MDA-MB-231 cells treated with CD74 siRNA displayed significantly higher levels of annexin V staining (± 55% and 58% respectively) compared with negative control siRNA-treated counterparts (± 8% and ± 13% respectively) (Figure 5-15 A). These observations indicate that CD74 might play important regulatory roles in apoptosis.

5.2.9 Determination of the effects of CD74 siRNA on CAMA-1 and MDA-MB-231 cell proliferation

CAMA-1 and MDA-MB-231 cell proliferation and viability was determined using the MTT metabolic and viability assay (Figure 5-15 B). CAMA-1 and MDA-MB-231 cells treated with CD74 siRNA displayed significantly reduced proliferation compared to cells treated with the negative control siRNA control sequence.

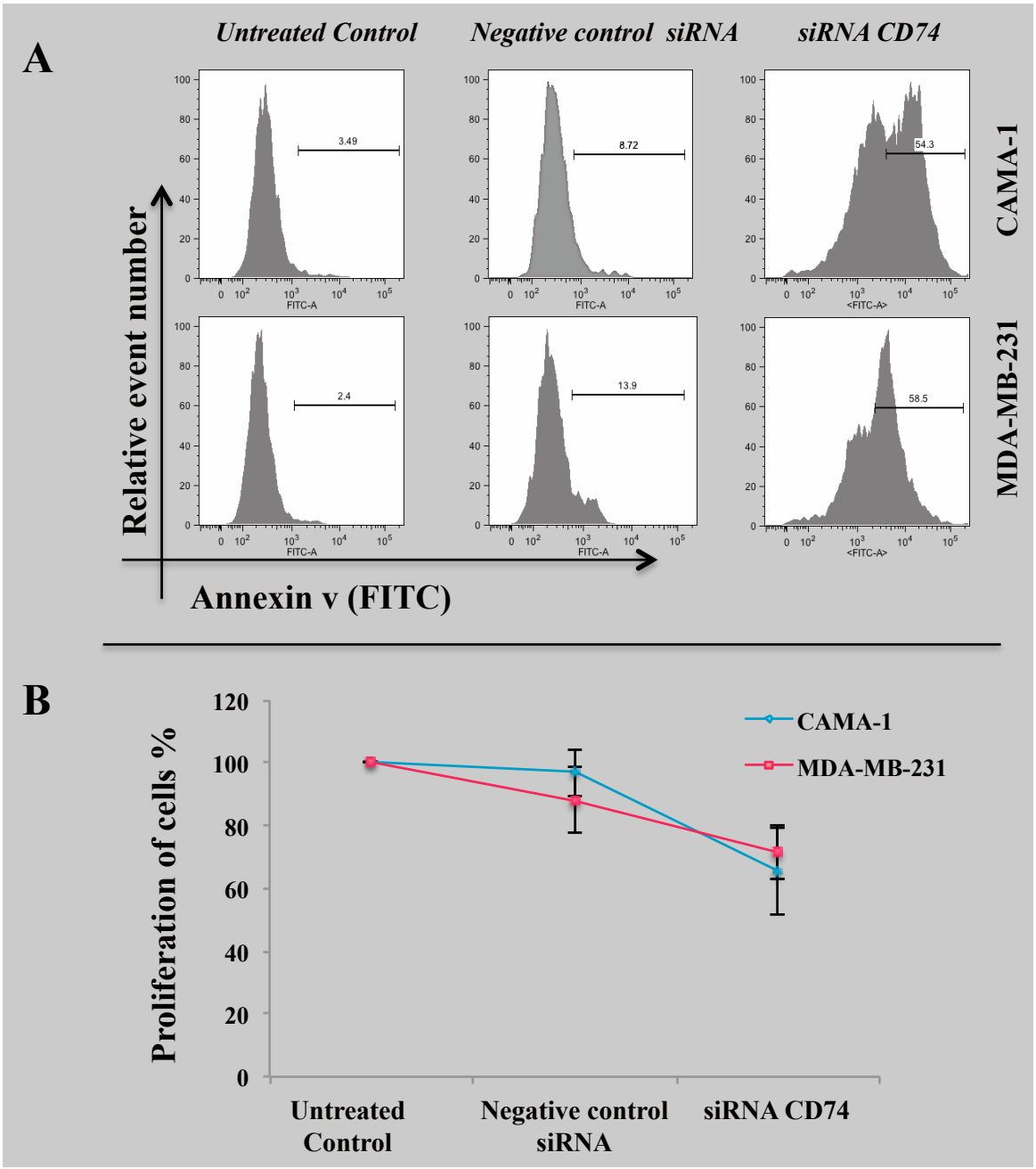

Figure 5-15: Effect of CD74 siRNA on the apoptosis and proliferation of CAMA-1 and MDA-MB-231 cells.

(A) Flow cytometric determination of the effect of CD74 siRNA on apoptosis of CAMA-1 and MDA-MB-231 cells. Cultured CAMA-1 and MDA-MB-231 cells were divided into three groups: nontransfected cells, cells transfected with negative control siRNA and cells transfected with CD74 siRNA. After a 24 hr treatment, the cells were harvested for quantitation of apoptosis by determining changes in the cell-surface expression of annexin V. Displayed is also a description of the observed frequency of cells undergoing apoptosis, which was found to be much higher in the CD74 siRNA treated cells than in the negative control treated group of CAMA-1 and MDA-MB-231 cells, respectively. (B) Effect of CD74 siRNA on the proliferation of CAMA-1 and MDA-MB-231 cells. MTT assay showed that treatment of CAMA-1 and MDA-MB-231 cells with CD74 siRNA inhibited their proliferation. Each point in the curve represents the arithmetic mean OD values ± SD from representative experiments that were performed in triplicate.

5.3 Conclusions

As it was suggested that co-expression CD74/MIF and CD44 might play a significant role in breast tumour progression and survival (Leng et al., 2003; Shi et al., 2006). This study found that CD74, MIF and CD44 were expressed in breast cancer cell lines; they were also associated with cell proliferation and apoptosis. Correlation analysis revealed that CD74 was positively correlated with MIF and both proteins were also associated with CD44. CD74 colocalise with MIF on the cell-surface and intra-cytoplasmic domain of CD74 colocalise with CD44 in CAMA-1, MDA-MB-231 and MDA-MB-435 cells, regardless of the degree of colocalisation. It was observed that the interaction of CD74 with MIF and CD74 with CD44 could be a potential tumour marker for breast cancer cells. Moreover, level of co-expression of MIF and CD74 or CD74 and CD44 could be a surrogate marker for the efficacy of anti-angiogenic drugs, particularly in breast cancer tumours. Also, knockdown of CD74 by CD74 siRNA significantly reduced CAMA-1 and MDA-MB-231 cell proliferation and increased the level of apoptotic cells.

In summary, by applying a pixel-based and object-based colocalisation quantification technique, it was possible precisely to quantify and detect subtle differences in the distribution of CD74, MIF and CD44 proteins. The breast cancer cell lines CAMA-1, MDA-MB-231 and MDA-MB-435 served as a good study model to develop this approach and to investigate baseline information on potential associations of CD74, MIF and CD44 molecules. It is concluded that CD74, MIF and CD44 molecules colocalise with each other, forming preferential associations on breast cancer derived cells. There appeared to be favoured combinations of certain CD74-MIF-CD44 complexes, and these may enhance cell-to-cell apposition. It is reasonable to assume that an immune-effector mechanism initiated a pro-survival signal, leading to the increase of proliferation and inhibition of apoptosis.

Chapter 6 Proteomics study of IFN-γ on CAMA-1 and MDA-MB-231 cells

6.1 Introduction

Proteomics is the large-scale study of localisation, identification, structure and function of the proteome. A proteome is the complete set of proteins expressed and modified by an organism under a specific set of environmental conditions. The application of mass spectrometry (MS) in proteomics analysis has made it a powerful tool for protein characterization (Cravatt et al., 2007). The classical method for the quantitative analysis of complex protein mixtures is the separation of proteins by two-dimensional gel electrophoresis (2-DE), and identification of resolved proteins by MS or tandem mass spectrometry (MS/MS) (Issaq and Veenstra, 2008). 2-DE accommodates a large mass range and permits the analysis of the entire set of proteins. Also, proteins are separated with high resolution by isoelectric point (pI) and molecular mass. Resolved protein spots are used for comparison among different samples and can be used for MS analysis. However, this method has some disadvantages such as the occurrence of gel to gel variation, a limited dynamic range, and difficulty in detection of basic or hydrophobic proteins and low range of molecular weights and limited range pIs of proteins (Zhu et al., 2009). Recent developments of non-gel-based and label-free shotgun proteomics techniques have rendered quantitative protein study faster, cleaner and simpler (Old et al., 2005; Chen and Yates, 2007; Patel et al., 2009).

Proteomics studies provide global analysis of protein expression and function. In contrast to the genome, the proteome is very dynamic in nature because of post-translational modifications (Aebersold and Cravatt, 2002; Aebersold and Mann, 2003). Therefore, in order to recognize the physiological and pathological events that occur in health and disease, it is important to detect and analyse the proteins from their native proteome. Taking into consideration the importance of proteomics, 2-DE was applied in the context of the breast cancer model system to investigate the effect of cytokines such as IFN-γ on

breast cancer cells. The ExPASy tool (http://web.expasy.org/tagident/) was used to identify and quantify breast cancer cell membrane proteins expressed in response to IFN-γ. This investigation will be a potential aid in developing our understanding of the molecular aspects breast cancer and drug discovery.

6.2 Results

6.2.1 Two dimensional gel analysis of CAMA-1 and MDA-MB-231 cells

CAMA-1 and MDA-MB-231 cells were used in this study as a model for breast cancer and differential expression of the breast cancer proteome in response to proinflammatory cytokines such as IFN-γ. This was investigated by 2-DE followed by protein spot analysis. The total proteome is separated by first dimension iso-electric focusing on the basis of the isoelectric points (pI) of the various proteins. The isoelectrically focused proteins were resolved by second dimension SDS-PAGE, as shown in Figure 6-1 and Figure 6-3. Silver stained protein spots in untreated CAMA-1 and MDA-MB-231 cells and IFN-γ treated cells, as well as a third unchallenged control group, are shown in (Figure 6-2 A-D and Figure 6-4 A-D). Gel images from three independent experiments were then analysed using Progenesis SameSpot software (Nonlinear Dynamics Limited), where a control untreated sample gel was used as a reference to identify differentially expressed proteins. Differentially expressed protein spots from CAMA-1 and MDA-MB-231 cells are shown in (Figure 6-1 and Figure 6-3) surrounded by a blue line and a spot number is given to each spot. Some selected differentially expressed spots are also indicated with red arrows in all four conditions: control cells only; in 10% FCS medium, cells treated with 100 IU/ml IFN-γ, cells treated with 500 IU/ml IFN-γ and cells treated with 1000 IU/ml IFN-γ (Figure 6-2 A-D and Figure 6-4 A-D). These data were used to gather preliminary results to discover the potential of differential protein expression in response to infections in the model system. An example of a 3D spot graph analysed by Progenesis SameSpot software is shown in Figure 6-5. Table 6-1 represents a summary of data obtained from a reference image showing all differentially expressed spots on an untreated control of CAMA-1 and MDA-MB-231 cells by PI and molecular weight. Representation and comparison of the number of spots in the untreated control of CAMA-

1 or MDA-MB-231 and IFN-γ treated CAMA-1 or MDA-MB-231 cells was identified by Progenesis SameSpot software and is shown in (Table 6-2 and Table 6-3).

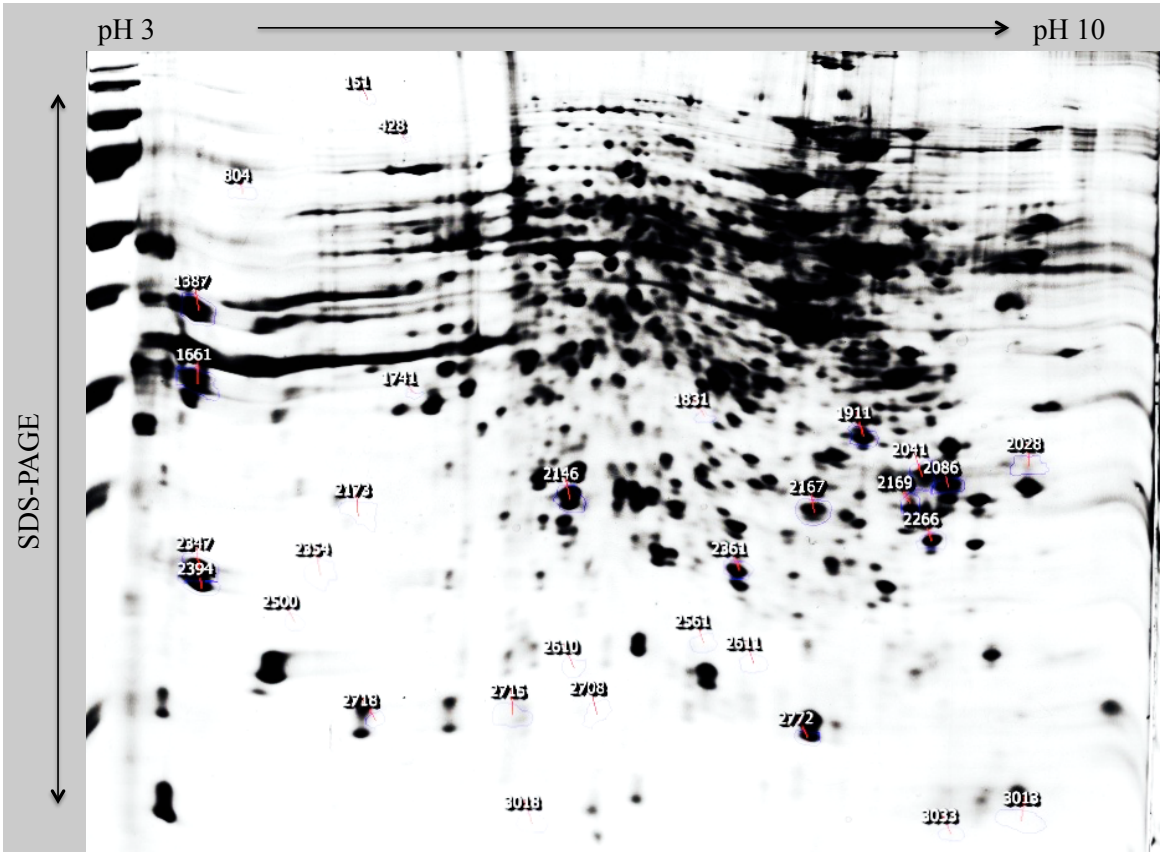

Figure 6-1: Representation of reference image showing an example image of spot detection on untreated CAMA-1 cells control.

Reference image used for image analysis that was carried out with Progenesis SameSpot software. Isoelectric point pI range is shown at the top, while the direction of the second dimension SDS-PAGE is represented by an arrow on the left.

.

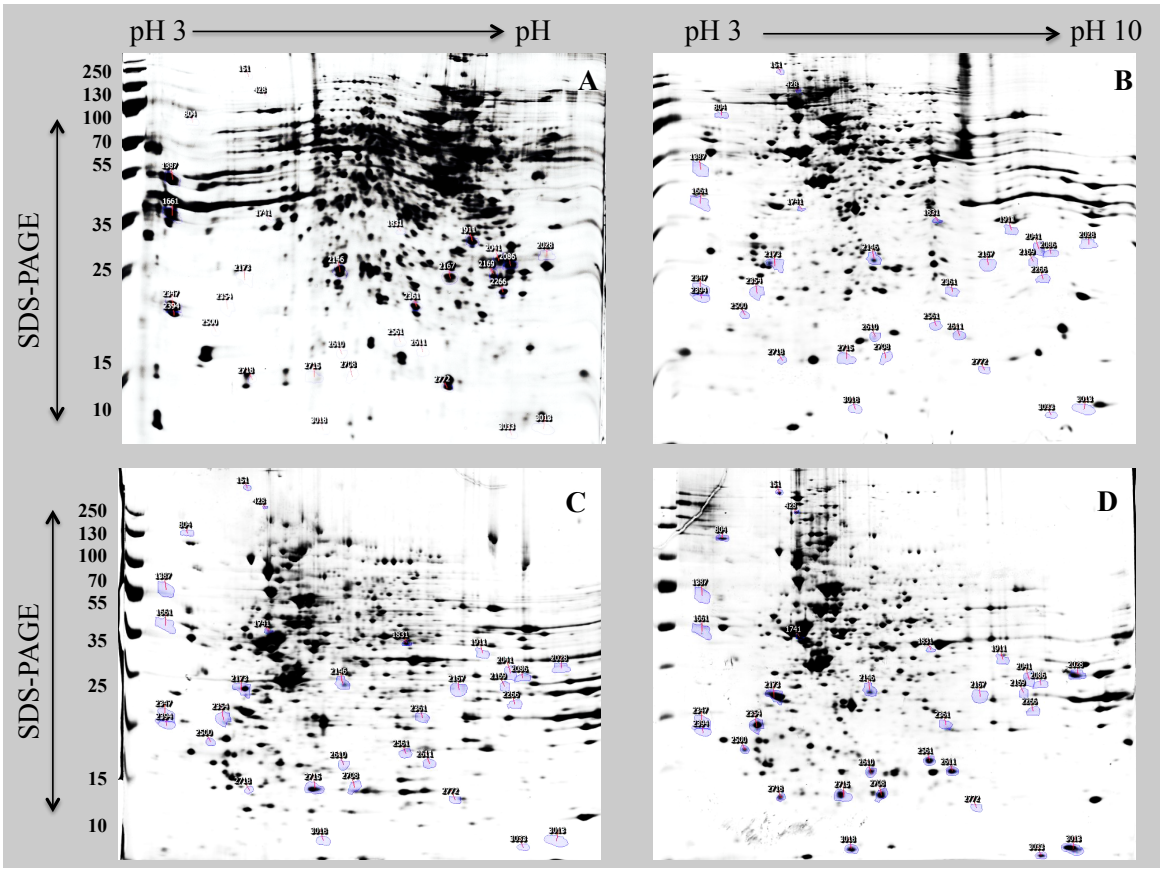

Figure 6-2: Representative 2D gel images of total cell proteins from CAMA-1 cells untreated and treated with IFN-γ.

(A) Control (untreated) cells only, in 10% FCS medium. (B) Cells treated with 100 IU/ml IFN-γ. (C) Cells treated with 500 IU/ml IFN-γ. (D) Cells treated with 1000 IU/ml IFN-γ. All incubations were for 72 hr. In the first dimension, 80 µg total soluble protein was separated on immobiline IPG strips (18 cm, pH 3-10 NL). Isoelectric focussing was performed using a IPG phor unit. The second dimension was performed on 12% SDS-PAGE gels, with image analysis carried out using Progenesis SameSpot software. M-Molecular mass standards are shown on the left side (kDa- kilo Daltons). Differentially expressed, user selected protein spots in four gels are marked by red arrows.

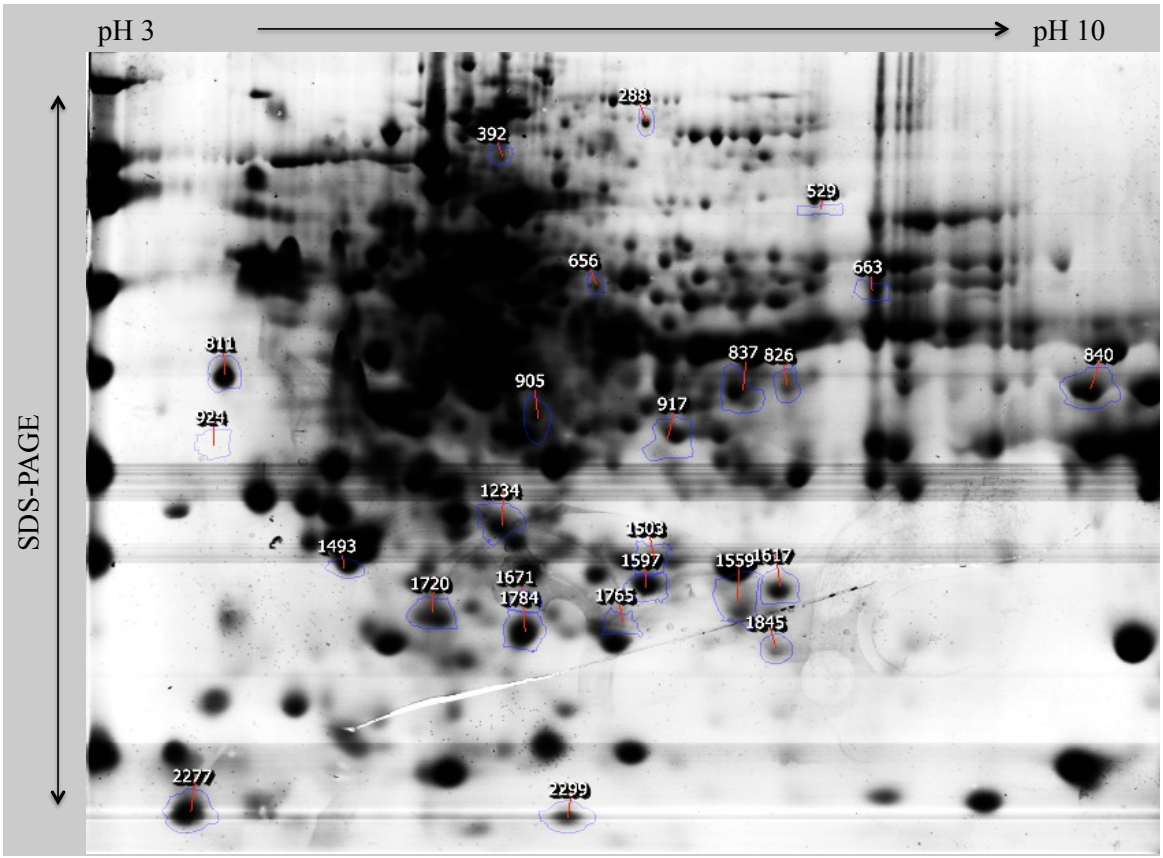

Figure 6-3:Representation of reference image showing an example image of spot detection on untreated of MDA-MB-231 cells control.

Reference image used for image analysis that was carried out with Progenesis SameSpot software. Isoelectric point pI range is shown at the top, while the direction of the second dimension SDS-PAGE is represented by an arrow on the left.

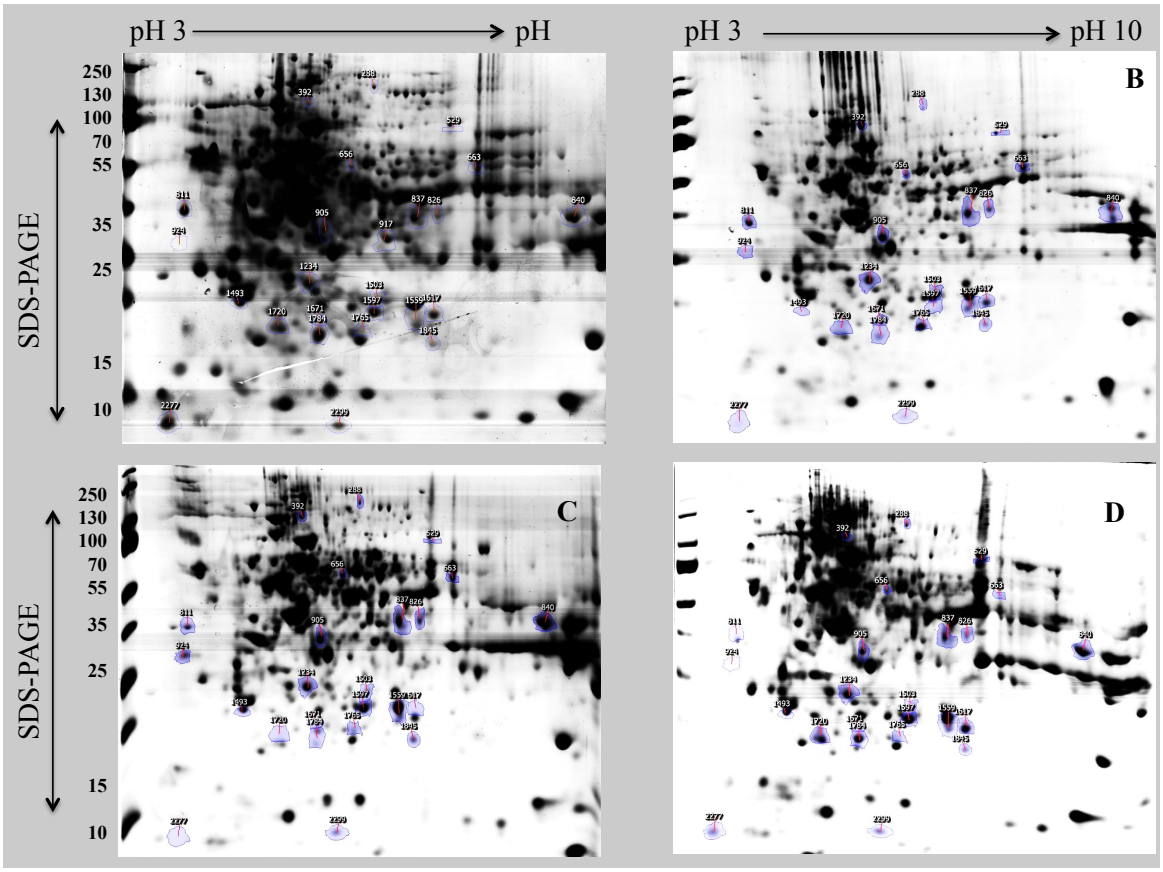

Figure 6-4: Representative 2D gel images of MDA-MB-231 total cell proteins from cells untreated and treated with IFN-γ.

(A) Control (untreated) cells only in 10% FCS medium. (B) Cells treated with 100 IU/ml IFN-γ. (C) Cells treated with 500 IU/ml IFN-γ. (D) Cells treated with 1000 IU/ml IFN-γ. Incubations were for 72 hr. In the first dimension, 80 µg total soluble protein was separated on immobiline IPG strips (18 cm, pH 3-10 NL). Isoelectric focussing was performed on an IPG phor unit. The second dimension was performed on 12% SDS-PAGE gels, with image analysis carried out with Progenesis SameSpot software. M-Molecular mass standards are shown on the left side (kDa- kilo Daltons). Differentially expressed, user selected protein spots in four gels are marked by red arrows.

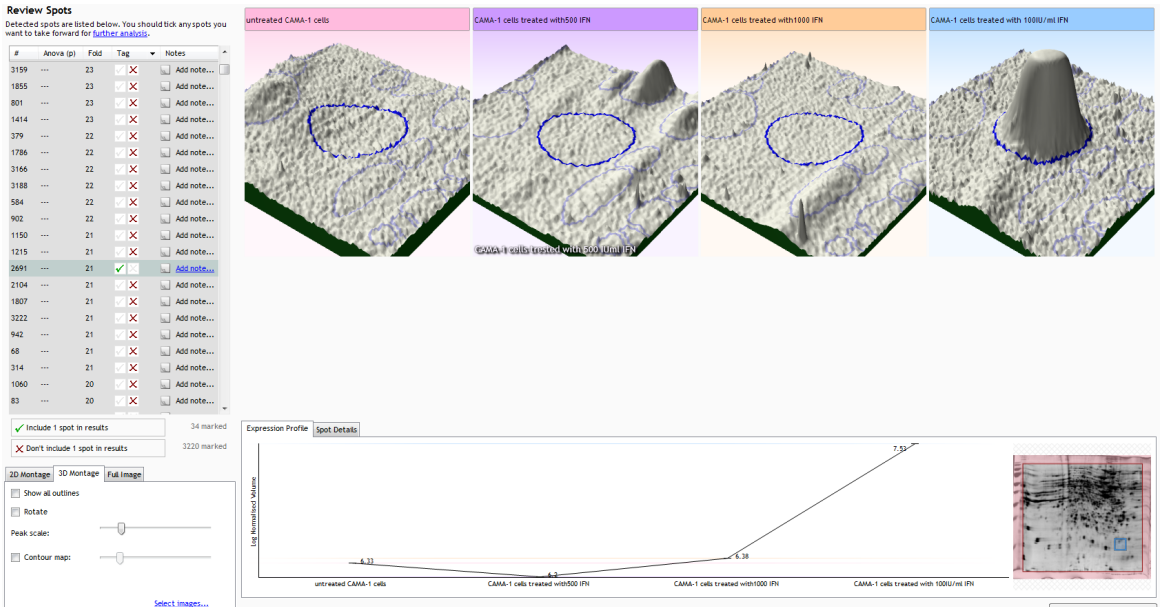

Figure 6-5: Example of 3D spot graph analysed by Progenesis SameSpot software.

Three-dimensional spot graph showing the difference between untreated (control) and treated CAMA-1 cells treated with different doses of IFN-γ. The images show the effect of IFN-γ on breast cancer cells.

Table 6-1: Summary of data obtained form reference image showing all differentially expressed spots on untreated CAMA-1 and MDA-MB-231 cells controls by PI and molecular weight.

CAMA-1 cells			MDA-MB-231 cells		
Spot Number	**PI (pH)**	**Molecular Weight (kDa)**	**Spot Number**	**PI (pH)**	**Molecular Weight (kDa)**
2610	6	16	1720	4	20
2708	7	12	1765	6	18
2561	7	18	1597	7	18
2611	8	17	1671	5	35
2715	7	16	2277	3	10
3018	7	12	2299	5	10
3033	8	11	1784	5	22
2718	5	15	1845	8	22
3013	10	12	1493	3	30
2500	4	18	663	9	65
2086	9	25	837	6	60
2167	8	22	392	4	110
1387	3	30	656	6	63
1741	6	25	1234	4	35
2266	9	20	1503	7	20
2361	7	20	826	7	60
2410	8	18	905	5	55
2347	3	20			
2354	5	22			

Table 6-2: Representation and comparison of the number of spots in untreated CAMA-1 cells control and in IFN-γ treated CAMA-1 cells, identified by Progenesis sameSpot software.

CAMA-1 cells were either untreated or treated with the indicated concentration of IFN-γ for a period of 72 hr. Both untreated and treated cell lysates were then subjected to isoelectric focusing. The second dimension was resolved with 12% SDS-PAGE. A plus sign (+) indicates the presence of spots or increase of spot size before or after treatment with IFN-γ. A minus sign (-) indicates the absence of spots before or after treatment with IFN-γ. Five spots out of the 19 polypeptide spots (highlighted in bold); generated from the CAMA-1 cell sample were randomly selected and analysed using ExPASy tool (http://web.expasy.org/tagident/).

Average normalised volumes of CAMA-1 cells spot				
Spot Number	**Untreated CAMA-1 (Control)**	**CAMA-1 treated with 100 IU/ml of IFN-γ**	**CAMA-1 treated with 500 IU/ml of IFN-γ**	**CAMA-1 treated with 1000 IU/ml of IFN-γ**
2610	**Spot -**	**Spot -**	**Spot +**	**Spot -**
2708	Spot -	Spot -	Spot +	Spot -
2561	Spot -	Spot -	Spot +	Spot -
2611	Spot -	Spot -	Spot +	Spot -
2715	Spot -	Spot ++	Spot +	Spot -
3018	Spot -	Spot -	Spot +	Spot -
3033	Spot -	Spot -	Spot +	Spot -
2718	Spot -	Spot -	Spot +	Spot -
3013	Spot -	Spot -	Spot +	Spot -
2500	Spot -	Spot -	Spot +	Spot -
2086	**Spot +**	**Spot -**	**Spot -**	**Spot -**
2167	Spot +	Spot -	Spot -	Spot -
1387	**Spot +**	**Spot -**	**Spot -**	**Spot -**
1741	**Spot -**	**Spot +**	**Spot +**	**Spot -**
2266	Spot +	Spot -	Spot -	Spot -
2361	**Spot +**	**Spot -**	**Spot -**	**Spot -**
2410	Spot +	Spot -	Spot -	Spot -
2347	Spot +	Spot -	Spot -	Spot -
2354	Spot -	Spot -	Spot +	Spot -

Table 6-3: Representation and comparison of the number of spots in untreated MDA-MB-21 cells control and in IFN-γ treated MDA-MB-231 cells, identified by Progenesis SameSpot software.

MDA-MB-231 cells were either untreated or treated with the indicated concentration of IFN-γ for a period of 72 hr. Both untreated and treated cell lysates were then subjected to isoelectric focusing. The second dimension was resolved with 12% SDS-PAGE. A plus sign (+) indicates the presence of spots or increase in spot size before or after treatment with IFN-γ. A minus sign (-) indicates the absence of spots before or after treatment with IFN-γ. Five spots out of the 17 polypeptide spots (highlighted in bold); generated from the MDA-MB-231 cell sample were randomly selected and analysed using ExPASy tool (http://web.expasy.org/tagident/).

Average normalised volumes of MDA-MB-231 cells spots				
Spot Number	**Untreated MDA-MB-231 (Control)**	**MDA-MB-231 treated with 100 IU/ml of IFN-γ**	**MDA-MB-231 treated with 500 IU/ml of IFN-γ**	**MDA-MB-231 treated with 1000 IU/ml of IFN-γ**
1720	**Spot ++**	**Spot +**	**Spot -**	**Spot -**
1765	Spot -	Spot -	Spot -	Spot +
1597	Spot +	Spot +	Spot +	Spot -
1671	Spot -	Spot -	Spot -	Spot +
2277	Spot ++	Spot +	Spot -	Spot -
2299	**Spot ++**	**Spot +**	**Spot +**	**Spot -**
1784	Spot +++	Spot ++	Spot +	Spot +
1845	Spot ++++	Spot +++	Spot ++	Spot +
1493	**Spot ++++**	**Spot +++**	**Spot ++**	**Spot -**
663	Spot ++	Spot -	Spot +++	Spot +
837	Spot ++	Spot +	Spot ++	Spot +
932	**Spot +**	**Spot +**	**Spot +**	**Spot +++**
656	Spot -	Spot -	Spot +	Spot +
1234	Spot -	Spot ++	Spot +++	Spot +++
1503	Spot +	Spot +	Spot +	Spot +
826	Spot +	Spot ++	Spot +++	Spot +++
905	**Spot +**	**Spot ++**	**Spot +++**	**Spot +++**

6.3 Conclusions

Two-dimensional gel electrophoresis is considered as one of the most powerful tools for protein separation and fractionation since its first introduction in 1975 (Klose, 1975; O'Farrell, 1975; Fernandez et al., 1990). The method has been improved over time to make it a more robust tool for proteome analysis. However, 2-DE is a robust technique only if samples are of low complexity and if subcellular fractions are used. This study made use of 2-DE to investigate breast cancer cell responses to proinflammatory cytokines such as IFN-γ through analysis of their proteome, and compared results with untreated conditions. Whole cell lysates of IFN-γ-stimulated and non-stimulated CAMA-1 and MDA-MB-231 breast cancer cells were used. Thus, 2-DE was utilized to obtain information about potential differential protein expression. Protein spots in the gels were visualized by silver staining and analysed by Progenesis SameSpot as previously used in a number of previous studies (Amiour et al., 2012; Brasier et al., 2012; Brunelli et al., 2012; Magdeldin et al., 2012; Brioschi et al., 2013). While results obtained from this analysis were used as preliminary data to identify differences between untreated and IFN-γ-treated samples, they were not used for further MS analysis.

The present proteomics study of the breast cancer cell lines CAMA-1 and MDA-MB-231 revealed that breast cancer cells respond to cytokines, including IFN-γ. Differentially expressed proteins in IFN-γ-stimulated and non-stimulated (control) CAMA-1 and MDA-MB-231 breast cancer cells were identified and quantified. Sub-cellular localisation, expression, and functions of the listed proteins have been discussed briefly. The data described and discussed here can be utilized for further data validation projects, and could assist the discovery of new breast cancer related proteins and molecular pathways.

Chapter 7 Discussion

7.1 Overview

Tumour immunology aims to investigate tumour markers that may affect normal immune function (Bissell and Radisky, 2001; Kindt et al., 2007). The field also seeks to identify tumour antigens that play a role in the immune response (Graziano and Finn, 2005). The present study has contemplated a number of issues associated with breast cancer, cancer immuoediting, immunogenicity and tumorigenicity in cases of health and disease. The non-invasive and invasive cell lines CAMA-1, MDA-MB-231 and MDA-MB-435 were employed as a study model because many of their biological and biochemical characteristics are shared with breast cancer (Holliday and Speirs, 2011). This study also employed 226LDM cells, immortalized normal breast luminal cells, as a model of healthy and normal breast tissue (Docquier et al., 2009).

7.1.1 Analysis and profiling of the expression of CD74, MIF and CD44

To further understand the immunogenicity and tumorigenicity of breast cancer cells, the expression of HLA-A, B, C and HLA-DR molecules in CAMA-1, MDA-MB-231, MDA-MB-435 and 226LDM cells was investigated. HLA-A, B, C expression was detected in MDA-MB231 and MDA-MB435 cells, but not in CAMA-1 and 226LDM cells. Conversely, HLA-DR was not detectable in any of the cell lines except MDA-MB-435 cells, which showed weak expression, as shown in (Figure 3-2). The expression of MHC class I and II in cancer cells, including lung, liver, melanoma, colon and breast cancer, has been previously observed (Moldenhauer et al., 1999; Kaczmarek et al., 2007; Huang et al., 2010; Thibodeau et al., 2012). Notably, Jabrane-Ferrat et al., (1990a,b) reported that four out of five different breast adenocarcinoma cell lines expressed cell-surface MHC class I proteins. On the other hand, MHC class I was either not expressed or downregulated in primary breast cancer tissue (Pistillo et al., 2000).

In this respect, it has been reported that coordinate expression of HLA-DR, CD74 and HLA-DM by tumour cells is an indicator of improved prognosis in breast carcinoma. Several groups have suggested that the expression of HLA molecules improves immunogenicity of tumour cells and therefore can induce an anti-tumour T-cell response (Meazza et al., 2003; Humphreys et al., 2004; Oldford et al., 2006). Thus, the expression of HLA-A, B, C and HLA-DR molecules in breast cancer cell lines could be of considerable value for tumour immunity, potentially leading to efficient tumour antigen processing and presentation to T cells (Feinmesser et al., 2000). In the tumour immunotherapy design field, MHC class II presentation has received much recent attention (Rajnavölgyi and Lanyi, 2003; Velders et al., 2003).

Recent published data show that CD74, MIF and CD44 can play a role in the pathogenesis of various solid tumours (Meyer-Siegler et al., 2004; 2006; Gore et al., 2008). The data obtained have confirmed that cell-surface and intracellular CD74, MIF and CD44 molecules are detectable by flow cytometry and by confocal microscopy on CAMA-1, MDA-MB-231 and MDA-MB-435 cells. The Western blotting results revealed that breast cancer cells express total protein of CD74, MIF and CD44. Significantly, Western blot analysis revealed that the CAMA-1, MDA-MB-231 and MDA-MB-435 cell lines express three different isoforms of CD74, the P33, P35 and P41 isoforms, which were detected at the expected molecular weights, the major form being the 33 kDa isoform (Figure 3-6 A) (Liu and Lin, 2014). These findings differ from those obtained by Verjans et al. (2009) who found that MDA-MB-231 and MDA-MB-468 cells express one CD74 isoform however it was not specified which isoform. Similarly, Metodieva et al. (2013) found that MDA-MB-435 also express P35 isoform of CD74. Using Western blot analysis, Martín-Ventura et al. (2009) found THP-1 cells to express the P33 and P43 isoforms of CD74. The cell-surface and the total protein expression of CD74 were also

studied in the MCF-7 cell line. Data obtained from flow cytometry showed that MCF-7 cells express a moderate level of CD74 compared to the positive control Raji cell lines. Western blot results confirmed that MCF-7 cells express the total protein of CD74. However, MCF-7 cells expressed the P33 and P41 isoforms of CD74, in contrast to breast cancer cells (Appendix 1; Figure A1.1). Theoretically, an additional 43 kDa form of CD74, the longest isoform, could be expected, but it has not yet been unequivocally detected in immunoprecipitates from human cells. The P33 and P35 isoforms are believed to be involved in regulating class II MHC antigen presentation while the P41 isoform may play a key role in T cell selection in the thymus (Mun et al., 2013; Liu and Lin, 2014). It is generally accepted that CD74 facilitates the export of MHC II/CD74 complexes from the endoplasmic reticulum, while blocking premature loading of peptides on to the MHC II molecules (Weenink and Gautam 1997; Datta et al., 2000; Neefjes et al., 2011; Bergmann, 2012; Genève et al., 2012). However, it has been recently suggested that high levels of CD74 expression might prevent tumour antigen presentation by blocking the MHC class II peptide-binding cleft, thus preventing binding of antigenic peptides for presentation to T cells, rendering tumours less immunogenic (Beswick and Reyes, 2009; Zheng et al., 2012). In humans, 80% of the CD74 protein pool is composed of the P33 isoform. However, P35 is considered the most enigmatic isoform (Bergmann, 2012). Genève et al. (2012) have suggested that P33 and P35, together, facilitate antigen presentation, and that this process does not require the co-expression of any other CD74 isoform (Beswick and Reyes, 2009; Genève et al 2012).

Western blotting also demonstrated that CAMA-1 cells express two different isoforms of CD44; CD44 variant (CD44v) and CD44 standard (CD44s) (Figure 3-6 A). Jung et al. (2009) showed that some breast cancer cell lines, such as MDA-MB-468 and SUM149, express several isoforms of CD44s and CD44v. It is possible that CD44 expression in

breast cancer is associated with highly aggressive breast tumour subtypes or highly invasive breast cancer cells (Montgomery et al., 2012).

To validate the present study, immortalized normal breast luminal cells (226LDM), breast (human) whole cell lysate obtained from adult normal tissue, and normal breast tissue slides were used as a model. The expression of CD74, MIF and CD44 was investigated by flow cytometry, Western blot and microscopy. The findings confirmed that 226LDM cells did not express CD74 on the cell-surface or intracellularly, while they do express MIF and CD44, although in low levels compared to breast cancer cells (Figure 3-10). In the same manner, the results obtained from Western blotting of normal breast lysate and histological immunostaining of breast tissue slides showed only positive detection of MIF and CD44 but not CD74 (Figure 3-11). This result was expected because it has been confirmed that the expression of CD74 is restricted to antigen-presenting cells, including B cells, monocytes, macrophages and dendritic cells (e.g. langerhans cells) (Gold et al., 2011).

7.1.2 The role of IFN-γ and LPS in the expression of CD74

This study investigated if IFN-γ or LPS played a role in the proliferation and migration of CAMA-1 and MDA-MB-231 cells. To determine the level of IFN-γ and LPS that is toxic to the cells, the MTT assay was performed, using concentrations of IFN-γ ranging from 100 to 1000 IU/ml and of LPS ranging from 100 to 1000 ng/ml. The results showed that the viability of CAMA-1 and MDA-MB-231 cells decreased after treatment with IFN-γ in contrast to that of cells treated with LPS, which enhanced cell proliferation of breast cancer cells. In this system, it was observed that 1000 IU/ml of IFN-γ or 1000 ng/ml of LPS was the optimal concentration. The results from migration assays indicated that MDA-MB-231 cells migrated towards FCS at a higher level than CAMA-1 cells. This

was carried out as an evaluation of the ability of cells to display migratory properties in an in vitro assay. The effect of the optimal concentration 1000 IU/ml of IFN-γ or 1000 ng/ml of LPS on cell migration and invasion was also investigated. The results showed that both cell lines migrated against IFN-γ or LPS (Figure 4-1).

In this context, Zhao et al. (2013) have shown that AGS, HGC-27 and GES-1 gastric cancer cells that were exposed to IFN-γ had significantly reduced colony formation, cell proliferation and migration ability. However, flow cytometry showed no effect of IFN-γ on apoptosis of the cells and no effect on cell ageing as assessed by beta-galactosidase (β-gal) staining. In contrast, results obtained from flow cytometry revealed that IFN-γ arrested the cells in the transition stage (G1/S) phase. It has also been shown that IFN-γ induces apoptosis in ovarian cancer cells in vivo and in vitro (Wall et al., 2003). Tate Jr et al. (2012) have shown that IFN-γ inhibits the proliferation of carcinoma cells.

This study has also demonstrated that LPS can induce the proliferation and migration of CAMA-1 and MDA-MB-231 cells. In this context, Goodier and Londei (2000) have shown that LPS stimulates the proliferation and expansion of human CD56+CD3− NK cells. Wang et al. (2013a) also demonstrated that LPS can induce the signalling of TLR-4, resulting in promotion of cell survival and proliferation in hepatocellular carcinoma. LPS has been found to induce NF-κB-dependent expression of antiapoptotic and prometastatic genes in tumour cells (Luo et al., 2004). However, Hsu et al. (2011) observed no proliferative or apoptotic changes in vitro after 4 hr of LPS treatment of colorectal cancer cells, despite evidence that LPS may alter proliferation and apoptosis in cancer cells.

The expression of CD74 can be induced in tumour cells upon their exposure to proinflammatory cytokines such as MIF and IFN-γ (Moldenhauer et al., 1999; Beswick and Reyes; 2009). Several researches have shown that IFN-γ reduces tumourgenicity *in*

vivo by upregulating the expression of MHC and related molecules such as CD74. IFN-γ in cancer cells can be modified by epigenetic changes in the promoter region of class II, major histocompatibility complex, transactivator (CIITA) (Beatty and Paterson, 2000). This may potentially disrupt the IFN-γ signalling pathway and impair T-cell activation, thus representing a possible tumour escape mechanism of cancer cells from immunosurveillance, (Matsushita et al., 2006). In the same manner, it is suggested that systemic inflammation and postoperative infections lead to cancer recurrence (Hsu et al., 2011). It has been shown that CD74 expression is increased by chronic inflammatory conditions and *Helicobacter pylori* infection (Beswick and Reyes, 2009; Zheng et al., 2012). Thus, to evaluate tumour cell responsiveness to treatment with different reagents, the expression of HLA-A, B, C and HLA-DR molecules on the surface of CAMA-1 and MDA-MB-231 cells, following their exposure to IFN-γ, was examined, as studied by flow cytometry. The results confirmed the viability of the cells in response to external reagents such as IFN-γ (Figures 4-2 and 4-3). The data also showed that CD74 expression increased upon treatment with IFN-γ or LPS in both the CAMA-1 and MDA-MB-231 cell lines.

A clear shift of CD74 mRNA expression was observed when the cells were incubated with 100, 500 or 1000 IU/ml of IFN-γ for 72 hr (Figure 4-5). Also, using flow cytometry and Western blotting, following IFN-γ treatment of the cells CD74 expression was found to increase both on the cell-surface and intracellularly (Figures 4-6, 4-8, 4-9 and 4-10). Verjans et al. (2009) showed that expression of the MIF receptor CD74 was elevated in MDA-MB-231 compared to non-invasive MDA-MB-468 and ZR-75-1 breast cancer cells. In contrast, the observations of this study revealed that the expression of CD74 was higher in non-invasive CAMA-1 cells compared to invasive MDA-MB-231 cells.

Using real-time PCR and immunostaining techniques, Maubach et al. (2007) observed that CD74 expression in hepatic stellate cells (HSCs) was upregulated after the cells were treated with IFN-γ for 30 hr. Similarly, Martín-Ventura et al. (2009) found the expression of CD74 to increase in human vascular smooth muscle cells (VSMCs) and THP-1 cells after IFN-γ treatment. Moldenhauer et al. (1999) have also shown that the expression of CD74, HLA-DR and HLA-A, B, C increased when colon carcinoma cell lines (HT-29 cells) were incubated with rIFN-γ for 72 hr. More specifically, Greenwood et al. (2012) revealed that the triple negative breast cancer cell lines MDA-MB-435, MDA-MB-231, MCF-7 and ZR-75 showed higher expression of CD74 after IFN-γ treatment for 72 hr using Western blot techniques. There are several potential explanations for increasing CD74 expression after IFN-γ treatment. It has been suggested that IFN-γ may directly induce CD74 intramembrane cleavage and release to the nucleus, or alternative indirect mechanism via cathepsin S upregulation or by an as yet unknown mechanism (Maubach et al., 2007; Martín-Ventura et al., 2009).

CD74 is classified as MIF receptor, which suggests that its expression might be induced directly after cytokine treatment (Beswick and Reyes; 2009; Borghese and Clanchy; 2011). For example, MIF induces the expression of CD74 via Bcl-2 and Bcl-XL (proteins family involved in the regulation of apoptosis) in tumour cells such as bladder cancer, prostate cancer, gastric cancer and breast cancer (Meyer-Siegler et al., 2004, 2006; Burton et al., 2004; Zheng et al., 2012). Verjan et al. (2009) confirmed that the expression of CD74 and MIF is somehow associated, since the cell lines that express high levels of MIF show higher expression of CD74 compared to those that have low expression of MIF. This might indicate that IFN-γ induces CD74 expression directly via the JAK-STAT-1 pathway, even though the exact mechanism is not well known yet.

It has been suggested that CD74 is upregulated directly via CITTA after IFN-γ treatment. When IFN-γ binds to its receptors; interferon gamma receptor (IFNAR1 and IFNGR2), it causes dimerization and the activation of JAK1 and JAK2 by tyrosine phosphorylation. Tyrosine phosphorylation of receptors in cytoplasmic regions allows for interaction to occur with STAT-1. STAT-1 is then activated by tyrosine phosphorylation, which also leads to dimerization causing STAT-1 to move to the nucleus. At the nucleus STAT-1 binds to the GAS element of the CIITA promoter IV and is stabilized by its interaction with USF-1 (upstream stimulatory factor-1). This then leads to the activation of the transcription of CIITA mRNA. CIITA then operates as the essential mediator of MHC-II gene induction and activates MHC II gene expression and related genes such as CD74 as a co-activator interacting with the promoter – bound transcription factors (Muhlethaler-Mottet et al., 1998).

Several studies have suggested that the expression of CD74 upon IFN-γ treatment might be induced via cathepsin S (Martín-Ventura et al., 2009). There are many different proteases involved in the processing of CD74 during antigen presentation. The most effective proteases involved in the last step of this process are cathepsins S and L. These enzymes release the class II-associated peptide (CLIP) region of the invariant chain from the lip10 (leupeptin induced polypeptide) (Maubach et al., 2007). Significantly, cathepsin S overexpression has been linked to human malignant tumour tissues and cells (Chang et al., 2007). Cathepsin S is involved in MHC class II expression and CD74 processing in human T-cell leukaemia cell lines (HuT-78) and keratinocyte cell lines (HaCaT) (Schönefuß et al., 2009). Schönefuß et al. (2009) showed that the expression of MHC class II and CD74 was downregulated after inhibition of cathepsin S with CATS-inhibitor in HuT-78 and HaCaT cells, even with IFN-γ treatment. This indicates that the expression of CD74 might be regulated by cathepsin S via IFN-γ treatment.

Recently, it was confirmed that most cytokines that alter MHC class II and CD74 expression, such as IFN-γ, tumour necrosis factor (TNF-α), transforming growth factor-β, IL-1, IL-4 and IL-10, either upregulate or downregulate CIITA and both MHC class II and CD74 accordingly. CIITA is known to respond to different proinflammatory stimuli and to induce the expression of the classical MHC class II molecules as well as the accessory molecule invariant chain CD74 (Harton and Ting; 2000; Maubach et al., 2007). Interestingly, Maubach et al. (2007), using real time PCR, have shown that mRNA expression of CIITA and CD74 increased in HSC cells upon treatment with IFN-γ. Following induction by inflammatory stimuli (IFN-γ), CD74 associates with class II alpha and beta chains. This is followed by the stepwise processing of CD74 into the CLIP starting from the C-terminus. In contrast, it has also been confirmed that mRNA expression of CIITA, HLA-DR and CD74 is not found in trophoblast cell lines such as JAR and JEG-3, even after treatment with IFN-γ (Murphy and Tomasi; 1998). Holtz et al. (2003) have shown that CD74 is not expressed in JAR and JEG-3 due the absence of the CIITA gene.

In terms of infection (chronic inflammatory conditions), accumulating evidence indicates that systemic inflammation and postoperative infections can lead to cancer recurrence (Tsujimoto et al., 2010). The mechanisms by which postoperative Gram-negative bacterial infections promote cancer recurrence are poorly understood (Hsu et al., 2011). It has been reported that the expression of CD74 is increased by inflammatory processes triggered by *H. Pylori* infection. This bacterium can also use CD74 as a point of attachment to gastric cancer cell lines (Beswick and Reyes; 2009; Zheng et al., 2012). Therefore, the dramatic increase in CD74 expression during infection suggests that *H.Pylori* can use CD74 as a receptor (Zheng et al., 2012). Zhang et al. (2013) have reported that CD74 is induced by LPS, polyinosinic acid: (polyI:C), and infection with

porcine circovirus type 2 (PCV2) in vitro. These findings suggest that CD74 may play a potential role in inflammatory diseases including cancer.

In this context, data obtained have shown that CD74 is overexpressed in both the CAMA-1 and MDA-MB-231 cell lines after LPS treatment. Maximum CD74 mRNA expression was detected when the cells were incubated with 1000 ng/ml of LPS for 24 hr (Figure 4-5). Similar findings were obtained from flow cytometry and Western blotting (Figures 4-7, 4-10 and 4-11). Relatedly, LPS treatment increased the expression of CD74 in MKN45 cells and the highest expression was found when the cells were incubated with 1000 ng/ml of LPS. It has been suggested that the expression of CD74 increases via MIF induction (Zheng et al., 2012). Zhang et al. (2013) have reported that LPS and polyI:C in porcine kidney (PK-15) cells induce CD74 when PK-15 cells are cultured and maintained with 1 μg/ml LPS or 10 μg/ml polyI:C for 48 hr.

Beswick et al. (2006) reported that *H.Pylori* binds CD74 on gastric epithelial cells and induces NF-κB, ERK1 and ERK2 activation and IL-8 predication. Another study has demonstrated that the stimulation of surface CD74 could induce a signalling cascade that results in the activation of Akt, NF-κB, and cell proliferation (Starlets et al., 2006). In addition, it was found that CD74 is processed in the endocytic compartments, which ensures its intramembrane cleavage to liberate the intracellular domain of CD74. This cleavage process is followed by nuclear translocation and transcriptional activation, including that of NF-κB (Brown et al., 2000). Induction of CD74 by LPS, leading to upregulation of the inflammation factors IL-6, IL-8 and COX-2, has also been proposed. Thus, it is believed that CD74 enhances the inflammatory response by regulating the NF-κB signalling pathway (Zhang et al. 2013). Interestingly, it has been found that diabetic patients overexpress MIF and CD74. Similarly, high glucose also upregulated MIF and CD74 expression in cultured HK2 human proximal tubular cells (Sanchez-Niño et al.,

2009). This suggests that the interaction between CD74 and LPS might take place in the polysaccharide core of the LPS. *H.pylori* is thought to bind directly to CD74 on the surface of cells via urease, a common bacterial protein involved in the catalysis of urea to CO_2 and NH_3 (Beswick and Reyes, 2009; Borghese and Clanchy, 2011).

The effect of concentrations of IFN-γ ranging from 100 to 1000 IU/ml and LPS ranging from 100 to 1000 ng/ml on the expression of CD44 in CAMA-1 and MDA-MB-231 cells was also studied. The expression of CD44 was found not affected upon IFN-γ and LPS treatment (Appendix 1; Figures A1.2, A1.3, A1.4 and A1.5). This result was not expected, since CD44 has been shown to be associated with inflammation conditions. However, CD44 has been linked to cancer due to its ability to increase tumour cell proliferation and invasiveness (Götte and Yip, 2006; Barshack et al., 1998).

7.1.3 The interrelation of CD74 with MIF and CD44

Several groups have studied the association of CD74 with MIF and CD44 in cancers since it was reported that CD74 and CD44 are involved in signalling with MIF (Shi et al., 2006; Gore et al., 2008; Borghese and Clanchy, 2011). In addition, it was shown that the formation of a molecular complex between MIF, CD74 and CD44 in prostate carcinoma cells lines (DU-145) could mediate signal transduction including (gene regulation, apoptosis and cell proliferation) in prostate cancer (Meyer-Siegler et al., 2006). So, the present study aimed to investigate the role of CD74 and its interrelation to MIF and CD44 in breast cancer cells. This was achieved by studying the colocalisation of CD74, MIF and CD44 molecules in the breast cancer cell lines CAMA-1, MDA-MB-231 and MDA-MB-435 and in THP-1 cells. THP-1 cells were used as a model in this study based on Leng et al.'s (2003) finding that MIF colocalises with CD74 with high affinity. THP-1 is a human leukemia monocytic cell line, which has been extensively used to study

monocyte/macrophage functions, mechanisms, signalling pathways, and nutrient and drug transport (Chanput et al., 2014). The results obtained from confocal microscopy demonstrated that CD74 and MIF are highly colocalised on the cell-surface of all breast cancer cells as well as THP-1 cells (Figures 5-2 and 5-3). Pearson's correlation coefficient and scatter plot (Figure 5-3) were used to analyse the colocalisation of CD74 and MIF (Bolte and Cordelieres, 2006). The colocalisation of CD74 and MIF was additionally investigated by segmentation methods using regional maximum detection of the images (Figure 5-6). These accurately depict the percentage of colocalised CD74 and MIF molecules.

One previous immunofluorescence study has confirmed the colocalisation of MIF and CD74 in non-small cell lung cancer (McClelland et al., 2009). Additionally, using correlation analysis, Zheng et al. (2012) identified a positive correlation between MIF and CD74 in gastric cancer cells. Correspondingly, Starlets et al. (2006) showed that, in malignant B cells obtained from patients with chronic lymphocytic leukemia (CLL), MIF binds to the extracellular domain of CD74 to initiate a signalling cascade leading to cell proliferation and survival. The interaction of MIF with CD74 and CD44 has been reported, suggesting that MIF in association with CD74 and CD44 as a complex plays a significant role in bladder cancer cell proliferation (Meyer-Siegler et al., 2004). Similarly, Meyer-Siegler et al. (2006) reported that the interaction between MIF and CD74 activates the ERK1 and ERK2 signalling pathway, presumably through interaction with CD44, in the prostate cancer cell lines DU-145 and LNCaP, but not in normal human prostate epithelial cells (PrEC) or benign prostate epithelial cells (BPH-1). However, human benign prostate hyperplasia epithelial cells (BPH-1) and PrEC prostate cancer cells do not express CD74 on the cell-surface, so for this reason, both cells do not interact with MIF and CD44 (Meyer-Siegler et al., 2006). Correspondingly, Shi et al. (2006) showed that

mammalian COS-7 cells do not bind MIF unless engineered to express the extracellular domain of CD74.

Using confocal microscopy, the present study investigated the colocalisation of CD74 with CD44, intracellularly, in CAMA-1, MDA-MB-231 and MDA-MB-435 cells. The results obtained show that CD74 and CD44 are highly colocalised intracellularly in all breast cancer cells as well as THP-1 cells (Figures 5-8 and 5-9). Figure 5-9 showed the colocalisation of CD74 and CD44 by scatter plot and the Pearson's correlation coefficient (Bolte and Cordelieres, 2006). Colocalisation of CD74 and CD44 was also investigated by segmentation methods using regional maximum detection of the images, which shows the percentage of colocalised CD74 and CD44 molecules (Figure 5-11).

It has been confirmed that CD74 alone is sufficient to mediate MIF binding to COS-7 cells. However, CD74 on its own is insufficient to signal with MIF in the absence of CD44. Shi et al. (2006) demonstrated that COS-7 cells are not capable of being involved in signalling when engineered to express CD74 and a truncated CD44 lacking its cytoplasmic signalling domain. Moreover, Shi et al. (2006) also observed that the phosphoserine content of CD74 increased only in cells that expressed CD74 and full-length CD44, which is consistent with the hypothesis that MIF-mediated phosphorylation of CD74 is dependent on the activity of the CD44 intracytoplasmic domain. Further, Gore et al. (2008) demonstrated that CD74 binds to CD44 to initiate a signalling pathway involving MIF in monocytes and macrophages. It has also been found that CD44-deficient cells are not able to participate in MIF-induced signalling cascade like MAPK/ERK pathway (Gore et al., 2008; Cohen and Shachar, 2014.).

In the light of the above findings, whether CD74 and CD44 colocalise on the cell-surface as well as CD44 with MIF was also studied by confocal microscopy. In this context, no evidence for the existence of cell-surface interaction between CD44 and CD74 or MIF

was obtained. Concomitantly, Shi et al. (2006) did not obtain evidence for a specific interaction between MIF and CD44 in COS-7/M6 cells. However, CD44 was suggested to mediate signalling of MIF by binding to a MIF that has undergone conformational modification as a result of binding to CD74. CD74 alone mediated MIF binding. However, MIF-induced ERK1 and ERK2 kinase phosphorylation required the co-expression of CD44 (Shi et al., 2006).

To confirm the colocalisation of CD74 with MIF and CD44 co-immunoprecipitation was performed, utilizing CAMA-1, MDA-MB-231 and MDA-MB-435 cells. So, either CD74 or CD44 was incubated with CAMA-1, MDA-MB-231 and MDA-MB-435 lysates. CD74 or CD44 was immunoprecipitated by the CD74 or CD44 antibody along with proteins bound to it. Western blotting using anti-MIF or anti-CD44 mAb revealed that CD74 was co-precipitated with MIF, and CD74 was co-precipitated with CD44. The result obtained from Co-IP confirmed that CD74 interacted with MIF and both CD44s and CD44v. However, Co-IP of CD44/74 showed that CD44s and CD44v interacted only with the P41 isoform of CD74, which is found to be the largest isoform present in breast cancer cells of this study. Moreover, this study confirmed there is no clear association between CD44 and MIF, which was further, supported by Co-IP data (Figures 5-12 and 5-13).

Meyer-Siegler et al. (2004) showed that CD44 binds to the P35 form of CD74 in bladder cancer cells, although P35 has been suggested to be involved in the antigen presentation process (Genève et al., 2012). However, Meyer-Siegler et al. (2006) did not study whether bladder cancer cells express different isoforms of CD74 or not. In the same manner, in prostate cancer cells (DU-145), CD44v interacts with CD74 and MIF, creating a complex. Moreover, BPH-1 and LNCaP cells do not express surface CD74; so both cell lines do not interact with CD44. LNCaP cells, however, have been demonstrated to interact with MIF (Meyer-Siegler et al., 2006). Zheng et al. (2012) have found a positive

correlation between MIF and CD74 and TLR4 in gastric cancer through correlation analysis. Therefore, the data suggest that MIF-CD74 interaction activates the ERK1 and ERK2 signalling pathway, presumably through interaction with CD44, as suggested by Naujokas et al, (1993). Interestingly, no information has been reported to show other pathways and/or signalling molecules (aside from ERK activation) that are affected by MIF-CD74 interaction, although a recent report suggests that MIF engagement of CD74 augments B cell survival by increasing the expression of Bcl-xL (Starlets et al., 2006; Xu et al., 2013). However, CD74 has been found to promote HLA-DR internalization by active physical association. So, this proposed a model for the dual role of CD74 as a molecule that promotes HLA-DR internalization by physical interaction with CD74 and as a ligand for MIF (Karakikes et al., 2012).

To investigate the role of CD74 in apoptosis and proliferation, siRNA that targeted CD74 was used. Western blot results (Figure 5-14 A and B) showed that CD74 expression was strongly knocked down in CAMA-1 and MDA-MB-231 cells in comparison with the control and CD74 siRNA. Microscopic results also confirmed that CD74 expression was strongly knocked down in both cell lines (Figure 5-14 C and D). When CD74 expression was knocked down, apoptosis was observed in CAMA-1 and MDA-MB-231 cells. Both cell lines, when treated with CD74 siRNA, displayed significantly higher levels of annexin V staining (± 55% and ± 58% respectively) compared to negative control siRNA-treated counterparts (± 8% and ± 13% respectively). In the same manner, it was found that in CAMA-1 and MDA-MB-231 cells treated with CD74 siRNA, a significantly reduced proliferation was observed compared to cells treated with the negative control siRNA control sequence and untreated cells.

Likewise, it has been reported that knockdown of MIF or CD74 expression by RNA interference inhibits DU-145 cell proliferation and downstream MIF signalling (Meyer-

Siegler et al., 2006; Ren et al., 2006). Guo et al. (2013) also reported that knockdown of the functional expression of MIF markedly decreased H460 cell proliferation and induced apoptosis, as seen by augmented expression of annexin A5 following treatment of H40 cells by MIF siRNA. In particular, Verjans et al. (2009) showed that anti-MIF and anti-CD74 antibodies potently blocked cell proliferation of non-invasive MDA-MB-468 and invasive MDA-MB-231 breast cancer cells however this was not observed in non-tumorous MCF-12A cells. This could be explained by the absence of the cell-surface portion of CD74 in MCF-12A cells. Berkova et al. (2014) reported that CD74 regulates Fas death receptor signalling in lymphomas by decreasing the levels of Fas receptors on the cell-surface. In the same manner, Liu et al. (2008) have shown that CD74 promotes tumour growth, angiogenesis, and cancer cell metastasis *in vivo*. The effect of CD74 in tumour growth and cell proliferation was studied by blocking the activity of MIF or CD74 in HEK/ CD74 or a renal cell carcinoma (Caki-1) cells. The data showed that CD74-upregulated vascular endothelial growth factor D (VEGF-D) positively regulates the expression of cyclin D and E, which results in the promotion of cell cycle progression (Liu et al., 2008). It was reported that G1/S phase proteins cyclin D and cyclin E, were upregulated by CD74 and promoted cell cycle progression (Starlets et al., 2006). In the light of this, it is here assumed that persistent high expression of CD74 in the intracellular compartment and on the cell-surface could impair MHC class II antigen presentation by tumour cells; it could also contribute to immune escape and tumour metastasis (Xu et al., 2000). Figure 7-1 shows proposed signal transduction pathway of MIF with CD74 and CD44.

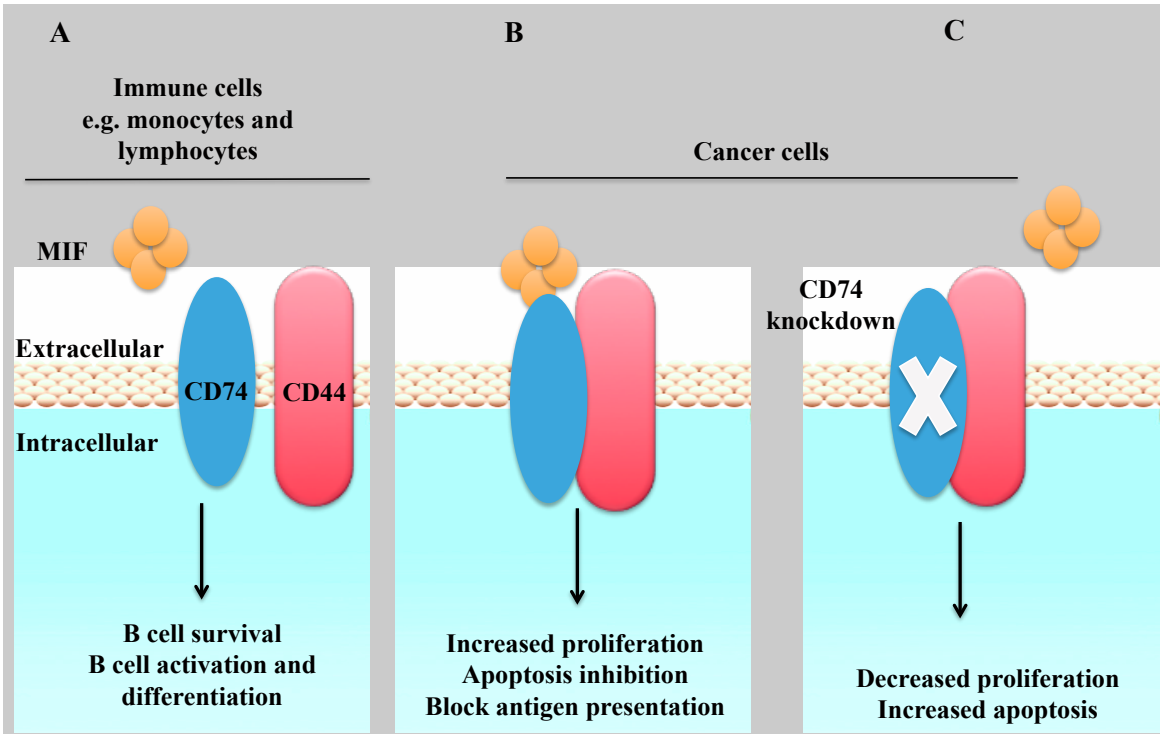

Figure 7-1: Diagram illustrating the proposed signal transduction pathway of MIF with CD74 and CD44 in human breast cancer cells CAMA-1, MDA-MB-231 and MDA-MB-435.

(A) MIF, CD74 and CD44 are key molecules in the immune system through the role that they have on their own or when they associate to form a multimeric complex. MIF/CD74/CD44 complex regulates the adaptive immune response by maintaining the mature B cell population and B cell activation and differentiation. However, when tumour cells express this complex, it shows different functions that are believed to be against the immune system. (B) Shows proposed model of an association between MIF and cluster of differentiation CD74 and CD44 based on the correlation analysis revealed on this study, which shows that MIF is positively correlated with CD74 and CD44. It was hypothesised that CD74 colocalise with MIF on the cell-surface and intra-cytoplasmic domain of CD74 colocalise with CD44 in CAMA-1, MDA-MB-231 and MDA-MB-435 cells. It is reasonable to assume that the MIF-CD74-CD44 complex formation activates Src-family kinase and (ERK1 and ERK2/MAPK), resulting in the activation of cyclin D1 and PI3K/Akt, to the downstream effects on cell cycle, cell proliferation, gene expression and inhibition of apoptosis on tumour cells however detailed mechanisms are not fully understood. (C) As it is proposed that blocking MIF-CD74 interaction selectively will decrease ERK1 and ERK2 activation, decrease cell proliferation, and increase apoptosis in tumour cells. The present study showed that knockdown of CD74 by CD74 siRNA significantly reduce CAMA-1 and MDA-MB-231 cell proliferation and increase the level of apoptotic cells.

7.1.4 Proteomics study of the effect of IFN-γ in CAMA-1 and MDA-MB-231 cells

A proteomics study using 2-DE was performed to identify differences between untreated and IFN-γ-treated CAMA-1 and MDA-MB-231 cells. In comparison with IFN-γ-stimulated and non-stimulated CAMA-1 and MDA-MB-231 cells, 19 protein spots resolved at a given pI and molecular weight were identified in CAMA-1 cells and 17 spots were identified in MDA-MB-231 cells. The 2-DE results were analysed using ExPASy tool that yielded several potential useful results. The polypeptide spots that randomly selected and analysed were highlighted shown in (Table 6-2 and Table 6-3).

Five spots out of the 19 polypeptide spots generated from the CAMA-1 cell sample were randomly selected and analysed. For example, the polypeptide spot number 1741 correlated with interferon-induced transmembrane protein 10, which has a pI of ~ 6 and a MW 25 kDa. The polypeptide spot number 2610, which it is believed to be related to programmed cell death protein 5 (PDCD5), was also evaluated. PDCD5 has a pI of ~ 6 and a MW 16 kDa which is very similar to spot number 2610. PDCD5 is widely expressed in most types of normal human tissue and is unregulated in cells undergoing apoptosis (Chen et al., 2013). It has since been confirmed that IFN-γ inhibits growth of human carcinoma cells via caspase-1 dependent induction of apoptosis (Detjen et al., 2001). It was assumed that IFN-γ played a critical role in the apoptosis inducing factors like PDCD5. The investigation of spot number 1387 which has a pI of ~ 3 and a MW 30 kDa, showed a strong similarity to cell cycle checkpoint protein RAD1. Cycle checkpoint proteins play an important role in controlling cell division of damaged cells (Abraham, 2001). Another interesting polypeptide spot number was 2086 which has a pI of ~ 9 and a MW 25 kDa. The search engine showed that this spot might be related TNF-α -induced protein 8-like protein 2 (TIPE2). TIPE2 is a novel immune negative molecule and an inhibitor of the oncogenic Ras in mice. However, its function in humans is still unclear

(Wang et al., 2013b). The polypeptide spot number 2361 which has a pI of ~ 7 and a MW 20 kDa showed correlation with cyclin-dependent kinase 4. Cyclin-dependent kinases (CDKs) play a central role in the orderly transition from one phase of the eukaryotic mitotic cell division cycle to the next (Ullah et al., 2009; Roberts et al., 2012). CDKs regulate cell proliferation and coordinate the cell cycle checkpoint response to DNA damage. Owing to this, it is assumed that the absence of spot number 2361 after IFN-γ treatment may act as a regulator of tumour cell division. CDK4/6 inhibitors have been proven to be attractive antineoplastic agents because of the importance of CDK4/6 activity in regulating cell proliferation (Roberts et al., 2012).

In the above manner, five spots out of the 17 the polypeptide spots obtained from MDA-MB-231 cell lysates were randomly selected and analysed. The polypeptide spot number 932, which has a pI of ~ 4 and a MW 110 kDa, was been investigated. This spot showed strong correlation with melanoma-associated antigen C. Melanoma-associated antigens (MAGEs) are classified into two subgroups, I and II. Subgroup I consists of antigens in which expression is generally restricted to tumour or germ cells, whereas subgroup II MAGEs are expressed in various normal adult human tissues (Xiao and Chen, 2004). Another polypeptide spot that was linked to ExPASy tool was number 905, which has a pI of ~ 5 and a MW 55 kDa. The database showed that spot number 905 corresponds to Myc proto-oncogene protein. The Myc proto-oncogene is a "master regulator" which controls many functions, including cellular metabolism and proliferation. The Myc oncogene has been shown to induce apoptosis, and has therefore been targeted to develop novel cancer therapies (Miller et al., 2012). It was noticed that the data obtained from 2-DE indicates that the intensity of spot number 905 increased after IFN-γ treatment. In this context, IFN-γ has been shown to induce apoptosis of human carcinoma cells via a caspase-1 dependent mechanism, which is believed to control Myc proto-oncogene

(Detjen et al., 2001). Therefore IFN-γ might increase the apoptosis of breast cancer cells via Myc proto-oncogene protein in the same manner. TP53-regulated inhibitor of apoptosis is linked to the polypeptide spot number 2299, which has a pI of ~ 5 and a MW 10 kDa. The polypeptide spot number 1720, which has a pI of ~ 4 and a MW 20 kDa, showed correlation with growth arrest and DNA damage-inducible protein (GADD45β). GADD45β has been reported to inhibit apoptosis via attenuating c-Jun N-terminal kinase (JNK) activation. It has been reported that TNF-α treatment induces GADD45β protein expression through NF-κB-mediated transcription, and transforming growth factor-b induces its expression (Yu et al., 2013). The polypeptide spot number 1493 was then evaluated, which it is believed to be related to the HLA-DR alpha chain. The HLA-DR alpha chain has a pI of ~ 2 and MW 30 kDa, which is very similar to spot, number 1493. The expression of HLA-DR on cancer cells closely relates to a more favourable prognosis for cancer patients, but the immunological and non-immunological mechanisms are still obscure (Matsushita et al., 2006).

The current study has found a number of differentially expressed proteins in the breast cancer model system in response to infectious agents. The data presented here could be used as baseline for further detailed investigation. In this regard, functional assays need to be employed to further validate the data presented. Further analysis by mass spectrometry is also required to identify sequences and differentially observed polypeptide spots.

7.2 Limitations and significance of the main findings

The use of breast cancer cells, normal breast luminal cells, normal breast tissues and solubilise cell extracts as well as the positive control cell lines, was a unique feature of this study. The study used a variety of techniques including RT-PCR, flow cyotemetry,

Western blotting, Co-IP, imaging of siRNA transfection, and 2-DE. There are, however, limitations to this study.

This study utilized *in vitro* cell lines that cannot serve as a replacement for *in vivo* or *ex vivo* primary cells, in that the precise cellular conditions in vivo could be replicated. Therefore, investigating clinical samples from breast cancer patients and normal women would improve this study, providing more accurate outcomes for comparison with previous research. One of the main limitations of this study is that it did not evaluate the effect of IFN-γ and LPS in a dose- and time-dependent manner. However, in accordance with previously published methods, optimum conditions were implemented (Moldenhauer et al., 1999; Zheng et al., 2012). Another limitation of this study is that the apoptosis assay did not include a direct measure of the total number of tumour cells after treatment with IFN-γ and LPS for comparison with the proliferation results.

This study did not attempt to explain the mechanism of MIF action and the role of interacting proteins in influencing MIF signalling pathways. Microscopic techniques such as fluorescence resonance energy transfer (FRET) could be applied to study the physical association between CD74, MIF and CD44 molecules. FRET is a mechanism describing energy transfer between two light-sensitive molecules (chromophores). A donor chromophore, initially in its electronic excited state, may transfer energy to an acceptor chromophore through nonradiative dipole–dipole coupling. The efficiency of this energy transfer is inversely proportional to the sixth power of the distance between donor and acceptor, making FRET extremely sensitive to small changes in distance. Investigating the interacting binding sites of MIF and CD74 as well as CD74 and CD44 would facilitate the design of a clinical drug blocking the interaction.

This study investigated the effect of IFN-γ on breast cancer cell lines by 2-DE, but no further analysis was performed, such us spot analysis by mass spectrometry. However, ExPASy tool was utilised to analyse the protein spots that were identified in CAMA-1 and MDA-MB-231 cells. Low recovery of hydrophobic proteins on 2-DE gels is another major limitation in proteome research. However, much progress has been made in the analysis of integral membrane proteins by 2-DE (Santoni et al., 1999).

7.3 Future directions

Tumour immunology is a growing field of research that aims to discover innovative cancer immunotherapies to treat the disease and prevent its progression. There are still key questions that could be further investigated in future research. A major challenge in the future will be to understand CD74 interactions and modifications with different molecules such as CXCR1 and CXCR2 in breast cancer. Since these molecules have been shown involve in signalling pathway with MIF and CD74; it may then become possible to target specific pathways and provide new therapeutic interventions.

Future studies of the role of CD74, along with that of CD44, in mediating MIF's signalling pathways would benefit from the application of RNA-Seq, a recently developed approach to transcriptome profiling that uses deep sequencing technologies. Using RNA-Seq to compare the transcriptome of normal and cancer breast tissues would permit the survey of the transcriptional dynamics implicated in health and disease. RNA-Seq based experiments could profitably be combined with proteomic surveys carried out with liquid chromatography mass spectrometry (LC-MS). Mass spectrometry operates in similar fashion to conventional flow cytometry, except that the detection of antigens of interest is based on elemental detection of lanthanide metals (via inductively coupled plasma mass spectrometry (ICP-MS)). The lanthanide metals are conjugated to probes

(usually an antibody) in place of the classical fluorescent labels of flow cytometry. By forgoing fluorescent measures, there is no need to compensate for fluorescent spill-over across channels. This greatly extends multiplexing potential, allowing simultaneous measurement of up to 35 antigens. Mass cytometry is the adaptation of ICP-MS to single-cell analysis based on the concept that a purified single isotope could be used to tag antibodies, and that these conjugates could be quantified in an ICP-MS detection system. Mass cytometry is also readily combined with imaging to provide a spatial distribution of the antigens of interest over times, thereby providing further insight into the CD74-MIF-CD44 network.

7.4 Closing remarks

In conclusion, this study indicates the feasibility of using immunological and proteomics techniques to find new connections between the ability of cancer cells to establish metastasis in distant organs and altered expression levels of specific proteins. The study was designed to focus on transmembrane proteins relative to the entire proteome, thereby increasing the likelihood of identifying proteins that could be targeted by antibodies and small molecule drugs as to inhibit the metastatic process. Several of the transmembrane proteins identified and characterized seem to be involved in the metastatic behaviour of human breast cancer. This indicates that further investigations hold promise for identifying novel mechanistically important targets for preventing metastasis and significantly advancing treatment of breast cancer. Because of novel technical improvements, future studies will also include identification and characterization of proteins with altered expression in subcellular compartments, bringing further insight to the tumour immunology field.

References

References

Abbas, A. K. & Lichtman, A. H. (2005). *Cellular and Molecular Immunology,* 5th edition, Elsevier Saunders, Philadelphia.

Abraham, R. T. (2001). Cell cycle checkpoint signaling through the ATM and ATR kinases. *Genes & development*, *15*(17), 2177-2196.

Adler, J., & Parmryd, I. (2010). Quantifying colocalization by correlation: the Pearson correlation coefficient is superior to the Mander's overlap coefficient. *Cytometry part A*, *77*(8), 733-742.

Aebersold, R., & Cravatt, B. F. (2002). Proteomics–advances, applications and the challenges that remain. *Trends in biotechnology*, *20*(12), s1-s2.

Aebersold, R., & Mann, M. (2003). Mass spectrometry-based proteomics. *Nature*, *422*(6928), 198-207.

Aickelin, U., & Cayzer, S. (2008). The danger theory and its application to artificial immune systems. *arXiv preprint arXiv:0801.3549*.

Al-Hajj, M., Wicha, M. S., Benito-Hernandez, A., Morrison, S. J., & Clarke, M. F. (2003). Prospective identification of tumourigenic breast cancer cells. *Proceedings of the national academy of sciences*, *100*(7), 3983-3988.

Ali, S., & Coombes, R. C. (2002). Endocrine-responsive breast cancer and strategies for combating resistance. *Nature reviews cancer*, *2*(2), 101-112.

Amiour, N., Imbaud, S., Clement, G., Agier, N., Zivy, M., Valot, B., Balliau, T., Armengaud, P., Quillere, I., Canas, R., Tercet-Laforgue, T., and Hirel, B. (2012). The use of metabolomics integrated with transcriptomic and proteomic studies for identifying key steps involved in the control of nitrogen metabolism in crops such as maize. *Journal of experimental botany*, *63*(14), 5017-5033.

Anand, M. T., & Kumar, S. (2014). CD44: A key player in breast cancer. *Indian journal of cancer*, *51*(3), 247-250.

Andersson, I. (2005). Invasive breast cancer. In *Radiologic-Pathologic Correlations from Head to Toe* (pp. 757-766). Springer Berlin Heidelberg.

Ashman, L. K. (1987). The immunogenicity of tumour cells. *Immunology and cell biology*, *65*(4), 271-277.

Assimakopoulos, D., Kolettas, E., Patrikakos, G., & Evangelou, A. (2002). The role of CD44 in the development and prognosis of head and neck squamous cell carcinomas. *Histology & histopathology, 17*(5), 1269-1281.

B Janakiram, N., Mohammed, A., S Bronze, M., & V Rao, C. (2012). Prophylactic vaccine approach for colon and pancreatic cancers: present and future. *Current medicinal chemistry*, *19*(22), 3664-3678.

Bach, J. P., Deuster, O., Balzer-Geldsetzer, M., Meyer, B., Dodel, R., & Bacher, M. (2009). The role of macrophage inhibitory factor in tumour igenesis and central nervous system tumour s. *Cancer*, *115*(10), 2031-2040.

Bach, J. P., Rinn, B., Meyer, B., Dodel, R., & Bacher, M. (2008). Role of MIF in inflammation and tumorigenesis. *Oncology*, *75*(3-4), 127-133.

Badve, S., Deshpande, C., Hua, Z., & Lennart, L. (2002). Expression of Invariant Chain (CD 74) and Major Histocompatibility Complex (MHC) Class II Antigens in the Human Fetus1. *Journal of histochemistry & cytochemistry*, *50*(4), 473-482.

Bando, H., Matsumoto, G., Bando, M., Muta, M., Ogawa, T., Funata, N., Nishihira, J., Koike, M., & Toi, M. (2002). Expression of macrophage migration inhibitory factor in human breast cancer: association with nodal spread. *Cancer science*, *93*(4), 389-396.

Barshack, I., Goldberg, I., Nass, D., Olchovsky, D., & Kopolovic, J. (1998). CD44 expression in normal adrenal tissue and adrenal tumours. *Journal of clinical pathology*, *51*(1), 52-54.

Basha, G., Omilusik, K., Chavez-Steenbock, A., Reinicke, A. T., Lack, N., Choi, K. B., & Jefferies, W. A. (2012). A CD74-dependent MHC class I endolysosomal cross-presentation pathway. *Nature immunology*, *13*(3), 237-245.

Bauer, K. R., Brown, M., Cress, R. D., Parise, C. A., & Caggiano, V. (2007). Descriptive analysis of estrogen receptor (ER)-negative, progesterone receptor (PR)-negative, and HER-2-negative invasive breast cancer, the so-called triple-negative phenotype. *Cancer*, *109*(9), 1721-1728.

Beatty, G. L., & Paterson, Y. (2000). IFN-γ can promote tumour evasion of the immune system in vivo by down-regulating cellular levels of an endogenous tumour antigen. *The Journal of immunology*, *165*(10), 5502-5508.

Becker-Herman, S., Arie, G., Medvedovsky, H., Kerem, A., & Shachar, I. (2005). CD74 is a member of the regulated intramembrane proteolysis-processed protein family. *Molecular biology of the cell*, *16*(11), 5061-5069.

Benigni, F., Atsumi, T., Calandra, T., Metz, C., Echtenacher, B., Peng, T., & Bucala, R. (2000). The proinflammatory mediator macrophage migration inhibitory factor induces glucose catabolism in muscle. *Journal of clinical investigation*, *106*(10), 1291-1300.

Bergmann, H. (2012). Business as usual: the p35 isoform of human CD74 retains function in antigen presentation. *Immunology and cell biology*, *90*(9), 839-840.

Berkova, Z., Wang, S., Ao, X., Wise, J. F., Braun, F. K., Rezaeian, A. H., Sehgal, L., Goldenberg, D.M., & Samaniego, F. (2014). CD74 interferes with the expression of fas receptor on the surface of lymphoma cells. *Journal of experimental & clinical cancer research*, *33*(1), 80-90.

Bernhagen, J., Krohn, R., Lue, H., Gregory, J. L., Zernecke, A., Koenen, R. R., Dewor, M., Georgiev, I., Schober, A., Leng, L., Kooistra, T., Fingerle-Rowson, G., Ghezzi, P., Kleemann, R., McColl, S. R., Bucala, R., Hickey, M.J & Weber, C. (2007). MIF is a noncognate ligand of CXC chemokine receptors in inflammatory and atherogenic cell recruitment. *Nature medicine*, *13*(5), 587-596.

Beswick, E. J., & Reyes, V. E. (2009). CD74 in antigen presentation, inflammation, and cancers of the gastrointestinal tract. *World journal of gastroenterology, 15*(23), 2855-2861.

Beswick, E. J., Pinchuk, I. V., Suarez, G., Sierra, J. C., & Reyes, V. E. (2006). Helicobacter pylori CagA-dependent macrophage migration inhibitory factor produced by gastric epithelial cells binds to CD74 and stimulates procarcinogenic events. *The iournal of immunology*, *176*(11), 6794-6801.

Bindea, G., Mlecnik, B., Fridman, W. H., & Galon, J. (2011). The prognostic impact of anti-cancer immune response: a novel classification of cancer patients. In *seminars in immunopathology, 33* (4), 335-3340.

Binsky, I., Lantner, F., Grabovsky, V., Harpaz, N., Shvidel, L., Berrebi, A., Goldenberg, D.M., Leng, L., Bucala, R., Alon, R., Haran, M., & Shachar, I. (2010). TAp63 regulates VLA-4 expression and chronic lymphocytic leukemia cell migration to the bone marrow in a CD74-dependent manner. *The journal of immunology*, *184*(9), 4761-4769.

Bissell, M. J., & Radisky, D. (2001). Putting tumours in context. *Nature reviews cancer*, *1*(1), 46-54.

Blankenstein, T., Coulie, P. G., Gilboa, E., & Jaffee, E. M. (2012). The determinants of tumour immunogenicity. *Nature reviews cancer*, *12*(4), 307-313.

Blazar, B. R., Lindberg, F. P., Ingulli, E., Panoskaltsis-Mortari, A., Oldenborg, P. A., Iizuka, K., Yokoyama, W.M., & Taylor, P. A. (2001). CD47 (integrin-associated protein) engagement of dendritic cell and macrophage counterreceptors is required to prevent the

clearance of donor lymphohematopoietic cells. *The journal of experimental medicine*, *194*(4), 541-550.

Bolte, S., & Cordelieres, F. P. (2006). A guided tour into subcellular colocalization analysis in light microscopy. *Journal of microscopy*, *224*(3), 213-232.

Borghese, F., & Clanchy, F. I. (2011). CD74: an emerging opportunity as a therapeutic target in cancer and autoimmune disease. *Expert opinion on therapeutic targets*, *15*(3), 237-251.

Boyton, R. J., & Altmann, D. M. (2007). Natural killer cells, killer immunoglobulin-like receptors and human leucocyte antigen class I in disease. *Clinical & experimental immunology*, *149*(1), 1-8.

Brandacher, G., Winkler, C., Schroecksnadel, K., Margreiter, R., & Fuchs, D. (2006). Antitumour al activity of interferon-involved in impaired immune function in cáncer patients. *Current drug metabolism*, *7*(6), 599-612.

Brasier, A. R., Garcia, J., Wiktorowicz, J. E., Spratt, H. M., Comach, G., Ju, H., Recinos, A., Soman, K., Forshey, B. M., Halsey, E. S., Blair, P. J., Rocha, C., Bazan, I., Victor, S. S., Wu, Z., Stafford, S., Watts, D., Morrison, A. C., Scott, T. W., and Kochel, T. J. (2012). Discovery proteomics and nonparametric modeling pipeline in the development of a candidate biomarker panel for dengue hemorrhagic fever. *Clinical and translational science*, *5*(1), 8-20.

Brioschi, M., Lento, S., Tremoli, E., & Banfi, C. (2013). Proteomic analysis of endothelial cell secretome: a means of studying the pleiotropic effects of Hmg-CoA reductase inhibitors. *Journal of proteomics*, *78*, 346-361.

Brody, J. R., Costantino, C. L., Berger, A. C., Sato, T., Lisanti, M. P., Yeo, C. J., Emmons, R.V., & Witkiewicz, A. K. (2009). Expression of indoleamine 2, 3-dioxygenase in metastatic malignant melanoma recruits regulatory T cells to avoid immune detection and affects survival. *Cell cycle*, *8*(12), 1930-1934.

Brown, M. S., Ye, J., Rawson, R. B., & Goldstein, J. L. (2000). Regulated intramembrane proteolysis: a control mechanism conserved from bacteria to humans. *Cell*, *100*(4), 391-398.

Brunelli, L., Campagna, R., Airoldi, L., Cauli, O., Llansola, M., Boix, J., Felipo, V., and Pastorelli, R. (2012). Exploratory investigation on nitro-and phospho-proteome cerebellum changes in hyperammonemia and hepatic encephalopathy rat models. *Metabolic brain disease*, *27*(1), 37-49.

Brunner, H., & Bernhagen, J. (2000). Intracellular action of the cytokine MIF to modulate AP-1 activity and the cell cycle through Jab1. *Nature*, *408*(6809), 211-216.

Bucala, R., & Donnelly, S. C. (2007). Macrophage migration inhibitory factor: a probable link between inflammation and cancer. *Immunity*, *26*(3), 281-285.

Burgess, D. J. (2012). Tumour immunogenicity: editorial selection demystified. *Nature reviews cancer*, *12*(4), 227-227.

Burnet, M. (1957). Cancer—a biological approach: I. The processes of control. II. The significance of somatic mutation. *British medical journal*, *1*(5022), 779.

Burton, J. D., Ely, S., Reddy, P. K., Stein, R., Gold, D. V., Cardillo, T. M., & Goldenberg, D. M. (2004). CD74 is expressed by multiple myeloma and is a promising target for therapy. *Clinical cancer research*, *10*(19), 6606-6611.

Burton, J. D., Stein, R., Chandra, A., Chen, S., Mishra, N., Shah, T., & Goldenberg, D. M. (2010). Expression of CD74 by AML blasts and cell lines, and enhanced in vitro cytotoxicity of anti-CD74 antibody after interferon-gamma (IFN-{gamma}) treatment. *Journal of clinical oncology, 28*(15), 6576.

Butrym, A., Majewski, M., Dzietczenia, J., Kuliczkowski, K., & Mazur, G. (2013). High CD74 expression correlates with ZAP70 expression in B cell chronic lymphocytic leukemia patients. *Medical oncology*, *30*(2), 1-6.

Cailleau, R., Olivé, M., & Cruciger, Q. V. (1978). Long-term human breast carcinoma cell lines of metastatic origin: preliminary characterization. *In vitro*, *14*(11), 911-915.

Calandra, T., & Roger, T. (2003). Macrophage migration inhibitory factor: a regulator of innate immunity. *Nature reviews immunology*, *3*(10), 791-800.

Calandra, T., Bernhagen, J., Mitchell, R. A., & Bucala, R. (1994). The macrophage is an important and previously unrecognized source of macrophage migration inhibitory factor. *The Journal of experimental medicine*,*179*(6), 1895-1902.

Calandra, T., Echtenacher, B., Roy, D.L., Pugin, J., Metz, C.N., Hultner, L., Heumann, D., Mannel, D., Bucala, R., and Glauser, M.P. (2000). Protection from septic shock by neutralization of macrophage migration inhibitory factor. *Nature medicine*, *6*(2), 164-170.

Capuco, A. V., & Ellis, S. E. (2013). Comparative aspects of mammary gland development and homeostasis. *Annual review of animal biosciences, 1*(1), 179-202.

Carlsson, B., Forsberg, O., Bengtsson, M., Tötterman, T. H., & Essand, M. (2007). Characterization of human prostate and breast cancer cell lines for experimental T cell-based immunotherapy. *The prostate*, *67*(4), 389-395.

Chambers, A. F. (2009). MDA-MB-435 and M14 cell lines: identical but not M14 melanoma?. *Cancer research*, *69*(13), 5292-5293.

Chang, F., Lee, J. T., Navolanic, P. M., Steelman, L. S., Shelton, J. G., Blalock, W. L., Franklin, R. A., & McCubrey, J. A. (2003a). Involvement of PI3K/Akt pathway in cell cycle progression, apoptosis, and neoplastic transformation: a target for cancer chemotherapy. *Leukemia*, *17*(3), 590-603.

Chang, F., Steelman, L. S., Shelton, J. G., Lee, J. T., Navolanic, P. M., Blalock, W. L., Franklin, R. A., & McCubrey, J. A. (2003b). Regulation of cell cycle progression and apoptosis by the Ras/Raf/MEK/ERK pathway (Review). *International journal of oncology*, *22*(3), 469-480.

Chang, W. S. W., Wu, H. R., Yeh, C. T., Wu, C. W., & Chang, J. Y. (2007). Lysosomal cysteine proteinase cathepsin S as a potential target for anti-cancer therapy. *Journal of cancer molecules*, *3*(1), 5-14.

Chanput, W., Mes, J. J., & Wichers, H. J. (2014). THP-1 cell line: An in vitro cell model for immune modulation approach. *International immunopharmacology, 23*(1), 37-45. Chicago

Chao, M. P., Weissman, I. L., & Majeti, R. (2012). The CD47–SIRPα pathway in cancer immune evasion and potential therapeutic implications. *Current opinion in immunology*, *24*(2), 225-232.

Charafe-Jauffret, E., Ginestier, C., Monville, F., Finetti, P., Adelaide, J., Cervera, N., Fekairi, S., Xerri, L., Birnbaum, D., & Bertucci, F. (2006). Gene expression profiling of breast cell lines identifies potential new basal markers. *Oncogene*, *25*(15), 2273-2284.

Cheah, P. L., & Looi, L. M. (2001). p53: an overview of over two decades of study. *The Malaysian journal of pathology*, *23*(1), 9-16.

Chen, E. I., & Yates, J. R. (2007). Cancer proteomics by quantitative shotgun proteomics. *Molecular oncology*, *1*(2), 144-159.

Chen, Y., Zou, Z., Xu, A., Liu, Y., Pan, H., & Jin, L. (2013). Serum programmed cell death protein 5 (PDCD5) levels is upregulated in liver diseases. *Journal of immunoassay and immunochemistry*, *34*(3), 294-304.

Cheng, S. P., Liu, C. L., Chen, M. J., Chien, M. N., Leung, C. H., Lin, C. H., Hsu, Y.C., & Lee, J. J. (2015). CD74 expression and its therapeutic potential in thyroid carcinoma. *Endocrine-related cancer*, *22*(2), 179-190.

Chesney, J., Metz, C., Bacher, M., Peng, T., Meinhardt, A., & Bucala, R. (1999). An essential role for macrophage migration inhibitory factor (MIF) in angiogenesis and the growth of a murine lymphoma. *Molecular medicine*, *5*(3), 181-191.

Chomczynski, P., & Mackey, K. (1995). Short technical reports. Modification of the TRI reagent procedure for isolation of RNA from polysaccharide-and proteoglycan-rich sources. *Biotechniques*, *19*(6), 942-945.

Cichy, J., & Puré, E. (2003). The liberation of CD44. *The Journal of cell biology*, *161*(5), 839-843.

Cohen, S., & Shachar, I. (2014). Midkine as a regulator of B cell survival in health and disease. *British journal of pharmacology*, *171*(4), 888-895.

Cohen, S., Shoshana, O. Y., Zelman-Toister, E., Maharshak, N., Binsky-Ehrenreich, I., Gordin, M., Hazan-Halevy, I., Herishanu, Y., Shvidel, L., Haran, M., Leng, L., Bucala, R., Harroch, S., & Shachar, I. (2012). The cytokine midkine and its receptor RPTPζ regulate B cell survival in a pathway induced by CD74. *The journal of immunology*, *188*(1), 259-269.

Conroy, H., Mawhinney, L., & Donnelly, S. C. (2010). Inflammation and cancer: macrophage migration inhibitory factor (MIF)—the potential missing link. *Quarterly journal of medicine*, *103*(11), 831-836.

Couldrey, C., Moitra, J., Vinson, C., Anver, M., Nagashima, K., & Green, J. (2002). Adipose tissue: a vital in vivo role in mammary gland development but not differentiation. *Developmental dynamics*, *223*(4), 459-468.

Coulie, P. G., Van den Eynde, B. J., van der Bruggen, P., & Boon, T. (2014). Tumour antigens recognized by T lymphocytes: at the core of cancer immunotherapy. *Nature reviews cancer*, *14*(2), 135-146.

Cravatt, B. F., Simon, G. M., & Yates Iii, J. R. (2007). The biological impact of mass-spectrometry-based proteomics. *Nature*, *450*(7172), 991-1000.

Crotzer, V. L., & Blum, J. S. (2010). Autophagy and adaptive immunity. *Immunology*, *131*(1), 9-17.

Culver, J. B., Hull, J., Levy-Lahad, E., Daly, M., & Burke, W. (2003). Breast cancer genetics: an overview. *GeneReviews at GeneTests: Medical Genetics Information Resource (database online). University of Washington, Seattle*.

Datta, M. W., Shahsafaei, A., Nadler, L. M., Freeman, G. J., & Dorfman, D. M. (2000). Expression of MHC class II-associated invariant chain (Ii; CD74) in thymic epithelial neoplasms. *Applied immunohistochemistry & molecular morphology*, *8*(3), 210-215.

de Dios Rosado, J., & Rodriguez-Sosa, M. (2011). Macrophage migration inhibitory factor (MIF): a key player in protozoan infections. *International journal of biological sciences*, *7*(9), 1239-1256.

DeLisser, H. M. (2009). CD44: target for antiangiogenesis therapy. *Blood*, *114* (25), 5114-5115.

DeSantis, C., Siegel, R., Bandi, P., & Jemal, A. (2011). Breast cancer statistics, 2011. *CA: a cancer journal for clinicians*, *61*(6), 408-418.

Detjen, K. M., Farwig, K., Welzel, M., Wiedenmann, B., & Rosewicz, S. (2001). Interferon γ inhibits growth of human pancreatic carcinoma cells via caspase-1 dependent induction of apoptosis. *An international peer-reviewed journal for health professionals and researchers in gastroenterology & hepatology*, *49*(2), 251-262.

Dimri, G., Band, H., & Band, V. (2005). Mammary epithelial cell transformation: insights from cell culture and mouse models. *Breast cancer research*, *7*(4), 171-9.

Disis, M. L. (2002). Immunologic targets for breast cancer. *Breast disease*, *15*(1), 83-90.

Docquier, F., Kita, G. X., Farrar, D., Jat, P., O'Hare, M., Chernukhin, I., Gretton, S., Mandal, A., Alldridge, L., & Klenova, E. (2009). Decreased poly (ADP-ribosyl) ation of CTCF, a transcription factor, is associated with breast cancer phenotype and cell proliferation. *Clinical cancer research*, *15*(18), 5762-5771.

Dodson, L. F., Hawkins, W. G., & Goedegebuure, P. (2011). Potential targets for pancreatic cancer immunotherapeutics. *Immunotherapy*, *3*(4), 517-537.

Donn, R. P., & Ray, D. W. (2004). Macrophage migration inhibitory factor: molecular, cellular and genetic aspects of a key neuroendocrine molecule. *Journal of endocrinology*, *182*(1), 1-9.

Dontu, G., Al-Hajj, M., Abdallah, W. M., Clarke, M. F., & Wicha, M. S. (2003). Stem cells in normal breast development and breast cancer. *Cell proliferation*, *36*(s1), 59-72.

Dranoff, G. (2004). Cytokines in cancer pathogenesis and cancer therapy. *Nature Reviews cancer*, *4*(1), 11-22.

Dunn, G. P., Bruce, A. T., Ikeda, H., Old, L. J., & Schreiber, R. D. (2002). Cancer immunoediting: from immunosurveillance to tumour escape. *Nature immunology*, *3*(11), 991-998.

Dunn, G. P., Old, L. J., & Schreiber, R. D. (2004). The immunobiology of cancer immunosurveillance and immunoediting. *Immunity*, *21*(2), 137-148.

DuPage, M., Mazumdar, C., Schmidt, L. M., Cheung, A. F., & Jacks, T. (2012). Expression of tumour-specific antigens underlies cancer immunoediting. *Nature*, *482*(7385), 405-409.

Eberth, S., Schneider, B., Rosenwald, A., Hartmann, E., Romani, J., Zaborski, M., Siebert, R., Drexler, G. H., & Quentmeier, H. (2010). Epigenetic regulation of CD44 in Hodgkin and non-Hodgkin lymphoma. *BMC cancer*, 10 (1), 517.

Eccles, S.A., Aboagye, E.O., Ali, S., Anderson, A.S., Armes, J., Berditchevski, F., Blaydes, J.P., Brennan, K., Brown, N.J., Bryant, H.E., Bundred, N.J., Burchell, J.M., Campbell, A.M., Carroll, J.S., Clarke, R.B., Coles, C.E., Cook, G.J., Cox, A., Curtin, N.J., Dekker, L.V., Dos Santos Silva, I., Duffy, S.W., Easton, D.F., Eccles, D.M., Edwards, D.R., Edwards, J, Evans, D, Fenlon, DF, Flanagan, JM, Foster, C, Gallagher, WM, Garcia-closas, M, Gee, JMW, Gescher, A.J., Goh, V., Groves, A.M., Harvey, A.J., Harvie, M., Hennessy, B.T., Hiscox, S., Holen, I., Howell, S.J., Howell, A., Hubbard, G., Hulbert-williams, N., Hunter, M.S., Jasani, B., Jones, L.J., Key, T.J., Kirwan, C.C., Kong, A., Kunkler, I.H., Langdon, S.P, Leach, M.O, Mann, D.J, Marshall, J.F, Martin, L., Martin, S.G., Macdougall, J.E., Miles, D.W., Miller, W.R., Morris, J.R., Moss, S.M., Mullan, P., Natrajan, R., O'Connor, J.P., O'Connor, R., Palmieri, C., Pharoah, P.D.P., Rakha, E.A., Reed, E., Robinson, S.P., Sahai, E., Saxton, J.M., Schmid, P., Smalley, M.J., Speirs, V., Stein, R., Stingl, J., Streuli, C.H., Tutt, A.N.J., Velikova, G., Walker, R.A.,Watson, C.J., Williams, K.J., Young, L.S. & Thompson, A.M.(2013). Critical research gaps and translational priorities for the successful prevention and treatment of breast cancer. *Breast cancer research*, *15*(5), R92.

El Bounkari, O., & Bernhagen, J. (2012). MIF and autophagy: a novel link beyond "eating". *Cell research*, *22*(6), 950-953.

Elenbaas, B., Spirio, L., Koerner, F., Fleming, M. D., Zimonjic, D. B., Donaher, J. L., Popescu, N.C., Hahn, W., & Weinberg, R. A. (2001). Human breast cancer cells generated by oncogenic transformation of primary mammary epithelial cells. *Genes & development*, *15*(1), 50-65.

Elias, A. D. (2010). Triple-negative breast cancer: a short review. *American journal of clinical oncology*, *33*(6), 637-645.

Eroles, P., Bosch, A., Pérez-Fidalgo, J. A., & Lluch, A. (2012). Molecular biology in breast cancer: intrinsic subtypes and signaling pathways. *Cancer treatment reviews*, *38*(6), 698-707.

Fabbri, A., Carcangiu, M. L., & Carbone, A. (2008). Histological classification of breast cancer. In *Breast Cancer* (pp. 3-14). Springer Berlin Heidelberg.

Fan, H., Hall, P., Santos, L. L., Gregory, J. L., Fingerle-Rowson, G., Bucala, R., Morand, E.F.& Hickey, M. J. (2011). Macrophage migration inhibitory factor and CD74 regulate macrophage chemotactic responses via MAPK and Rho GTPase. *The Journal of immunology*, *186*(8), 4915-4924.

Farrar, M. A., & Schreiber, R. D. (1993). The molecular cell biology of interferon-gamma and its receptor. *Annual review of immunology*, *11*(1), 571-611.

Fata, J. E., Werb, Z., & Bissell, M. J. (2003). Regulation of mammary gland branching morphogenesis by the extracellular matrix and its remodeling enzymes. *Breast cancer research*, *6*(1), 1.

Fedorchenko, O., Stiefelhagen, M., Peer-Zada, A. A., Barthel, R., Mayer, P., Eckei, L., Breuer, A., Crispatzu, G., Rosen, N., Landwehr, T., Lilienthal, N., M ¨ollmann, M., Montesinos-Rongen, M., Heukamp, L., D ¨urig, J., Hallek, M., Fingerle-Rowson, G., & Herling, M. (2013). CD44 regulates the apoptotic response and promotes disease development in chronic lymphocytic leukemia. *Blood*, *121*(20), 4126-4136.

Feinmesser, M., Sulkes, A., Morgenstern, S., Sulkes, J., Stern, S., & Okon, E. (2000). HLA-DR and β2 microglobulin expression in medullary and atypical medullary carcinoma of the breast: histopathologically similar but biologically distinct entities. *Journal of clinical pathology*, *53*(4), 286-291.

Ferlay, J., Shin, H. R., Bray, F., Forman, D., Mathers, C., & Parkin, D. M. (2010). Estimates of worldwide burden of cancer in 2008: GLOBOCAN 2008. *International journal of cancer*, *127*(12), 2893-2917.

Ferlay, J., Steliarova-Foucher, E., Lortet-Tieulent, J., Rosso, S., Coebergh, J. W. W., Comber, H., Forman, D., & Bray, F. (2013). Cancer incidence and mortality patterns in Europe: estimates for 40 countries in 2012. *European journal of cancer*, *49*(6), 1374-1403.

Fernandez, N., Labeta, M., Kurpisz, M., Nakatsuji, T., Sachs, J., & Festenstein, H. (1990). Major histocompatibility complex (MHC) protein analysis by optimised two-dimensional electrophoretic methods. *Electrophoresis, 11*(2), 167-174.

Fillmore, C., & Kuperwasser, C. (2007). Human breast cancer stem cell markers CD44 and CD24: enriching for cells with functional properties in mice or in man. *Breast cancer research*, *9*(3), 303-306.

Finn, O. J. (2012). Immuno-oncology: understanding the function and dysfunction of the immune system in cancer. *Annals of oncology*, *23*(suppl 8), viii6-viii9.

Flaster, H., Bernhagen, J., Calandra, T., & Bucala, R. (2007). The macrophage migration inhibitory factor-glucocorticoid dyad: regulation of inflammation and immunity. *Molecular endocrinology*, *21*(6), 1267-1280.

Fuchs, E. J., & Matzinger, P. (1996). Is cancer dangerous to the immune system? In *Seminars in immunology, 8*(5), 271-280.

Gabriel, C. A., & Domchek, S. M. (2010). Breast cancer in young women. *Breast cancer research*, *12*(5), 212-222.

Gajewski, T. F., Meng, Y., Blank, C., Brown, I., Kacha, A., Kline, J., & Harlin, H. (2006). Immune resistance orchestrated by the tumour microenvironment. *Immunological reviews*, *213*(1), 131-145.

Gajewski, T. F., Schreiber, H., & Fu, Y. X. (2013). Innate and adaptive immune cells in the tumour microenvironment. *Nature immunology*, *14*(10), 1014-1022.

Garrido, F., Cabrera, T., & Aptsiauri, N. (2010). "Hard" and "soft" lesions underlying the HLA class I alterations in cancer cells: implications for immunotherapy. *International journal of cancer*, *127*(2), 249-256.

Geddes, D. T. (2007). Inside the lactating breast: the latest anatomy research. *Journal of midwifery & women's health*, *52*(6), 556-563.

Genève, L., Chemali, M., Desjardins, M., Labrecque, N., & Thibodeau, J. (2012). Human invariant chain isoform p35 restores thymic selection and antigen presentation in CD74-deficient mice. *Immunology and cell biology*, *90*(9), 896-902.

Gil-Yarom, N., Herman, S. B., & Shachar, I. (2014). *Gene Section*. http://AtlasGeneticsOncology. org, 2014: p. 879.

Gold, D. V., Stein, R., Burton, J., & Goldenberg, D. M. (2011). Enhanced expression of CD74 in gastrointestinal cancers and benign tissues. *International journal of clinical and experimental pathology*, *4*(1), 1.

Goldsby, R.A., Kindt, T.J., Osborne, B.A., Kuby, J. 2003. *Immunology* 5th edn W. H. Freeman and Company, New York.

Gooch, J. L., Herrera, R. E., & Yee, D. (2000). The role of p21 in interferon gamma-mediated growth inhibition of human breast cancer cells. *Cell growth & differentiation: the molecular biology journal of the american association for cancer research*, *11*(6), 335-342.

Goodier, M. R., & Londei, M. (2000). Lipopolysaccharide stimulates the proliferation of human CD56+ CD3− NK cells: a regulatory role of monocytes and IL-10. *The journal of immunology*, *165*(1), 139-147.

Goodison, S., Urquidi, V., & Tarin, D. (1999). CD44 cell adhesion molecules. *Molecular pathology*, *52*(4), 189-196.

Gordin, M., Tesio, M., Cohen, S., Gore, Y., Lantner, F., Leng, L., Bucala, R., & Shachar, I. (2010). c-Met and its ligand hepatocyte growth factor/scatter factor regulate mature B

cell survival in a pathway induced by CD74. *The journal of immunology*, *185*(4), 2020-2031.

Gore, Y., Starlets, D., Maharshak, N., Becker-Herman, S., Kaneyuki, U., Leng, L., Bucala, R., & Shachar, I. (2008). Macrophage migration inhibitory factor induces B cell survival by activation of a CD74-CD44 receptor complex. *Journal of biological chemistry*, *283*(5), 2784-2792.

Götte, M., & Yip, G. W. (2006). Heparanase, hyaluronan, and CD44 in cancers: a breast carcinoma perspective. *Cancer research*, *66*(21), 10233-10237.

Graziano, D. F., & Finn, O. J. (2005). Tumour antigens and tumour antigen discovery. *In tumour immunology and cancer vaccines* (pp. 89-111). Springer US.

Greenwood, C., Metodieva, G., Al-Janabi, K., Lausen, B., Alldridge, L., Leng, L., & Metodiev, M. V. (2012). Stat1 and CD74 overexpression is co-dependent and linked to increased invasion and lymph node metastasis in triple-negative breast cancer. *Journal of proteomics*, *75*(10), 3031-3040.

Gregers, T. F., Nordeng, T. W., Birkeland, H. C., Sandlie, I., & Bakke, O. (2003). The cytoplasmic tail of invariant chain modulates antigen processing and presentation. *European journal of immunology*, *33*(2), 277-286.

Grivennikov, S. I., Greten, F. R., & Karin, M. (2010). Immunity, inflammation, and cancer. *Cell*, *140*(6), 883-899.

Guo, Y., Hou, J., Luo, Y., & Wang, D. (2013). Functional disruption of macrophage migration inhibitory factor (MIF) suppresses proliferation of human H460 lung cancer cells by caspase-dependent apoptosis. *Cancer cell international*, *13*(1), 28-37.

Hakim, F. T., Flomerfelt, F. A., Boyiadzis, M., & Gress, R. E. (2004). Aging, immunity and cancer. *Current opinion in immunology*, *16*(2), 151-156.

Hanahan, D., & Weinberg, R. A. (2000). The hallmarks of cancer. *Cell, 100*(1), 57-70.

Hanahan, D., & Weinberg, R. A. (2011). Hallmarks of cancer: the next generation. *Cell*, *144*(5), 646-674.

Hardaway, R. M. (2000). A review of septic shock. *The american surgeon*, *66*(1), 22-29.

Harton, J. A., & Ting, J. P. Y. (2000). Class II transactivator: mastering the art of major histocompatibility complex expression. *Molecular and cellular biology*, *20*(17), 6185-6194.

Hashimoto, M. (Oct12, 2015). LPS and toll-like receptor. *Glycoforum*: *http://www.glycoforum.gr.jp.18/10/2015*

Hassiotou, F., & Geddes, D. (2013). Anatomy of the human mammary gland: Current status of knowledge. *Clinical anatomy*, *26*(1), 29-48.

Helzlsouer, K. J., Harris, E. L., Parshad, R., Perry, H. R., Price, F. M., & Sanford, K. K. (1996). DNA repair proficiency: potential susceptibility factor for breast cancer. *Journal of the national cancer institute*, *88*(11), 754-755.

Henne, C., Schwenk, F., Koch, N., & Möller, P. (1995). Surface expression of the invariant chain (CD74) is independent of concomitant expression of major histocompatibility complex class II antigens. *Immunology*, *84*(2), 177-188.

Hennighausen, L., & Robinson, G. W. (2005). Information networks in the mammary gland. *Nature reviews molecular cell biology*, *6*(9), 715-725.

Hens, J. R., & Wysolmerski, J. J. (2005). Key stages of mammary gland development: molecular mechanisms involved in the formation of the embryonic mammary gland. *Breast cancer research*, *7*(5), 220-224.

Hens, J. R., Dann, P., Zhang, J. P., Harris, S., Robinson, G. W., & Wysolmerski, J. (2007). BMP4 and PTHrP interact to stimulate ductal outgrowth during embryonic mammary development and to inhibit hair follicle induction. *Development*, *134*(6), 1221-1230.

Hinck, L., & Silberstein, G. B. (2005). The mammary end bud as a motile organ. *Breast cancer research*, *7*(6), 245-251.

Holliday, D. L., & Speirs, V. (2011). Choosing the right cell line for breast cancer research. *Breast cancer research*, *13*(4), 215-222.

Holtz, R., Choi, J. C., Petroff, M. G., Piskurich, J. F., & Murphy, S. P. (2003). Class II transactivator (CIITA) promoter methylation does not correlate with silencing of CIITA transcription in trophoblasts. *Biology of reproduction*, *69*(3), 915-924.

Houghton, A. N. (1994). Cancer antigens: immune recognition of self and altered self. *The Journal of experimental medicine*, *180*(1), 1-4.

Hsu, R. Y., Chan, C. H., Spicer, J. D., Rousseau, M. C., Giannias, B., Rousseau, S., & Ferri, L. E. (2011). LPS-induced TLR4 signaling in human colorectal cancer cells increases β1 integrin-mediated cell adhesion and liver metastasis. *Cancer research*, *71*(5), 1989-1998.

Huang, C. S., Shen, C. Y., Wang, H. W., Wu, P. E., & Cheng, C. W. (2007). Increased expression of SRp40 affecting CD44 splicing is associated with the clinical outcome of lymph node metastasis in human breast cancer. *Clinica chimica acta*, *384*(1), 69-74.

Huang, X., van den Berg, A., Gao, Z., Visser, L., Nolte, I., Vos, H., & Diepstra, A. (2010). Expression of HLA class I and HLA class II by tumour cells in Chinese classical Hodgkin lymphoma patients. *PloS one*, *5*(5), e10865-e10871.

Humphreys, R. E., Hillman, G. G., von Hofe, E., & Xu, M. (2004). Forcing tumour cells to present their own tumour antigens to the immune system: a necessary design for an efficient tumour immunotherapy. *Cellular & molecular immunology*, *1*(3), 180-185.

Humphreys, Robin C., Maryla Krajewska, Susanne Krnacik, Richard Jæger, Hans Weiher, Stanislaw Krajewski, John C. Reed, and Jeffrey M. Rosen. (1996). Apoptosis in the terminal endbud of the murine mammary gland: a mechanism of ductal morphogenesis. *Development 122*, (12), 4013-4022.

Hutchinson, L. (2010). Breast cancer: challenges, controversies, breakthroughs. *Nature reviews clinical oncology*, *7*(12), 669-670.

Hynes, N. E., & Watson, C. J. (2010). Mammary gland growth factors: roles in normal development and in cancer. *Cold spring harbor perspectives in biology*, *2*(8), a003186-a003206.

Iczkowski, K. A. (2011). Cell adhesion molecule CD44: its functional roles in prostate cancer. *American journal of translational research*, *3*(1), 1-7.

Igney, F. H., & Krammer, P. H. (2002). Immune escape of tumour s: apoptosis resistance and tumour counterattack. *Journal of leukocyte biology*, *71*(6), 907-920.

Ikeda, H., Old, L. J., & Schreiber, R. D. (2002). The roles of IFNγ in protection against tumor development and cancer immunoediting. *Cytokine & growth factor reviews*, *13*(2), 95-109.

Ishigami, S., Natsugoe, S., Tokuda, K., Nakajo, A., Iwashige, H., Aridome, K., Hokita, S., & Aikou, T. (2001). Invariant chain expression in gastric cancer. *Cancer letters, 168*(1), 87-91.

Issaq, H. J., & Veenstra, T. D. (2008). Two-dimensional polyacrylamide gel electrophoresis (2D-PAGE): advances and perspectives. *Biotechniques*, *44*(5), 697-700.

Jabrane-Ferrat, N., Calvo, F., Faille, A., Lagabrielle, J. F., Boisson, N., Quillet, A., & Fradelizi, D. (1990a). Recombinant gamma interferon provokes resistance of human breast cancer cells to spontaneous and IL-2 activated non-MHC restricted cytotoxicity. *British journal of cancer*, *61*(4), 558-562.

Jabrane-Ferrat, N., Faille, A., Loiseau, P., Poirier, O., Charron, D., & Calvo, F. (1990b). Effect of gamma interferon on HLA class-I and-II transcription and protein expression in

human breast adenocarcinoma cell lines. *International journal of cancer*, *45*(6), 1169-1176.

Jaggupilli, A., & Elkord, E. (2012). Significance of CD44 and CD24 as cancer stem cell markers: an enduring ambiguity. *Clinical and developmental immunology*, *2012*.

Jaiswal, S., Jamieson, C. H., Pang, W. W., Park, C. Y., Chao, M. P., Majeti, R., Traver, D., Rooijen, N & Weissman, I. L. (2009). CD47 is upregulated on circulating hematopoietic stem cells and leukemia cells to avoid phagocytosis. *Cell*, *138*(2), 271-285.

Ji, H., Stout, L. E., Zhang, Q., Zhang, R., Leung, H. T., & Leung, B. S. (1994). Absence of transforming growth factor-β responsiveness in the tamoxifen growth-inhibited human breast cancer cell line CAMA-1. *Journal of cellular biochemistry*, *54*(3), 332-342.

Jiang, W., Crossman, D. K., Mitchell, E. H., Sohn, P., Crowley, M. R., & Serra, R. (2013). WNT5A inhibits metastasis and alters splicing of CD44 in breast cancer cells. *PloS one*, *8*(3), e58329-e58341.

Jiang, Z., Xu, M., Savas, L., LeClair, P., & Banner, B. F. (1999). Invariant chain expression in colon neoplasms. *Virchows archive*, *435*(1), 32-36.

Jung, T., Castellana, D., Klingbeil, P., Hernández, I. C., Vitacolonna, M., Orlicky, D. J., Roffler, S.R., Brodt, P., & Zöller, M. (2009). CD44v6 dependence of premetastatic niche preparation by exosomes. *Neoplasia*, *11*(10), 1093-1105.

Kaboord, B., & Perr, M. (2008). Isolation of proteins and protein complexes by immunoprecipitation. In *2D PAGE: sample preparation and fractionation* (pp. 349-364). Humana Press.

Kaczmarek, M., Frydrychowicz, M., Rubis, B., Mizera-Nyczak, E., Nieruchalska, E., Sikora, J., & Kaczmarek, E. (2007). Analysis of expression of MHC class I molecules and TAP genes in malignant human cell lines. *Folia histochemica et cytobiologica*, *45*(3), 205-214.

Karakikes, I., Morrison, I. E., O'Toole, P., Metodieva, G., Navarrete, C. V., Gomez, J., Miranda-Sayago , J.M., Cherry, R.J., Metodiev, M., & Fernandez, N. (2012). Interaction of HLA-DR and CD74 at the cell surface of antigen-presenting cells by single particle image analysis. *The FASEB Journal*, *26*(12), 4886-4896.

Kenny, P. A., Lee, G. Y., Myers, C. A., Neve, R. M., Semeiks, J. R., Spellman, P. T., Lorenz, K., Lee, E. H., Helen Barcellos-Hoff, M., Petersen, O.W., Gray, W.O., & Bissell, M. J. (2007). The morphologies of breast cancer cell lines in three-dimensional assays correlate with their profiles of gene expression. *Molecular oncology*, *1*(1), 84-96.

Kikuchi, Y., Uno, S., Kinoshita, Y., Yoshimura, Y., Iida, S. I., Wakahara, Y., Tsuchiya, M., Yamada-Okabe, H., & Fukushima, N. (2005). Apoptosis inducing bivalent single-

chain antibody fragments against CD47 showed antitumour potency for multiple myeloma. *Leukemia research*, *29*(4), 445-450.

Kim, M. J., Lee, J. C., Lee, J. J., Kim, S., Lee, S. G., Park, S. W., Sung, M.W., & Heo, D. S. (2008). Association of CD47 with natural killer cell-mediated cytotoxicity of head-and-neck squamous cell carcinoma lines. *Tumour biology*, *29*(1), 28-34.

Kindt, T.J., Goldsby, R.A., & Osborne. (2007). *Immunology, 5th edition*, W.H.Freeman & company. USA.

Kleemann, R., Hausser, A., Geiger, G., Mischke, R., Burger-Kentischer, A., Flieger, O., Johannes, F. J., Roger, T., Calandra, T., Kapurniotu, A., Grell, M., Finkelmeier, D.,

Klein, G., & Klein, E. (2005). Surveillance against tumours—is it mainly immunological?. *Immunology letters*, *100*(1), 29-33.

Klingbeil, P., Natrajan, R., Everitt, G., Vatcheva, R., Marchio, C., Palacios, J., & Isacke, C. M. (2010). CD44 is overexpressed in basal-like breast cancers but is not a driver of 11p13 amplification. *Breast cancer research and treatment*, *120*(1), 95-109.

Klose, J. (1975). Protein mapping by combined isoelectric focusing and electrophoresis of mouse tissues. A novel approach to testing for induced point mutations in mammals. *Humangenetik 26*(3), 231-243

Kouros-Mehr, H., Slorach, E. M., Sternlicht, M. D., & Werb, Z. (2006). GATA-3 maintains the differentiation of the luminal cell fate in the mammary gland. *Cell*, *127*(5), 1041-1055.

Kowalczyk, Dariusz W. "Tumors and the danger model." *ACTA BIOCHIMICA POLONICA-ENGLISH EDITION*- 49, no. 2 (2002): 295-302.

Kumar, U., Grigorakis, S. I., Watt, H. L., Sasi, R., Snell, L., Watson, P., & Chaudhari, S. (2005). Somatostatin receptors in primary human breast cancer: quantitative analysis of mRNA for subtypes 1–5 and correlation with receptor protein expression and tumour pathology. *Breast cancer research and treatment*, *92*(2), 175-186.

Laakso, M., Loman, N., Borg, Å., & Isola, J. (2005). Cytokeratin 5/14-positive breast cancer: true basal phenotype confined to BRCA1 tumours. *Modern pathology*, *18*(10), 1321-1328.

Lachmanovich, E., Shvartsman, D. E., Malka, Y., Botvin, C., Henis, Y. I., & Weiss, A. M. (2003). Co-localization analysis of complex formation among membrane proteins by computerized fluorescence microscopy: application to immunofluorescence co-patching studies. *Journal of microscopy*, *212*(2), 122-131.

Lacroix, M., & Leclercq, G. (2004). Relevance of breast cancer cell lines as models for breast tumours: an update. *Breast cancer research and treatment*, *83*(3), 249-289.

Lai, Y. L., Mau, B. L., Cheng, W. H., Chen, H. M., Chiu, H. H., & Tzen, C. Y. (2008). PIK3CA exon 20 mutation is independently associated with a poor prognosis in breast cancer patients. *Annals of surgical oncology*, *15*(4), 1064-1069.

Landsverk, O. J. B., Bakke, O., & Gregers, T. F. (2009). MHC II and the endocytic pathway: regulation by invariant chain. *Scandinavian journal of immunology*, *70*(3), 184-193.

Lane, D. (2004). p53 from pathway to therapy. *Carcinogenesis*, *25*(7), 1077-1081.

Lanigan, F., O'Connor, D., Martin, F., & Gallagher, W. M. (2007). Molecular links between mammary gland development and breast cancer. *Cellular and molecular life sciences: CMLS*, *64*(24), 3159-3184.

Lantner, F., Starlets, D., Gore, Y., Flaishon, L., Yamit-Hezi, A., Dikstein, R., Leng, L., Bucala, R., Machluf, Y., Oren, M., & Shachar, I. (2007). CD74 induces TAp63 expression leading to B-cell survival. *Blood*, *110*(13), 4303-4311.

Le Hiress, M., Tu, L., Ricard, N., Phan, C., Thuillet, R., Fadel, E., Dorfmüller, P., Montani,D., de Man, F., Humbert, M., Huertas, A., & Guignabert, C. (2015). Pro-inflammatory Signature of the Dysfunctional Endothelium in Pulmonary Hypertension: Role of MIF/CD74 Complex. *American journal of respiratory and critical care medicine*, *192*(8), 913-915.

Lee, H., Rhee, H., Kang, H. J., Kim, H. S., Min, B. S., Kim, N. K., & Kim, H. (2008). Macrophage migration inhibitory factor may be used as an early diagnostic marker in colorectal carcinomas. *American journal of clinical pathology*, *129*(5), 772-779.

Lee, P. P., Yee, C., Savage, P. A., Fong, L., Brockstedt, D., Weber, J. S., Johnson, D., Swetter, S., Thompson, J., Greenberg, P. D., Roederer, M., Davis, M. M. (1999). Characterization of circulating T cells specific for tumour -associated antigens in melanoma patients. *Nature medicine*, *5*(6), 677-685.

Lee, S., & Margolin, K. (2012). Tumour -infiltrating lymphocytes in melanoma. *Current oncology reports*, *14*(5), 468-474.

Lemaine, V., & Simmons, P. S. (2013). The adolescent female: Breast and reproductive embryology and anatomy. *Clinical anatomy*, *26*(1), 22-28.

Leng, L., & Bucala, R. (2006). Insight into the biology of macrophage migration inhibitory factor (MIF) revealed by the cloning of its cell-surface receptor. *Cell research*, *16*(2), 162-168.

Leng, L., Metz, C. N., Fang, Y., Xu, J., Donnelly, S., Baugh, J., Delohery, C. Y., Mitchell, R.A., & Bucala, R. (2003). MIF signal transduction initiated by binding to CD74. *The Journal of experimental medicine*, *197*(11), 1467-1476.

Lesley, J., & Hyman, R. (1998). CD44 structure and function. *Front Biosci*, *3*, 616-630.

Leth-Larsen, R., Lund, R., Hansen, H. V., Laenkholm, A. V., Tarin, D., Jensen, O. N., & Ditzel, H. J. (2009). Metastasis-related plasma membrane proteins of human breast cancer cells identified by comparative quantitative mass spectrometry. *Molecular & cellular proteomics*, *8*(6), 1436-1449.

Li, X., Lin, G., Wu, B., Zhou, X., & Zhou, K. (2007). Overexpression of PTEN induces cell growth arrest and apoptosis in human breast cancer ZR-75-1 cells. *Acta biochimica et biophysica Sinica*, *39*(10), 745-750.

Ligresti, G., Libra, M., Militello, L., Clementi, S., Donia, M., Imbesi, R., Malaponte, A., Cappellani, A., Mccubrey, J., & Stivala, F. (2008). Breast cancer: Molecular basis and therapeutic strategies (Review). *Molecular medicine reports*, *1*(4), 451-458.

Liu, H., Zang, C., Fenner, M. H., Possinger, K., & Elstner, E. (2003). PPARγ ligands and ATRA inhibit the invasion of human breast cancer cells in vitro. *Breast cancer research and treatment*, *79*(1), 63-74.

Liu, S., Clouthier, S. G., & Wicha, M. S. (2012). Role of microRNAs in the regulation of breast cancer stem cells. *Journal of mammary gland biology and neoplasia*, *17*(1), 15-21.

Liu, Y. H., & Lin, J. Y. (2014). Recent advances of cluster of differentiation 74 in cancer. *The world journal of immunology*, *4*(3), 174-184.

Liu, Y. H., Lin, C. Y., Lin, W. C., Tang, S. W., Lai, M. K., & Lin, J. Y. (2008). Up-regulation of vascular endothelial growth factor-D expression in clear cell renal cell carcinoma by CD74: a critical role in cancer cell tumourigenesis. *The journal of immunology*, *181*(9), 6584-6594.

Louderbough, J. M., & Schroeder, J. A. (2011a). Understanding the dual nature of CD44 in breast cancer progression. *Molecular cancer research*, *9*(12), 1573-1586.

Louderbough, J. M., Brown, J. A., Nagle, R. B., & Schroeder, J. A. (2011b). CD44 promotes epithelial mammary gland development and exhibits altered localization during cancer progression. *Genes & cancer*, *2*(8), 771-781.

Lue, H., Kapurniotu, A., Fingerle-Rowson, G., Roger, T., Leng, L., Thiele, M., Calandrad, T., Bucalae, R., & Bernhagen, J. (2006). Rapid and transient activation of the ERK MAPK signalling pathway by macrophage migration inhibitory factor (MIF) and dependence on JAB1/CSN5 and Src kinase activity. *Cellular signalling*, *18*(5), 688-703.

Lue, H., Thiele, M., Franz, J., Dahl, E., Speckgens, S., Leng, L., Fingerle-Rowson, G., Bucala, R., Lüscher, B., & Bernhagen, J. (2007). Macrophage migration inhibitory factor (MIF) promotes cell survival by activation of the Akt pathway and role for CSN5/JAB1 in the control of autocrine MIF activity. *Oncogene*, *26*(35), 5046-5059.

Luo, J. L., Maeda, S., Hsu, L. C., Yagita, H., & Karin, M. (2004). Inhibition of NF-κB in cancer cells converts inflammation-induced tumour growth mediated by TNFα to TRAIL-mediated tumour regression. *Cancer cell*, *6*(3), 297-305.

Ma, Z., Chang, M. J., Shah, R. C., & Benveniste, E. N. (2005). Interferon-γ-activated STAT-1α suppresses MMP-9 gene transcription by sequestration of the coactivators CBP/p300. *Journal of leukocyte biology*, *78*(2), 515-523.

Macéa, J. R. & Fregnani, J. H. T. G. (2006). Anatomy of the thoracic wall, axilla and breast. *International journal of morphology*, *24*(4), 691-704.

Maddams, J., Brewster, D., Gavin, A., Steward, J., Elliott, J., Utley, M., & Møller, H. (2009). Cancer prevalence in the United Kingdom: estimates for 2008. *British journal of cancer*, *101*(3), 541-547.

Maddams, J., Utley, M., & Møller, H. (2012). Projections of cancer prevalence in the United Kingdom, 2010–2040. *British journal of cancer*, *107*(7), 1195-1202.

Magdeldin, S., Zhang, Y., Xu, B., Yoshida, Y., and Yamamoto, T. (2012). "Two-Dimensional Polyacrylamide Gel Electrophoresis - A Practical Perspective," InTech, http://www.intechopen.com/books/gel-electrophoresis-principles-and-basics/two-dimensional-polyacrylamide-gel-electrophoresis-a-practical-perspective.

Maharshak, N., Cohen, S., Lantner, F., Hart, G., Leng, L., Bucala, R., & Shachar, I. (2010). CD74 is a survival receptor on colon epithelial cells. *World journal of gastroenterology*, *16*(26), 3258.

Malhotra, G. K., Zhao, X., Band, H., & Band, V. (2010). Histological, molecular and functional subtypes of breast cancers. *Cancer biology & therapy*, *10*(10), 955-960.

Malmberg, K. J., Levitsky, V., Norell, H., de Matos, C. T., Carlsten, M., Schedvins, K., Rabbani, H., Moretta, A., Söderström, K., Levitskaya, J., & Kiessling, R. (2002). IFN-γ protects short-term ovarian carcinoma cell lines from CTL lysis via a CD94/NKG2A-dependent mechanism. *The journal of clinical investigation*, *110* (10), 1515-1523.

Manders, E. M. M. (1997). Chromatic shift in multicolour confocal microscopy. *Journal of microscopy*, *185*(3), 321-328.

Manders, E. M. M., Verbeek, F. J., & Aten, J. A. (1993). Measurement of co-localization of objects in dual-colour confocal images. *Journal of microscopy*, *169*(3), 375-382.

Mani, S. A., Guo, W., Liao, M. J., Eaton, E. N., Ayyanan, A., Zhou, A. Y., Brooks, M., Reinhard, F., Zhang, C.C., Shipitsin, M., Campbell, L.L., Polyak, K., Brisken, C., Yang, J., & Weinberg, R. A. (2008). The epithelial-mesenchymal transition generates cells with properties of stem cells. *Cell*, *133*(4), 704-715.

Manna, P. P., & Frazier, W. A. (2004). CD47 mediates killing of breast tumour cells via Gi-dependent inhibition of protein kinase A. *Cancer research*, *64*(3), 1026-1036.

Mantovani, A., Allavena, P., Sica, A., & Balkwill, F. (2008). Cancer-related inflammation. *Nature*, *454*(7203), 436-444.

Marhaba, R., & Zöller, M. (2004). CD44 in cancer progression: adhesion, migration and growth regulation. *Journal of molecular histology*, *35*(3), 211-231.

Martín-Ventura, J. L., Madrigal-Matute, J., Muñoz-Garcia, B., Blanco-Colio, L. M., Van Oostrom, M., Zalba, G., Fortuño, A., Gomez-Guerrero, C., Ortega, L., Ortiz, A., Diez, J & Egido, J. (2009). Increased CD74 expression in human atherosclerotic plaques: contribution to inflammatory responses in vascular cells. *Cardiovascular research*, *83*(3), 586-594.

Maruyama, K., Selmani, Z., Ishii, H., & Yamaguchi, K. (2011). Innate immunity and cancer therapy. *International immunopharmacology*, *11*(3), 350-357.

Mateo, V., Brown, E. J., Biron, G., Rubio, M., Fischer, A., Le Deist, F., & Sarfati, M. (2002). Mechanisms of CD47-induced caspase-independent cell death in normal and leukemic cells: link between phosphatidylserine exposure and cytoskeleton organization. *Blood*, *100*(8), 2882-2890.

Matsushita, H., Vesely, M. D., Koboldt, D. C., Rickert, C. G., Uppaluri, R., Magrini, V. J., & Schreiber, R. D. (2012). Cancer exome analysis reveals a T-cell-dependent mechanism of cancer immunoediting. *Nature*, *482*(7385), 400-404.

Matsushita, K., Takenouchi, T., Shimada, H., Tomonaga, T., Hayashi, H., Shioya, A., Komatsu, A., Matsubara, H., & Ochiai, T. (2006). Strong HLA-DR antigen expression on cancer cells relates to better prognosis of colorectal cancer patients: Possible involvement of c-myc suppression by interferon-γ in situ. *Cancer science*, *97*(1), 57-63.

Matza, D., Kerem, A., & Shachar, I. (2003). Invariant chain, a chain of command. *Trends in immunology*, *24*(5), 264-268.

Matza, D., Lantner, F., Bogoch, Y., Flaishon, L., Hershkoviz, R., & Shachar, I. (2002). Invariant chain induces B cell maturation in a process that is independent of its chaperonic activity. *Proceedings of the national academy of sciences*, *99*(5), 3018-3023.

Matza, D., Wolstein, O., Dikstein, R., & Shachar, I. (2001). Invariant chain induces B cell maturation by activating a TAFII105-NF-κB-dependent transcription program. *Journal of biological chemistry*, *276*(29), 27203-27206.

Matzinger, P. (1994). Tolerance, danger, and the extended family. *Annual review of immunology*, *12*(1), 991-1045.

Matzinger, P. (2001). The Danger model in its historical context. *Scandinavian journal of immunology*, *54*(1-2), 4-9.

Matzinger, P. (2002). The danger model: a renewed sense of self. *Science*, *296*(5566), 301-305.

Maubach, G., Lim, M. C. C., Kumar, S., & Zhuo, L. (2007). Expression and upregulation of cathepsin S and other early molecules required for antigen presentation in activated hepatic stellate cells upon IFN-γ treatment. *Biochimica et biophysica acta (BBA)-molecular cell research*, *1773*(2), 219-231.

McClelland, M., Zhao, L., Carskadon, S., & Arenberg, D. (2009). Expression of CD74, the receptor for macrophage migration inhibitory factor, in non-small cell lung cancer. *The american journal of pathology*, *174*(2), 638-646.

Meazza, R., Comes, A., Orengo, A. M., Ferrini, S., & Accolla, R. S. (2003). Tumour rejection by gene transfer of the MHC class II transactivator in murine mammary adenocarcinoma cells. *European journal of immunology*, *33*(5), 1183-1192.

Melvold, R. W., & Sticca, R. P. (2007). Basic and tumour immunology: a review. *Surgical oncology clinics of north america*, *16*(4), 711-735.

Metodieva, G., Nogueira-de-Souza, N. C., Greenwood, C., Al-Janabi, K., Leng, L., Bucala, R., & Metodiev, M. V. (2013). CD74-dependent deregulation of the tumour suppressor scribble in human epithelial and breast cancer cells. *Neoplasia*, *15*(6), 660-IN21.

Meyer-Siegler, K. L., Iczkowski, K. A., Leng, L., Bucala, R., & Vera, P. L. (2006). Inhibition of macrophage migration inhibitory factor or its receptor (CD74) attenuates growth and invasion of DU-145 prostate cancer cells. *The journal of immunology*, *177*(12), 8730-8739.

Meyer-Siegler, K. L., Leifheit, E. C., & Vera, P. L. (2004). Inhibition of macrophage migration inhibitory factor decreases proliferation and cytokine expression in bladder cancer cells. *BMC cancer*, *4*(1), 34-46.

Miller, D. M., Thomas, S. D., Islam, A., Muench, D., & Sedoris, K. (2012). c-Myc and cancer metabolism. *Clinical cancer research*, *18*(20), 5546-5553.

Mitchell, R. A., Metz, C. N., Peng, T., & Bucala, R. (1999). Sustained mitogen-activated protein kinase (MAPK) and cytoplasmic phospholipase A2 activation by macrophage migration inhibitory factor (MIF) Regulatory role in cell proliferation and glucocorticoid action. *Journal of biological chemistry*, *274*(25), 18100-18106.

Moldenhauer, G., Henne, C., Karhausen, J., & Möller, P. (1999). Surface-expressed invariant chain (CD74) is required for internalization of human leucocyte antigen-DR molecules to early endosomal compartments. *Immunology-Oxford-*, *96*, 473-484.

Möller, G., & Möller, E. (1976). The concept of immunological surveillance against neoplasia. *Immunological reviews*, *28*(1), 3-17.

Möller, P., & Moldenhauer, G. (1999). CD74. *Journal of biological regulators and homeostatic agents*, *14*(4), 299-301.

Molyneux, G., Regan, J., & Smalley, M. J. (2007). Common Molecular Mechanisms of Mammary Gland Development and Breast Cancer (Mammary stem cells and breast cancer). *Cellular and molecular life sciences*, *64*(24), 3248-3260.

Montgomery, N., Hill, A., McFarlane, S., Neisen, J., O'Grady, A., Conlon, S., Conlon, S., Jirstrom, K., Kay, E. W., & Waugh, D. J. (2012). CD44 enhances invasion of basal-like breast cancer cells by upregulating serine protease and collagen-degrading enzymatic expression and activity. *Breast cancer research*, *14*(3), R84.

Monti, P., Ciribilli, Y., Jordan, J., Menichini, P., Umbach, D. M., Resnick, M. A., Luzzatto, L., Inga, A., & Fronza, G. (2007). Transcriptional functionality of germ line p53 mutants influences cancer phenotype. *Clinical cancer research*, *13*(13), 3789-3795.

Morel, A. P., Lièvre, M., Thomas, C., Hinkal, G., Ansieau, S., & Puisieux, A. (2008). Generation of breast cancer stem cells through epithelial-mesenchymal transition. *PloS one*, *3*(8), e2888-e2895.

Moretta, A., Pende, D., Locatelli, F., & Moretta, L. (2009). Activating and inhibitory killer immunoglobulin-like receptors (KIR) in haploidentical haemopoietic stem cell transplantation to cure high-risk leukaemias. *Clinical & experimental immunology*, *157*(3), 325-331.

Muhlethaler-Mottet, A., Di Berardino, W., Otten, L. A., & Mach, B. (1998). Activation of the MHC class II transactivator CIITA by interferon-γ requires cooperative interaction between Stat1 and USF-1. *Immunity, 8*(2), 157-166.

Mun, S. H., Won, H. Y., Hernandez, P., Aguila, H. L., & Lee, S. K. (2013). Deletion of CD74, a putative MIF receptor, in mice enhances osteoclastogenesis and decreases bone mass. *Journal of bone and mineral research*, *28*(4), 948-959.

Murphy, S. P., & Tomasi, T. B. (1998). Absence of MHC class II antigen expression in trophoblast cells results from a lack of class II transactivator (CIITA) gene expression. *Molecular reproduction and development*, *51*(1), 1-12.

Naor, D., Sionov, R. V., & Ish-Shalom, D. (1997). CD44: structure, function and association with the malignant process. *Advances in cancer research*, *71*, 241-319

Naujokas, M. F., Morin, M., Anderson, M. S., Peterson, M., & Miller, J. (1993). The chondroitin sulfate form of invariant chain can enhance stimulation of T cell responses through interaction with CD44. *Cell*, *74*(2), 257-268.

Neefjes, J., Jongsma, M. L., Paul, P., & Bakke, O. (2011). Towards a systems understanding of MHC class I and MHC class II antigen presentation. *Nature reviews immunology*, *11*(12), 823-836.

Nowarski, R., Gagliani, N., Huber, S., & Flavell, R. A. (2013). Innate immune cells in inflammation and cancer. *Cancer immunology research*, *1*(2), 77-84.

O'Farrell, P. H. (1975). High resolution two-dimensional electrophoresis of proteins. *Journal of biological chemistry*, *250*(10), 4007-4021.

Old, W. M., Meyer-Arendt, K., Aveline-Wolf, L., Pierce, K. G., Mendoza, A., Sevinsky, J. R., Resing, K. A., and Ahn, N. G. (2005). Comparison of label-free methods for quantifying human proteins by shotgun proteomics. *Molecular & cellular proteomics*, *4*(10), 1487-1502.

Oldenborg, P. A., Zheleznyak, A., Fang, Y. F., Lagenaur, C. F., Gresham, H. D., & Lindberg, F. P. (2000). Role of CD47 as a marker of self on red blood cells. *Science*, *288*(5473), 2051-2054.

Oldford, S. A., Robb, J. D., Codner, D., Gadag, V., Watson, P. H., & Drover, S. (2006). Tumour cell expression of HLA-DM associates with a Th1 profile and predicts improved survival in breast carcinoma patients. *International immunology*, *18*(11), 1591-1602.

Olsson, E., Honeth, G., Bendahl, P. O., Saal, L., Gruvberger-Saal, S., Ringnér, M., & Hegardt, C. (2011). CD44 isoforms are heterogeneously expressed in breast cancer and correlate with tumour subtypes and cancer stem cell markers .*BMC cancer*, *11*(1), 418-431.

Orian-Rousseau, V. (2015). CD44 acts as a signalling platform controlling tumour progression and metastasis. *Frontiers in immunology*, *6*, 154-158.

Otterstrom, C., Soltermann, A., Opitz, I., Felley-Bosco, E., Weder, W., Stahel, R. A., Triponez, F., Robert, J.H., & Serre-Beinier, V. (2014). CD74: a new prognostic factor for patients with malignant pleural mesothelioma. *British journal of cancer*, *110*(8), 2040-2046.

Pandha, H., Rigg, A., John, J., & Lemoine, N. (2007). Loss of expression of antigen-presenting molecules in human pancreatic cancer and pancreatic cancer cell lines. *Clinical & experimental immunology*, *148*(1), 127-135.

Paralkar, V., & Wistow, G. (1994). Cloning the human gene for macrophage migration inhibitory factor (MIF). *Genomics*, *19*(1), 48-51.

Parkin, J., & Cohen, B. (2001). An overview of the immune system. *The lancet*, *357*(9270), 1777-1789.

Parmiani, G., De Filippo, A., Novellino, L., & Castelli, C. (2007). Unique human tumour antigens: immunobiology and use in clinical trials. *The journal of immunology*, *178*(4), 1975-1979.

Patel, V. J., Thalassinos, K., Slade, S. E., Connolly, J. B., Crombie, A., Murrell, J. C., & Scrivens, J. H. (2009). A comparison of labeling and label-free mass spectrometry-based proteomics approaches. *Journal of proteome research*,*8*(7), 3752-3759.

Pestalozzi, B. C., Zahrieh, D., Mallon, E., Gusterson, B. A., Price, K. N., Gelber, R. D., Holmberg, S.B., Lindtner, J., Snyder, R., Thu¨rlimann, B., Murray, E., Viale, G., Castiglione-Gertsch, M., Coates, A.S., & Goldhirsch, A. (2008). Distinct clinical and prognostic features of infiltrating lobular carcinoma of the breast: combined results of 15 International Breast Cancer Study Group clinical trials. *Journal of clinical oncology*, *26*(18), 3006-3014.

Pestka, S., Langer, J. A., Zoon, K. C., & Samuel, C. E. (1987). Interferons and their actions. *Annual review of biochemistry*, *56*(1), 727-777.

Pistillo, M. P., Nicolò, G., Salvi, S., Capanni, P., Perdelli, L., Pasciucco, G., & Ferrara, G. B. (2000). Biochemical analysis of HLA class I subunits expression in breast cancer tissues. *Human immunology*, *61*(4), 397-407.

Platt, J. S., & Hunt, J. S. (1998). Interferon-gamma gene expression in cycling and pregnant mouse uterus: temporal aspects and cellular localization. *Journal of leukocyte biology*, *64*(3), 393-400.

Polyak, K. (2011). Heterogeneity in breast cancer. *The Journal of clinical investigation*, *121*(10), 3786.

Ponti, D., Costa, A., Zaffaroni, N., Pratesi, G., Petrangolini, G., Coradini, D., Pilotti, S., Pierotti, M.A., & Daidone, M. G. (2005). Isolation and in vitro propagation of tumour igenic breast cancer cells with stem/progenitor cell properties. *Cancer research*, *65*(13), 5506-5511.

Poschke, I., Mougiakakos, D., & Kiessling, R. (2011). Camouflage and sabotage: tumour escape from the immune system. *Cancer Immunology, Immunotherapy*, *60*(8), 1161-1171.

Prasad, V. V., & Gopalan, R. O. (2015). Continued use of MDA-MB-435, a melanoma cell line, as a model for human breast cancer, even in year, 2014.*npj Breast Cancer*, *1*, 15002.

Press, W. H., Teukolsky, S. A., Vetterling, W. T., and Flannery, B. P. (1992). "Numerical recipes in C (2nd ed.): the art of scientific computing," Cambridge University Press.

Propper, D. J., Chao, D., Braybrooke, J. P., Bahl, P., Thavasu, P., Balkwill, F., Turley, T., Dobbs, N., Gatter, K., Talbot, D.C., Harris, A. H., & Ganesan, T. S. (2003). Low-dose IFN-γ induces tumour MHC expression in metastatic malignant melanoma. *Clinical cancer research*, *9*(1), 84-92.

Pyrz, M., Wang, B., Wabl, M., & Pedersen, F. S. (2010). Research A retroviral mutagenesis screen identifies Cd74 as a common insertion site in murine B-lymphomas and reveals the existence of a novel IFNγ-inducible CD74 isoform. *Molecular cancer, 86*(9), 2-17.

Qiao, S., Luo, Q., Zhao, Y., Zhang, X. C., & Huang, Y. (2014). Structural basis for lipopolysaccharide insertion in the bacterial outer membrane. *Nature*, 511, 108–111.

Rajnavölgyi, É., & Lanyi, A. (2003). Role of CD4+ T lymphocytes in antitumour immunity. *Advances in cancer research*, *87*, 195-249.

Rakha, E. A., & Ellis, I. O. (2009). Triple-negative/basal-like breast cancer: review. *Pathology*, *41*(1), 40-47.

Rangel, L. B., Agarwal, R., Sherman-Baust, C. A., de Mello-Coelho, V., Pizer, E. S., Ji, H., Taub, D.D., & Morin, P. J. (2004). Anomalous expression of the HLA-DR alpha and beta chains in ovarian and other cancers. *Cancer biology & therapy*, *3*(10), 1021-1027.

Reddy, K. B. (2011). Triple-negative breast cancers: an updated review on treatment options. *Current Oncology*, 18(4), e173.

Ren, Y., Chan, H. M., Fan, J., Xie, Y., Chen, Y. X., Li, W., & Tam, P. K. H. (2006). Inhibition of tumour growth and metastasis in vitro and in vivo by targeting macrophage migration inhibitory factor in human neuroblastoma. *Oncogene*, *25*(25), 3501-3508.

Revillion, F., Lhotellier, V., Hornez, L., Bonneterre, J., & Peyrat, J. P. (2008). ErbB/HER ligands in human breast cancer, and relationships with their receptors, the bio-pathological features and prognosis. *Annals of oncology*, *19*(1), 73-80.

Reya, T., Morrison, S. J., Clarke, M. F., & Weissman, I. L. (2001). Stem cells, cancer, and cancer stem cells. *Nature*, *414*(6859), 105-111.

Rice, E. K., Tesch, G. H., Cao, Z., Cooper, M. E., Metz, C. N., Bucala, R., ... & Nikolic-Paterson, D. J. (2003). Induction of MIF synthesis and secretion by tubular epithelial cells: a novel action of angiotensin II. *Kidney international*, *63*(4), 1265-1275.

Rich, A.R., & Lewis M.R. (1932). Migration of neutrophils and macrophages. *Bulletin of the johns hopkins hospital* (50), 115–31.

Richard, V., Kindt, N., Decaestecker, C., Gabius, H. J., Laurent, G., Noël, J. C., & Saussez, S. (2014). Involvement of macrophage migration inhibitory factor and its receptor (CD74) in human breast cancer. *Oncology reports*, *32*(2), 523-529.

Rizk, A., Paul, G., Incardona, P., Bugarski, M., Mansouri, M., Niemann, A., Ziegler, U., Berger, P., & Sbalzarini, I. F. (2014). Segmentation and quantification of subcellular structures in fluorescence microscopy images using Squassh. *Nature protocols*, *9*(3), 586-596.

Roberts, P. J., Bisi, J. E., Strum, J. C., Combest, A. J., Darr, D. B., Usary, J. E., Zamboni, W.C., Wong, K.K., Perou, C.M., & Sharpless, N. E. (2012). Multiple roles of cyclin-dependent kinase 4/6 inhibitors in cancer therapy. *Journal of the national cancer institute*, *104*(6), 476-487.

Rosengren, E., Bucala, R., Aman, P., Jacobsson, L., Odh, G., Metz, C. N., & Rorsman, H. (1996). The immunoregulatory mediator macrophage migration inhibitory factor (MIF) catalyzes a tautomerization reaction. *Molecular medicine*, *2*(1), 143-149.

Roskoski, R. (2012). ERK1/2 MAP kinases: structure, function, and regulation. *Pharmacological research*, *66*(2), 105-143.

Russo, J., and Russo, I. H. (2004). Development of Human Breast. *Mururitas, 49*(1), 2-15.

Sanchez-Niño, M. D., Sanz, A. B., Ihalmo, P., Lassila, M., Holthofer, H., Mezzano, S., Aros, C., Groop, P., Saleem, M.A., Mathieson, P.W., Langham, R., Kretzler, M., Nair, V., Lemley, K.V., Nelson, R.G., Mervaala, E., Mattinzoli, D., Pia Rastaldi, M., Ruiz-Ortega, M., Martin-Ventura, J.L., Egido, J., & Ortiz, A. (2009). The MIF receptor CD74 in diabetic podocyte injury. *Journal of the american society of nephrology*, *20*(2), 353-362.

Santoni, V., Rabilloud, T., Doumas, P., Rouquié, D., Mansion, M., Kieffer, S., Garin, J., & Rossignol, M. (1999). Towards the recovery of hydrophobic proteins on two-dimensional electrophoresis gels. *Electrophoresis*, *20*(4-5), 705-711.

Sapoznikov, A., Pewzner-Jung, Y., Kalchenko, V., Krauthgamer, R., Shachar, I., & Jung, S. (2008). Perivascular clusters of dendritic cells provide critical survival signals to B cells in bone marrow niches. *Nature immunology*, *9*(4), 388-395.

Schedin, P., & Keely, P. J. (2011). Mammary gland ECM remodeling, stiffness, and mechanosignaling in normal development and tumour progression. *Cold spring harbor perspectives in biology*, *3*(1), a003228.

Schneppenheim, J., Dressel, R., Hüttl, S., Lüllmann-Rauch, R., Engelke, M., Dittmann, K., Wienands, J., Eskelinen, E., Hermans-Borgmeyer, I., Fluhrer, R., Saftig, P., & Schröder, B. (2013). The intramembrane protease SPPL2a promotes B cell development and controls endosomal traffic by cleavage of the invariant chain. *The journal of experimental medicine*, *210*(1), 41-58.

Schönefuß, A., Wendt, W., Schattling, B., Schulten, R., Hoffmann, K., Stuecker, M., Tigges, C., Lu¨bbert, H., & Stichel, C. (2010). Upregulation of cathepsin S in psoriatic keratinocytes. *Experimental dermatology*, *19*(8), e80-e88.

Schreiber, R. D., Old, L. J., & Smyth, M. J. (2011). Cancer immunoediting: integrating immunity's roles in cancer suppression and promotion. *Science*, *331*(6024), 1565-1570.

Schroder, K., Hertzog, P. J., Ravasi, T., & Hume, D. A. (2004). Interferon-γ: an overview of signals, mechanisms and functions. *Journal of leukocyte biology*, *75*(2), 163-189.

Shachar, I., & Haran, M. (2011). The secret second life of an innocent chaperone: the story of CD74 and B cell/chronic lymphocytic leukemia cell survival. *Leukemia & lymphoma*, *52*(8), 1446-1454.

Shastry, M., & Yardley, D. A. (2013). Updates in the treatment of basal/triple-negative breast cancer. *Current opinion in obstetrics and gynecology*, *25*(1), 40-48.

Shi, X., Leng, L., Wang, T., Wang, W., Du, X., Li, J., McDonald, C., Chen, Z., Murphy, J. M., Lolis, E., Noble, P., Knudson, W., & Bucala, R. (2006). CD44 is the signaling component of the macrophage migration inhibitory factor-CD74 receptor complex. *Immunity*, *25*(4), 595-606.

Sieuwerts, A. M., Kraan, J., Bolt, J., van der Spoel, P., Elstrodt, F., Schutte, M., Marens, M.W.J., Gratama, J., Sleijfer, S., & Foekens, J. A. (2009). Anti-epithelial cell adhesion molecule antibodies and the detection of circulating normal-like breast tumour cells. *Journal of the national cancer institute*, *101*(1), 61-66.

Sikora, K., & Smedley, H. (1983). Interferon and cancer. *British medical journal*, *286*(6367), 739-740.

Sloane, B. F. (2012). On How Mammary Gland Reprogramming Metalloproteinases Couple Form with Function. *Cold spring harbor perspectives in biology*, *4*(7), a013474.

Sneath, R. J., & Mangham, D. C. (1998). The normal structure and function of CD44 and its role in neoplasia. *Molecular pathology*, *51*(4), 191-200.

Standish, L. J., Sweet, E. S., Novack, J., Wenner, C. A., Bridge, C., Nelson, A., Martzen, M., & Torkelson, C. (2008). Breast cancer and the immune system. *Journal of the society for integrative oncology*, *6*(4), 158-168.

Starlets, D., Gore, Y., Binsky, I., Haran, M., Harpaz, N., Shvidel, L., Becker-Herman, S., Berrebi, A., & Shachar, I. (2006). Cell-surface CD74 initiates a signaling cascade leading to cell proliferation and survival. *Blood*, *107*(12), 4807-4816.

Stein, R., Mattes, M. J., Cardillo, T. M., Hansen, H. J., Chang, C. H., Burton, J., & Goldenberg, D. M. (2007). CD74: a new candidate target for the immunotherapy of B-cell neoplasms. *Clinical cancer research*, *13*(18), 5556s-5563s.

Sternlicht, M. D., Kouros-Mehr, H., Lu, P., & Werb, Z. (2006). Hormonal and local control of mammary branching morphogenesis. *Differentiation*, *74*(7), 365-381.

Stingl, J., & Caldas, C. (2007). Molecular heterogeneity of breast carcinomas and the cancer stem cell hypothesis. *Nature reviews cancer*, *7*(10), 791-799.

Strubin, M., Berte, C., & Mach, B. (1986). Alternative splicing and alternative initiation of translation explain the four forms of the Ia antigen-associated invariant chain. *The EMBO journal*, *5*(13), 3483-3488.

Stumptner-Cuvelette, P., & Benaroch, P. (2002). Multiple roles of the invariant chain in MHC class II function. *Biochimica et biophysica acta (BBA)-Molecular cell research*, *1542*(1), 1-13.

Swann, J. B., & Smyth, M. J. (2007). Immune surveillance of tumours. *Journal of clinical investigation*, *117*(5), 1137-1146.

Takahashi, N., Nishihira, J., Sato, Y., Kondo, M., Ogawa, H., Ohshima, T., Une, Y., & Todo, S. (1998). Involvement of macrophage migration inhibitory factor (MIF) in the mechanism of tumor cell growth. *Molecular medicine*, *4*(11), 707-714.

Tate Jr, D. J., Patterson, J. R., Velasco-Gonzalez, C., Carroll, E. N., Trinh, J., Edwards, D., Aiyar, A., Finkel-Jimenez, B., & Zea, A. H. (2012). Interferon-gamma-induced nitric oxide inhibits the proliferation of murine renal cell carcinoma cells. *International journal of biological sciences*, *8*(8), 1109-1120.

Thibodeau, J., Bourgeois-Daigneault, M. C., & Lapointe, R. (2012). Targeting the MHC Class II antigen presentation pathway in cancer immunotherapy. *Oncoimmunology*, *1*(6), 908-916.

Thiery, J. P., & Sleeman, J. P. (2006). Complex networks orchestrate epithelial–mesenchymal transitions. *Nature reviews molecular cell biology*, *7*(2), 131-142.

Tian, B., Zhang, Y., Li, N., Liu, X., & Dong, J. (2012). CD74: a potential novel target for triple-negative breast cancer. *Tumour Biology*, *33*(6), 2273-2277.

Tillmann, S., Bernhagen, J., & Noels, H. (2013). Arrest functions of the MIF ligand/receptor axes in atherogenesis. *Frontiers in immunology*, *4*(115), 1-20.

Toole, B. P., & Slomiany, M. G. (2008). Hyaluronan, CD44 and Emmprin: partners in cancer cell chemoresistance. *Drug resistance updates, 11*(3), 110-121.

Topper, Y. J. (2013). Multiple hormone interactions in the development of mammary gland in vitro. *Recent progress in hormone research*, *26*, 287-3.

Torre, C., Wang, S. J., Xia, W., & Bourguignon, L. Y. (2010). Reduction of Hyaluronan-CD44–Mediated Growth, Migration, and Cisplatin Resistance in Head and Neck Cancer Due to Inhibition of Rho Kinase and PI-3 Kinase Signaling. *Archives of otolaryngology–head & neck surgery*, *136*(5), 493-501.

Trapé, A. P., & Gonzalez-Angulo, A. M. (2012). Breast cancer and metastasis: on the way toward individualized therapy. *Cancer genomics-proteomics*, *9*(5), 297-310.

Tsai, R. K., & Discher, D. E. (2008). Inhibition of "self" engulfment through deactivation of myosin-II at the phagocytic synapse between human cells. *The journal of cell biology*, *180*(5), 989-1003.

Tsujimoto, H., Ueno, H., Hashiguchi, Y., Ono, S., Ichikura, T., & Hase, K. (2010). Postoperative infections are associated with adverse outcome after resection with curative intent for colorectal cancer. *Oncology letters*, *1*(1), 119-125.

Tsunawaki, S., Nakamura, S., Ohyama, Y., Sasaki, M., Ikebe-Hiroki, A., Hiraki, A., Kadena, T., Kawamura, E., Kumamaru, W., Shinohara, M. and Shirasuna, K. (2002). Possible function of salivary gland epithelial cells as nonprofessional antigen-presenting cells in the development of Sjögren's syndrome. *The Journal of rheumatology*, *29*(9), pp.1884-1896.

Turashvili, G., Bouchal, J., Burkadze, G., & Kolar, Z. (2005). Mammary gland development and cancer. *Czecho-Slovak pathology*, *41*(3), 94-101.

Ullah, Z., Lee, C. Y., & DePamphilis, M. L. (2009). Cip/Kip cyclin-dependent protein kinase inhibitors and the road to polyploidy. *Cell division*, *4*(10).

Uno, S., Kinoshita, Y., Azuma, Y., Tsunenari, T., Yoshimura, Y., Iida, S., Kikuchi, Y., Yamada-Okabe, H., & Fukushima, N. (2007). Antitumour activity of a monoclonal

antibody against CD47 in xenograft models of human leukemia. *Oncology reports*, *17*(5), 1189-1194.

Urosevic, M., & Dummer, R. (2008). Human Leukocyte Antigen–G and Cancer Immunoediting. *Cancer research*, *68*(3), 627-630.

Uyttenhove, C., Pilotte, L., Théate, I., Stroobant, V., Colau, D., Parmentier, N., Boon, T., & Van den Eynde, B. J. (2003). Evidence for a tumour al immune resistance mechanism based on tryptophan degradation by indoleamine 2, 3-dioxygenase. *Nature medicine*, *9*(10), 1269-1274.

van der Geer, P. (2013). Analysis of protein-protein interactions by coimmunoprecipitation. *Methods in enzymology*, *541*, 35-47.

Vargo-Gogola, T., & Rosen, J. M. (2007). Modelling breast cancer: one size does not fit all. *Nature reviews cancer*, *7*(9), 659-672.

Velasco-Velázquez, M. A., Homsi, N., De La Fuente, M., & Pestell, R. G. (2012). Breast cancer stem cells. *The international journal of biochemistry & cell biology*, *44*(4), 573-577.

Velders, M. P., Markiewicz, M. A., Eiben, G. L., & Martin Kast, W. (2003). CD4+ T cell matters in tumour immunity. *International reviews of immunology*, *22*(2), 113-140.

Verjans, E., Noetzel, E., Bektas, N., Schütz, A. K., Lue, H., Lennartz, B., Hartmann, A., Dahl, E., & Bernhagen, J. (2009). Dual role of macrophage migration inhibitory factor (MIF) in human breast cancer. *BMC cancer*, *9*(1), 230.

Vesely, M. D., Kershaw, M. H., Schreiber, R. D., & Smyth, M. J. (2011). Natural innate and adaptive immunity to cancer. *Annual review of immunology*, *29*, 235-271.

Viale, G. (2012). The current state of breast cancer classification. *Annals of oncology*, *23*(suppl 10), x207-x210.

Vollebergh, M. A., Jonkers, J., & Linn, S. C. (2012). Genomic instability in breast and ovarian cancers: translation into clinical predictive biomarkers. *Cellular and molecular life sciences*, *69*(2), 223-245.

Vyas, J. M., Van der Veen, A. G., & Ploegh, H. L. (2008). The known unknowns of antigen processing and presentation. *Nature reviews immunology*, *8*(8), 607-618.

Wall, L., Burke, F., Barton, C., Smyth, J., & Balkwill, F. (2003). IFN-γ induces apoptosis in ovarian cancer cells in vivo and in vitro. *Clinical cancer research*, *9*(7), 2487-2496.

Wang, C., Navab, R., Iakovlev, V., Leng, Y., Zhang, J., Tsao, M. S., Siminovitch, K., McCready, D.R., & Done, S. J. (2007). Abelson interactor protein-1 positively regulates

breast cancer cell proliferation, migration, and invasion. *Molecular cancer research*, *5*(10), 1031-1039.

Wang, L., Zhu, R., Huang, Z., Li, H., & Zhu, H. (2013a). Lipopolysaccharide-induced toll-like receptor 4 signaling in cancer cells promotes cell survival and proliferation in hepatocellular carcinoma. *Digestive diseases and sciences*, *58*(8), 2223-2236.

Wang, X., Chen, Y. H., & Zhang, L. (2013b). Human tumour necrosis factor (TNF)-alpha-induced protein 8-like 2 suppresses hepatocellular carcinoma metastasis through inhibiting Rac1. *Molecular cancer, 12*(149), 1-10.

Watson, C. J. (2006). Involution: apoptosis and tissue remodelling that convert the mammary gland from milk factory to a quiescent organ. *Breast cancer research*,*8*(2), 203.

Watson, C. J., & Khaled, W. T. (2008). Mammary development in the embryo and adult: a journey of morphogenesis and commitment. *Development*, *135*(6), 995-1003.

Weenink, S. M., & Gautam, A. M. (1997). Antigen presentation by MHC class II molecules. *Immunology and cell biology*, *75*(1), 69-81.

Weigelt, B., Geyer, F. C., & Reis-Filho, J. S. (2010). Histological types of breast cancer: how special are they?. *Molecular oncology*, *4*(3), 192-208.

Weiser, W. Y., Temple, P. A., Witek-Giannotti, J. S., Remold, H. G., Clark, S. C., & David, J. R. (1989). Molecular cloning of a cDNA encoding a human macrophage migration inhibitory factor. *Proceedings of the national academy of sciences*, *86*(19), 7522-7526.

Welcsh, P. L., & King, M. C. (2001). BRCA1 and BRCA2 and the genetics of breast and ovarian cancer. *Human molecular genetics*, *10*(7), 705-713.

Wen, Y., Zhang, D., Liu, H., Wang, F., & Zhang, Y. (2015). Heterogeneity in Breast cancer. Cancer Genetics and Epigenetics, 3.

Whiteside, T. L. (2006). Immune suppression in cancer: effects on immune cells, mechanisms and future therapeutic intervention. In *Seminars in cancer biology*, 16 (1) 3-15.

Wilson, K. M., Labeta, M. O., Pawelec, G., & Fernandez, N. (1993). Cell-surface expression of human histocompatibility leucocyte antigen (HLA) class II-associated invariant chain (CD74) does not always correlate with cell-surface expression of HLA class II molecules. *Immunology*, *79*(2), 331-335.

Wiseman, B. S., & Werb, Z. (2002). Stromal effects on mammary gland development and breast cancer. *Science*, *296*(5570), 1046-1049.

Wolchok, J. D., & Chan, T. A. (2014). Cancer: Antitumour immunity gets a boost. *Nature, 515*(7528), 496-498.

Wortzel, I., & Seger, R. (2011). The ERK cascade distinct functions within various subcellular organelles. *Genes & cancer*, *2*(3), 195-209.

Wortzel, R. D., Philipps, C., & Schreiber, H. (1983) Multiple tumour specific antigens expressed on a single tumour cell. *Nature,* 304, 165– 167.

Wu, G., Sun, Y., Wang, X., Ma, B., & Xia, Z. (2014). The role of CD74 in experimental and clinical acute lung injury. *European respiratory journal*, *44*(Suppl 58), P3927.

Xiao, J., & Chen, H. S. (2004). Biological functions of melanoma-associated antigens. *World journal of gastroenterology*, *10*(13), 1849-1853.

Xu, L., Li, Y., Sun, H., Zhen, X., Qiao, C., Tian, S., & Hou, T. (2013). Current developments of macrophage migration inhibitory factor (MIF) inhibitors. *Drug discovery today*, *18*(11), 592-600.

Xu, M., Qiu, G., Jiang, Z., von Hofe, E., & Humphreys, R. E. (2000). Genetic modulation of tumour antigen presentation. *Trends in biotechnology*, *18*(4), 167-172.

Xu, X., Wang, B., Ye, C., Yao, C., Lin, Y., Huang, X., Zhang, Y., & Wang, S. (2008). Overexpression of macrophage migration inhibitory factor induces angiogenesis in human breast cancer. *Cancer letters*, *261*(2), 147-157.

Yaddanapudi, K., Putty, K., Rendon, B. E., Lamont, G. J., Faughn, J. D., Satoskar, A., Lasnik, A., Eaton, J.W., & Mitchell, R. A. (2013). Control of tumour -associated macrophage alternative activation by macrophage migration inhibitory factor. *The journal of immunology*, *190*(6), 2984-2993.

Yamamoto, K., Floyd-Smith, G., Francke, U., Koch, N., Lauer, W., Dobberstein, B., & Hämmerling, G. J. (1985). The gene encoding the Ia-associated invariant chain is located on chromosome 18 in the mouse. *Immunogenetics*, *21*(1), 83-90.

Yan, J. X., Wait, R., Berkelman, T., Harry, R. A., Westbrook, J. A., Wheeler, C. H., and Dunn, M. J. (2000). A modified silver staining protocol for visualization of proteins compatible with matrix-assisted laser desorption/ionization and electrospray ionization-mass spectrometry. *Electrophoresis, 21*(17), 3666-72.

Yan, W., & Chen, S. S. (2005). Mass spectrometry-based quantitative proteomic profiling. *Briefings in functional genomics & proteomics*, *4*(1), 27-38.

Yaprak, M., Erdogan, G., Aricic, G., Ozcan, B., Mesci, A., Dınckan, A., Erdogan, O., & Arici, C. (2015). Prognostic Value of CD74 and HLA-DR Expressions in Invasive Ductal Breast Cancer. *Advances in breast cancer research*, *4*(03), 71-76.

Yin, K. B. (2011). The Mesenchymal-Like Phenotype of the MDA-MB-231 Cell Line. In: *Textbook of Breast Cancer - Focusing Tumour Microenvironment, Stem cells and* Metastasis (ed Mehmet, G). pp. 385-402. Rijeka. InTech.

Young, A. N., Amin, M. B., Moreno, C. S., Lim, S. D., Cohen, C., Petros, J. A., Marshall, F.F., & Neish, A. S. (2001). Expression profiling of renal epithelial neoplasms: a method for tumour classification and discovery of diagnostic molecular markers. *The american journal of pathology*, *158*(5), 1639-1651.

Yu, Y., Huang, H., Li, J., Zhang, J., Gao, J., Lu, B., & Huang, C. (2013). GADD45β mediates p53 protein degradation via Src/PP2A/MDM2 pathway upon arsenite treatment. *Cell death & disease*, *4*(5), e637.

Zaidi, M. R., & Merlino, G. (2011). The two faces of interferon-γ in cancer. *Clinical cancer research*, *17*(19), 6118-6124.

Zamarron, B. F., & Chen, W. (2011). Dual roles of immune cells and their factors in cancer development and progression. *International journal of biological sciences*, *7*(5), 651-658.

Zernecke, A., Bernhagen, J., & Weber, C. (2008). Macrophage migration inhibitory factor in cardiovascular disease. *Circulation*, *117*(12), 1594-1602.

Zhang, H., Liu, C., Cheng, S., Wang, X., Li, W., Charreyre, C., Audonnet, C. A., & He, Q. (2013). Porcine CD74 is involved in the inflammatory response activated by nuclear factor kappa B during porcine circovirus type 2 (PCV-2) infection. *Archives of virology*, *158*(11), 2285-2295.

Zhang, J., & Liu, Y. (2008). HER-2 over-expression and response to different chemotherapy regimens in breast cancer. *Journal of zhejiang university science B*, *9*(1), 5-9.

Zhang, L., Ye, S. B., Ma, G., Tang, X. F., Chen, S. P., He, J., Liu, W., Xie, D., Zeng, Y., & Li, J. (2013). The expressions of MIF and CXCR4 protein in tumour microenvironment are adverse prognostic factors in patients with esophageal squamous cell carcinoma. *Journal of translational medicine*, *11*, 60.

Zhao, Y. H., Wang, T., Yu, G. F., Zhuang, D. M., Zhang, Z., Zhang, H. X., Zhao, D., P., & Yu, A. L. (2013). Anti-proliferation effects of interferon-gamma on gastric cancer cells. *Asian pacific journal of cancer prevention*, *14*(9), 5513-5518.

Zheng, Y. X., Yang, M., Rong, T. T., Yuan, X. L., Ma, Y. H., Wang, Z. H., Shen, Z., & Cui, L. (2012). CD74 and macrophage migration inhibitory factor as therapeutic targets in gastric cancer. *World journal of gastroenterology*, *18*(18), 2253.

Zhu, W., Smith, J. W., & Huang, C. M. (2009). Mass spectrometry-based label-free quantitative proteomics. *Biomedical research international*, *2010*, 1-6

Zöller, M. (2011). CD44: can a cancer-initiating cell profit from an abundantly expressed molecule? *Nature reviews cancer*, *11*(4), 254-267.

Appendices

Appendix 1 Supplemental results

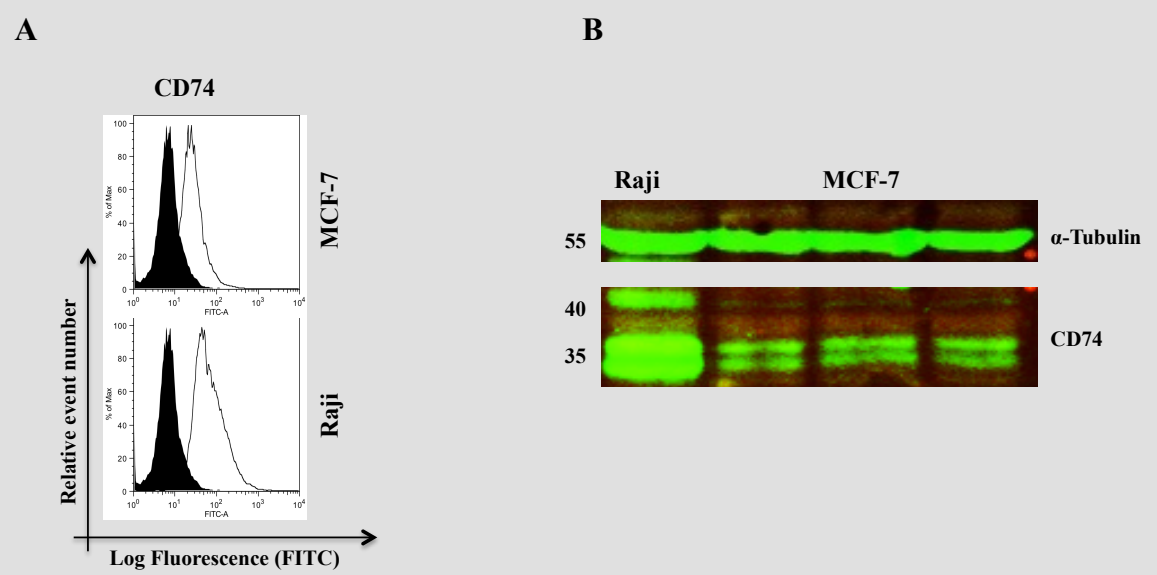

Figure A1.1: The expression of CD74 in breast cancer cells (MCF-7).

(A) Cell-surface expression of CD74 was acquired by flow cytometry using By2 (anti-CD74. (Empty histograms), displayed as mean fluorescence intensity, at the cell-surface of MCF-7 cells stained with indicated antibody. Negative controls were performed by using an isotype-matched control antibody (black filled histograms). (B) Total protein of CD74 detected by western blot and α-Tubulin was used as a loading control.

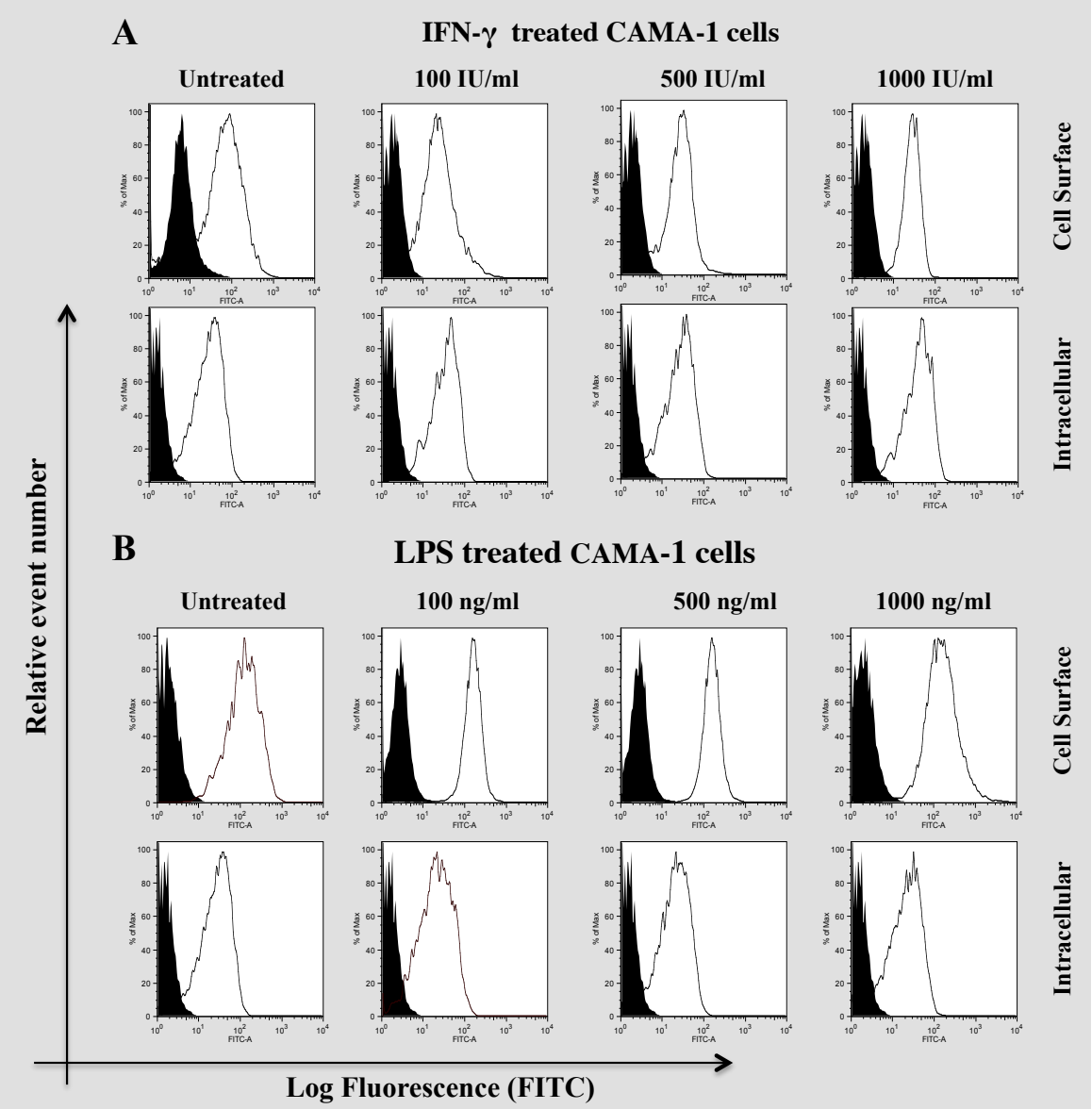

Figure A1.2: Cell-surface and intracellular expression of CD44 on IFN-γ or LPS treated CAMA-1 cells.

CAMA-1 cells were cultured in the presence of the indicated concentrations of IFN-γ (100-1000 IU/ml) for 72 hr or LPS (100-1000 ng/ml) for 24 hr were acquired by flow cytometry using 156-3C11 (anti-CD44). Empty histograms represent the expression of CD44 on untreated CAMA-1 and IFN-γ or LPS treated CAMA-1 cells whereas black filled histograms show negative controls. Cells were labelled with an FITC-labelled secondary anti-mouse antibody. (A) Represent cells surface and intracellular expression of CD44 on untreated CAMA-1cells and on IFN-γ treated cells. (B) Represents the expression of CD44 after LPS treatment with indicated concentration. The results show that CD44 expression does increases upon IFN-γ or LPS treatment and no significant change is detected in CD44 expression after exposing the cells to IFN-γ or LPS.

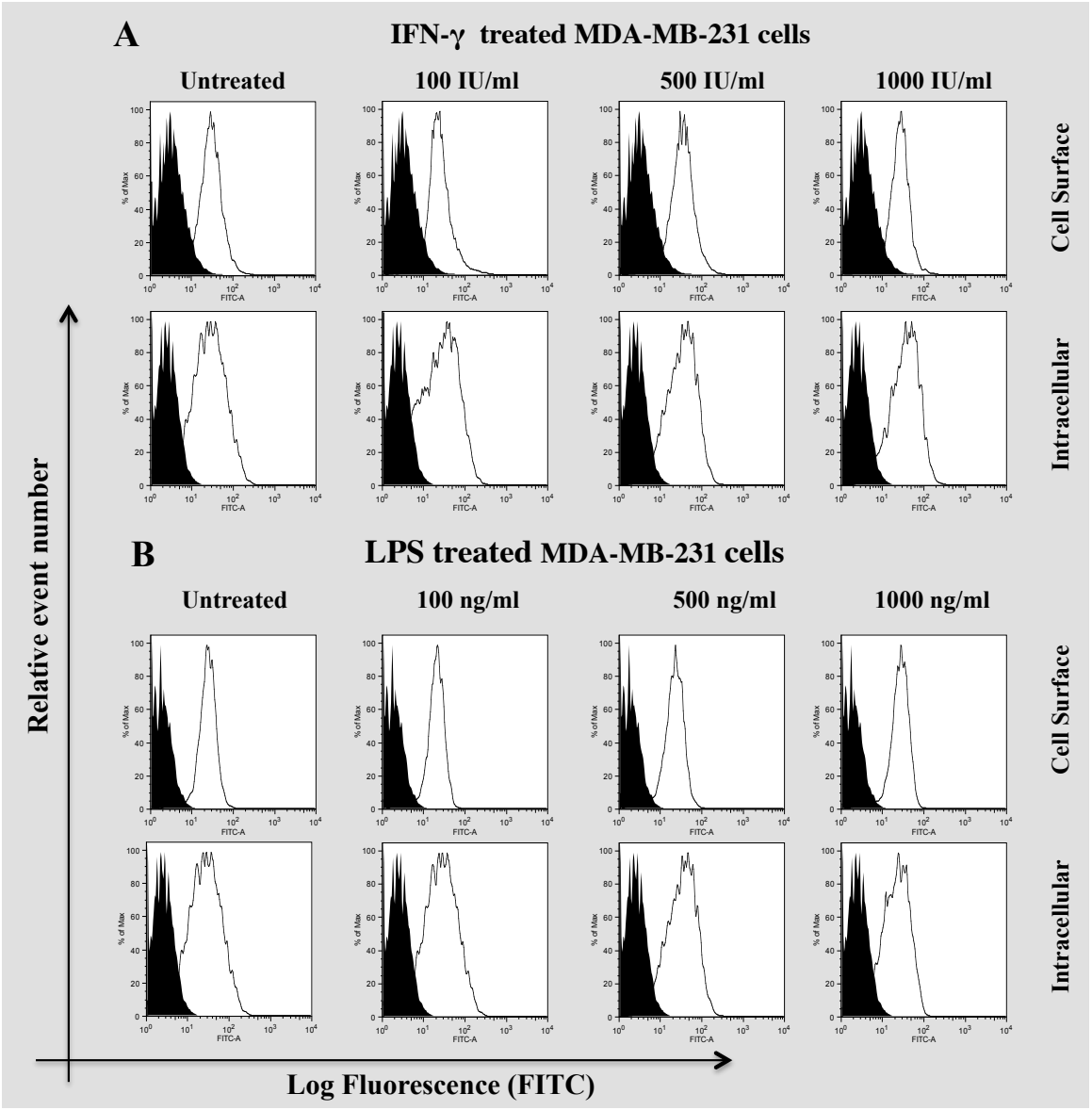

Figure A1.3: Cell-surface and intracellular expression of CD44 on IFN-γ or LPS treated MDA-MB-231 cells.

MDA-MB-231 cells were cultured in the presence of the indicated concentrations of IFN-γ (100-1000 IU/ml) for 72 hr or LPS (100-1000 ng/ml) for 24 hr were acquired by flow cytometry using 156-3C11 (anti-CD44). Empty histograms represent the expression of CD44 on untreated MDA-MB-231 and IFN-γ or LPS treated MDA-MB-231 cells whereas black filled histograms show negative controls. Cells were labelled with an FITC-labelled secondary anti-mouse antibody. (A) Represent cells surface and intracellular expression of CD44 on untreated MDA-MB-231cells and on IFN-γ treated cells. (B) Represents the expression of CD44 after LPS treatment with indicated concentration. The results show that CD44 expression does increases upon IFN-γ or LPS treatment and no significant change is detected in CD44 expression after exposing the cells to IFN-γ or LPS.

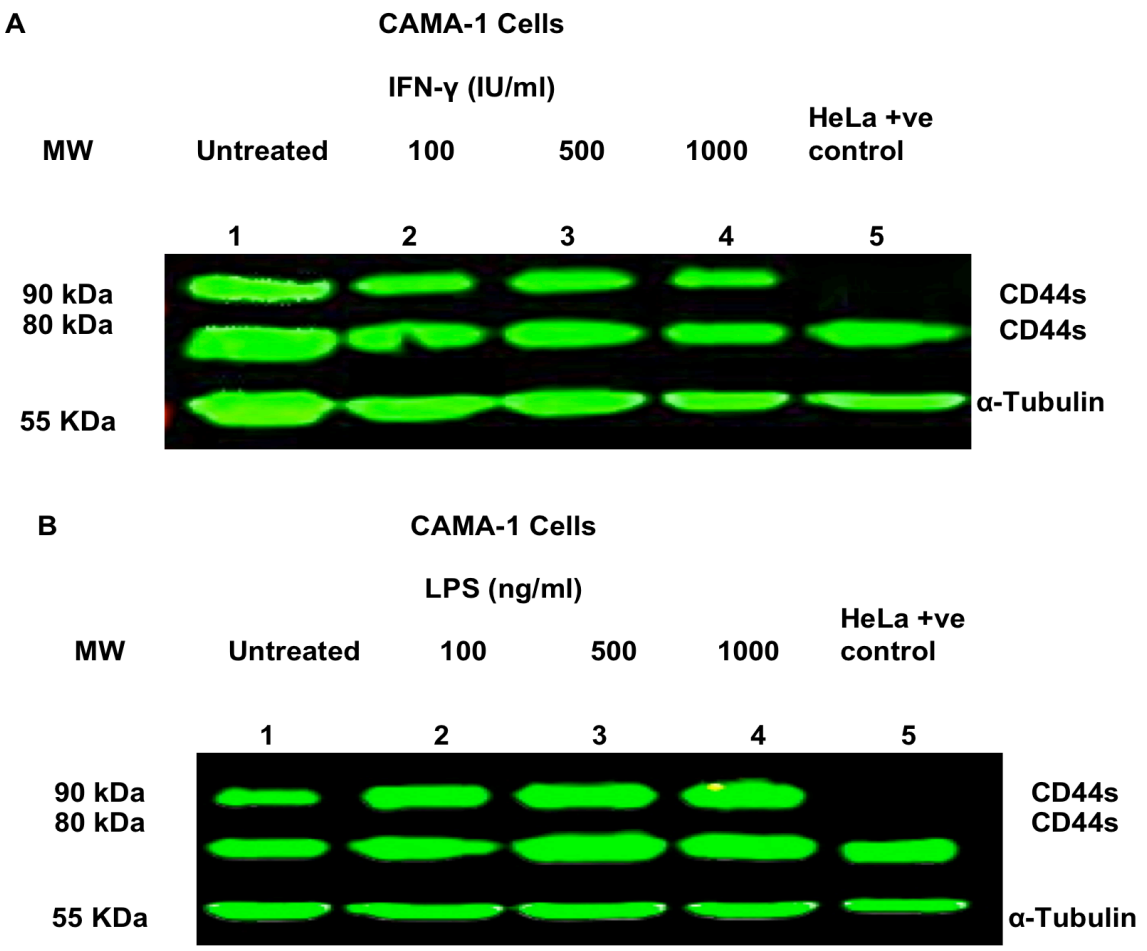

Figure A1.4: CD44 and α-Tubulin expression according to their molecular weight in IFN-γ or LPS treated CAMA-1 cells.

(A and B) Primary monoclonal antibodiesTU-02 (anti α-Tubulin as loading control) and 156-3C11 (anti-CD44) were used. α-Tubulin is detected at 55 kDa molecular weight. The cervical cancer cells line HeLa was used as a positive control as it expresses high levels of CD44 without any stimulation of cytokines (lane 5; A and B). CAMA-1 cells, cultured in the presence of the indicated concentrations of IFN- γ for 72 hr or LPS for 24 hr. (A) Lane 1 represents α-Tubulin, CD44s and CD44v on untreated CAMA-1 cells. (A) IFN-γ treated CAMA-1 cells with indicated concentrations are shown in lane 2, 3 and 4. (B) LPS treated CAMA-1 cells with indicated concentrations are shown in lane 2, 3 and 4. CD44 isoforms were detected at expected molecular weights; 80 and 90 kDa. No significant difference in CD44 isoform expression was detectable after treating CAMA-1 cells with IFN-γ or LPS.

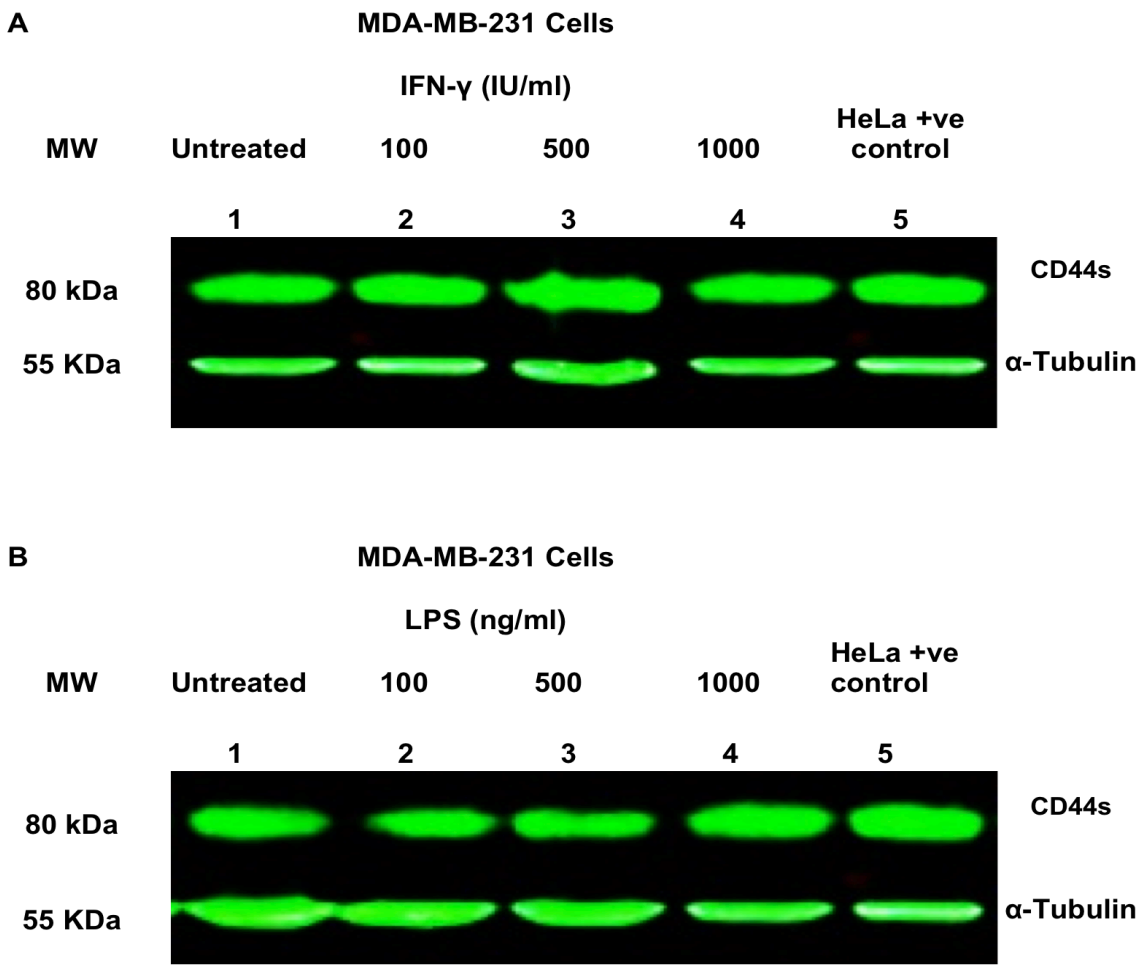

Figure A1.5: CD44 and α-Tubulin expression according to their molecular weight in IFN-γ or LPS treated MDA-MB-231 cells.

(A and B) Primary monoclonal antibodiesTU-02 (anti α-Tubulin as loading control) and 156-3C11 (anti-CD44) were used. α-Tubulin is detected at a molecular weight of 55 kDa. The monocytes cell line Raji was used as a positive control as it expresses high levels of CD74 without any stimulation of cytokines (lane 5; A and B). MDA-MB-231 cells, cultured in the presence of the indicated concentrations of IFN- γ for 72 hr or LPS for 24 hr. (A) Lane 1 represents α-Tubulin and CD74 on untreated MDA-MB-231 cells. (A) IFN-γ treated MDA-MB-231 cells with indicated concentrations are shown in lane 2, 3 and 4. (B) LPS treated MDA-MB-231 cells with indicated concentrations are shown in lane 2, 3 and 4. CD44 isoforms were detected at expected molecular weights; 80 and 90 kDa. No significant difference in CD44 isoform expression was detectable after treating MDA-MB-231 cells with IFN-γ or LPS.

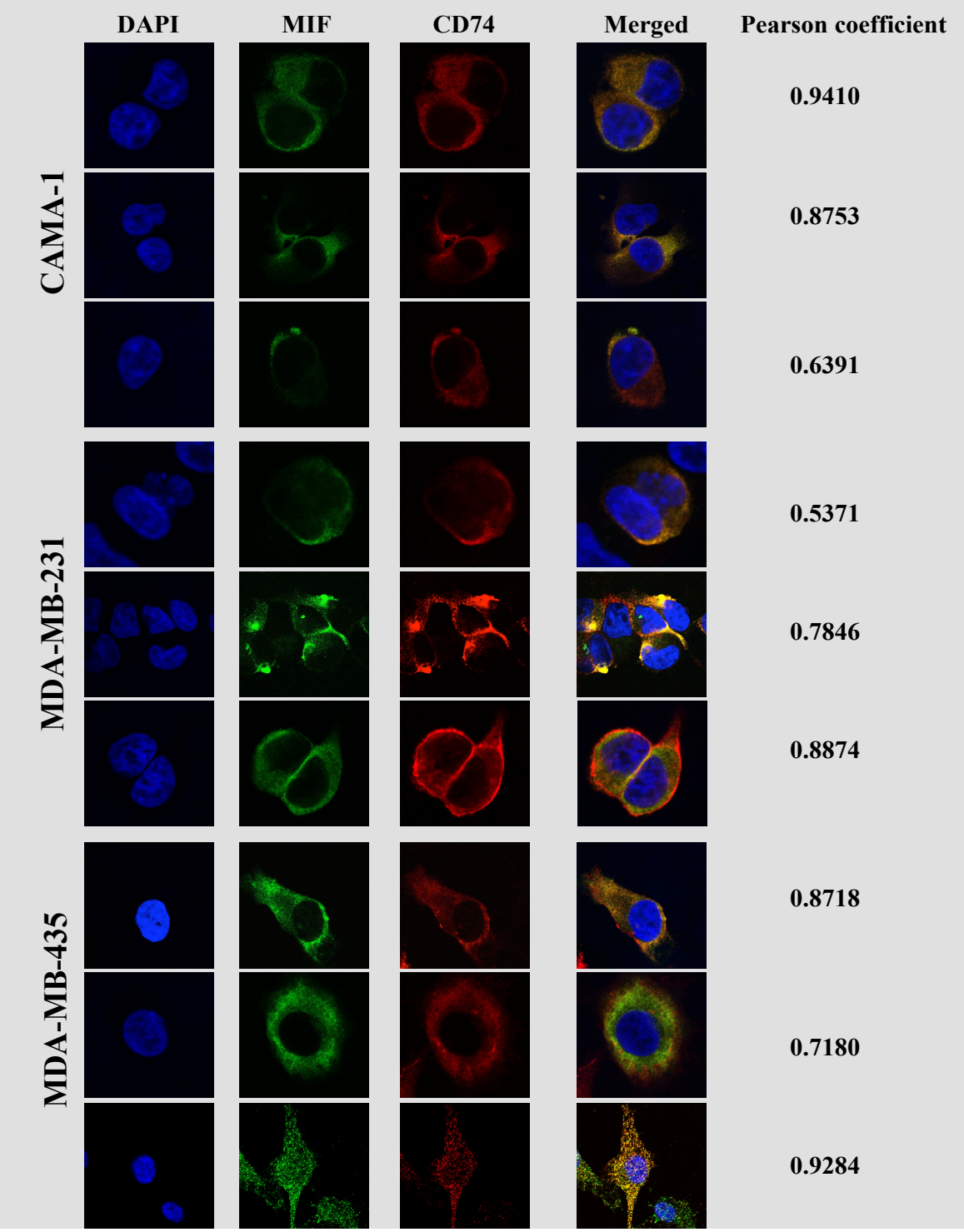

Figure A1.6: Calculated Pearson's product-moment correlation coefficients of MIF and CD74 for each image in CAMA-1, MDA-MB-231 and MDA-MB-435 cells.

The coefficients were generated using Fiji software and specific plugins. For every batch of double immunostaining of MIF and CD74 cells, three samples were used for quantification. Yellow/ orange signals achieved by merging fluorochromes (Alexa Fluor® 488 and Alexa Fluor® 555) separately using using Fiji software. Florescence reveals the colocalisation and Pearson's correlation coefficients was used to study the degree of colocalisation.

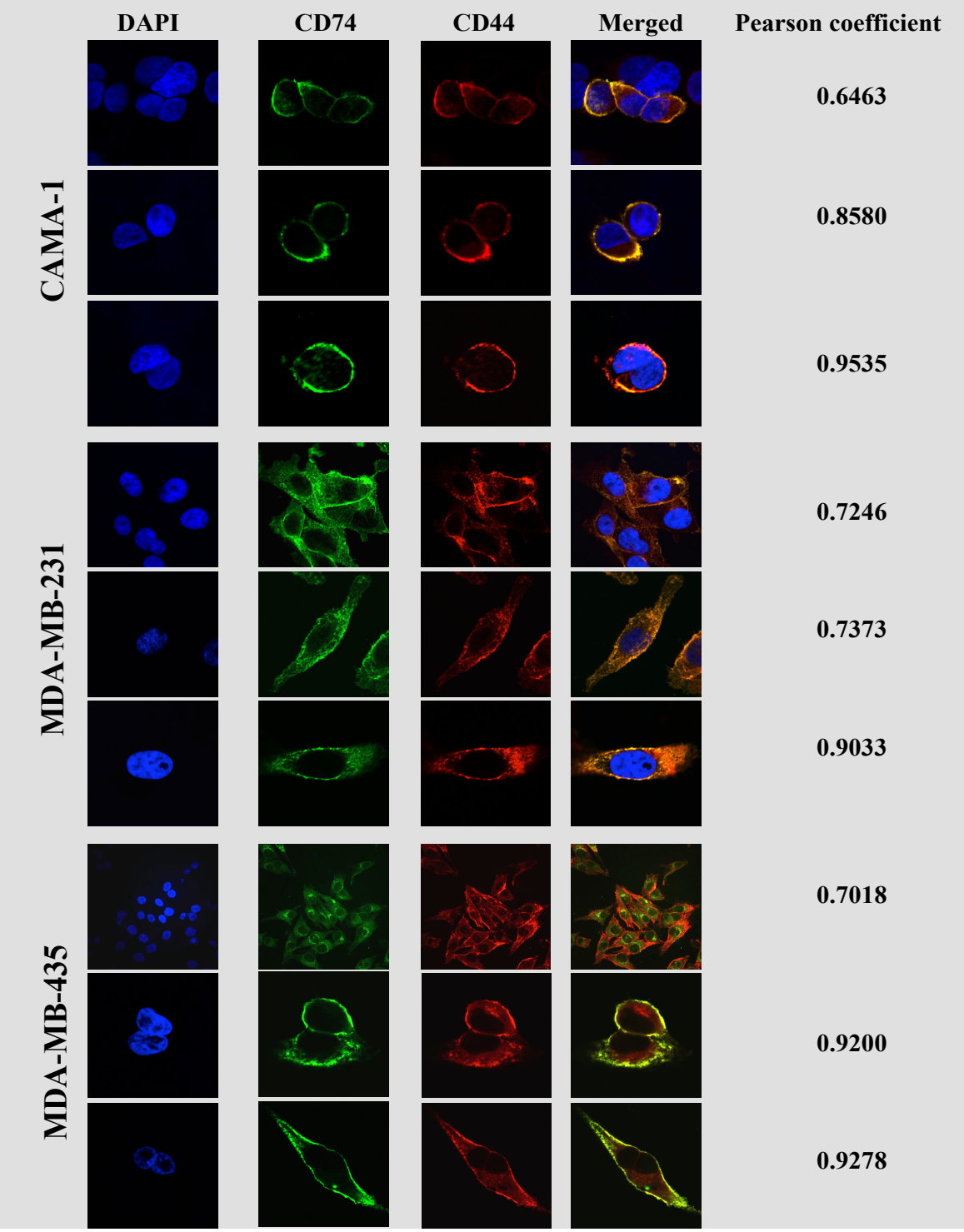

Figure A1.7: Calculated Pearson's product-moment correlation coefficients of CD74 and CD44 for each image in CAMA-1, MDA-MB-231 and MDA-MB-435 cells.

The coefficients were generated using Fiji software and specific plugins. For every batch of double immunostaining of CD74 and CD44 cells, three samples were used for quantification. Yellow/ orange signals achieved by merging fluorochromes (Alexa Fluor® 488 and Alexa Fluor® 555) separately using using Fiji software. Florescence reveals the colocalisation and Pearson's correlation coefficients was used to study the degree of colocalisation.

Appendix 2 Buffer Recipes

1X PBS (1000 ml)

Reagent	Amount	Final Concentration
NaCl	8.0gm	138 mM
KCl	0.25gm	2.6 mM
KH_2PO_4	0.25gm	1.5 mM
Na_2HPO_4	0.25gm	6.3 mM
Distilled Water	1000 ml	-

(PH 7.3; Store at 4°C).

4% Paraformaldehyde (100 ml)

Reagent	Amount
PFA	4.0 g
PBS	100 ml

(PH 7.3; Store at 4°C).

Blocking buffer (1000 ml)

Reagent	Amount	Final concentration
FCS	10 ml	1 %
PBS	1000 ml	-

(PH 7.3; Store at 4°C).

Coomasie Blue stain (1000 ml)

Reagent	Amount	Final concentration
Coomasie Blue R-250	1 g	0.1 %
Methanol	450 ml	45 %
Glacial acetic acid	100 ml	10 %
Distilled Water	450 ml	

Coomasie Blue destain (1000 ml)

Reagent	Amount	Final concentration
Methanol	100 ml	10 %
Glacial acetic acid	100 ml	10 %
Distilled Water	800 ml	-

5X electrophoresis running buffer (1000 ml)

Reagent	Amount	Final concentration
Tris	15.1 g	25 mM
Glycine	72 g	250 mM
10% SDS	5 g	0.1 %

1X electrophoresis Buffer (1000 ml)

Reagent	Amount
5X electrophoresis running buffer	200 ml
Distilled Water	800 ml

Ammonium Persulfate (10%) (1 ml)

Reagent	Amount
Ammonium Persulfate	0.1 g
Distilled Water	1 ml

Transfer buffer (1000 ml)

Reagent	Amount	Final concentration
Tris	3.03 g	25 mM
Glycine	14.4 g	192 mM
Methanol	200 ml	20 %
Distilled Water	800 ml	

(PH 8.3; Store at 4°C).

Wash buffer (PBS-T) (1000 ml)

Reagent	Amount	Final concentration
PBS	999 ml	-
Tween 20	1 ml	0.1 %

Blocking buffer (100 ml)

Reagent	Amount	Final concentration
Non- fat dry milk	5 g	5 %
PBS-T	100 ml	-

Sodium dodecyl sulfate SDS (10 %)(100 ml)

Reagent	Amount
Sodium dodecyl sulfate	10 g
Distilled Water	100 ml

1.5 M Tris-HCl, pH 8.8 (100 ml)

Reagent	Amount
Tris base	10 g
Distilled Water	100 ml Adjust to pH 8.8 with HCl

(PH 8.8; Store at 4°C).

0.5 M Tris-HCl, pH 6.8 (100 ml)

Reagent	Amount
Tris base	6.6 g
Distilled Water	100 ml Adjust to pH 6.8 with HCl

(PH 6.8; Store at 4°C).

Resolving and stacking gel

Reagent	Resolving gel (ml)	Stacking gel (ml)
Distilled Water	4.9	6.1
1.5 M Tris-HCL	3.8	-
0.5 M Tris-HCL	-	2.5
Bis acrylamide	6	1.33
10% SDS	0.15	0.1
APS	0.15	0.05
TEMED	0.006	0.01

Appendix 3 Chemicals

1. Accutase Sigma-Aldrich Dorset, UK
2. Acrylamide 30% BIO-RAD, UK
3. Agarose Invitrogen, UK
4. Brilliant Blue G-Colloidal Concentrate Sigma-Aldrich, UK
5. Bromophenol blue sodium salt Sigma-Aldrich, UK
6. Calcium chloride Merck, Darmstadt
7. CHAPS AppliChem, Darmstadt Chloroform Merck, Darmstadt
8. Ethanol Fisher Scientific, UK
9. Ethidiumbromide Roth, Karlsruhe
10. Giemsa stain Sigma-Aldrich, UK
11. Glutathione Amersham, Freiburg Glycerol Merck, Darmstadt
12. Glycine Sigma-Aldrich, Steinheim
13. Guanidine hydrochloride Sigma-Aldrich, Steinheim
14. Imidazole Fluka, Steinheim
15. Isopropylthio-β-D-galactoside Serva, Heidelberg
16. Leupeptin Sigma-Aldrich, Steinheim
17. Lipopolysaccharide Sigma-Aldrich, Steinheim
18. Magnesium chloride Merck, Darmstadt
19. Magnesium sulfate Sigma-Aldrich, Steinheim
20. Methanol Fisher Scientific, UK
21. N,N,N',N’-Tetramethylethylenediamin Roth, Karlsruhe
22. Non-fat dry milk Bio-Rad, UK
23. Paraformaldehyde Sigma, Germany
24. Phenylmethylsulfonyl fluoride Sigma-Aldrich, Steinheim
25. Ponceau S Roth, Karlsruhe
26. Potassium chloride Fisher Scientific, UK
27. Sodium acetate Roth, Karlsruhe
28. Sodium azide Merck, Darmstadt
29. Sodium carbonate Roth, Karlsruhe
30. Sodium chloride Sigma-Aldrich, Steinheim
31. Sodium citrate Merck, Darmstadt
32. Sodium dodecyl sulfate Merck, Darmstadt

33. Sodium periodate Sigma-Aldrich, Steinheim

34. Sodium thiosulfate Roth, Karlsruhe

35. Sodium thiosulfate Roth, Karlsruhe

36. Tris (hydroxymethyl) aminomethane Roth, Karlsruhe

37. Triton $_X$-100 Sigma-Aldrich, UK

38. Trypan blue Gibco, USA

39. Tween-20 Roth, Karlsruhe

40. Urea Merck, Darmstadt

41. β-Mercaptoethanol AppliChem, Darmstadt

Appendix 4 Training sessions attended during the period of PhD programme

1. Advance project management
2. Assertive communications boards
3. Building an academic profile
4. Communicating your research
5. Communication skills for sciences postgraduates
6. Completing your PhD
7. Confocal microscopy training (Nikon and Bio-Rad Training)
8. Correct referencing and avoiding plagiarism
9. Diversity and quality training course
10. Effective use of voice
11. EndNote training
12. Engaging your audience
13. Flow cytometry training
14. Focus group session
15. General safety in the department and regulations in biology and risk assessment
16. Getting published in science
17. Graduate laboratory assistant
18. How to be an effective researcher
19. Intellectual property in bioscience research
20. Poster presentation
21. Presentations skills
22. Surviving the viva
23. The seven secretes of highly successful research students

Appendix 5 Conferences attended during the period of PhD programme

Two abstracts have been submitted to European Society for Immunodeficiencies (ESID) conference, which was held in Prague, Czech Republic from the 29th October to the 1st November 2014.

1. **The tittle**: "Analysis of the expression and interrelationship between the CD74 and CD44 receptors expressed on human breast cancer derived cells"

   The authors: Hussain Alssadh, Waleed Al Abdulmenaim and Nelson Fernández

The abstract: CD74 is a transmembrane protein that functions as a chaperone of MHC class II and is also thought to be involved in signalling via MIF and CD44. CD44 is a transmembrane glycoprotein that acts as the receptor for hyaluronan and it is considered as a member of cell adhesion molecules. The relationship between these two proteins is not well understood; one hypothesis postulates that the expression of CD74 and CD44 is associated with inflammatory disorders including cancer. We have examined the expression of CD74 and CD44 by flow cytometry and western blot in three breast tumour cell lines, CAMA-1, MDA-MB-231 and MDA-MB-435. The cell-surface membrane expression of CD44 is higher than CD74 in all examined cell lines. On the other hand, the level of expression of CD74 in MDA-MB-435 cell lines was higher than in CAMA-1 and MDA-MB-231. To evaluate the physical association of these two proteins, co-localization experiments using bioimaging were carried out. It was observed that CD74 and CD44 are highly co-localized suggesting a possible mode of function in facilitating signalling.

2. **The tittle**: "Lack of Trophoblast-specific isoforms of CD74 may protect human pregnancy"

   The authors: Waleed Al Abdulmenaim, Hussain Alssadh and Nelson Fernández

The abstract: During pregnancy the maternal immune system protects the allogeneic foetus from rejection. At the same time the mother maintains immunity defences intact against potential pathogens. We wish to know whether immunological receptors associated with antigen presentation and hence strong inflammatory responses play a role at the feto-maternal tolerance. One such receptor is CD74, a membrane-bound protein involved in HLA Class mediated antigen presentation and as Macrophage Migration Inhibitory Factor (MIF) receptor. Consequently, we wish to investigate the expression of CD74 at mRNA and protein levels in trophoblast derived cells, JEG-3 and ACH-3P and human placenta. We also wish to obtain knowledge on the effect of IFN-γ and LPS-mediated infection, in particular in the regulation of CD74 isoform expression.

One abstract has been submitted to 7th Saudi Students Conference-UK, which was held in Edinburgh International Conference Centre, in Edinburgh, UK from the 1st to 2nd February 2014

3. **The tittle**: "Role of MHC class II in association with CD74 on human breast cancer cell lines"

   The authors: Hussain Alssadh and Nelson Fernández

The abstract: The expression of HLA-DR and CD74 has been identified in several types of cancer and is believed to play a role in immunotolerance. CD74 is a type II transmembrane protein that plays a role in the assembly of MHC class II molecule-peptide complexes in antigen presentation. Their selective expression is assumed to activate certain mechanisms/signal transduction pathways that suppress or modulate the immune system and protect the developing of cancerous cells including metastasis. A recent study has shown that CD74 is over-expressed on various cancer cells, i.e., prostate cancer cells, B lymphomas and gastric carcinomas. So, it is believed that CD74 and HLA-DR might be considered as tumour markers.

Publications

A manuscript has been in progress for publications as described below:

1. Title: Interactions between CD74 and CD44 receptors expressed by human breast cancer cells

   Authors: Al Ssadh Hussain, Alabdulmenaim Waleed and Nelson Fernández

   Journal: Journal of Immunology

Interactions between CD74 and CD44 receptors expressed by human breast cancer cells

Al Ssadh Hussain, Alabdulmenaim Waleed, Alghamdi Rana and Nelson Fernández

School of Biological Sciences, University of Essex, Wivenhoe Park, Colchester, Essex CO4 3SQ, United Kingdom

Corresponding author: nelson@essex.ac.uk; Tel: +44 1206 873330; Fax: +44 1206 872592

Abstract

Increasingly the interactions of pairs of membrane-bound receptors acting in synergy have been linked to tumor progression; in this study we show that, indeed, CD74 and CD44 act in synergy and thus could promote breast cancer progression. The transmembrane receptor, which is also known as Cluster of Differentiation (CD) 74 functions as a chaperone of MHC class II biosynthesis, it is also involved in signaling via (macrophage migration inhibitory factor) MIF and the adhesion receptor CD44. The latter is also a transmembrane receptor, which is a member of a large family of cell adhesion molecules that is responsible for mediating communication and adhesion between adjacent cells, and between cells and the extracellular matrix (ECM). We have employed flow cytometry and western blot to examine the breast tumor cell lines, CAMA-1, MDA-MB-231 and MDA-MB-435 for CD74 and CD44. We observed that CD44 was higher than CD74 in all examined cancer cells. On the other hand, the level of expression of CD74 in MDA-MB-435 cell lines was higher than in CAMA-1 and MDA-MB-231. We conclude that CD74 and CD44 showed significant quantitative variations and they associate in cytoplasmic compartments, suggesting a mechanistic and functional mode of action. Co-localization experiments using bioimaging indicate that CD74 and CD44 are physically associated suggesting a possible mode of function in facilitating signaling and hence tumor progression.

Introduction

Breast cancer is the most frequently diagnosed cancer in women worldwide and the most common cause of malignancy-associated death [1-3]. Breast cancer is found in breast sites and it is more common in females than males [3]. Each year, 458,000 women die from breast cancer globally, making it the most common cause of female cancer death in both the developed and developing world [4]. In the UK, the age-standardised incidence of breast cancer in women has increased by 6% over the last decade, between 1999 to 2001 and 2008 to 2010 [5]. Statistical surveys have estimated that around 550,000-570.000 people are diagnosed with breast cancer in the United Kingdom [6]. The number of women who are diagnosed with breast cancer is expected to increased three times by 2040 [7]. Recently, breast cancer research indicates that the annual cost of breast cancer healthcare increased over a third compared to the last 10 years [4].

The expression of CD74 and CD44 has been identified in several types of cancer and is believed to play a role in immunotolerance [8]. Recently, Greenwood et al. [9] have determined that high expression of Stat1, Max1 and CD74 is associated with triple-negative breast cancer. It has also been demonstrated that adhesion of tumour cells on the reconstituted membrane matrix Matrigel increases after IFN-γ-induced over-expression of CD74 [9]. Jiang et al [10] have shown that WNT5A, a lipid-modified glycoprotein, inhibits metastasis and alters splicing of CD44 in breast cancer cells. Therefore, it is believed that selective expression of CD74 and CD44 activates certain mechanisms and signal transduction pathways that suppress or modulate the immune system and protect the development of cancerous cells and metastasis [11].

CD74, also known as invariant chain (Ii) or macrophage migration inhibitory factor (MIF) receptor, is classified as a type II transmembrane glycoprotein that is expressed on antigen-presenting cells [11-13]. However, recent studies have demonstrated that CD74 is also expressed in numerous types of cancer cell, including prostate, bladder and breast cancer cells [14, 15]. Additionally, CD74 is thought to be involved in signalling via MIF, suggesting it has a crucial role in tumor progression [15, 16]. However, because the short cytoplasmic sequence of CD74 does not appear to signal directly, MIF-induced extracellular signal-regulated kinase (ERK) signalling appears to be reliant upon CD44 [15, 17]. Thus CD74 is modified by the addition of chondroitin sulfate, permitting interaction with CD44 to form a receptor complex of MIF-CD74-CD44 [18, 19].

CD44 is an integral membrane glycoprotein expressed in many cell types that serves as the principal receptor for hyaluronan, a glycosaminoglycan constituent of extracellular matrix [20]. Through alternative splicing, cells produce a family of CD44 including (CD44s and CD44v) protein isoforms that are involved in multiple distinct cellular functions, including proliferation, adhesion, and migration. The expression of CD44 has been associated to particular cancer types such as prostate tumours, head and neck squamous tumours, nervous system tumours, respiratory track tumours, melanomas and breast cancer [21-24]. CD44 expression in human breast cancer has been correlated with both favourable and unfavourable clinical outcomes [1, 25].

The present study aimed to characterize the cell-surface and total protein expression of CD74 and CD44 on human breast cancer cell lines (CAMA-1, MDA-MB-231 and MDA-MB-435). I also studied the interactive partners of CD74 and CD44 by target imaging and coimmunoprecipitation. We investigated the expression of CD74 and CD44 in immortalized normal breast luminal cells (226LDM) to validate the study.

Materials and Methods

Cell lines and cell culture

Three human mammary gland cell lines, CAMA-1, MDA-MB-231 and MDA-MB-435, all derived from malignant pleural effusion, were used. The CAMA-1 and MDA-MB-435 cell lines were maintained in RPMI 1640 medium (LONZA-Belgium), supplemented with 10% of (v/v) fetal calf serum (FCS; Imperials Laboratories). Although MDA-MB-435 has been debated to be melanoma cells due to its gene profile expression, it is yet widely used as breast cancer cells [26]. The MDA-MB-231 cell line was maintained in D-MEM (high glucose), supplemented with 10 % FCS. 226LDM immortalized normal breast luminal cells (kindly provided by Elena Klenova, School of Biological Sciences, University of Essex), were used as positive control cells. Raji cells (human negroid Burkitt's lymphoma) and HeLa cells (human cervical cancer), expressing high levels of CD74 and CD44, respectively, served as additional positive controls. The 226LDM cell line was maintained in Dulbecco's Modified Eagle's Medium (DMEM)/F-12, supplemented with 10% FCS, 5 mg/ml gentamicine, 5 ug/m insulin, l ng/ml hydrocortine, 20 ng/ml epidermal growth factor and 20 ng/ml cholera toxin. Raji and HeLa cells were cultured in RPMI -1640 (LONZA-Belgium) containing 10% FCS and cultured in a humidified atmosphere of 5% CO_2 and 37°C. HeLa cell line was generous gift from Professor Glyn Stanway, School of Biological Sciences, University of Essex .All media used for this study were purchased from PAA Laboratories GmbH (Pasching, Austria).

Reagents

The monoclonal primary antibodies mouse anti-human CD74 (clone: By2) and mouse anti-human α-tubulin (clone: TU-02) were purchased from Santa Cruz Biotechnology, USA. Mouse antibody CD44 (clone: 156-3c11) was purchased from Cell Signaling Technology, USA. Rabbit anti-human β-actin (clone: poly 6221) was purchased from (BioLegend, UK). The secondary antibody used for flow cytometry was a goat anti-Mouse antibody conjugated with the fluorophore FITC (clone: poly4053) and was purchased from Bio-legend, UK. The secondary antibody used for Western blotting was either goat anti-mouse (IRDye 800CW) or goat anti-rabbit (IRDye 680 LT), purchased from LI-COR Biosciences. Finally, Alex 488 (green) and Alex 555 (red) antibodies were purchased from Life Technologies, UK.

Flow cytometry analysis

Cell lines were lifted with accutase (Sigma) and $1x10^6$ cells were used per sample. Monoclonal antibodies By2 (anti-CD74) and 156-3c11 (anti-CD44) were employed in indirect immunofluorescence staining. Cells were preincubated with saturating concentrations of primary antibody, followed by washing and labeling with FITC-conjugated goat anti-mouse IgG (Bio-legend). For cell-surface staining, cells were fixed with 4% formaldehyde solution, and washed with 1X PBS. The cells were then blocked with blocking buffer (PBS/0.1 %BSA) followed by washing steps in PBS. Primary and secondary antibodies were diluted with 0.1% BSA in PBS. Samples were analysed on BD FACSAria and analyzed by FlowJo 8.8.6.

Western blotting and immunedetection

Cells were lysed with CelLytic reagent (Sigma) and total protein concentration was determined by Bradford assay. The Total cell lysate was separated on a 12% SDS-PAGE gel. A total of 40 µg protein was loaded per well, and, after electrophoresis, protein was transferred to a polyvinylidene fluoride (PVDF) membrane (Immobilon-FL, Merck Millipore, Merck KGaA, Darmstadt, Germany). Membranes were blocked with 5% skimmed milk in PBS-Tween-20 (Sigma) for 1 hr at room temperature and incubated in anti-CD74 (clone: By2) at a concentration of 1:200, and anti- CD44 (clone: 156-3C11) at a concentration of 1:1000. As a control, an alpha subunit-specific tubulin mouse monoclonal antibody was used to probe the cell extracts at a concentration of 1:200, followed by washing in PBS-T for 30 min. The membranes were then incubated with IRDye 800CW Donkey anti-Mouse IgG (Li-Cor Bioscience, Licoln, NE, USA) at a concentration of 1:1000 for 1 hr followed by washing in PBS-T for 30 min. Signals were detected using the ODYSSEY Infrared Imaging System (Li-Cor Biosciences). Fermentas PageRuler^{TM} Plus Prestained Protein Ladder (Thermo Fisher Scientific, Waltham, MA, USA) was used in order to estimate the molecular weight of the respective protein bands.

Immunofluorescence staining

CAMA-1, MDA-MB-231 and MDA-MB-435 cell lines were cultured in LabTek 8-well chambers (Thermo Fisher Scientific) at a density of 6×10^3 cells per well for two days and following that they were seeded. The cells were fixed with 4% paraformaldehyde for 20 min on ice. For immunofluorescence staining all procedures were carried out at ambient

temperature. Cells were permeabilized and then blocked with 2% (w/v) bovine serum albumin (BSA) prepared in 1x phosphate-buffered saline (PBS) for 1 h at room temperature. For single staining of each antigen, cells were incubated with anti-CD74 (clone: By2) at a concentration of 1:500, and anti- CD44 (clone: 156-3C11) at a concentration of 1:400, for 1 h followed by three washes with PBS. Secondary antibody, anti-mouse IgG conjugated with Alexa Fluor® 488 or Alexa Fluor® 555 (Invitrogen, Carlsbad, CA, USA), was used at a dilution of 0.25 µg/100ml for 1 h. For double staining, cells were blocked again with 2% BSA and the staining process was repeated for each desired pair. 4', 6-diamidino-2-phenylindole dihydrochloride (DAPI) counter stain (Vector Laboratories, Burlingame, CA, USA) was used at a 1:250 dilution. Cells were thoroughly washed with PBS, the chambers removed, and the slide was mounted with anti-fade mounting medium (Vector Shield) covered with a cover slip (Chance proper LTD, West Midlands, England) and sealed with Marabu fixogum rubber cement (Marabuwerke GmbH & Co. KG, Tamm, Germany).

Confocal microscopy

For image acquisition, a Nikon A1Si confocal microscope (Nikon Instruments Inc.) was used with a plan-apochromatic VC1.4 N.A. 60x magnifying the oil-immersion objective. NIS-Elements Advanced Research Software (version 4.13.01, build 916; Nikon Instruments Inc.) was used for image acquisition. Images were acquired in three channels, using one-way sequential line scans. DAPI was excited at 398.7 nm with laser power 1.6 arbitrary units, and its emission was collected at 450 nm with a PMT gain of 86. Alexa Fluor 488 was excited at 488 nm with laser power 5.8, its emission was collected at 525 nm with a PMT gain of 117. Alexa Fluor 555 was excited at 560.5 nm with laser power 3.7, and was collected at 595 nm with a PMT gain of 98.The scan speed was ¼ frames/s (galvano scanner). The pinhole size was 35.76 µm, approximating 1.2 times the Airy disk size of the 1.4-NA objective at 525 nm. Scanner zoom was centered on the optical axis and set to a lateral magnification of 60 nm/pixel. Axial step size was 105 nm, with 80-100 image planes per z-stack.

Image processing

NIS-Elements software (version 3.21.03, build 705; Nikon Instruments Inc.) was used for image processing. CD74 (green) and CD44 (red) channels were segmented using regional maxima detection tools followed by manual threshold. The generated binary areas were visually inspected; the overlap of the green and red channels which were generated by the overlay tool, resulted in a new layer (yellow) that represents the intersection of CD74 and

CD44. Finally, automated volume measurement was carried out for CD74, CD44 and their intersection was measured by a volume measurements tool.

Immunoprecipitation and coimmunoprecipitation

Cells were lysed with the RIPA Lysis Buffer System (Santa Cruz Biotechnology, USA) and total protein concentration was determined by Bradford assay.1 mg/ml of each sample was incubated overnight with 4 µg of anti-CD74 (clone: By2), at 4°C. Following that 40 µl of protein A/G PLUS- Agarose (Santa Cruz Biotechnology, USA) was added. To promote immunoglobulin binding, this solution was kept overnight on a rotator at 4°C. The samples were spun down for 30 s and the supernatant was discarded. Beads were then washed twice using PBS and the samples were boiled at 100°C after adding 50 µl of SDS-PAGE sample loading buffer containing dithiothreitol. Then 20 µl of each sample was loaded in each well of the gel that was left for 1 hr and 30 min at 120 V. After electrophoresis, protein was transferred to a PVDF membrane. Membranes were blocked with 5% skimmed milk in PBS-Tween-20 (Sigma) for 1 h at room temperature and incubated in either anti-CD74 (clone: By2) at a concentration of 1:200, or anti-CD44 (clone: 156-3C11) at a concentration of 1:1000, and flowed by washing in PBS-T for 30 min. The membranes were then incubated with secondary antibody (IRDye 800CW Donkey anti-Mouse IgG ;Li-Cor Bioscience, Licoln, NE, USA) at a concentration of 1:1000 for 1 h, followed by washing in PBS-T for 30 min. Signals were detected using the ODYSSEY Infrared Imaging System (Li-Cor Biosciences).

Results

Identification and quantification of CD74 and CD44

The cell surface expression of CD74 and CD44 was analyzed for CAMA-1, MDA-MB-231, and MDA-MB-435 and Raji cell lines. Non-permeabilized cells were stained with an appropriate concentration of By2 (anti-CD74) and 156-3C11 (anti-CD44) antibodies followed by 1 μl RAM-FITC secondary antibody. Cells only, without staining, and isotype cells, stained with only secondary antibody, were used as a negative control. CD74 and CD44 were detected on the cell-surface membrane of CAMA-1, MDA-MB-231 and MDA-MB-435 cells (Fig 1).

Immunostaining of CD74 and CD44

Laser scanning confocal microscopy using different wavelengths was used to visualize intracellular expression of CD74 and CD44 molecules. The CAMA-1, MDA-MB-231 and MDA-MB-435 cell lines all showed expression of CD74 and D44 on the intracellular membrane (Fig 2).

Immunoblot analysis of CD74 and CD44 proteins

CD74 and CD44 protein expression in CAMA-1, MDA-MB-231, MDA-MB-435, Raji and HeLa cells was studied by Western blot analysis using By2 (anti-CD74), 156-3C11 (anti-CD44) and Poly6221 (anti β-Actin). By2 (anti-CD74) is specific for CD74 isoforms 31-45 kDa and 156-3C11 (anti-CD44) is a mouse mAb which detects endogenous levels of total CD44 protein that is specific for most isoforms 80-90 kDa.

Results in figure 3 show that CD74, CD44 and anti β-actin have molecular weights of 33-41 kDa, 80-90 kDa and 45 kDa respectively. β-actin was used as a loading control. Most of the cell lines expressed three different isoforms of CD74 (Fig. 3*A*). However CAMA-1 cells expressed two different isoforms of CD44 (Fig. 3*A*). To evaluate the differences in protein loading during the experiment, the percentage of expression was calculated after the intensity of each band was adjusted according to its respective β-actin band intensity using the Image Studio Lite software (LI-COR Biosciences) (Fig. 3*B*).

Validation study of tumour antigens

In order to validate our study, we investigated the expression of CD74 and CD44 receptors in immortalized normal breast luminal cells (226LDM). Cell-surface and intracellular expression of both CD74 and CD44 was assessed by flow cytometry (Fig 4.*A*). Total protein of CD74 and CD44 was detected by Western blotting and α-Tubulin was used as a loading control (Fig 4.*B*). Confocal laser-scanning microscopy was utilized to study the intracellular staining of CD74 and CD44 in 226LDM cells (Fig 4.*C*). The results show that 226LDM cells do not seem to express CD74 however they do express CD44. Additionally, The expression of CD44 is very weak in the cell surface but it is higher intracellularly.

Colocalization analysis of CD74 and CD44

To investigate whether CD74 and CD44 are co-localized in CAMA-1, MDA-MB-231 and MDA-MB-435 cells, all cell lines were immunostained with an appropriate primary antibody followed by a secondary antibody. CD74 was labeled with FITC Alexa Fluor 488 (green) and CD44 was labeled with Alexa Flour 555 (red) (Fig 5 A.B.C). All breast cancer cells show expression of CD74 and CD44. Colocalization was assessed by merging green and red channels and the Pearson's correlation coefficient was used to analyse the degree of colocalization. The scale lay between -1 and 1, where 1 stands for colocalization, -1 stands for negative colocalization and 0 stands for no colocalization Fig 5D shows the comparison of colocalization in all cell lines versus the negative control. The colocalization of DAPI against FITC was used as a negative control. For more accuracy, 3D images were acquired in stack, with z-direction and segmented by NIS elements to calculate the exact degree of colocalized molecules of CD74 and CD44 against the total volume in each of the images in (Fig 6.A.B.C). The results colocalization were obtained by correlation coefficient and total segmented volume showed that CAMA-1 cells seem to have the highest degree of colocalized CD74 and CD44 molecules followed by MDA-MB-435 and then MDA-MB-231.

Interaction of CD74 and CD44

CD74-CD44 interaction in cell lysates as demonstrated by coimmunoprecipitation showed that there is an interaction between CD74 and CD44 in breast cancer cells (CAMA-1, MDA-MB-231 and MDA-MB-435) (Fig 7.*B*). It was further revealed that

CD74 interacts with both CD44s and CD44v isoforms, in CAMA-1 cells. MDA-MB-231 and MDA-435 cells express only CD44s isoform, which also interact with CD74. To test whether CD44s and CD44v interact with all isoforms of CD74 we performed the Co-IP of CD44-CD74. The results obtained showed that CD44s and CD44v bind only to p41 of CD74 (Fig 7.*C*).

Discussion

Characterization and identification of tumour antigens that are highly immunogenic in human tumours are considered important in tumour immunology [27]. Recent data suggest that CD74 and CD44 can play a significant role in the pathogenesis of various solid tumours [15, 16, 28]. For example, CD74 can mediate MIF binding, and MIF-induced ERK1 and ERK2 kinase phosphorylation requires the co-expression of CD44 [17]. Greenwood et al. [9] found that Stat1, Max1 and CD74 are expressed at high levels in triple-negative breast tumours . It has also been shown that CD44 expression is associated with a high rate of cell division and proliferation status [22].

Our data have confirmed that cell-surface CD74 and CD44 molecules are detectable by flow cytometry on CAMA-1, MDA-MB-231 and MDA-MB-435 cells. We also confirmed intracellular expression of CD74 and CD44 by confocal microscopy in all breast cancer cell lines. Our immunoblot results revealed that CAMA-1, MDA, MB-231 and MDA-MB-435 cells express total protein of CD74 and CD44. In addition, our data, obtained from Western blotting and immuneprecipitation, reveal that the CAMA-1, MDA-MB-231 and MDA-MB-435 cell lines express three different isoforms of CD74 (Fig. 4). These findings differ from that made by Verjans et al. [27] who found that MDA-MB-231 and MDA-MB-468 cells express only one isoform of CD74 [29]. Similarly, Metodieva et al. [30] found that MDA-MB-435 express one isoform of CD74.

It is generally accepted that CD74 facilitates export of MHC II/CD74 complexes from the endoplasmic reticulum, while blocking premature loading of peptides on to the MHC II molecules [31-34]. In humans, 80% of the CD74 protein pool is composed of the p33 isoform, and p35 is considered the most enigmatic isoform [32]. Genève et al. [32] have suggested that p33 and p35, together, facilitate antigen presentation, and this process does not require the co-expression of any other CD74 isoform [11, 32]. However, it has been recently suggested that high levels of CD74 expression might prevent tumour antigen presentation by blocking the MHC class II peptide-binding cleft, thus preventing binding of antigenic peptides for presentation to T cells, rendering tumors less immunogenic [11, 35]. Moreover, several studies have shown that the level of CD74 expression is proportionality associated with tumour grade [10, 35, 36]. Chao et al. [36]

have shown that upregulation of CD74 expression influences tumor growth and dissemination.

It was previously shown that MIF binds to the CD74 extracellular domain on macrophages and B cells to facilitate signaling [28, 37]. However, the interaction of MIF and CD74 requires CD44, due to lack of direct signal in the cell surface domain of CD74 [38]. When CD74 forms a complex with CD44, CD74 is modified by the addition of chondroitin sulfate, which is essential for the MIF-induced signaling cascade [39-41].

CD44, which is a multifunctional, class I transmembrane glycoprotein that generally acts as a specific receptor for hyaluronic acid, promotes migration in normal cells. It is widely expressed in almost all cells [42], and in its standard or variant form CD44 expression is found in most cancer cells [43]. CD44 has been the subject of extensive research for more than three decades because of its role in breast cancer. It has been demonstrated that CD44's role in breast cancer is twofold [25]. It was shown that CD44 activates and inhibits oncogenic signalling by both promoting and inhibiting tumour progression in response to extracellular cues [25, 44]. CD44 has also been linked to cancer due to its ability to increase the proliferation and invasion of tumour cells [1].

We have shown, by flow cytomtery, Western blotting and imaging, that CD44 is expressed in the CAMA-1, MDA-MB-231 and MDA-MB-435 cell lines. Equivalently, Sieuwerts et al. [43] observed that MDA-MB-435, ZR 75 and MDA-MB-231 cells express high levels of CD44. Western blot results have shown that CAMA-1 cells express two different CD44 isoforms: CD44s and CD44v. Jung et al. [45] showed that some breast cancer cell lines, such as MDA-MB-468 and SUM149, express several isoforms of CD44s and CD44v. It is possible that CD44 expression in breast cancer is associated with highly aggressive breast tumour subtypes or highly invasive breast cancer cells [46].

To validate our study we have used immortalized normal breast luminal cells (226LDM) as a model. We have investigated the expression of CD74 and CD44 by flow cytometry, Western blotting and bioimaging. Our findings confirmed that 226LDM cells do not express CD74 on the cell surface and intracellularly, while them do express CD44. This result was expected because it has been confirmed that the expression of CD74 can only be found antigen-presenting cells, including B cells, monocytes, macrophages, dendritic

cells, and Langerhans cells [47]. The presence of CD44 in normal breast cells is normal, since CD44 has a wide range of functions in normal tissues.

In view of the fact that CD74 and CD44 are involved in signalling with MIF [19], several groups have studied the association of CD74 and CD44 in cancers . Meyer-Siegler et al. [16] have shown that CD44 binds to the p35 isoform of CD74 in bladder cancer cells, although this isoform has been suggested to be involved in antigen presentation [32]. Meyer-Siegler et al. [16] did not specify, however, whether bladder cancer cells express different CD74 isoforms. Yet, they found that CD44v interacts with CD74 and MIF, creating a complex in prostate cancer cells (DU-145). However, human benign prostate hyperplasia epithelial cells (BPH-1) and LNCaP prostate cancer cells do not express CD74 on the cell surface. For this reason, both cells do not interact with CD44; however, LNCaP has been demonstrated to interact with MIF [15].

Our study has confirmed that CD74 and CD44 are expressed on the cell surface and intracellularly in the breast cancer cell lines CAMA-1, MDA-MB231 and MDA-MB435. Confocal microscopy allowed for the determination that CD74 and CD44 are highly colocalized in cytoplasmic domain in all breast cancer cells. Pearson's correlation coefficient was used to analyse the colocalization of CD74 and CD44 [48]. The segmentation of the images also showed the percentage of colocalized CD74 and CD44 molecules. The result from Co-IP confirmed that CD74 interacts with CD44s and CD44v. However, CD44s and CD44v interact only with p41, the most abundant isoform of CD74. Shi et al. [17] have shown that mammalian COS-7 cells do not bind MIF unless engineered to express CD74 [37]. It has been confirmed that CD74 alone is sufficient to mediate MIF binding to cells [17] however, CD74 alone is insufficient to signal with MIF in the absence of CD44. It has also been demonstrated that although phosphorylation of serine takes place in the p35 variant of Ii, the short cytoplasmic sequence of CD74 does not appear to signal directly and depends on CD44 [19]. Shi et al. [17] showed that COS-7 cells cannot instigate signalling when engineered to express CD74 and a truncated CD44 lacking its cytoplasmic signalling domain. Gore et al. [28] have also shown that CD74 binds to CD44 to initiate a signaling pathway involving with MIF in monocytes and macrophages. Furthermore, CD44-deficient cells do not have any activity that might involve in signaling pathway [28].

In summary, the present study has confirmed that all above used cell lines express CD74 and CD44. In addition, CAMA-1, MDA-MB-231 and MDA-MB-435 cells have significant amounts of cell surface CD74, an event that was not observed immortalized normal breast luminal cells 226LDM. Colocalization analysis has demonstrated that CD74 and CD44 are colocalized at cytoplasmic membrane suggestion a crucial role in breast cancer cells. In specific, coimmunoprecipitation result has confirmed that CD44 interact only with p41, the most abundant isoform of CD74. The emerging role of CD74 and CD44 in breast tumorigenesis may have selective, therapeutic modalities for women with breast cancer.

Acknowledgment

We would like to thank a Professor Elena Klenova Research Group Coordinator (Molecular and Cellular Bioscience) Director of Essex Biomedical Sciences Institute for providing us with breast normal cells 226LDM. We would like also a Professor Glyn Stanway the Chair Biological Hazards Committee for providing us HeLa cell line

Figure 1

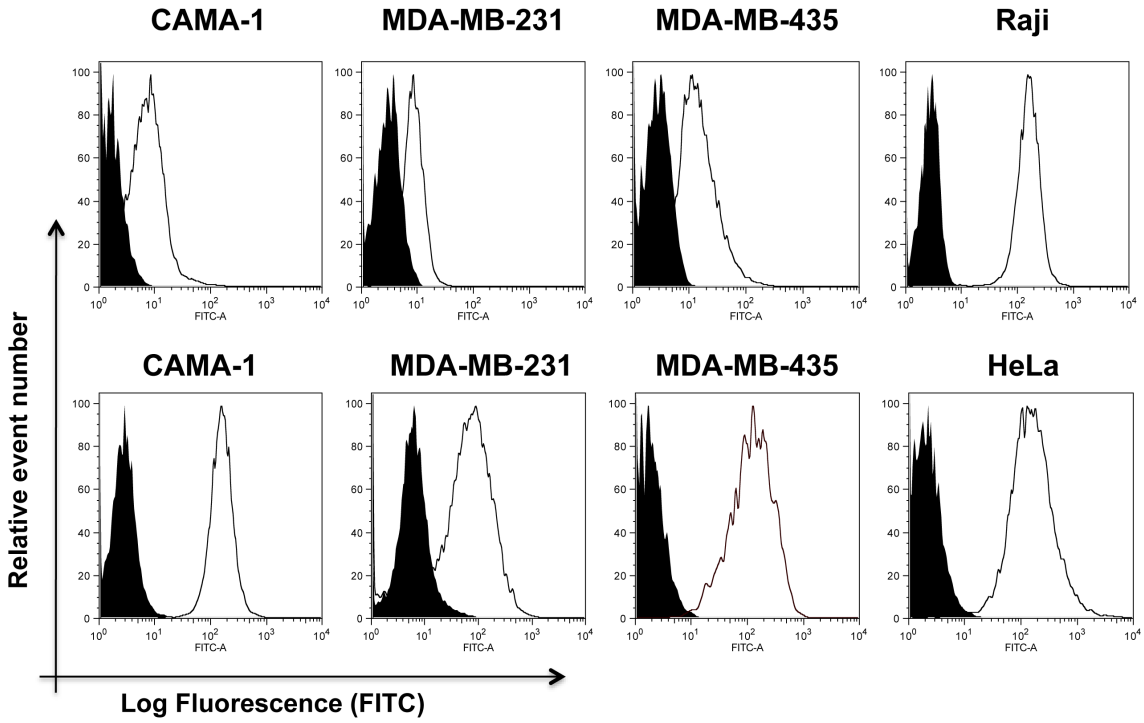

FIGURE 1: Cell surface expression of CD74 and CD44 on CAMA-1, MDA-MB-231, MDA-MB-435, Raji and HeLa cells. All cells were cultured in the appropriate media and were acquired by flow cytometry using By2 (anti-CD74) and 156-3C11 (anti-CD44). (A and B) Empty histograms represent the aforementioned cell lines labeled with anti-CD74 and anti-CD44 antibody. Black-filled histograms show the isotype as negative controls. Cells were labelled with an FITC-labelled secondary anti-mouse antibody. Expression levels were analyzed by flow cytometry (Aria cell sorter) and FlowJo 8.8.6 software was used to analyze the data. Mean fluorescence intensity (MFI) values were measured based on geometric means. Mouse IgG was used as a negative control.

Figure 2

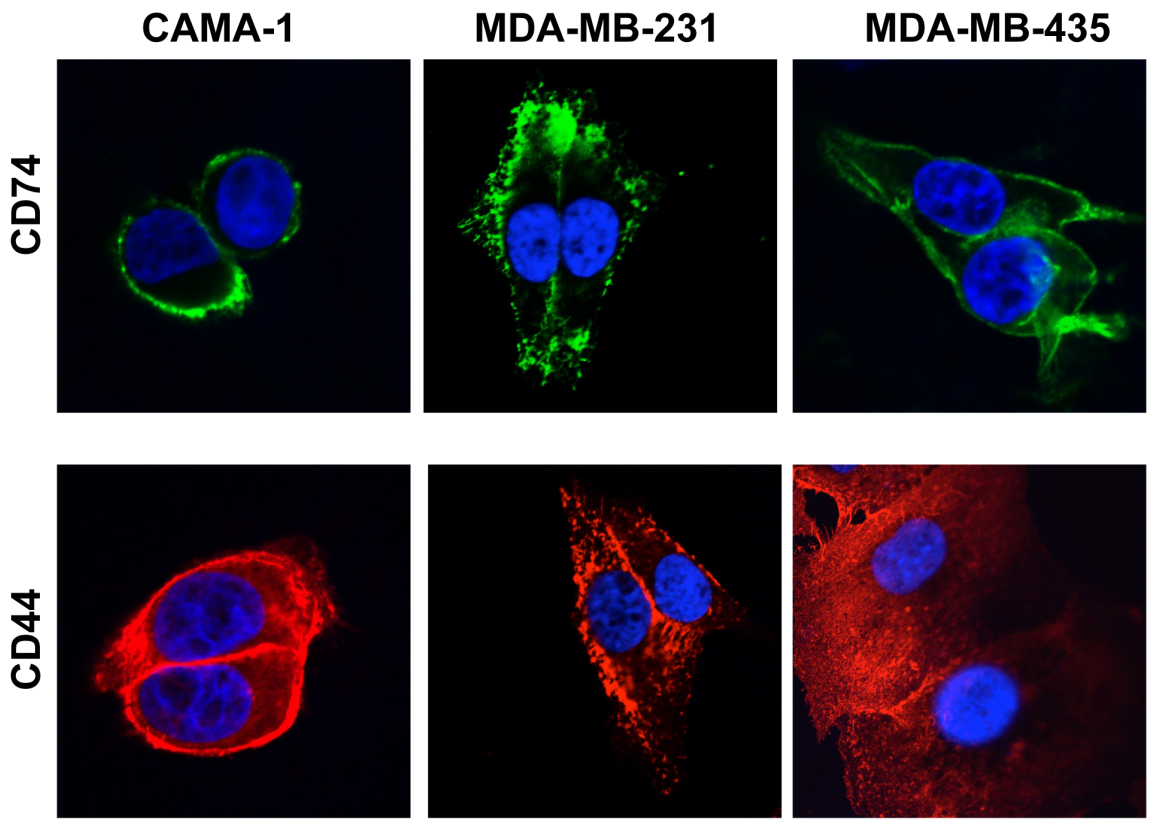

FIGURE 2: Confocal laser scanning microscopy images of intracellular staining of CD74 and CD44 in CAMA-1, MDA-MB-231 and MDA-MB-435 cells. The cells were cultured in LabTek 8-well chambers at a density of 6 x 10^3 cells per well overnight. CD74 was labelled with Alexa Fluor 488 (green) and CD44 with Alexa Fluor 555 (red). 4', 6-diamidino-2-phenylindole (DAPI) was used for nuclear staining (blue). Fluorochromes were acquired separately to evaluate the expression of CD74 and CD44 using the image-analysis software platform Fiji. Scale bar 10 µm.

Figure 3

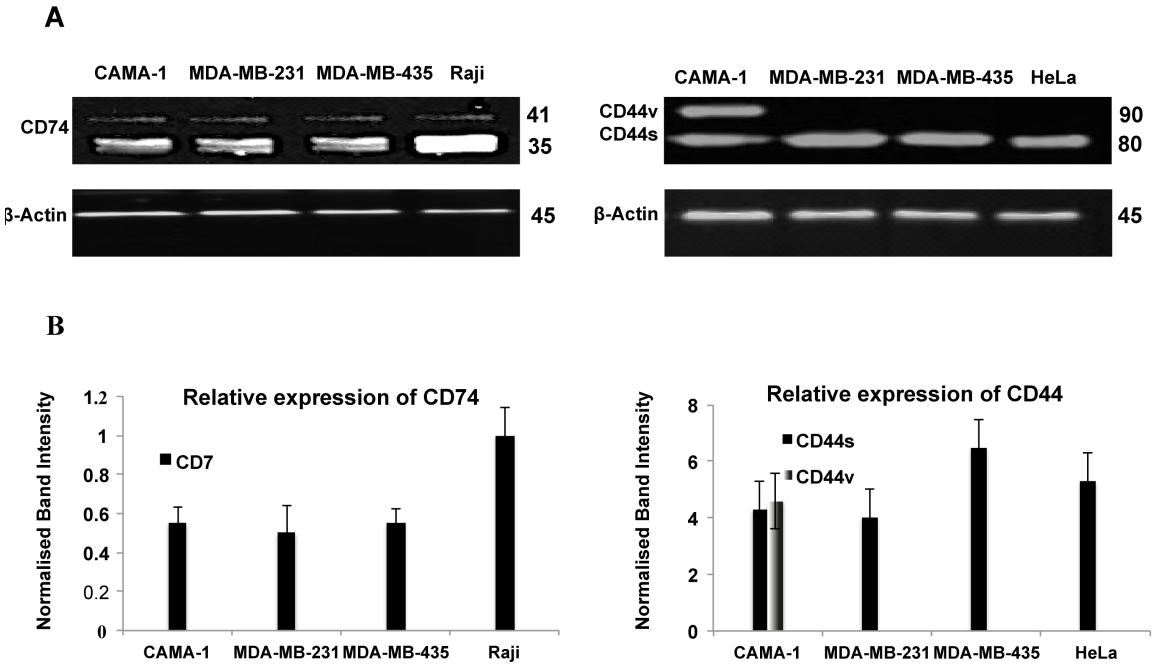

FIGURE 3: Western blotting was utilized to detect CD74, CD44 and β-actin expression in CAMA-1, MDA-MB-231, MDA-MB-435 and Raji cell lines. (A) Primary monoclonal antibodies Poly6221 (anti β-actin as loading control), By2 (anti-CD74) and 156-3C11 (anti-CD44) were used. β-actin is detected at a molecular weight of 50 kDa; CD74 isoforms were detected at molecular weights 33 and 45 kDa, whereas CD44 isoforms were detected at molecular weights 80 and 90 kDa. (B) CD74 and CD44 levels are normalized against β-actin. To account for the difference in protein loading during the experiment, the percentage of expression was calculated after the intensity of each band was adjusted according to its respective β-actin band intensity using the Image Studio Lite software (LI-COR Biosciences).

Figure 4

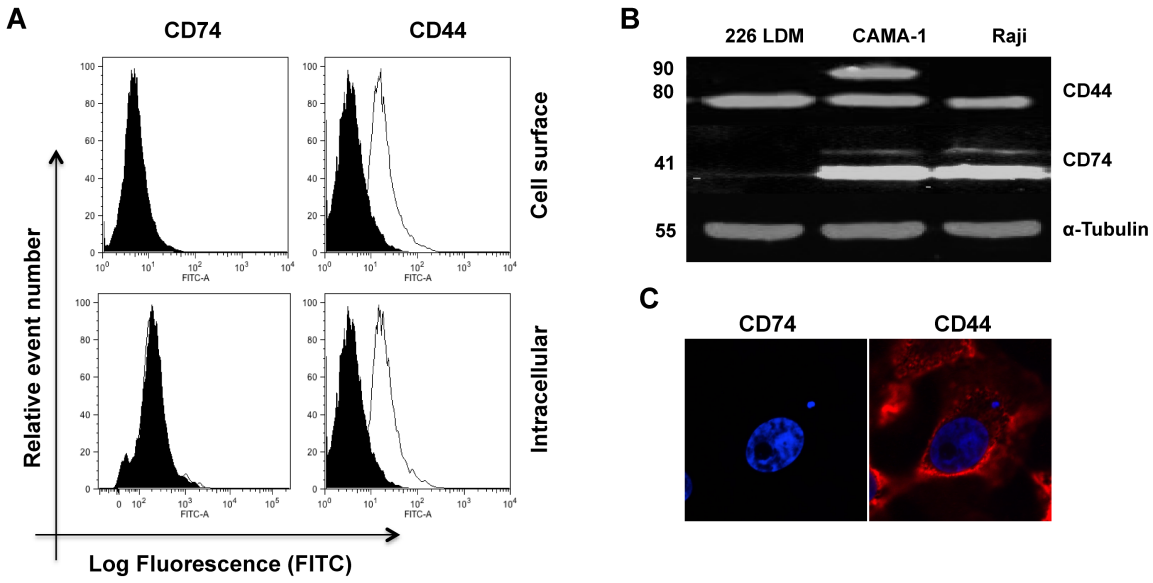

FIGURE 4: The expression of CD74 and CD44 receptors in immortalized normal breast luminal cells (226LDM). (A) Cell-surface and intracellular expression of CD74 and CD44 was acquired by flow cytometry using By2 (anti-CD74) and 156-3C11 (anti-CD44). Empty histograms represent the 226LDM cells stained with indicated antibody. Black-filled histograms show the isotype as negative controls. (B) Total protein of CD74 and CD44 was detected by Western blotting and α-tubulin was used as a loading control. (C) Intracellular staining of CD74 and CD44 in 226LDM cells by confocal laser scanning microscopy. Scale bar 10 μm.

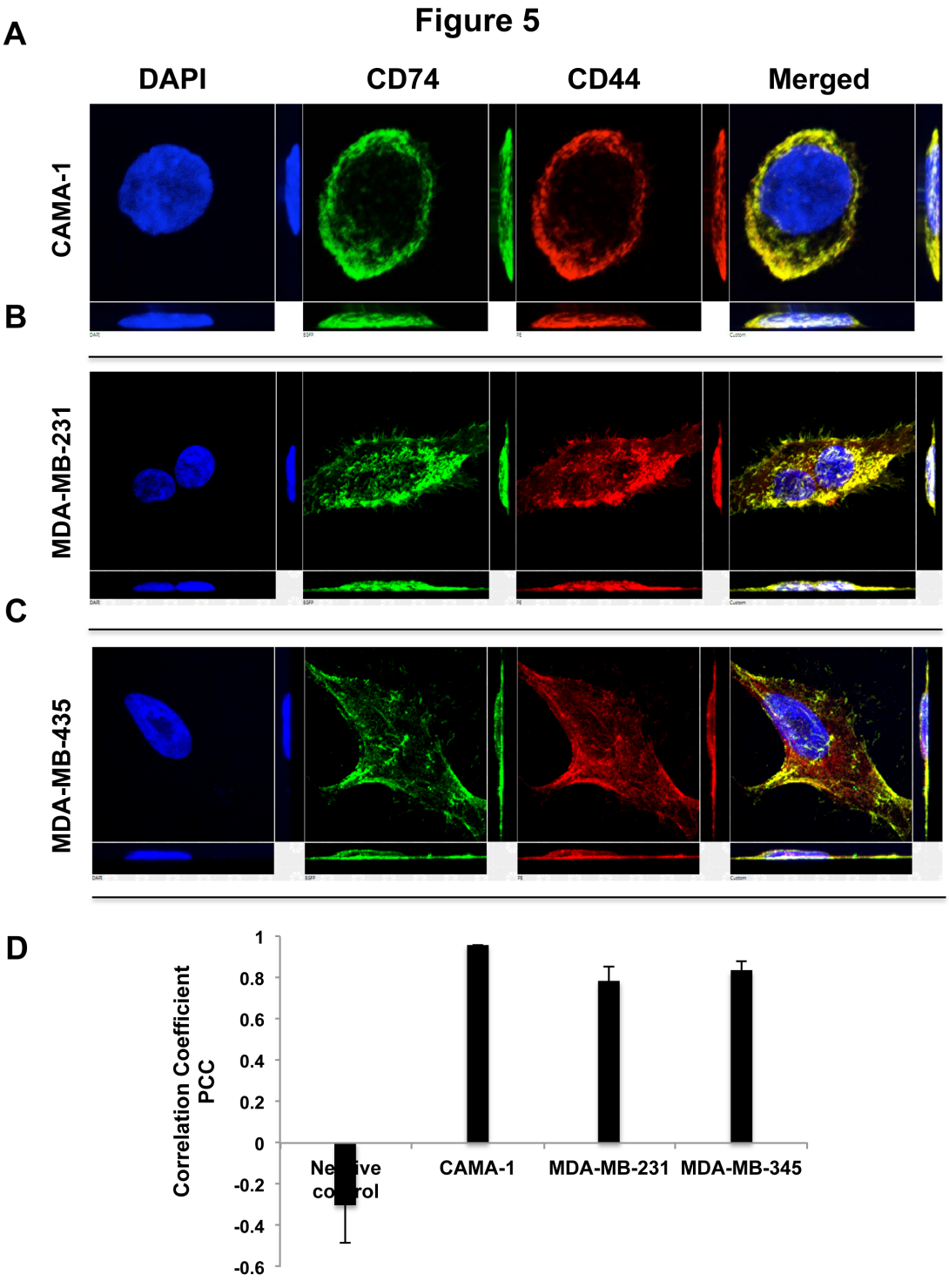

FIGURE 5: Colocalization of CD74 and CD44 at intracellular level on (A) CAMA-1, (B) MDA-MB-231 and (C) MDA-MB-435 cells, determined by confocal microscopy analysis. Yellow/orange fluorescence reveals the potential colocalization of two antigens. 3 D images were acquired in stack, with z-direction step size 0.14 µm using NIS element. Single-plane of z-stack is shown in three directions as xy, yz and zx. (D) Graphical representation of colocalization analysis based on PCC on each cells.

Figure 6

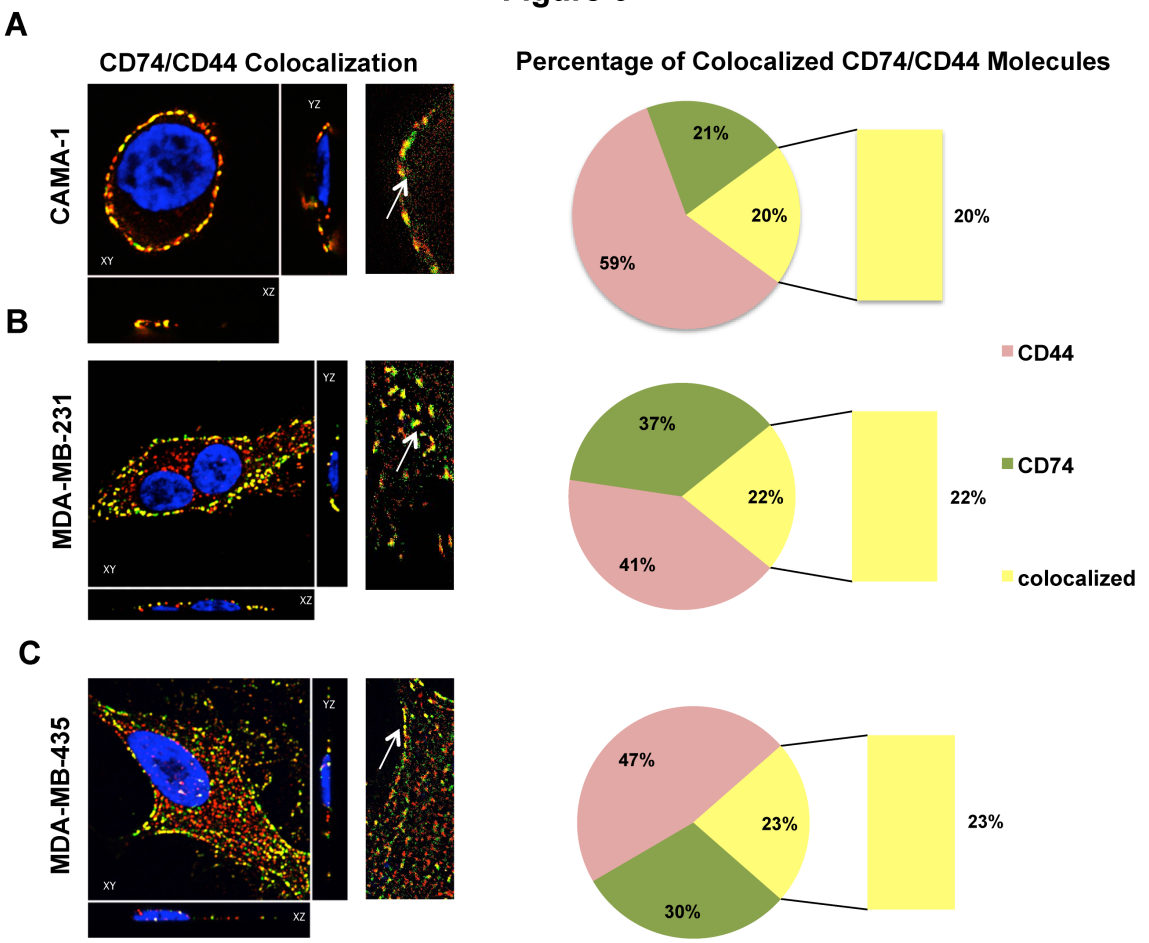

FIGURE 6: The colocalisation of CD74 with CD44 was quantified on segmented 3D images. Maximum intensity projections of CAMA-1, MDA-MB-231 and MDA-MB-435 cells are represented in A, B and C. CD74 was labelled with Alexa Fluor 488 (green) and CD44 with Alexa Fluor 555 (red). Nuclei are visualized with blue 4', 6-diamidino-2-phenylindole (DAPI) staining. Segmentation results from both channels merged with the DAPI. The percentages of the total volumes of CD74, CD44 and the colocalisation from each image are represented by pie charts. The result shows that CAMA-1 cells have the highest correlation between CD74 and CD44 followed by MDA-MB435 and MDA-MB231.

Figure 7

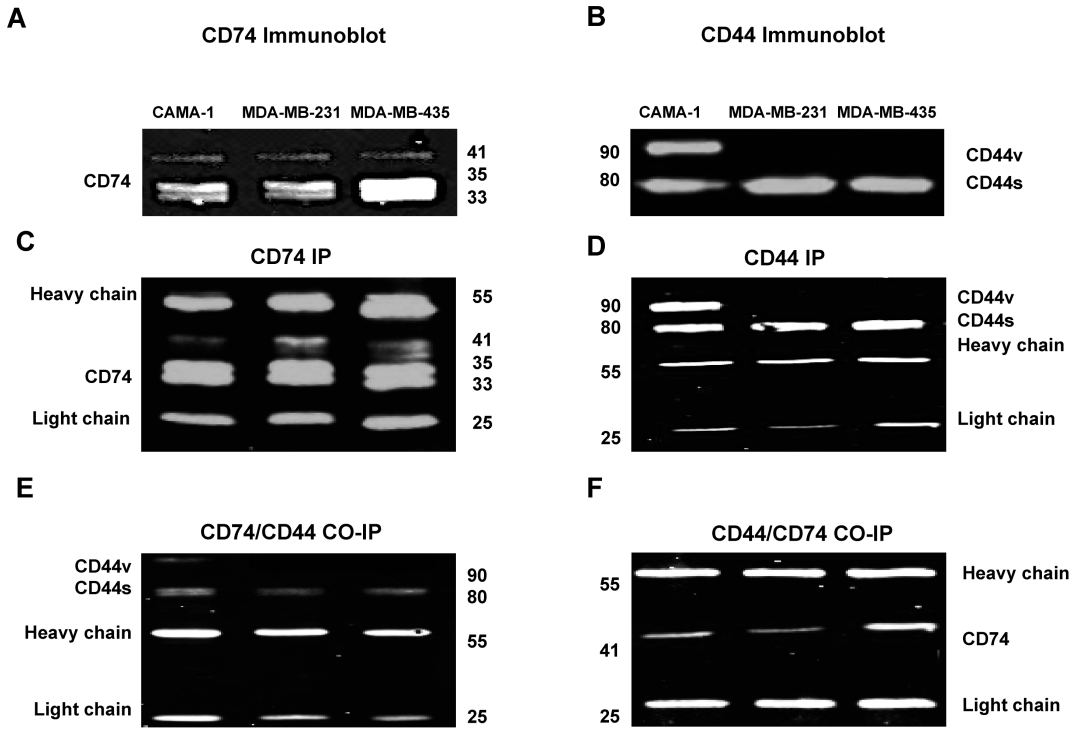

FIGURE 7: Coimmunoprecipitation to study the interaction of CD74 and CD44 in CAMA-1, MDA-MB-231 and MDA-MB-435 cell lines. (A and B) Immunoblot of CD74 and CD44 from breast cancer cell lysate. The blots were probed with either mouse anti-CD74 or anti-CD44 antibodies. (C and D) IP was subjected to pull down either CD74 or CD44.The antibody (Ab) heavy and light chain bands are indicated so that Ab heavy and light chain fragments can be observed at approximately 55 and 25 kDa respectively. (E and F) Co-IP was applied to study the interaction of CD74/CD44 and CD44/CD74. The Co-IP of CD74 /CD44 confirmed that all CD44 isoforms, including CD44s and CD44, interact with CD74. However, Co-IP of CD44/CD74 confirmed that only p41 of CD74 interacts with CD44.

Reference

1. Götte, Martin and George W Yip, *Heparanase, hyaluronan, and CD44 in cancers: a breast carcinoma perspective.* Cancer Research, 2006. 66(21): p. 10233-10237.

2. Trapé, Adriana Priscila and Ana Maria Gonzalez-Angulo, *Breast cancer and metastasis: on the way toward individualized therapy.* Cancer Genomics-Proteomics, 2012. 9(5): p. 297-310.

3. Richard, Vincent, Nadège Kindt, Christine Decaestecker, Hans‐Joachim Gabius, Guy Laurent, Jean-Christophe Noël, and Sven Saussez, *Involvement of macrophage migration inhibitory factor and its receptor (CD74) in human breast cancer.* Oncology reports, 2014. 32(2): p. 523-529.

4. Eccles, Suzanne A, Eric O Aboagye, Simak Ali, Annie S Anderson, Jo Armes, Fedor Berditchevski, Jeremy P Blaydes, Keith Brennan, Nicola J Brown, and Helen E Bryant, *Critical research gaps and translational priorities for the successful prevention and treatment of breast cancer.* Breast Cancer Research, 2013. 15(5): p. R92.

5. Ferlay, Jacques, Hai-Rim Shin, Freddie Bray, David Forman, Colin Mathers, and Donald Maxwell Parkin, *Estimates of worldwide burden of cancer in 2008: GLOBOCAN 2008.* International journal of cancer, 2010. 127(12): p. 2893-2917.

6. Maddams, J, D Brewster, A Gavin, J Steward, J Elliott, M Utley, and H Møller, *Cancer prevalence in the United Kingdom: estimates for 2008.* British Journal of Cancer, 2009. 101(3): p. 541-547.

7. Maddams, J, M Utley, and H Møller, *Projections of cancer prevalence in the United Kingdom, 2010–2040.* British journal of cancer, 2012. 107(7): p. 1195-1202.

8. Becker-Herman, Shirly, Galit Arie, Helena Medvedovsky, Anat Kerem, and Idit Shachar, *CD74 is a member of the regulated intramembrane proteolysis-processed protein family.* Molecular biology of the cell, 2005. 16(11): p. 5061-5069.

9. Greenwood, Christina, Gergana Metodieva, Khalid Al-Janabi, Berthold Lausen, Louise Alldridge, Lin Leng, Richard Bucala, Nelson Fernandez, and Metodi V Metodiev, *Stat1 and CD74 overexpression is co-dependent and linked to increased invasion and lymph node metastasis in triple-negative breast cancer.* Journal of proteomics, 2012. 75(10): p. 3031-3040.

10. Jiang, Zhong, Minzhen Xu, Louis Savas, Paula LeClair, and BF Banner, *Invariant chain expression in colon neoplasms.* Virchows Archiv, 1999. 435(1): p. 32-36.

11. Beswick, Ellen J and Victor E Reyes, *CD74 in antigen presentation, inflammation, and cancers of the gastrointestinal tract.* World journal of gastroenterology: WJG, 2009. 15(23): p. 2855.

12. Burton, Jack D, Scott Ely, Praveen K Reddy, Rhona Stein, David V Gold, Thomas M Cardillo, and David M Goldenberg, *CD74 is expressed by multiple myeloma and is a promising target for therapy.* Clinical Cancer Research, 2004. 10(19): p. 6606-6611.

13. Stein, Rhona, M Jules Mattes, Thomas M Cardillo, Hans J Hansen, Chien-Hsing Chang, Jack Burton, Serengulam Govindan, and David M Goldenberg, *CD74: a new candidate target for the immunotherapy of B-cell neoplasms.* Clinical Cancer Research, 2007. 13(18): p. 5556s-5563s.

14. Pyrz, Magdalena, Bruce Wang, Matthias Wabl, and Finn Skou Pedersen, *Research A retroviral mutagenesis screen identifies Cd74 as a common insertion site in murine B-lymphomas and reveals the existence of a novel IFNγ-inducible Cd74 isoform.* 2010.

15. Meyer-Siegler, Katherine L, Kenneth A Iczkowski, Lin Leng, Richard Bucala, and Pedro L Vera, *Inhibition of macrophage migration inhibitory factor or its receptor (CD74) attenuates growth and invasion of DU-145 prostate cancer cells.* The Journal of Immunology, 2006. 177(12): p. 8730-8739.

16. Meyer-Siegler, Katherine L, Erica C Leifheit, and Pedro L Vera, *Inhibition of macrophage migration inhibitory factor decreases proliferation and cytokine expression in bladder cancer cells.* BMC cancer, 2004. 4(1): p. 34.

17. Shi, Xuerong, Lin Leng, Tian Wang, Wenkui Wang, Xin Du, Ji Li, Courtney McDonald, Zun Chen, James W Murphy, and Elias Lolis, *CD44 is the signaling component of the macrophage migration inhibitory factor-CD74 receptor complex.* Immunity, 2006. 25(4): p. 595-606.

18. Naujokas, Marisa F, Michelle Morin, Mark S Anderson, Mary Peterson, and Jim Miller, *The chondroitin sulfate form of invariant chain can enhance stimulation of T cell responses through interaction with CD44.* Cell, 1993. 74(2): p. 257-268.

19. Borghese, Federica and Felix IL Clanchy, *CD74: an emerging opportunity as a therapeutic target in cancer and autoimmune disease.* Expert opinion on therapeutic targets, 2011. 15(3): p. 237-251.

20. Fillmore, Christine and Charlotte Kuperwasser, *Human breast cancer stem cell markers CD44 and CD24: enriching for cells with functional properties in mice or in man.* Breast Cancer Res, 2007. 9(3): p. 303.

21. Assimakopoulos, D, E Kolettas, G Patrikakos, and A Evangelou, *The role of CD44 in the development and prognosis of head and neck squamous cell carcinomas.* 2002.

22. Sneath, RJ and DC Mangham, *The normal structure and function of CD44 and its role in neoplasia.* Molecular Pathology, 1998. 51(4): p. 191.

23. Iczkowski, Kenneth A, *Cell adhesion molecule CD44: its functional roles in prostate cancer.* American journal of translational research, 2011. 3(1): p. 1.

24. Eberth, Sonja, Björn Schneider, Andreas Rosenwald, Elena M Hartmann, Julia Romani, Margarete Zaborski, Reiner Siebert, Hans G Drexler, and Hilmar Quentmeier, *Epigenetic regulation of CD44 in Hodgkin and non-Hodgkin lymphoma.* BMC cancer, 2010. 10(1): p. 517.

25. Louderbough, Jeanne MV and Joyce A Schroeder, *Understanding the dual nature of CD44 in breast cancer progression.* Molecular Cancer Research, 2011. 9(12): p. 1573-1586.

26. Chambers, Ann F, *MDA-MB-435 and M14 cell lines: identical but not M14 melanoma?* Cancer research, 2009. 69(13): p. 5292-5293.

27. Parmiani, Giorgio, Annamaria De Filippo, Luisa Novellino, and Chiara Castelli, *Unique human tumor antigens: immunobiology and use in clinical trials.* The Journal of Immunology, 2007. 178(4): p. 1975-1979.

28. Gore, Yael, Diana Starlets, Nitsan Maharshak, Shirly Becker-Herman, Utako Kaneyuki, Lin Leng, Richard Bucala, and Idit Shachar, *Macrophage migration inhibitory factor induces B cell survival by activation of a CD74-CD44 receptor complex.* Journal of Biological Chemistry, 2008. 283(5): p. 2784-2792.

29. Verjans, Eva, Erik Noetzel, Nuran Bektas, Anke K Schütz, Hongqi Lue, Birgitt Lennartz, Arndt Hartmann, Edgar Dahl, and Jürgen Bernhagen, *Dual role of macrophage migration inhibitory factor (MIF) in human breast cancer.* BMC cancer, 2009. 9(1): p. 230.

30. Metodieva, Gergana, Naiara Correa Nogueira-de-Souza, Christina Greenwood, Khalid Al-Janabi, Lin Leng, Richard Bucala, and Metodi V Metodiev, *CD74-dependent deregulation of the tumor suppressor scribble in human epithelial and breast cancer cells.* Neoplasia, 2013. 15(6): p. 660-IN21.

31. Neefjes, Jacques, Marlieke LM Jongsma, Petra Paul, and Oddmund Bakke, *Towards a systems understanding of MHC class I and MHC class II antigen presentation.* Nature Reviews Immunology, 2011. 11(12): p. 823-836.

32. Genève, Laetitia, Magali Chemali, Michel Desjardins, Nathalie Labrecque, and Jacques Thibodeau, *Human invariant chain isoform p35 restores thymic selection and antigen presentation in CD74-deficient mice.* Immunology and cell biology, 2012. 90(9): p. 896-902.

33. Datta, Milton W, Aliakbar Shahsafaei, Lee M Nadler, Gordon J Freeman, and David M Dorfman, *Expression of MHC class II-associated invariant chain (Ii; CD74) in thymic epithelial neoplasms.* Applied Immunohistochemistry & Molecular Morphology, 2000. 8(3): p. 210-215.

34. Bergmann, Hannes, *Business as usual: the p35 isoform of human CD74 retains function in antigen presentation.* Immunology and cell biology, 2012. 90(9): p. 839-840.

35. Zheng, Ying-Xia, Ming Yang, Ting-Ting Rong, Xiang-Liang Yuan, Yan-Hui Ma, Zhi-Hao Wang, Li-Song Shen, and Long Cui, *CD74 and macrophage migration inhibitory factor as therapeutic targets in gastric cancer.* World journal of gastroenterology: WJG, 2012. 18(18): p. 2253.

36. Chao, Mark P, Irving L Weissman, and Ravindra Majeti, *The CD47–SIRPα pathway in cancer immune evasion and potential therapeutic implications.* Current opinion in immunology, 2012. 24(2): p. 225-232.

37. Leng, Lin, Christine N Metz, Yan Fang, Jing Xu, Seamas Donnelly, John Baugh, Thomas Delohery, Yibang Chen, Robert A Mitchell, and Richard Bucala, *MIF signal transduction initiated by binding to CD74.* The Journal of experimental medicine, 2003. 197(11): p. 1467-1476.

38. Starlets, D., Y. Gore, I. Binsky, M. Haran, N. Harpaz, L. Shvidel, S. Becker-Herman, A. Berrebi, and I. Shachar, *Cell-surface CD74 initiates a signaling cascade leading to cell proliferation and survival.* Blood, 2006. 107(12): p. 4807-4816.

39. Stumptner-Cuvelette, Pamela and Philippe Benaroch, *Multiple roles of the invariant chain in MHC class II function.* Biochimica et biophysica acta, 2002. 1542(1-3): p. 1.

40. Maharshak, N., S. Cohen, F. Lantner, G. Hart, L. Leng, R. Bucala, and I. Shachar, *CD74 is a survival receptor on colon epithelial cells.* World journal of gastroenterology: WJG, 2010. 16(26): p. 3258.

41. Gil-Yarom, Naama, Shirly Becker Herman, and Idit Shachar, *Gene Section.* http://AtlasGeneticsOncology. org, 2014: p. 879.

42. Jaggupilli, Appalaraju and Eyad Elkord, *Significance of CD44 and CD24 as cancer stem cell markers: an enduring ambiguity.* Clinical and Developmental Immunology, 2012. 2012.

43. Sieuwerts, Anieta M, Jaco Kraan, Joan Bolt, Petra van der Spoel, Fons Elstrodt, Mieke Schutte, John WM Martens, Jan-Willem Gratama, Stefan Sleijfer, and John A Foekens, *Anti-epithelial cell adhesion molecule antibodies and the detection of circulating normal-like breast tumor cells.* Journal of the National Cancer Institute, 2009. 101(1): p. 61-66.

44. Marhaba, R and M Zöller, *CD44 in cancer progression: adhesion, migration and growth regulation.* Journal of molecular histology, 2004. 35(3): p. 211-231.

45. Jung, Thorsten, Donatello Castellana, Pamela Klingbeil, Ines Cuesta Hernández, Mario Vitacolonna, David J Orlicky, Steve R Roffler, Pnina Brodt, and Margot Zöller, *CD44v6 dependence of premetastatic niche preparation by exosomes.* Neoplasia, 2009. 11(10): p. 1093-IN17.

46. Montgomery, Nicola, Ashleigh Hill, Suzanne McFarlane, Jessica Neisen, Anthony O'Grady, Susie Conlon, Karin Jirstrom, Elaine W Kay, and David JJ Waugh, *CD44 enhances invasion of basal-like breast cancer cells by upregulating serine protease and collagen-degrading enzymatic expression and activity.* Breast Cancer Res, 2012. 14(3): p. R84.

47. Gold, David V, Rhona Stein, Jack Burton, and David M Goldenberg, *Enhanced expression of CD74 in gastrointestinal cancers and benign tissues.* International journal of clinical and experimental pathology, 2011. 4(1): p. 1.

48. Bolte, S and FP Cordelieres, *A guided tour into subcellular colocalization analysis in light microscopy.* Journal of microscopy, 2006. 224(3): p. 213-232.